EXPRES 2016

Proceedings

8th International Symposium on Exploitation of Renewable Energy Sources and Effectiveness

EXPRES 2016

8th International Symposium on
Exploitation of Renewable Energy Sources and Efficiency

Subotica, Serbia
March 31- April 02, 2016

_____

Proceedings

http://Expres 2016 ISBN 978-86-919769-0-3

Table of contents

Committees

HONORARY COMMITTEE
Imre J. Rudas, Óbuda University, Budapest
Branislav Todorović, University of Beograd
Janos Fodor, Óbuda University, Budapest

GENERAL CHAIR
József Nyers, Óbuda University, Budapest

INTERNATIONAL ADVISORY COMMITTEE
János Beke, SzIE University , Gödöllő-, Budapset
Ján Takács, University of Technology in Bratislava, Slovakia
Felix Stachowicz, University of Rzesov, Poland

ORGANIZING COMMITTEE CHAIR
Zoltán Pék, V3ME, Subotica**,   László Veréb,** V3ME, Subotica

ORGANIZING COMITTEE
Slavica Tomić, University, Novi Sad
Laszlo Kajtar, BME, Budapest

TECHNICA PROGRAM COMMITTE CHAIRS
Péter Láng, BME, Budapest
Péter Kádár, Óbuda University, Budapest
Péter Odry, Subotica Tech

TECHNICAL PROGRAM COMMITTE
Marija Todorović, Univ. Beograd, Serbia
Milorad Bojić, Univ. Kragujevac, Serbia
László Garbai, BME, Budapest¸ Hungary
Dušan Gvozdenac, Univ. Novi Sad, Serbia
Jenő Kontra, BME, Budapes, Hungary
Belo Furi, University of Technology in Bratislava, Slovakia
László Tóth, Univ. SzIE, Gödöllő, Hungary
István Farkas Univ. SzIE,. Gödöllő, Hungary
Stevan Firstner,SuboticaTech, Serbia
Ferenc Kalmar, Univ. Debrecen, Hungary
Djordje Kozić, Univ. Beograd, Serbia
Laszlo Sikolya, Nyiregyhaza College, Hungary
Dusan Golubović, Univ. East Sarajevo, Bosna and Hercegovina.
Zoltan Magyar, BME, Budapest¸ Hungary
Laslo Šereš, University, Novi Sad
Miklos Kassai, BME, Budapest¸ Hungary

PROCEEDINGS EDITOR
József Nyers, Óbuda University, Budapest

Cooling energy saved investigation of air-to-air heat-and energy exchangers

Miklos Kassai*, Laszlo Kajtar*

* Budapest University of Technology and Economics/Department of Building Service Engineering and Process, Budapest, Hungary
kas.miklos@gmail.com
kajtar@epgep.bme.hu

Abstract—**The aim of this research study was to investigate the cooling energy saved of five different air-to-air heat-and energy exchangers in three different weather European countries. Using the ambient temperature and enthalpy duration curves, detailed mathematical expressions are presented to determine the energy saved by air-to-air heat-and energy recovery units operating in ventilation systems during the cooling period. The three different climate cities are: Palermo (as Mediterranean zone), Krakow (as temperate zone) and to Helsinki (as cold climate region). The investigated heat recoveries that are suitable only for heat transfer are the fixed-plate heat exchanger, the run around coil and the heat-pipe technology. Energy exchangers allow both heat-and moisture transfer with higher moisture transfer effectiveness by a sorption rotor and with lower without sorption coating. Using the developed method it is easy to see that during the selection of heat-and energy recovery units when a ventilation system is designed, the energy saved of the units have to be considered not only for heating, but also for cooling period depending of the climate location.**

INTRODUCTION

The demands in the building sector regarding energy conservation have been growing for many years in the whole world. Generally less energy use for HVAC systems is required but without compromising a comfortable and acceptable indoor environment. Decreasing the energy consumption in different enduse sectors, especially in buildings [1], is one of the main energy concerns of the European Union (EU) countries. People nowadays spend about 90% of their time in indoor spaces [2]. This means that, without any indoor air is treating and fresh air supplying, people are subject to an unhealthy and uncomfortable environment for prolonged periods. With fresh air demand increasing, energy consumption also increases in order to condition this required fresh air. Due to the increasing indoor air quality (IAQ) standard, the ventilation loads represent about 20–50% part of the total heating demand for new and retrofitted buildings [2,4,9,10,11,12], depending on the building's insulation, compactness, air change rate, indoor heat sources, indoor set points and outdoor climate. Therefore, there is a need for residential buildings and their systems to provide a comfortable and acceptable indoor environment. This is often accomplished through the use of heating, ventilation, and air conditioning systems, particularly in the summer (cooling) and winter (heating) seasons. Nearly 87% of residential homes in the United States of America use air conditioning, including 89% of single family homes, and 84% of multi-family homes [13]. In more extreme hot climates air conditioning penetration is nearly 100%. Air conditioning penetration is lower in many other parts of the world, but is predicted to grow worldwide by 72% between 2000 and 2100, particularly in the face of predicted climate change. Worldwide, the use of central heating is also predicted to increase by 34% by 2100 [14]. Since HVAC systems impact energy use, thermal comfort and indoor air quality, it is important to understand how and when these systems operate. However, there is limited information available on the operational characteristics, and specifically on runtimes and energy consumption of these HVAC systems. With new building codes, EU countries also intend to reduce the total energy consumption in buildings by making the buildings well-insulated and tighter [2–7]. The first retrofit options to be considered for existing buildings are the improvement of the thermal insulation and air tightness. Improving the building envelope increases the relative part of the energy consumption due to ventilation. The usage of mechanical ventilation system equipped with an air-to-air recovery heat-and energy exchanger is a solution to ensure a high global energy performance of the building and reach the requirements in terms of IAQ [15]. In these systems, indoor air extracted from the building is used to pre-heat (in winter) or pre-cool (in summer) the fresh air flow rate coming from the outdoor environment. While such exchangers have been on the market for many years, only a few modeling works are presented in technical and scientific literature. Only the parameters having an impact on the energy performance of heat recovery ventilation have been investigated deeper in the last years. Mardiana and Riffat [16] list physical characteristics ofthe main components: heat exchanger and fans that influence the efficiency of heat or energy recovery. Roulet et al. [17] discuss the effect of leakages and shortcuts on heat recovery unit and show that the conventional methods to determine the heat recovery efficiency are not sufficient to outline the global performance of ventilation systems; and propose a method based on the specific net energy savings to characterise the energy performance. Manz et al. [18] investigate the

same effect on a single room ventilation system and define a heat recovery efficiency based on heating load reduction. External parameters like the climate location also play a key role in the determination of the performances of ventilation systems [19]. Based on the above mentioned facts it is easy to see that the calculation of energy consumption and energy saved of ventilation systems is a complex design problem requiring many pieces of information such as outdoor weather condition, indoor set point temperature and relative humidity, mass flow rate of ventilation air, effectiveness of the exchanger, technique to add auxiliary heating and cooling. The calculations needed to evaluate the operating energy consumption involve functions of these parameters integrated over time and are quite complex (ASHRAE 2000). Several studies on heating energy consumption of ventilation systems operated with heat-and energy recovery units have been done, but investigation of cooling energy saved of these systems have been not taken much attention in the literature [20-30].

The object of this research study was to investigate the energy saved of five different constructed air-to-air heat-and energy exchangers in three in different weather European countries in cooling period. Using the ambient temperature and enthalpy duration curves, developing a novel approach to describe the changing of the cooling air condition parameters during the cooling period, detailed mathematical expressions were worked out to determine the energy consumption of the ventilation systems and the energy saved by air-to-air heat-and energy recovery units during the cooling period. The three different climate cities are: Palermo (as mediterranean zone), Krakow (as temperate zone) and to Helsinki (as cold climate region). The investigated heat recoveries that are suitable only for heat transfer are the fixed-plate heat exchanger, the run around coil and the heat-pipe technology. Energy exchangers, that were also considered, allow both heat-and moisture transfer with higher moisture transfer effectiveness by a sorption rotor and with lower without sorption coating. Using the developed method it is easy to see that during the selection of heat-and energy recovery units when a ventilation system is designed, the energy saved of the units have to considered not only for heating, but also for cooling period depending of the climate location. The results by the developed method show that before the selection of the heat-and energy recovery unit into an air handling unit, their energy saved has to investigate not only for the heating, but also for the cooling period depending on the climate zone.

METHOLOGIES

The energy saved of different heat-and energy recovery technologies were investigated in three different climate cities (Palermo as a hot, Krakow as temperate, and Helsinki as a cold climate city) in cooling period. The energy saving investigation for the heating period in these three cities have been already investigated in a previous study [49]. During our investigation a steady air volume flow rate was assumed to 1000 m3/h, and the air density was assumed to constant 1,2 kg/m3. For heat recovery systems, that are suitable only for heat transfer, temperature controlling was considered during calculations, which means the heat exchanger works only when outer air temperature is higher than the exhaust temperature delivered from the conditioned space. In case

of energy recovery systems that are suitable for both heat-and moisture transfer, enthalpy controlling was considered, thus energy exchanger operates until enthalpy of ambient air decreases to the exhaust air enthalpy value. During our research a comparative energetic investigation was performed for the heat-and energy recovery systems most commonly applied in HVAC practice. Among heat recovery technologies that transfer only heat energy, cross flow plate heat recovery, run around coil heat recovery and heat pipe heat exchangers were investigated. Among energy recovery systems that are suitable for both heat and moisture transfer rotary energy recovery unit with sorption and non sorption coating were investigated. The object was to predict the energy savings in the different cases for cooling season. The heat and moisture transfer effectiveness values for each exchangers were selected (Table 1) based on VDI 2071 standard.

HEAT-AND MOISTURE TRANSFER EFFECTIVENESS VALUES OF THE INVESTIGATED ENERGY RECOVERY UNITS [34]

Type of the investigated heat-and energy recovery	Heat transfer effectiveness	Moisture transfer effectiveness
-	η_h [-]	η_m [-]
Cross flow plate heat recovery	0,6	0
Run around coil heat recovery	0,4	0
Heat pipe heat exchangers	0,3	0
Rotary energy recovery unit with sorption coating	0,8	0,65
Rotary energy recovery unit with non sorption coating	0,8	0,15

Air handling process for sizing state is plotted to diagram Mollier h-x is in Figure 1. As the ambient air (to) passes the cooling coil the air temperature is decreased to the cooling temperature (tc) and finally the air is heated up by a re-heater to the suppy air tempareture (ts) to provide the required indoor air parameters (ti; φi) in cooling season.

Figure 1. Air handling process without heat-and energy exchanger in diagram h-x, in cooling period, Palermo

To determine the energy consumption of the system ambient air enthalpy duration curve was used. Figure 2 shows the areas that are proportional with the energy consumption of the cooling („C") and the re-heater („RH").
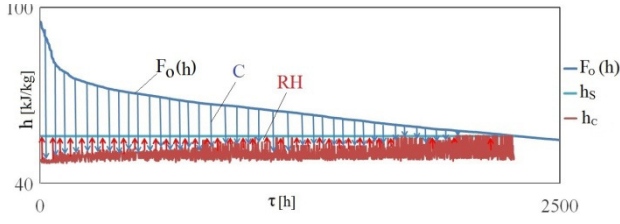
Figure 2. Areas proportional to the energy consumption of cooling and re-heating without heat-and energy exchanger in Palermo in cooling period

Using the amount of energy determined with the areas on the ambient air enthalpy duration curve, the energy consumption of the ventilation system could be calculated described bellow way.

Energy consumption of the cooling coil:

$$Q_C = \rho \cdot \dot{V} \cdot \int_{h_O}^{h_C} F_O(h)dh \quad [\text{MJ/year}] \qquad (1)$$

Energy consumption of the re-heater:

$$Q_{RH} = \rho \cdot \dot{V} \cdot \int_{h_C}^{h_S} F_O(h)dh \quad [\text{MJ/year}] \qquad (2)$$

DETERMINING THE ENERGY CONSUMPTION OF VENTILATION SYSTEM OPERATED WITH CROSS FLOW PLATE HEAT EXCHANGER IN PALERMO IN COOLING PERIOD

Air handling process for sizing state is plotted to diagram Mollier h-x is in Figure 3. As the ambient air (to) passes the heat recovery the air temperature is decreased to the heat recovered temperature (t_{HR}), then, passing the cooling coil, to the cooling temperature (tc) and finally the air is heated up by a re-heater to the suppy air temperature (ts) to provide the required indoor air parameters (ti; φi) in cooling season.
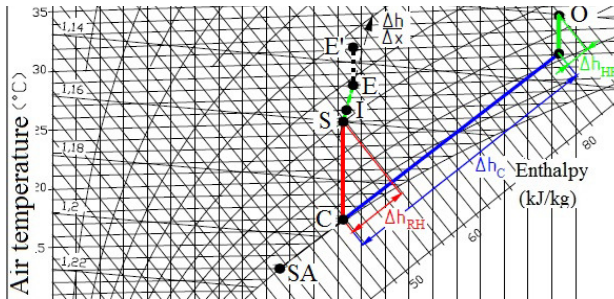
Figure 3. Air handling process with cross flow plate heat exchanger on diagram h-x in cooling period in Palermo
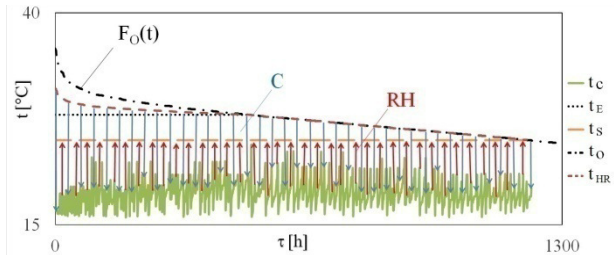
Figure 4. Areas proportional to the energy consumption of cooling and re-heating with cross flow plate heat exchanger in Palermo in cooling period

Using the amount of energy determined with the areas on the ambient air temperature duration curve (Figure 4), the energy consumption of the ventilation system for cooilng period could be calculated described below way.

Energy consumption of the cooling coil:

$$Q_C = c_{pl} \cdot \rho \cdot \dot{V} \cdot \int_{t_C}^{t_{HR}} F_O(t)dt \quad [\text{MJ/year}] \qquad (3)$$

Energy consumption of the re-heater:

$$Q_{RH} = c_{pl} \cdot \rho \cdot \dot{V} \cdot \int_{t_C}^{t_S} F_O(t)dt \quad [\text{MJ/year}] \qquad (4)$$

DETERMINING THE ENERGY CONSUMPTION OF VENTILATION SYSTEM OPERATED WITH ROTARY ENERGY EXCHANGER WITH SORPTION COATING IN PALERMO IN COOLING PERIOD

The determination method for energy consumption investigation looks almost the same for run around coil heat recovery and heat pipe heat exchanger. Figure 5 shows the air handling process of the ventilation system that is plotted to Mollier h-x diagram for sizing state in cooling season.
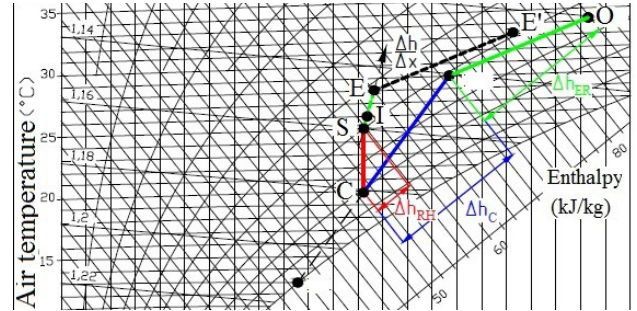
Figure 5. Air handling process with rotary energy exchanger with sorption coating on diagram h-x in cooling period in Palermo

Figure 6 shows the areas that are proportional with the energy consumption of the cooling („C") and the re-heater („RH") using the ambient air enthalpy duration curve.
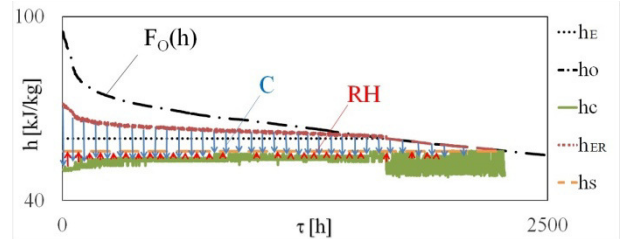
Figure 6. Areas proportional to the energy consumption of cooling and reheating, air conditioner operating with sorption coating rotary heat exchanger, Palermo

Energy consumption of the cooling coil:

$$Q_C = \rho \cdot \dot{V} \cdot \int_{h_C}^{h_{ER}} F_O(h)\,dh \quad \text{[MJ/year]} \qquad (5)$$

Energy consumption of the re-heater:

$$Q_{RH} = \rho \cdot \dot{V} \cdot \int_{h_C}^{h_S} F_O(h)\,dh \quad \text{[MJ/year]} \qquad (6)$$

The determination method for energy consumption investigation looks almost the same for non sorption rotary heat exchanger technology.

RESULTS

Figure 7-10 show the predicted energy saved of the ventilating systems operating with different heat-and energy recovery technologies.
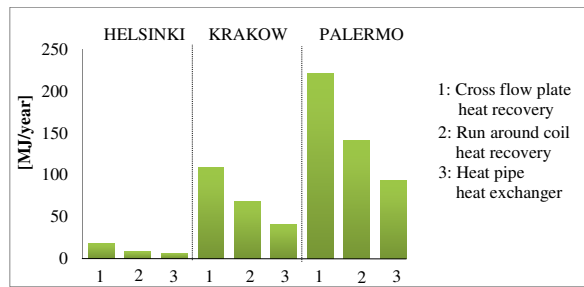
Figure 7. Energy saved of the investigated heat recovery technologies in cooling period
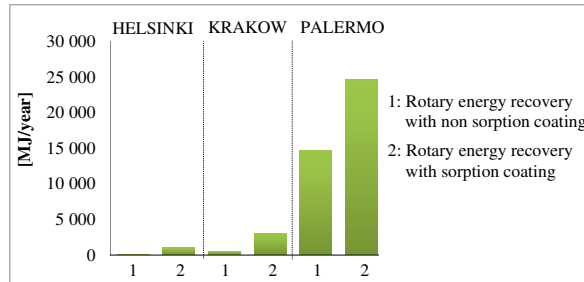
Figure 8. Energy saved of the investigated energy recovery technologies in cooling period
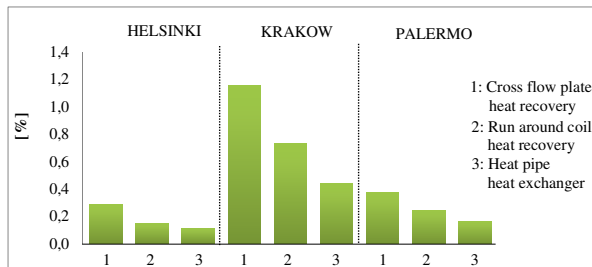
Figure 9. Energy saved of the investigated heat recovery technologies correlated to consumption without heat recovery operation in cooling period
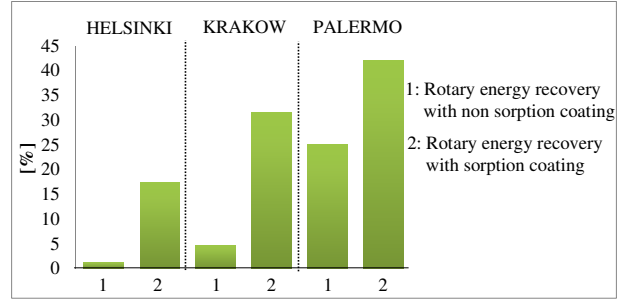
Figure 10. Energy saved of the investigated energy recovery technologies correlated to consumption without energy recovery operation in cooling period

Based on the results the highest amount of energy saved can be reached with rotary energy recovery (especially with sorption coating) in cooling period. In Helsinki nearly 1100 MJ/year, in Krakow 3000 MJ/year, and in Palermo approximately 25 000 MJ/year energy can be saved in the cooling period. Naturally there are differences in the energy consumption of the different located cities; therefore it is worth taking into consideration even the percentage format of the savings beside the values themselves. The results show that highest percentage of energy saved can be reached in Palermo by 42%, followed by Krakow (31,5 %), finally Helsinki (17,5 %) (compared to the ventilation system without any heat-and energy recovery technologies).

CONCLUSIONS

According to the above it can be concluded that in cooling period higher rate of energy saved can be performed in a mediterranean climate area. In case of the heat recovery systems that transfer only for heat energy, the maximal energy saved is only some 100 MJ/year, in percentage it means only 1-2%. Its reason is the higher energy consumption of re-heating compared to the ventilation system without any heat-and energy recovery. Namely the cooling air temperature is lower related to the same ambient air condition parameters, by this way the re-heater has to heat up the air from a lower cooling air temperature value (according to Fig. 2). It must be noted, that the values were not determined regarding the annual energy savings, only for the cooling period, thus the above results relevant only for this period. Selecting any heat-and energy recovery technology is worth for heating period, since the heating period is generally much longer than the necessary cooling hours' number especially in cold climates. Obviously the higher proportion cooling period compared to heating period, the much more it worth considering the energy saving for this period, for example in case of Palermo the energy saved by the heat-energy recovery can be significant even in the cooling period.

ACKNOWLEDGMENT

REFERENCES

EU-Directive 2010/31/EC of the European Parliament and of the council of 19 May 2010 on the energy performance of buildings (recast). *European Commission*. 2010.

C.A. Roulet, F.D. Heidt, F. Foradini, M.C. Pibiri, "Real heat recovery with air handling units", *Energy and Buildings* 2001;33:495–502.

M. Fehrm, W. Reiners, M. Ungemach, "Exhaust air heat recovery in buildings", *International Journal of Refrigeration* 2002;25:439–449.

M. Orme, "Estimates of the energy impact of ventilation and financial expenditures". *Energy and Buildings* 2001;33:199–205.

R.M. Lazzarin, A. Gasparella, "Technical and economical analysis of heat recovery in building ventilation systems". *Applied Thermal Engineering* 1998;18:47–67.

A. Dodoo, L. Gustavsson, R. Sathre, "Primary energy implications of ventilation heat recovery in residential buildings", *Energy and Buildings* 2011;43:1566–1572.

J. Nyers, L. Kajtar .S. Tomic, A. Nyers, "Investment-savings method for energy-economic optimization of external wall thermal insulation thickness." *Energy and Buildings*, 2015;86:268-274.

U.S. Environmental Protection Agency, Report to Congress on indoor air quality: volume 2. EPA/400/1-89/001C. Washington, DC, 1989.

M.W. Liddament, M. Orme, "Energy and ventilation." *Applied Thermal Engineering*, 1998;18:1101–1109.

J.S. Carey, "Energy consumption and ventilation performance of naturally ventilated ecological house in a cold climate." *Energy and Buildings* 2005;37:23–35.

R.K. Calay, B.A. Borresen, A.E. Holdø, "Selective ventilation in large enclosures". *Energy and Buildings*, vol. 2000;32:281–289.

K.C. Rajnish, C.W. Wen, "A study of an energy efficient building ventilation system", *RoomVent 2011 - 12th International conference on air distribution in rooms*, Trondheim, Juny 19-22, pp. 1-8. 2011.

United States Energy Information Administration, RECS, Residential Energy Consumption Survey, *U.S. Department of Energy*, Washington, DC, USA, 2009.

M. Isaac, P.V.V. Detlef, "Modeling global residential sector energy demand for heating and air conditioning in the context of climate change". *Energy Policy*, 2009;37:507–521.

C. Cristiana, N. Ilinca, B. Florin, M. Amina, D. Angel, "Thermal comfort models for indoor spaces and vehicles - Current capabilities and future perspectives". *Renewable and Sustainable Energy Reviews*. 2015;44:304–318.

A. Mardiana, S.B. Riffat, "Review on physical and performance parameters ofheat recovery systems for building applications". *Renewable Sustainable Energy* Rev. 2013;28:174–190.

C.A. Roulet, F.D. Heidt, F. Foradini, M.C. Pibiri, "Real heat recovery with air handling units", *Energy Build*. 2001;33:495–502.

H. Manz, H. Huber, D. Helfenfinger, "Impact of air leakages and short circuits inventilation units with heat recovery on ventilation efficiency and energyrequirements for heating." *Energy Build*. 2001;33:133–139.

J. Laverge, A. Janssens A,"Heat recovery ventilation operation traded off againstnatural and simple exhaust ventilation in Europe by primary energy factor, carbon dioxide emission, household consumer price and exergy." *Energy Build*. 2012;50:315–323.

W. Yang, F.Y. Zhao, J. Kuckelkorn, D. Liu, L.Q. Liu, Pan XC. "Cooling energy efficiency and classroom air environment of a school building operated by the heat recovery air conditioning unit." *Energy* 2014;64:991-1001

L. Kajtar, J. Nyers, J. Szabo, "Dynamic thermal dimensioning of underground spaces" *Energy* 2015;87:361–368.

T. Poos, M. Orvos, "Heat- and mass transfer in agitated, co-, or countercurrent, conductive-convective heated drum dryer", *Drying Technology* 2012;30:1457-1468.

T. Poos, V. Szabo, "Equations of volumetric heat transfer coefficients and mathematical models at rotary drum dryers", *Eurodrying'2015: 5th European Drying Conference*. Budapest, October 21-23. 2015:322-328.

L.Z. Zhang, J.K. Niu, "Energy requirements for conditioning fresh air and the longterm savings with a membrane-based energy recovery ventilator in Hong Kong", *Energy*, 2011;26,2001.

Z. Radu, X.Y. Wu, "Energy and exergy performance of residential heating systems with separate mechanical ventilation", *Energy*, 2007;32:187–195.

J. Wallin, H. Madani, J. Claesson, "Run-around coil ventilation heat recovery system: A comparative study between different system configurations", *Applied Energy* 2012;90:258–265.

K.C. Rajnish, C.W. Wen, "A study of an energy efficient building ventilation system", *RoomVent 2011 - 12th International conference on air distribution in rooms*. Trondheim. Juny 19-22. 2011:1-8.

C. Guangyu, A. Hazim, Y. Runming, F. Yunqing, S. Kai, Risto K, J.Z. Jianshun, "A review of the performance of different ventilation and airflow distribution systems in buildings", *Building and Environment*. 2014;73:171-186.

W. Lihui, B. Xinhui, C. Rui, J.Z. Jianshun, "The synamic thermal comfort index analysis under the air supply vent coupled with the cross-flow". *Procedia Engineering*. 2015;121:544 – 551.

C. Cristiana, N. Ilinca, B. Florin, M. Amina, D. Angel, "Thermal comfort models for indoor spaces and vehicles - Current capabilities and future perspectives". *Renewable and Sustainable Energy Reviews*, 2015;44:304–318.

L. Šereš L., O. Grljević, S. Bošnjak, „*IT Support of Buildings Energy Efficiency Improvement*", International Conference on Energy Efficiency and Environmental Sustainability, EEES2012, Conference proceedings, ISBN: 978-86-7233-320-6, pp. 55-62

Power Efficiency of Thermopile Technology

I. Farkas[*], A. Szente[**], D. Nyitri[***] and P. Odry[***]

[*] University of Dunaújváros/Computer Engineering, Dunaújváros, Hungary
[**] Paks Nuklear Power Plant, Paks, Hungary
[***]Polytechnic of Subotica/Electrical Engineering, Szabadka, Serbia
imka26@gmail.com, szentea@npp.hu, odry@appl-dsp.com

Abstract—*Thermopile technology enables us to convert the waste heat to useful electricity. This article is going to deal with two applications of the thermoelectric generators. Firstly we are going to overview the current state in the field of battery charging using the heat from the exhaust pipe in automobiles and to choose the right TEG module to ensuring the energy supply for the cooling system of nuclear plants in a case of natural disaster, or any system failure.*

INTRODUCTION

Thermoelectric generators (TEG) could be used in the near future in many industrial applications ranging from solar energy applications and automotive industry to nuclear power production and several other fields of engineering. Application of thermoelectric generators to recover wasted heat from the exhaust system of an automobile could be a promising utilization of the thermoelectric technology to improve the efficiency of an internal combustion engine. Currently this area is a rapidly evolving segment of the application of TEG technology.

On the other hand the safety applications of the thermoelectric generators is huge. In case of a natural disaster the nuclear plant shuts down, but the decay heat continues to elevate the temperature in the plant. Without the cooling system the plant is going to explode. It is possible to build a safety net with TEG modules to keep the temperature under a critical value for a few days for the help to arrive.

Thermoelectric generators (TEGs) allow direct conversion of heat energy to electricity without any moving parts and have advantages such as durability and maintenance-free and noiseless operation.

The thermoelectric generator is a semiconductor device which is governed by the following physical effects that describe the heat flow inside a thermoelectric generator. These are the Seebeck effect, Fourier effect, Joule effect and the Thomson effect. Generally the simplest mathematical description of the energy conservation of a TEG element can be modeled by one dimensional heat transfer and electrical current flow process.

Zorbas *et al.* [1] developed a model for the evaluation of the performance of a thermoelectric generator. The developed model takes into account the thermal contact resistant effect and also the thermal resistance of the applied ceramic plates of the TEG. The model has been applied to describe the behavior of a commercial TEG which has been tested in an exhaust system of a gasoline engine. Carmo *et al.* [2] presents a characterization of thermoelectric generators by measuring the load dependent behavior. The investigation has been carried out for modest temperature differences ($\Delta T<=51$). Waste heat recovery of a low cost thermoelectric generator for a stove investigated by Nuwayhid *et al.* [3]. They have studied an alternative electric power supply from a wood or petroleum heated stove in regions where the constant electric power supply cannot be achieved. F. Meng *et al.* [4] developed a complete numerical model with inner and external multi-irreversibilities of commercial thermoelectric generator in which physical properties, geometric dimensions, and flow parameters are all considered. It has been concluded that the main loss among the losses caused by inner effects is the Fourier heat leakage. The impact of the Thomson effect has been investigated by Chen *et al.* [5]. The thermal behavior and cooling power of three different TECMs have been investigated numerically with the aim to recognize the performance of miniature TEC in the presence\absence of Thomson effect.

Currently the following semiconductor material pairs have been investigated most widely, these are the BiTe, PbTe and SiGe semiconductor materials which can be operated efficiently in different temperature range. Higher the temperature more efficient the TEG device to produce electricity but there is an upper temperature limit where the materials melt. Table I. contains the approximate upper limit temperature and the thermal efficiency of the semiconductor material pairs by Schaevitz [10].

TABLE I.

TEMPERATURE UPPER LIMIT AND THE THERMAL EFFICIENCY OF THE SEMICONDUCTOR MATERIAL PAIRS

Material pair	Temperature limit [ºC]	Efficiency [%]
BiTe	300	6
PbTe	600	9
SiGe	1100	11.5

In addition to this the approximate temperature distribution of an exhaust system of automobiles are needed to calculate a good estimation of the electrical power harvested by thermoelectric generators. Temperature of the different location of the exhaust system has been measured by Gonzales [6] to test the ignition capability of different diesel engine driven vehicles for forest fuels. Characteristic temperatures have

been measured at different locations of the exhaust system which is significantly differs from a common gasoline engine driven vehicle.

The aim of this study is to present a comparison of the efficiency of different commercially available TEG modules applying in the exhaust system of different diesel or gasoline engine automobile.

Table 1 contains the studied thermoelectric modules all of them commercially available. The table shows the geometric dimension of the TEG modules, the maximum tested temperature differences between the cold and hot side of the TEG, and the produced maximum electrical power.

TABLE II.
THERMOELECTRIC MODULES OF THEM COMMERCIAL USE

Module name	Dimensions	ΔT [ºC]	P_{max} [W]
TEC1-12707	40 mm x 40 mm	51	0.5
TEC1-12708	40 mm x 40 mm	68	0.85
Melcor HT9-3-25 Bi2Te3 N=31	25 mm x 25 mm	190	2.5
		61	0.4
Melcor HT6-12-40 Bi2Te3	40 mm x 40 mm	68	0.75

TEMPERATURE DISTRIBUTION OF TYPICAL EXHAUST SYSTEMS

Recent progress in thermoelectric device technology has revealed the possibility of practical large-scale TEGs and various applications such as vehicles and microelectronic devices.

This is especially interesting with the vehicles on diesel drive like cars and boats. Application of the thermopile technology reduces overall diesel consumption. By applying the thermopile technology it is possible to cover energy costs for eg light and computer systems etc. This way it isn't necessary to use the diesel generator because dissipated thermo energy can be converted to electricity.

The four following potential sources are recoverable by a thermoelectric generator on a long-haul truck Diesel engine [7]:

– Coolant water (between 90_C and 110_C);
– Exhaust gases (between 250_C and 350_C, Fig. 1b);
– Exhaust gas recirculation (EGR) gases (between 400_C and 500_C, Fig. 1a);
– Charge air cooler outlet gases (CAC) (usually around 150_C).

Exergy calculations show that the most energy can be extracted from exhaust gases. Despite the lower exhaust gas temperature (due to temperature loss in the turbocompressor) compared with the EGR temperature, exhaust gases exhibit a higher mass flow rate, which increases their exergy (available recovery).

Thermoelectric generators utilizing as a source of heat the exhaust gas from internal combustion engines mounted in vehicles, primarily automobiles, are well known. It should be noted, however, that the requirements imposed on such generators are rather complex and diverse. They must be compact, lightweight, and able to endure heavy vibration during transport. Furthermore, thermoelectric generators for such applications must operate efficiently in different engine operating modes, which entails additional difficulties.

The temperature distribution of the exhaust system of the automobiles depends on the engine type. An approximate temperature distribution of a gasoline fueled automobile (BMW 318i) with two different operating modes (full and a usual or averaged load) can be seen in

Figure 1 shows the structure of the Exhaust system in one diesel drive car, with marked points of the thermo energy dissipation area like Diesel Oxidizing Catalyst, Diesel Particulate Filter and Exhaust Cooler.

This construction allows effective application of the thermopile technology on larger surface.
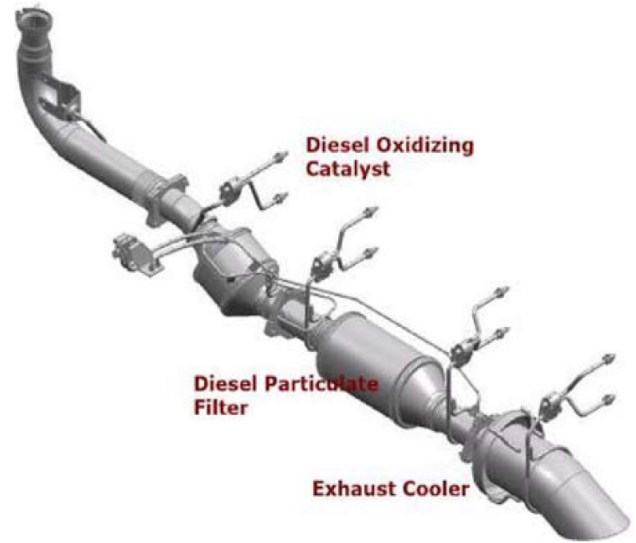
Figure 1. An approximate temperature distribution of a gasoline fueled automobile (BMW 318i) with two different operating modes

Figure 2 from qualitative point of view the temperature of the exhaust system is monotonically decreasing along the exhaust pipe from the engine toward the tail of the pipe.

The use of thermoelectric materials in vehicular engines for wasted heat recovery, can help considerably in the world need for energy saving and reduction of pollutants.

The allocated power and the temperatures that prevail in the exhaust pipe of an intermediate size car are satisfactory enough for the efficient application of a thermoelectric device. The most advisable place appears to be precisely after the catalyst, where high temperatures prevail. The output power and the efficiency of the device depend on the operational situation of the engine and on the effective designing of the heat exchanger.

Each TE element experiences a small temperature difference, so that greater surface area will improve performance. As the system is fully scalable and modular, different layouts can be designed for specific needs such as optimized electrical output, power density, and size. Heat pipes are one solution for carriage of heat to TEMs, providing a large heating area that can support many modules.
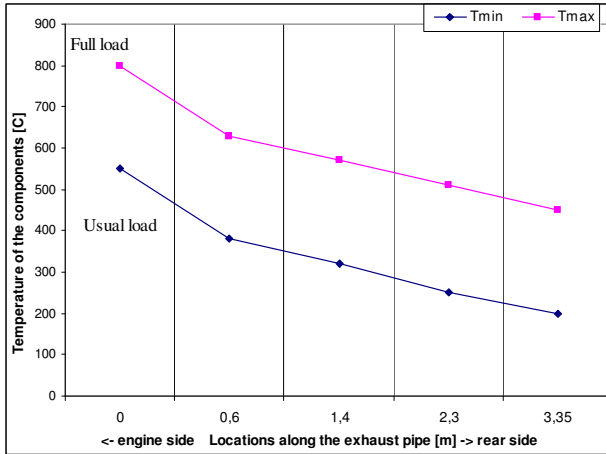
Figure 2. An approximate temperature distribution of a gasoline fueled automobile (BMW 318i) with two different operating modes

The temperature distribution of a diesel engine automobile is different compared to a gasoline fueled automobile because of the additional equipments (Diesel Particulate Filter DPF, Diesel Oxidizing Catalyst DOC). On smaller vehicles the DPF should be active (additionally fueled) equipment which further increases the temperature of the exhaust system around and after the DPF. Generally the highest temperatures occurred after the DPF [6]. This information is important to designers to specify the best location of the TEG modules to convert as much wasted heat as possible to electricity. Table 2 shows the temperature distribution of the exhaust system of smaller sized diesel engine trucks.

TABLE III.
TEMPERATURE DISTRIBUTION OF THE EXHAUST SYSTEM

Location	Ford	Dodge	Sterling	GMC
Diesel Particulate Filter DPF	295	168	196	307
After DPF	375	300	293	446
Before DOC	231	193	241	435
Diesel Oxidizing Catalyst DOC	356	218	228	308

It can be clearly seen from Figure 3 that the generated electrical power is strongly depend on the location of the thermocouples because the temperature of the exhaust system is varying along the different components.

In the same operating environment the TEG modules give a slightly better performance in case of electrical power production than the other modules. But the reliability of the modules have not been tested which is also an important factor of the practical applications.

III. COMMERTIALLY AWAILABLE TEG MODULES FOR NUCLEAR PLANTS

In case of a natural disaster the reason for the nuclear plant explosion is the lack of cooling. The cooling system gets cut from the electricity so the decay heat can further increase the temperature, resulting in an explosion. [10]

There is a theoretical solution, which requires further examination. In this theoretical solution TEG modules could be used on the primary circle for generating power

to the cooling system, resulting in a safety net for extreme instances.

In case of a power plant the upper temperature limit is around 300 °C. Because of this the material of the examined TEG module is BiTe. There are however new hybrid units on the market, which have more power output on the same temperature difference. [12]

Hot Side Temperature (°C)	350	Hot Side Temperature (°C)	300
Cold Side Temperature (°C)	30	Cold Side Temperature (°C)	30
Open Circuit Voltage (V)	9.2	Open Circuit Voltage (V)	8.4
Matched Load Resistance (ohms)	0.97	Matched Load Resistance (ohms)	1.2
Matched Load Output Voltage (V)	4.6	Matched load output voltage (V)	4.2
Matched Load Output Current (A)	4.7	Matched load output current (A)	3.4
Matched Load Output Power (W)	21.7	Matched load output power (W)	14.6
Heat Flow Across the Module (W)	≈310	Heat flow across the module(W)	≈ 365
Heat Flow Density (W cm^{-2})	≈9.88	Heat flow density(Wcm^{-2})	≈ 11.6
AC Resistance (ohms) Measured under 27 °C @ 1000 Hz	0.42~0.52	AC Resistance(ohms) Measured under 27 °C at 1000Hz	0.5~0.7

Figure 3. Difference between two commercially available TEG modules

On the Figure above we can see the comparison between a two commercially available modules, the TEG1-PB hybrid module and the TEG1-12611-6.0 module. The hybrid module gives more power in almost the same temperature difference. [11]
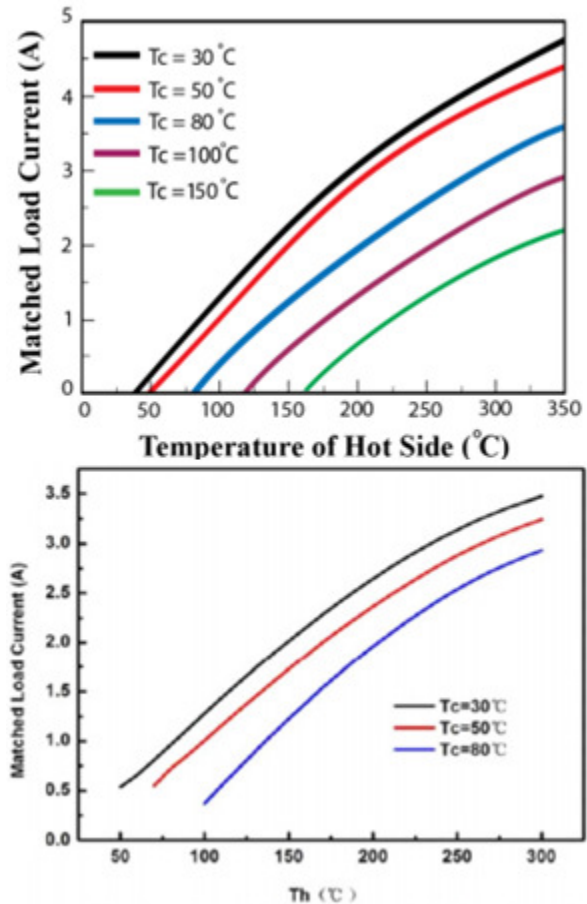
Figure 4. Matched load current comparison between the two modules

In Figure 4 we can see the difference in the matched load current of the two modules.
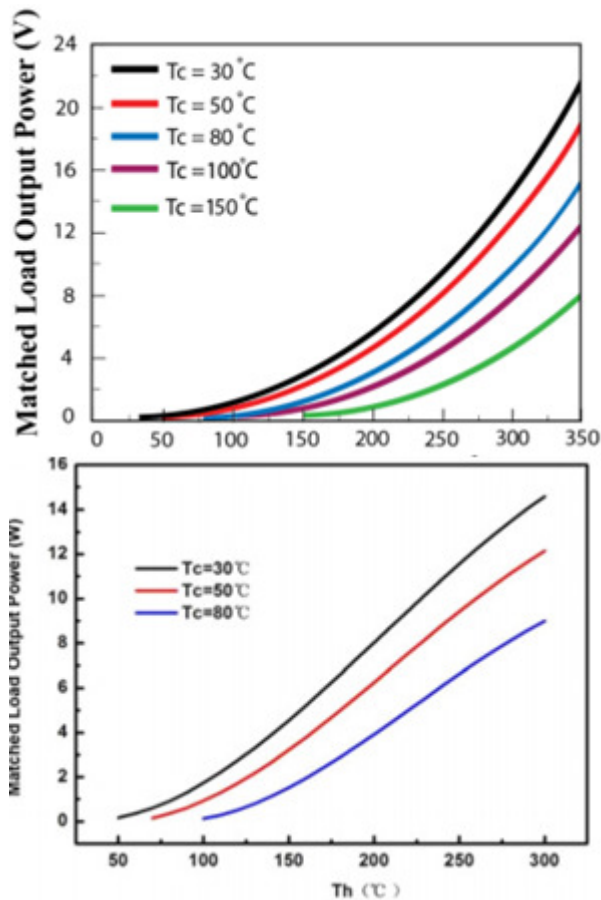
Figure 5. Matched load power output comparison between the two TEG modules

As we can see from the diagrams given by the manufacturers the hybrid module has a slightly better performance in the same temperature difference.

CONCLUSION

In the same operating environment the Melcor modules give a slightly better performance in case of electrical power production than the other modules. But the reliability of the modules have not been tested which is also an important factor of the practical applications.

The data presented in the tables clearly indicates that even with today's thermopile technology we have means to cover part of the electrical consumption in automobiles. On the other hand, at present it is only justified to use the thermopile technology in the vehicles with greater fuel consumption. With further development of the new types of the TEG converters it will became more and more economical to install the thermopile technology in the vehicles with small diesel consumption.
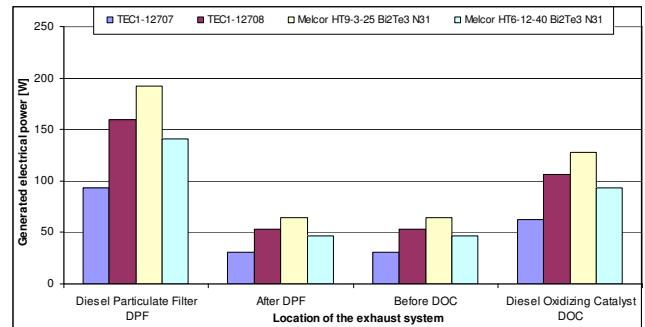
Figure 3. The influence of the position TEG generator on the amount of the generated electrical power

Based on the data given by the manufacturers the most efficient TEG modules are the hybrid modules, particularly the PB-1261-6.0.

REFERENCES

K. T. Zorbas, E. Hatzikraniotis, K. M. Paraskevopoulos, Power and efficiency calculation in commercial TEG and application in wasted heat recovery in automobile.

J.P. Carmo, J. Antunes, M.F. Silva, J.F. Riberio, L.M. Goncalves, J.H. Correia, Characterization of thermoelectric generators by measuring the load-dependence behavior, *Measurement* 44, (2011), 2194-2199.

R.Y. Nuwayhid, D.M. Rowe, G. Min, Low cost stove-top thermoelectric generator for regions with unreliable electricity supply, Renewable Energy 28, (2003), 205-222.

Fankai Meng, Lingen Chen, Fengrui Sun, Numerical model and comparative investigation of a thermoelectric generator with multi-irreversibilities, *Energy*, 36, (2011) 3513-3522.

Wei-Hsin Chen, Chen-Yeh Liao, Chen-I Hung, A numerical study on the performance of miniature thermoelectric cooler affected by Thomson effect, Applied Energy, 89, (2012) 464-473.

Ralph H. Gonzales, Diesel exhaust emission system temperature test, San Dimas Technology & Development Center, San Dimas, California, December 2008.

N.ESPINOSA, M.LAZARD, L.AIXALA, H.SCHERRER: "Modeling a Thermoelectric Generator Applied to Diesel Automotive Heat Recovery" Journal of ELECTRONIC MATERIALS, Vol. 39, No. 9, 2010 pp: 1446-1455

MOLAN LI, SHAOHUI XU, QIANG CHEN, LI-RONG ZHENG: "Thermoelectric-Generator-Based DC–DC Conversion Networks for Automotive Applications" Journal of ELECTRONIC MATERIALS, Vol. 40, No. 5, 2011, pp: 1136-1143

HIROSHI NAGAYOSHI, TATSUYA NAKABAYASHI, HIROSHI MAIWA, TAKENOBU KAJIKAWA: "Development of 100-W High-Efficiency MPPT Power Conditioner and Evaluation of TEG System with Battery Load" Journal of ELECTRONIC MATERIALS, Vol. 40, No. 5, 2011 pp: 657-661

S. B. Schaevitz, A MEMS Thermoelectric generators, Master Thesis, MIT, September 2000.

[10] M. Ragheb (22 March 2011). *"Decay Heat Generation in Fission Reactors"*. University of Illinois at Urbana-Champaign. *Retrieved 26 January 2013*

[11] www.tecteg.com

[12] ANDREAS BITSCHI Diss. ETH No. 18441, Modelling of thermoelectric devices for electric power generation, Technical University of Vienna

[13] J. Nyers, A. Nyers: "COP of Heating-Cooling System with Heat Pump" IEEE International Symposium "EXPRES 2011." Proceedings, ISBN 978-1-4577-0095-8, pp.17-21, Subotica, Serbia. 11-12 03. 2011.
*

Steady-state Mathematical Model of the Liquid-Suction Heat Exchanger of Heat Pump with R134a

Jozsef Nyers[*], Daniel Stuparic[**], Dorottya Boros[**]
[*]University Obuda, Budapest Hungary
[**]BME, Budapest Hungary
nyers@uni-obuda.hu

Absrtract – **This paper presents a stationary mathematical model of the liquid-suction heat exchanger of the heat pump with the concentrated state variables. Model contains the basic equations based on the heat balance and auxiliary equations for heat transfer of the superheated vapor and condensate as well as the state equation for the refrigerant. The model is solved analytically and numerically the obtained numerical results are presented graphically. The main objective was to analyze the obtained heat flow between the condensate and the superheated vapor as a function of the refrigerant mass flow rate. An additional objective was to determine the outlet temperature of the condensate and superheated vapor.**

INTRODUCTION

For heating systems with the heat pump the energy efficiency plays a very important role. Energy efficiency of the heating system increases with decreasing the temperature of water in the heating loop, it can achieve with increasing the surface of heaters. Large heating surface is possible to form in the panels for example primarily in the floor then in the wall and in the ceiling. However often in the application are radiators and fan-coils with the smaller heating surface. Due to the reduced heating surface, heating water temperature increases and as consequence reduces the energy efficiency, i.e. COP.

Some compensation of the COP deterioration can be achieved by applying liquid-suction exchanger. The liquid-suction exchanger is more effective when the temperature of the heating water increases. The heat pump with CO_2 refrigerant without liquid-suction exchanger cannot function. Besides the benefits liquid-suction exchanger has drawbacks: 1. Vapor temperature after compression can achieve a very high value 2. High temperature of vapor has a practical limit. 3. The temperature limit of the superheated vapor limits the sub cooling of the condensate. 4. Use of the liquid-suction heat exchanger may cause oscillations in the flow of the refrigerant. Regulator, TEV can become unstable.

The main goal of this research is to determine and examine the heat flux between the condensate and superheated vapor depending on the mass flow rate of the refrigerant. Additional aim is to determine the outlet temperature of the condensate and the superheated vapor.

PHYSICAL MODEL

The considered physical system consists of evaporator, condenser, compressor, controller TEV, and liquid-suction heat exchanger. Practically, the traditional refrigerating machine is expanded with the liquid-suction exchanger. In liquid-suction heat exchanger is exchanged the heat between the condensate and superheated vapor. The aim is to the optimum level sub cool the condensate.
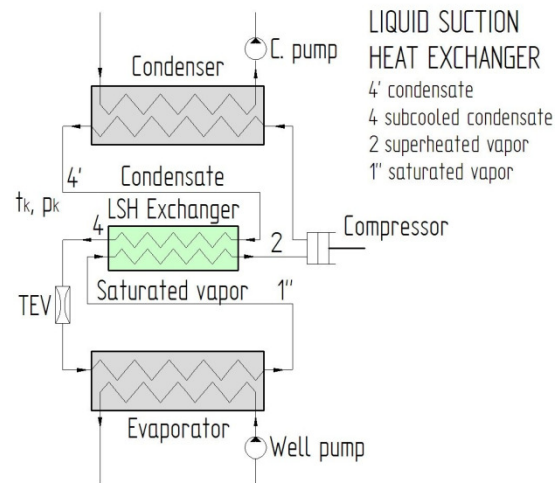
Figure 1. Physical model of the heat pump with liquid-suction exchanger
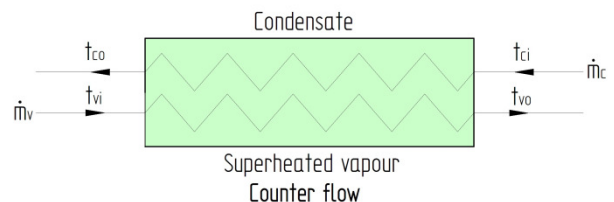
Figure 2. Physical model of the liquid-suction exchanger with variables

PROCESS IN THE STATE DIAGRAM

In the state diagram, logp-i, of the refrigerant R134a exactly can see quantity and location of the heat transfer between the sub-cooled condensate and superheated refrigerant vapor. The aim of the condensate sub-cooling is the COP improvement of the heat pump. The lack of the process is beside increases the COP after compression increases the superheated vapor temperature, as well.

Between the state of 4'-4 takes place sub-cooling of condensate, while between 1 "-2 superheating of the refrigerant vapor.
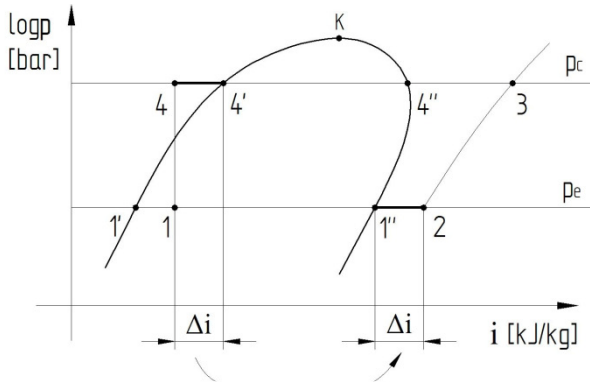
Figure 3. Liquid-suction process in logp-i diagram

MATHEMATICAL MODEL

Introduction

A mathematical model was created for the steady-state regime of the heat pump. The equations in the model are algebraic with lumped parameters and variables. The governing equations were derived based on the heat balance for the condensate, the superheated vapor and for the heat flux through the wall of the plate exchanger. Auxiliary equations are: coefficient of convective and conductive heat transfer, specific heat and dynamic viscosity of the condensate and vapor. The accuracy of the obtained results largely depends on the accuracy of the model for the convective heat transfer coefficient.

Governing equations

By governing equations is determined the heat flux of the condensate, through the exchanger wall on the superheated vapor.

At the steady-state operation mode the heat flux is constant through the each layer.

$$q = q_v = q_w = q_c$$

(1)

Heat flux of the refrigerant superheated vapor

$$q = C_{pv} \cdot \dot{m}_v \cdot (t_{vo} - t_{vi})$$

(2)

Heat flux through the exchanger's wall

$$q = k \cdot F \cdot \Delta t_{ln}$$

(3)

Heat flux of the refrigerant condensate

$$q = C_{pc} \cdot \dot{m}_c \cdot (t_{ci} - t_{co})$$

(4)

In case of the steady-state operation mode the mass flow rate is constant that means the mass flow rate of the condensate and the superheated vapor is equal.

$$\dot{m} = \dot{m}_c = \dot{m}_v$$

(5)

Auxiliary equations

The logarithmic temperature difference in the case of the parallel flow

$$\Delta t_{ln,v} = \frac{(t_{ci} - t_{vi}) - (t_{co} - t_{vo})}{ln[(t_{ci} - t_{vi})/(t_{co} - t_{vo})]}$$

(6)

The logarithmic temperature difference in the case of the counter flow

$$\Delta t_{ln,c} = \frac{(t_{ci} - t_{vo}) - (t_{co} - t_{vi})}{ln[(t_{ci} - t_{vo})/(t_{co} - t_{vi})]}$$

(7)

The overall heat transfer coefficient

The wall of the plate heat exchanger is usually of the steel and very thin only 0.3-0.4 mm for this reason the thermal resistance can be neglected.

$$k \cong \frac{\alpha_v \cdot \alpha_c}{(\alpha_v + \alpha_c)}$$

(8)

Heat transfer coefficient of the condensate and the vapor for the plate heat exchangers from Holger Martin [7] is.

$$\alpha_{c,v} = 0.205 \cdot \frac{\lambda_{c,v}}{d_{ekv}} \cdot f_{vis} \cdot Re^2_{ekv,c,v} \cdot sin2\beta \cdot Pr_{c,v}^{1/3}$$

(9)

Where:

• Reynolds number of the one channel is.

$$Re_{ekv,c,v} = \frac{d_{ekv} \cdot \dot{m}_{ekv}}{\eta_{c,v}}$$

(10)

• Equivalent mass flow rate in the one channel

$$\dot{m}_{ekv} = \dot{m} / (0.5 \cdot n \cdot A) \cdot$$

(11)

• Hydraulic diameter of the channel suggested by Shah and Wanniarachchi , d_{ekv}, is defined as

$$d_{ekv} = 2 \cdot b$$

(12)

• Mean channel spacing, b, is defined as the pitch, *p*, minus thickness of the plate, *t*.

$$b = p - t$$

• β - angle of the chevron
• f_vis- Fanning friction factor

• Prandtl number

$$Pr_{c,v} = \frac{\eta_{c,v} \cdot C_{p_{c,v}}}{\lambda_{c,v}}$$

(13)

Surface of the liquid-suction plate heat exchanger

$$F = L \cdot B \cdot n$$

(14)

Channel flow area is determined as the mean channel spacing, *b,* multiplied by width, *B*.

$$A = b \cdot B$$

(15)

Physical parameters of the refrigerant R 134a [2]

The temperatures conversion from [°C] to [K].

$$T_{ci} = t_{ci} + 273.15 [K]$$
$$T_{vi} = t_{vi} + 273.15 [K]$$

(16)

Coefficient of the saturated-liquid thermal conductivity

$$\lambda_c = 2,1099 \cdot 10^{-1} - 3.9431 \cdot 10^{-4} \cdot T_{ci} - 1.2983 \cdot 10^{-7} \cdot T_{ci}^2 [W/m^2K]$$

(17)

Coefficient of the saturated-vapor thermal conductivity

$$\lambda_v = -9.7578 \cdot 10^{-2} + 1.0504 \cdot 10^{-3} \cdot T_{vi} - 3.6079 \cdot 10^{-6} \cdot T_{vi}^2 - 4.4965 \cdot 10^{-9} \cdot T_{vi}^3 [W/m^2K]$$

(18)

Specific heat of the saturated-vapor
(R134a from -10C to +76C)

$$C_{p,v} = 10^3 \cdot (1.32414229572 - 0.0141445706134 \cdot t_{vi})^{-1/2.42033191871} \; [J/kgK]$$

(19)

Specific heat of the saturated-liquid valid for
(R134a from -10C to +76C)
$$C_{p,c} = 10^3 \cdot (0.228875401689 - 0.00254596034689 \cdot t_{ci})^{-1/5.02398498631} \; [J/kgK]$$

(20)

Coefficient of the dynamic viscosity of saturated-liquid, valid for (R134a from 260 K to 350 K)
$$\eta_c = 10^{-6} \cdot (5.09945402169 \cdot 10^3 - 39.8934446413 \cdot T_{ci} + 0.110393778874 \cdot T_{ci}^2 - 1.06441629968 \cdot 10^{-4} \cdot T_{ci}^3) \; [Pa \cdot s]$$

(21)

Coefficient of the dynamic viscosity of saturated-vapor, valid for (R134a from 260 K to 350 K)
$$\eta_v = 10^{-6} \cdot (-1.45311377254 \cdot 10^2 + 1.56986671388 \cdot T_{vi} - 5.36538485646 \cdot 10^{-3} \cdot T_{vi}^2 + 6.26125027795 \cdot 10^{-6} \cdot T_{vi}^3) \; [Pa \cdot s]$$

(22)

ANALITICAL PROCEDURE

Analytical solution of the governing equations is possible only with approximation of the logarithmic temperature difference to the arithmetic mean value. Deviation due to approximation is only 2-3%, because during the heat transfer the temperature variation is slightly nonlinear.

The arithmetic mean value of the parallel and counter flow is:

Parallel flow.

$$\Delta t_{lnp} \cong \frac{[\Delta t_{max} + \Delta t_{min}]}{2} = $$
$$= 1/2 \cdot [(t_{ci} - t_{vi}) + (t_{co} - t_{vo})] = $$
$$= 1/2 \cdot (t_{ci} + t_{co} - t_{vi} - t_{vo})$$

(23)

Counter flow.

$$\Delta t_{lnc} \cong \frac{[\Delta t_{max} + \Delta t_{min}]}{2} = $$
$$= 1/2 \cdot [(t_{ci} - t_{vo}) + (t_{co} - t_{vi})] = $$
$$= 1/2 \cdot (t_{ci} + t_{co} - t_{vi} - t_{vo})$$

(24)

It can be seen, the arithmetic mean value of the parallel and the counter flow exactly the same. The known i.e. the input independent variables are the input temperature of the condensate and superheated refrigerant vapor. The unknown i.e. the output temperature can be expressed as a function of the known input temperature and replace them in the relation of the arithmetic temperature difference.

Using the equation (1) can be obtained outlet temperature of the superheated vapor.

$$t_{vo} = t_{vi} + \frac{q}{C_{p,v} \cdot \dot{m}_v}$$

(25)

Using the equation (3) can be obtained outlet temperature of the condensate.

$$t_{co} = t_{ci} - \frac{q}{C_{p,c} \cdot \dot{m}_c}$$

(26)

Substituting the terms of the outlet temperatures (25), (26) and the arithmetic temperature difference (24) in the equation (2), the heat flux through the exchanger wall is obtained as a function of the input-known temperatures.

$$q = k \cdot F \cdot \Delta t_{ln} \cong k \cdot F \cdot 1/2 \cdot (t_{ci} + t_{co} - t_{vi} - t_{vo})$$

$$q \cong k \cdot F \cdot \frac{1}{2} \cdot (t_{ci} + t_{ci} - \frac{q}{C_{pc} \cdot \dot{m}_c} - t_{vi} - t_{vi} - \frac{q}{C_{pv} \cdot \dot{m}_v})$$

$$2 \cdot \frac{q}{k \cdot F} + \frac{q}{C_{pc} \cdot \dot{m}_c} + \frac{q}{C_{pv} \cdot \dot{m}_v} \cong 2 \cdot (t_{ci} - t_{vi})$$

(27)

Because of steady-state regime the mass flow rate is constant and shares by channels. Channels number of the condensate and vapor side is same, fifty-fifty of the total number of channels n/2. In an ideal case, by the same ratio is divided the mass flow rate.

$$\dot{m}_c = \dot{m}_v = \dot{m}$$

(28)

The analytical relation of the heat flux in the final form is.

$$q \cong 2 \cdot (t_{ci} - t_{vi}) \cdot \left(\frac{2}{k \cdot F} + \frac{1}{C_{pc} \cdot \dot{m}} + \frac{1}{C_{pv} \cdot \dot{m}} \right)^{-1}$$

(29)

NUMERICAL PROCEDURE

Introduction

Mathematical model of the liquid-suction heat exchanger contains coupled, nonlinear, explicit and implicit algebraic equations. Analytical approximate solution is possible only by negligence. Without negligence, to obtain the solution is possible only numerically applying one of the numerical methods from mathematical software package "Matlab".

Variables analyzes

Independent variables in the considered system are the input temperature of the condensate, *(t_{ci})*, and the saturated vapor, *(t_{vi})*, heat exchanger surface area, *(F)* or number of plat , and the mass flow rate of the refrigerant, *(ṁ)*.

Dependent variables are condensate output temperature, *(t_{co})*, and the superheated vapor temperature, *(t_{vo})*.

CASE STUDY

The behavior simulation of the liquid-suction heat exchanger was performed by applying the presented mathematical model with the following data.

Input data i.e. independent variables:
- Refrigerant is R134a
- Input temperature of the condensate t_{ci} = 50; 60 [°C]
- Input temperature of the superheated vapor t_{vi} = 0 °C
- mass flow rate of the refrigerant ṁ = 0.01; 0.02; 0.03 [kg/s]

Physical parameters of the plate heat exchanger:
- Length, L = 470 mm
- Width, B = 115 mm
- Number of plate, n = 2; 4; 6; 8; 10.
- Plate thickness t = 0.4 mm

- Mean channel spacing b = 2 mm

Physical parameters of the R134a:
- Coefficient of the saturated-liquid thermal conductivity (17)
- Coefficient of the saturated-vapor thermal conductivity (18)
- Specific heat of the saturated-vapor (19)
- Specific heat of the saturated-liquid valid for (20)
- Coefficient of the dynamic viscosity of saturated-liquid, valid for (R134a from 260 K to 350 K) (21)
- Coefficient of the dynamic viscosity of saturated-vapor, valid for (R134a from 260 K to 350 K) (22).

Remarks:

The specific heat of the sub-cooled condensate or of the superheated vapor, C_p, is calculated using the correlations of the saturated condensate or of the superheated vapor. Due to approximation the maximum deviation is less as 1%.

Output data i.e. dependent variables:
- Condensate outlet temperature, t_{co},
- Outlet temperature saturated vapor, t_{vo},
- Heat flux, q.

Output data may be as a function of the exchanger's surface, refrigerant mass flow rate, inlet temperature of the condensate and the superheated vapor.

VIII RESULTS
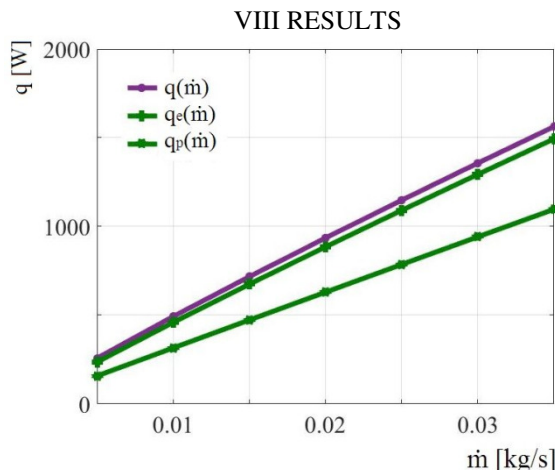
Figure 4. Heat transfer variation as a function of the refrigerant mass flow rate. q(m)-arithmetic model, q_e(m)-parallel flow, q_p(m)-counter flow by use the logarithmic model.

CONCLUSION

In the paper is presented a stationary lumped parameters mathematical model for describing the behavior of heat liquid-suction exchangers in the heat pump. The model is solved analytically and numerically. Numerical solution has been done, for parallel and counter flow of condensate and superheated vapor. Analytical solution is obtained by approximating the logarithmic with the arithmetic temperature difference. Correlation is not different for parallel and the counter flow because in this case the arithmetic mean temperature difference is same for both flows.

Numerically obtained simulation results show that:
• The results of analytical model are closer to the results obtained using the counter- than parallel flow numerical model.
• The choice of the surface size of the liquid-suction heat exchangers, possible to set the desired output temperature of the superheated vapor. Figure 4.
• As an alternative solution of the temperature regulation is applying the by-pass for regulating the mass flow of the condensate or the superheated vapor.
• The outlet temperature of the superheated vapor is limited by the outlet temperature of the superheated vapor after compression.

REFERENCES

A. Laesecke, R.A. Perkins, and C.A. Nieto de Castrob:" Thermal, conductivity of R134a" Fluid Phase Equilibrium, 80 (1992) pp. 263-274, Elsmier Science publishers B.V., Amsterdam.

Du Point's thermodynamic properties of the R134a, http://www.pfri.uniri.hr/~pkralj/R134a_thermo_prop_si.pdf.

Scalabrina and P. Marchi: "A Reference Multi parameter Viscosity Equation for 134a with an Optimized Functional Form". J. Phys. Chem. Ref. Data, Vol. 35, No. 2, 2006. pp 839-868.

P. A. Domanski, D. A. Didion and J. P. Doyle: "Evaluation of Suction Line-Liquid Line Heat Exchanger in the Refrigeration Cycle" International Refrigeration and Air Conditioning Conference 1992. Purdue University Purdue e-Pubs.

R.K. Shah, A.S. Wanniarachchi: Plate heat exchanger design theory in industry heat exchanger in: J.-M. Buchlin (Ed). Lecture Series, No 1991-04. Von Karman Institute for Fluid Dynamics, Belgium, 1992

Daniel Walraven, Ben Laenen and William D'haeseleer: Comparison of shell-and-tube with plate heat exchangers for the use in low-temperature organic Rankine cycles. Energy Conversion and Management, Volume 87, November 2014, Pages 227–237.

H. Martin, A theoretical approach to predict the performance of chevron-type plate heat exchangers, Chemical Engineering and Processing 35 (4) (1996) 301{310.

Pavlovic, S., Stefanovic, V., Suljkovic S., Optical Modeling of Solar Dish Thermal Concentrator Based on Square Flat Facets, Thermal Science 2014, 989-998.

László Kajtár, Miklós Kassai, László Bánhidi: Computerised simulation of the energy consumption of air handling units. 2011. Energy and Buildings, ISSN: 0378-7788, (45) pp. 54-59.

Saša R. Pavlovic, Velimir P. Stefanović , Dragan Kuštrimović: Review of Heat Transfer Fluids for Concentrating Solar Collectors. "EXPRES 2014 VTS." Subotica. Serbia, 2014. pp. 90-96. ISBN 978-86-85409-96-7.

Kajtár L., Hrustinszky T.: Investigation and influence of indoor air quality on energy demand of office buildings. WSEAS Transactions on Heat and Mass Transfer, Issue 4, Volume 3, October 2008. 219-228 p.

M. Kassai, C. J. Simonson, "Performance investigation of liquid-to-air membrane energy exchanger under low solution/air heat capacity rates ratio conditions," *Building Services Engineering Research & Technology*. vol. 36. n. 5. pp. 535-545, 2015.

T. Poós, M. Örvös, L. (2013) Legeza Development and Thermal Modeling of a New Construction Biomass Dryer, DRYING TECHNOLOGY 31:(16) pp. 1919-1929.

K. Dabis, Z. Szánthó: Control of Domestic Hot Water production is instantaneous heating system with a speed controlled pump, 6th International symposium "EXPRES 2014 VTS." Subotica. Serbia, 2014. pp. 101-106. ISBN 978-86-85409-96-7.

Balázs Both, Zoltán Szánthó, Róbert Goda: "Numerical investigation of offset jet attaching to a wall". EXPRES 2015. Subotica. Serbia, 2015. pp. 70-73. ISBN 978-86-82621-15-7

Mária Kurcová: The effect of thermal insulation of an apartment house on thermo-hydraulic stability of the space heating system. EXPRES 2015. Subotica. Serbia, 2015. pp. 88-91. ISBN 978-86-82621-15-7

Ferenc Kalmár, Sándor Hámori: Investigation of unbalancing problems in central heating systems. EXPRES 2015. Subotica. Serbia, 2015. pp. 7-12. ISBN 978-86-82621-15-7.

Ján Takács: Enhance of the efficiency of exploitation of geothermal energy. EXPRES 2015. Subotica. Serbia, 2015. pp. 46-49. ISBN 978-86-82621-15-7.

Ferenc Kalmár, Tünde Kalmár: Alternative personalized ventilation, ENERGY AND BUILDINGS 65:(4) pp. 37-44. (2013)

Magyar Zoltán, Révai Tamás: Thermal Insulation of the Clothing 2nd Royal Hungarian Army in Winter Campaign in the Light of Thermal Manikin Measurements. ACTA POLYTECHNICA HUNGARICA 11: (7) pp. 197-207. (2014)

Magyar Zoltán, Garbai László, Jasper Andor: Risk-based determination of heat demand for central and district heating by a probability theory approach. ENERGY AND BUILDINGS 110: pp. 387-395. (2016)

Miklos Kassai, Mohammad Rafati Nasr, Carey J. Simonson: A developed procedure to predict annual heating energy by heat-and energy recovery technologies in different climate European countries. Energy and Buildings. Vol. 109, pp. 267-273, DOI:10.1016/j.enbuild.2015.10.008 (2015).

L. Šereš L., O. Grljević, S. Bošnjak, „*IT Support of Buildings Energy Efficiency Improvement*", International Conference on Energy Efficiency and Environmental Sustainability, EEES2012, Conference proceedings, ISBN: 978-86-7233-320-6, pp. 55-62.

A. Szente, I. Farkas, and P. Odry: *The application of Thermopile Technology in high Energy Nuclear Power Plants,* EXPRES 2014, pp.23-28, 2014, ISBN 978-86-85409-96-7

Ferenc Kalmár, Sándor Hámori: Investigation of unbalancing problems in central heating systems, EXPRES 2015, pp. 7-12. ISBN 978-86-82621-15-7. 2015

Füri, B.: Practical experiences with multi-compressor refrigeration systems, Proceedings of 6th International Conference on Compressors and Coolants – Compressors 2006, 27. - 29. 9. 2006, Častá – Papiernička, p. 158– 161. ISBN 80-968986-5-5

Füri, B. Švingál, J.: Some experimental results with ammonia base azeotropic refrigerant R 723 in small heat pump, p. 139 – 142. Proceedings of 7th International Conference on Compressors and Coolants – Compressors 2009, 30. 9.- 2. 10. 2009, Častá - Papiernička, ISBN: 978-80-89376-02-2

Ján Takács, Marek Bukoviansky: Utilization of Geothermal Energy for Residential Sector of the City District Galanta North. EXPRES 2014, pp.82-85, ISBN 978-86-85409-96-7, 2014.

F.E. Kiss and D. P. Petkovic: Revealing the costs of air pollution caused by coal-based electricity generation in Serbia, EXPRES 2015, pp. 96-101. ISBN 978-86-82621-15-7, 2015.

Slavica Tomic, Aleksandra Stoiljkovic: Energy efficiency as a precondition of sustainable tourism. EXPRES 2015, pp. 134-139. ISBN 978-86-82621-15-7, 2015.

A. Nagy: Determination of the Gasket Load Drop at Large Size Welding Neck Flange Joints in the Case of Nonlinear Gasket Model. Int. J. Pres. Ves. & Piping. 67 (1996) 243-248.

A. Nagy: Time Depending Characteristics of Gasket at Flange Joints. Int. J. Pres. Ves. & Piping. (1997).

[33] Nagy Károly, Divéki Szabolcs, Odry Péter, Sokola Matija, Vujicic Vladimir:"A Stochastic Approach to Fuzzy Control", I.J. Acta Polytechnica Hungarica, Vol. 9, No 6, 2012, pp. 29-48. (ISSN: 1785-8860).

Experimental Measurements with Methanol filled vertical Thermo-siphon for receiving Energy of Environment

Belo B. FÜRI,

Slovak University of Technology, Faculty of Civil Engineering, Department of Building Services, Bratislava, Slovakia
e-mail: belo.furi@stuba.sk

Abstract **- The principle of a heat pipe or vertical thermo siphon has been well-known for a long time. This type of heat pipe is known as gravity assisted heat pipe, closed two-phase thermo siphon or wickless gravity assisted heat pipe. Gravity assisted heat pipes have received considerable attention in terrestrial applications due their efficient heat transfer capability, simple construction and durability. This paper reports on experience with functional model of methanol filled vertical thermo siphon.**

I. INTRODUCTION

The "heat pipe" is as its name implies, simply a pipe through which heat passes if there is a small temperature differences between its ends. If one end of the pipe is placed in contact with a warm medium heat will be extracted from the medium and transferred to the cooler end of the pipe. It can therefore be used as means of either extracting heat from a warm medium or introducing heat into a cold medium. A functional model of methanol (CH_3OH) filled vertical thermo-siphon as a ground source for heat pumps. The experimental measurements simulated ground source at temperature level approximately + 10 °C as water bath supplied from water supply. The thermo-siphon was immersed in water bath (simulated ground source of heat at approximately by 10 °C). Arithmetic average temperature between the top and bottom of the water bath define T_b, the mean temperature of heat source for thermo-siphon. The condenser temperature T_c, was measured with thermocouple inside pipe mounted in condenser section.

Obtained heat flow in condenser was subscribed by a spiral heat exchanger connected with water supply.

The supplied heat flow in condenser is hardy depended on the temperature difference between bath and condenser section and fill ratio (FR) of methanol in thermo-siphon. The fill ratio of heat pipe is determined as the ratio of amount of liquid in the pipe to the volume of the thermo-siphon.

In our case was investigated performance of thermo-siphon at different the fluid FR (5, 10 and 15 %) experimentally. The temperature distribution along the thermo-siphon was monitored and output heat from condenser was indirectly measured.
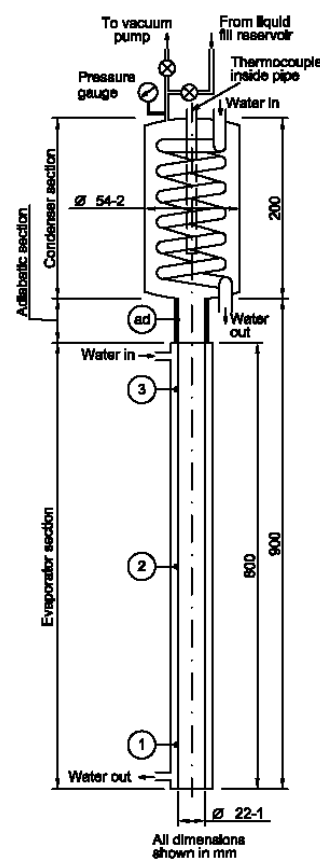
Figure 1 Experimental setup of methanol filed thermo-siphon measurements

Measurements could be conducted in which the thermo-siphon could be considered with different fill ratios. The thermo-siphon was filled with CH_3OH. Before charging the pipe, the tube was cleaned thoroughly to remove any grease or oil from the inner surface. After charging with the working fluid and confirming the absence of non-condensable gases in the tube, the thermo-siphon was set up for the experiments. Vacuuming was donning to 3 mbar vacuum pressure. Experiments were performed using different water flow rates in condenser. Condenser flow rates were supplied from domestic cold water supply. Condenser water flow, was measured using a rota meter, while inlet and outlet, temperatures of water were

measured using E type thermocouples. Data were recorded when the system reached steady-state condition.

Numerous investigations have been made to obtain the thermal performance of the wickless heat pipe or thermo-siphon [1, 2, and 3]. Water, ammonia, some refrigerants were the common working fluids investigated [1-4]. In last time were successful experiences with carbon dioxide (CO_2) thermo-siphon in conjunction with a ground source heat pump [5]. The presented investigation serves to present how a methanol-filled thermo-siphon perform. The heat pipe is a thermal device, which affords efficient transport of thermal energy by use of an intermediate heat transfer fluid. Heat pipes working under gravity with the condenser above the evaporator do not need any external power or capillary structure for return of the heat transfer fluid to the evaporator. The wickless heat pipe, which is essentially a two phase closed thermo-siphon tube, is a highly efficient device for heat transmission. It utilizes the evaporation and condensation of its internal working fluid to transport heat.

II. EXPERIMENTAL APARATUS

The experimental apparatus is shown in **Fig. 1.** It consisted of a 900 mm long x 22 mm O/D x 20 mm I/D copper tube. The thermo-siphon was immersed in a water bath as a heat exchanger. The effect of temperature difference between bath and condenser section, fill ratio and coolant mass flow rates on the performance of the thermo-siphon were determined. Various parameters affect the heat transfer performance of thermo-siphons. Conclusions have been drawn for the optimum-filling ratio (FR) at which the thermo-siphon operates best. The following calculations were carried out to determine overall heat performance of the thermo-siphon.

III. PERFORMANCE CHARACTERISTIC

For the description of condenser performance Φ_c (W) due the general equation for thermal load balance

$$\Phi_c = \dot{m}_w . c_w . (T_{out} - T_{in}) \quad (W)$$

(1)

where $\dot{m}_w$ (kg/s) is the mass flow of water (measured and adjusted quantity),

c_w $(J/(kg.K))$ - specific heat capacity of water,

$T_{out}(K) = \theta_{out}(°C) + 273{,}15$ - arise water temperature (measured parameter) and

$T_{in}(K) = \theta_{in}(°C) + 273{,}15$ - entry water temperature (measured parameter).

Likewise it is possible definition of specific performance for whole of condenser dividing condenser performance Φ (W) with surface of evaporation section of heat pipe

$$\phi = \frac{\Phi}{S_{es}} \quad (W/m^2)$$

(2)

where S_{es} (m^2) is the surface evaporation section of heat pipe.
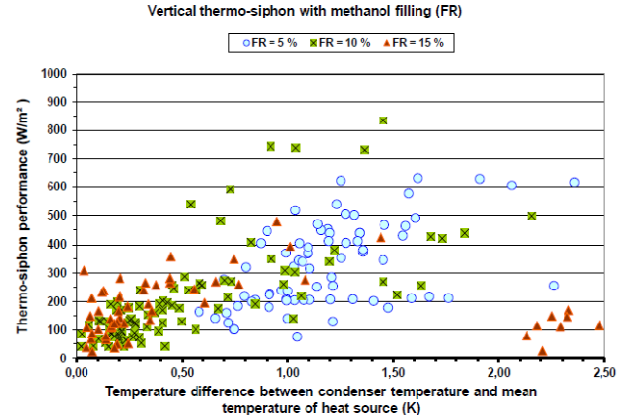
Figure 2 **Overall performance characteristic for CH₃OH filled thermosyphon**
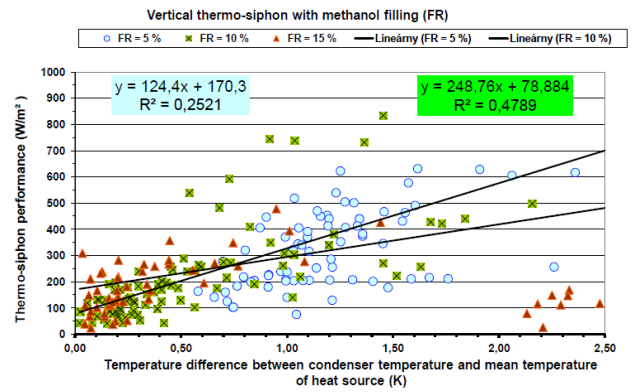
Figure 3 **Approximation of performance data at different fill ratios of CH₃OH filled thermo siphon**
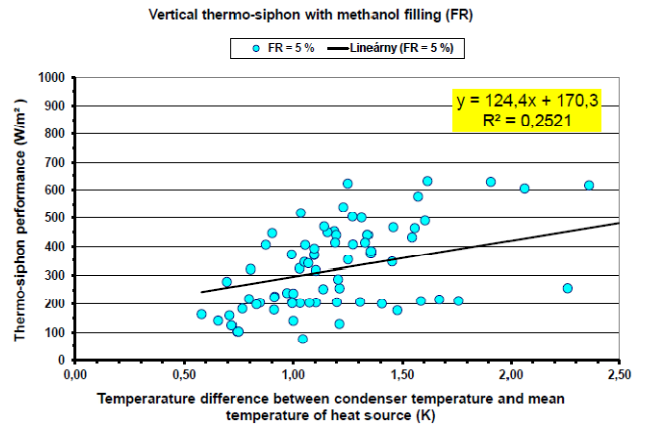
Figure 4 **Specific heat output at 10 % filling ratio of methanol**

The results of measurements are shown in **Fig. 2** and **Fig. 3** according to methodic of [1, 2]. It means illustrate performance parameters (condenser performance or specific heat output) depending on difference of methanol condensation temperature and mean temperature of heat source. In this case the heat source was simulated a heat exchanger cold water network with transparent glass coat. On the **Fig. 4** and **Fig. 5** are presented results of measurements of functional model of ground borehole

heat exchanger expression on active surface of heat pipe. Processed results of measurements are evident, that optimum filling rate (FR) of thermo-siphon with methanol is approximately 10 %. At lower filling rate 5 % and also at higher filling rate 15 %, also was decrease of siphon performance. Latest phenomenon is well known at heat pipes as swallow with filling matter.
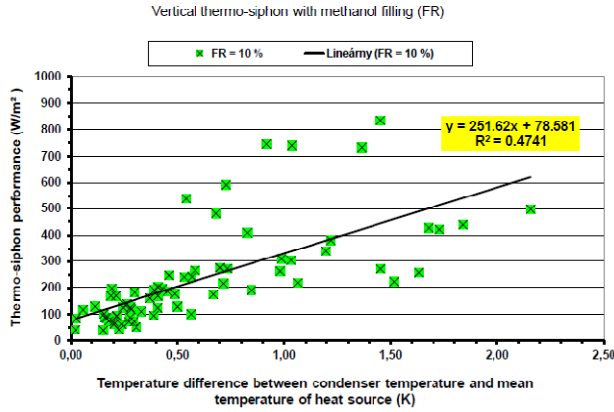
Figure 5 **Specific heat output at 10 % filling ratio of methanol**

Drawing of trend lines demonstrate different performance characteristic at widely different filling rates. Trend line on *Fig. 5* indicate in optimal conditions of specific heat output at 10 % filling ratio expressed with equation

$$\phi = 78,581 + 251,782 . \Delta\theta_s \quad \left(W/m^2 \right) \qquad (3)$$

where $\Delta\theta_s (K)$ is difference of methanol condensation temperature and mean temperature of heat source. According of realized experimental measurements its possible to obtain specific performance of ϕ from 200 onto 300 W/m² by actual difference $\Delta\theta_s$ of methanol
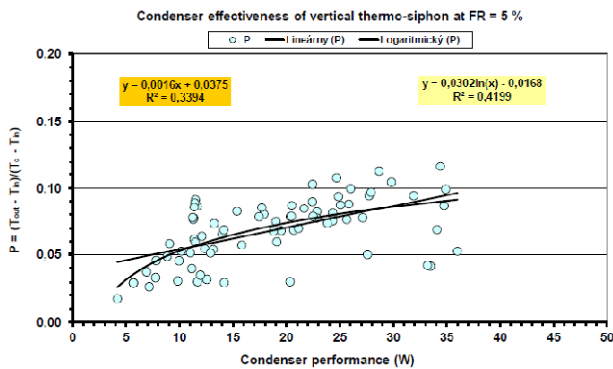
Figure 6 Effectiveness **of condenser at 5 % methanol filling rate**

condensation temperature and mean temperature 0,5 až 1,5 K of heat source (from earth massive). In case of actually realized vertical thermo siphons with length (depth) of approximately 100 m, is assume gentle growth of $\Delta\theta_s$ thankfulness of gravitation force, permit higher value of heat performance $\phi \left(W/m^2 \right)$.
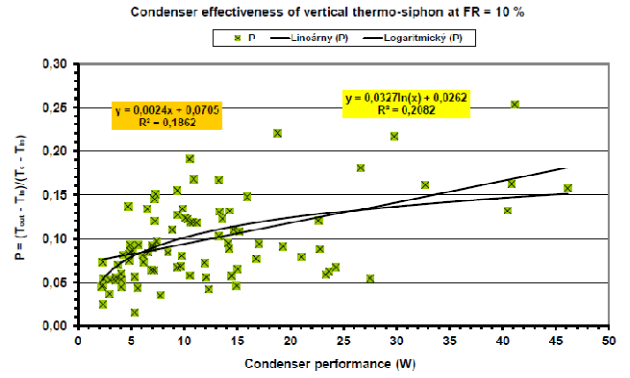
Figure 7 **Effectiveness of condenser at 10 % methanol filling**

IV. EFFECTIVENESS OF VERTICAL THERMO-SIPHON

On the formulation of characteristic work of condenser serve value of effectiveness well known for heat exchangers [6]. Effectiveness is a rate of temperature change flowing substance on secondary side of heat exchanger separating surface to whole temperature difference on HEX inlets. In case of condensers the effectiveness $P \left(- \right)$ maybe expressed with equation

$$P = \frac{T_{out} - T_{in}}{T_c - T_{in}} \quad (-)$$

(4)

where $T_c = \theta_c (°C) + 273,15 (K)$ is a measured temperature of methanol condensation in heat pipe ,

$T_{out} = \theta_{out} (°C) + 273,15 (K)$ - output temperature of water from condenser,

$T_{in} = \theta_{in} (°C) + 273,15 (K)$ - input water temperature into condenser,

$\theta_{out} (°C)$ - output water temperature from condenser (measured quantity),

$\theta_{in} (°C)$ - input temperature into condenser (measured quantity) .

On *Fig. 6* and *Fig.7* illustrate condenser effectiveness of vertical thermo siphon depending on measured achieved heat performance at two different filling rate of methanol. Comparison of trends lines of vertical thermo siphon condenser for methanol filling rates 5 % and 10 % give evidence, that optimal filling rate is approximately near at 10 % of methanol quantity.

CONCLUSIONS

The experimental results and its linear approximation indicate that, filling ratios of 10 % is a optimal value for successful operation of the thermo-siphon. Experiences from measurements on a functional model of methanol filled vertical thermo-siphon due to application of methods of similarity serves for design of really thermo siphons for utilization of ambient heat from the earth.

NOMENCLATURE

Φ - total performance of condenser (W),
m_w - water flow in condenser (kg/s),
c_w - heat capacity of water (J./(kg.K)),
T_{wout} - output temperature of water from condenser (°C),
T_{win} - entry temperature of water to condenser (°C),
ϕ - thermo-siphon performance (W/m^2),
S   - surface of thermo-siphon evaporator section (m^2),
T_c - measured condensation temperature (°C),
T_b - mean temperature of evaporator water bath (°C),
P   - effectiveness of heat exchanger (-).

REFERENCES

[1] ONG, K. S. HAIDER, A. M. Experimental investigations on the hysteresis effect in vertical two-phase closed thermosyphons, Applied Thermal Engineering 19 (1999), 399-408.

[2] JOUDI, K. A. WITWIT, A. M. Improvements of gravity assisted wickless heat pipes, Energy Conversion & Management 41 (2000), 2041-2061.

[3] ONG, K. S. HAIDER, A. M. Performance of a R-134a filled thermo-siphons, Applied Thermal Engineering 23 (2003), 2373-2381.

[4] NOIE, S. H. Heat transfer characteristic of a two-phase closed thermosyphon, Applied Thermal Engineering 25 (2005), 495-506.

[5] OCHSNER, K. Carbon dioxide heat pipes in conjunction with a ground source heat pump (GSHP), Applied Thermal Engineering 28 (2008), 2007-2082.

[6] KAKAÇ, S. BERGES, A. E. MAYINGER, F. Heat Exchangers – Thermal-Hydraulic Fundamentals and Design 1980, Hemisphere Publishing Corporation, ISBN 0-89116-225-9.

[7] J. Nyers, L. Nyers: "Monitoring of heat pumps". 'Studies in Computational Intelligence', Springer's book series, ISBN 978-3-642-15220-7 Vol. pp. 243, 573-581, Heiderberg, Germany. 2009.

[8] J. Nyers, A. Nyers: "COP of Heating-Cooling System with Heat Pump" IEEE International Symposium "EXPRES 2011." Proceedings, ISBN 978-1-4577-0095-8, pp.17-21, Subotica, Serbia. 11-12 03. 2011.

[9] L. Herczeg, T. Hrustinszky, L. Kajtár: Comfort in closed spaces according to thermal comfort and indoor air quality. Periodica Polytechnica-Mechanical Engineering 44: (2) pp.249-264. (2000)

[10] L. Kajtár, L. Herczeg, E. Láng: Examination of influence of CO2 concentration by scientific methods in the laboratory. 7th International Conference Healthy Buildings 2003. Singapore, 12. 07-11. 2003. pp. 176-181, 2003.

[11] Nyers J., Nyers A. : " Investigation of Heat Pump Condenser Performance in Heating Process of Buildings using a Steady-State Mathematical Model ". International J. Energy and Buildings. Vol.75, pp. 523–530, June 2014. DOI: 0.1016/j.enbuild.2014.02.046

[12] Kajtar L., Nyers J., Szabo J.: "Dynamic thermal dimensioning of underground spaces". International J. Energy. Vol. 87, pp. 361-368,1 July 2015. doi:10.1016/j.energy.2015.04.112

[13] J. Nyers, L. Garbai, A. Nyers: A modified mathematical model of heat pump's condenser for analytical optimization. International J. Energy. Vol. 80, pp. 706-714, 2015. (IF 4.844)

23

eMIS Energy Monitoring System as a Means of Increasing Energy Efficiency in Buildings

L. Šereš*, K. Bogataj** , S. Bošnjak* and O. Grljević*

* University of Novi Sad, Faculty of Economics in Subotica, Subotica, Serbia
** Iskra Sistemi d.d., Ljubljana, Slovenia
laslo.seres@ef.uns.ac.rs, kristina.bogataj@iskrasistemi.si, bsale@ef.uns.ac.rs

Abstract — the efficient consumption of energy, especially those coming from non-renewable sources, is one of the central aspects of functioning and sustainable development of contemporary society. As more than one third of world primary energy is consumed by buildings savings that residents / working staff can achieve by rational energy consumption are significant. IT/IS technologies can be of great help in achieving better energy efficiency in buildings. Energy information systems monitor, organize and process building energy consumption and related trend data in order to identify energy consumption anomalies and manage consumption costs. The use of such system helps to change people's attitudes towards energy consumption and impact on quitting their bad habits that stem from ignorance or negligence. This paper presents a web-based energy monitoring system developed in order to enhance energy awareness and efficiency, especially in the region of Western Balkans. Experiences gained through the implementation of the pilot project are also described. The paper also comprises future improvements of the system, which should contribute to more comprehensive support of efforts to increase the buildings energy efficiency

INTRODUCTION

There are many motivations to improve energy efficiency. Reducing energy use reduces energy costs and may result in a financial cost saving to consumers if the energy savings offset any additional costs of implementing an energy efficient technology. Reducing energy use is also seen as a solution to the problem of reducing greenhouse gas emissions. Energy efficiency and renewable energy are said to be the twin pillars of sustainable energy policy [3] and are high priorities in the sustainable energy hierarchy. In many countries energy efficiency is also seen to have a national security benefit because it can be used to reduce the level of energy imports from foreign countries and may slow down the rate at which domestic energy resources are depleted.

It is estimated that up to 40% of the total energy consumption can be allocated to buildings, while the potential savings of energy amounts to 27% for residential buildings and some 30% for commercial buildings [3]. On the other hand, the share of renewable energy in total energy consumption of the EU for the year 2010 was only 12.5% [4], and Serbia is only at the beginning of use of renewable energy sources.

Although the population can have little influence on energy offer due to the natural resources given, they can influence the energy demand by reducing energy consumption. In order to achieve substantial and sustainable energy savings, energy-efficient techniques, products and services must be developed and consumption habits must be changed so that less energy is used to maintain the same quality of life. This is achievable by improving energy efficiency.

The paper presents a low cost, easy to use monitoring system for instantaneous consumption monitoring and transparent energy efficiency indicator evaluation – energy management information system (in the following eMIS).

This system is an efficient and comprehensive solution for automatic energy monitoring task, based on established metering and communication infrastructure for data retrieving and storage, and Web based application giving insight into energy consumption, monitoring of energy efficiency, automatic creation of reports and data transmission to other systems and institutions.

The structure of the paper is as follows. Following this introduction the second section presents the theoretical backgrounds of the system presented in this paper. The set of indicators identified for the purpose of buildings energy efficiency assessment (and implemented in eMIS) are presented in the third section. Detailed illustration of the eMIS architecture, as well as its' main functionalities is given in the fourth section. Section five provides guidance and potential directions for further research and improvements of the developed system. The last section summarizes the results and stresses the benefits from the utilization of energy efficiency monitoring and management system in a real-time environment.

BACKGROUND

Energy Information Systems (EIS) refer to software, data acquisition hardware, and communication protocols administered by a single company, a partnership, or a collective to provide energy information to commercial building energy managers and electric utilities. An EIS may include numerous classes of information such as energy use, building characteristics, HVAC (Heating, Ventilating, and Air Conditioning) or other building system data, weather data, energy price signals, or energy demand-response event information. This paper summarizes key features available in today's EIS, along with a categorization framework to understand the relationship between EIS, EMCS (Energy Monitoring and Controlling Systems), and similar technology.

In a typical EIS architecture, the EIS server hardware and software located at the EIS service provider's physical site record interval data via the Internet, as shown in

Figure 1. The EIS receives these data from signals dispatched by meters installed in a customer's building, or directly communicates with meters. The EIS users can access the server with a password, and access the archived energy data either in real-time or in hourly, or daily updates from anywhere via a web browser. The typical functions of EIS are described in the following three features:

- Visualizing tabular and graphical metered usage data.
- Comparing load profiles within and across multiple facilities.
- Varying degrees of billing and rate information.

THE EVALUATION METHOD OF BUILDINGS ENERGY EFFICIENCY

The assessment of building energy efficiency is one of the most effective measures for reducing building energy consumption. One of the prerequisites for the development of the energy efficiency-related information systems is to define methods of energy efficiency evaluation.

The main parameters that are used as indicators of energy efficiency consumption are defined as follows:

- Electrical efficiency (EF_e): Total amount of electrical energy consumed per square meter of the observed building [kWh/m^2]
- Thermal efficiency (EF_t): Total amount of heating energy consumed per square meter of the observed building [kWh/m^2]
- Overall energy efficiency (EF_U): $EF_U=EF_e+ EF_t$ [kWh/m^2]
- Electrical cost efficiency (TE_e): Total cost of electrical energy per unit of measurement (RSD/kWh)
- Heat cost efficiency (TE_t): Total cost of heat energy consumed per unit of measurement (RSD/kWh)
- Total cost efficiency (TE_U): $TE_U=TE_e+ TE_t$ [RSD/m^2]
- Electrical efficiency of cost per square meter (TEK_e): Total cost of electrical energy per square meter of the observed building [RSD/m^2]
- Thermal efficiency cost per square meter (TEK_t): Total cost of heating energy consumed per square meter of the observed building [RSD/m^2]
- Total cost efficiency per square meter (TEK_U): $TEK_U=TEK_e+ TEK_t$ [RSD/m^2]

Along with defining the theoretical and methodological basis for the construction of the system for a period of one year data on energy consumption were collected in a
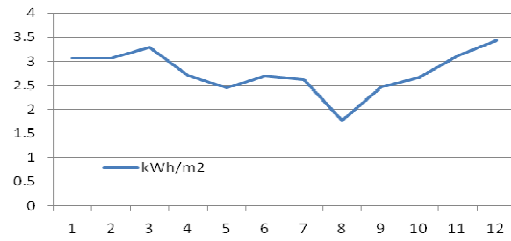
Figure 1.   Diagram of electrical energy consumption efficiency over the year

building that has been selected for the purpose of implementation of the pilot project. Also, the relevant data on temperature trends over the respective year were collected from the nearest meteorological station in order to analyze the energy consumption per temperature degree and in excess temperature (18°C). We obtained the Monthly Degree Days[1] (18°C Base) for the territory of Subotica, where the building is located, directly from http://www.sumeteo.info/index.php?lang=en.

The calculated values of energy consumption indicators of the observed building are shown in Table 1.

Figure 1 shows the changes in electric energy efficiency over this time interval, measured on a monthly level. It can be seen that the electricity consumption had risen in winter months, while it was at the lowest point in August, when the whole employees are on the collective summer holiday. The higher energy consumption is a result of additional heating in some offices during the winter, when the working staff found the offices temperature not sufficient.

One indicator of heating energy efficiency in buildings can be obtained by comparison of heat energy consumption per square meter with the division of amount of energy spent on heating and an annual degree-day (denoted K-day). At the selected location in Subotica the total annual K-day in 2011 was 2864,1. The correlation of heating energy consumption and monthly degree-days is shown in Figure 2, while Figure 3 displays the heating energy efficiency at annual level.

The level of electricity consumption in the selected building is greatly above the average electricity consumption in similar buildings, mainly due to the fact that there is neither a central cooling system installed nor an air conditioner in majority of offices.
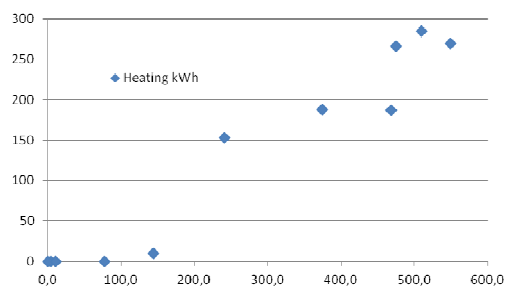
Figure 2.   Correlation of heating energy consumption and degree-days

According to international reviews, the average energy

---

[1] A Degree Day is a unit of measurement equal to a difference of one degree between the mean outdoor temperature and a reference temperature (18°C). Degree Days are used in estimating the energy needs for heating or cooling a building.

TABLE I.
CALCULATED VALUES OF ENERGY EFFICIENCY INDICATORS OF THE OBSERVED BUILDING

Energy	Consumption	Unit/m^2	RSD/Unit	RSD/m^2
Electricity	196,869 KWh	EF_e= 33.40	TE_e= 5.04	TEK_e= 168.27
Heating	1,408,454 MW	EF_t= 238.95	TE_t= 9.18	TEK_t= 2193.65
TOTAL:		EF_U= 272.35	TE_U= 14.22	TEK_U= 2361.92
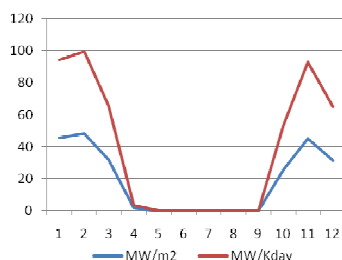
Figure 3. Heating energy consumption efficiency over the year

consumption for heating and hot water supply in buildings is 138 kWh/m^2/year[2]. In Serbia this average is even higher: 171 kWh/m^2/year in residential buildings and 194 kWh/m^2/year in non-residential buildings[3]. In comparison to these values, the selected building in Subotica is quite inefficient, with heating energy consumption over 250kWh/m^2 in November, January and February 2011.

The statistical correlation of heating energy and degree-days shows that the energy was consumed with caution, but the engineering and constructional characteristics reinforced a higher heating energy demand.

CHARACTERISTICS OF ENERGY MANAGEMENT
INFORMATION SYSTEM (eMIS)

One of the main goals, in the light of the orientation to energy savings and efficient energy consumption, was to develop a user friendly, transparent, and affordable energy management information system that would provide energy consumption monitoring, and abreast energy efficiency indicators evaluation and end-user energy consumption efficiency process improvement. The energy management information system is expected to present efficient and comprehensive solution for automatic energy monitoring task, based on established metering and communication infrastructure for data retrieving and storage, and Web based application giving insight into energy consumption, monitoring of energy efficiency, automatic creation of reports and data transmission to other systems and institutions.

System Architecture

From the architectural point of view eMIS is comprised of four layers of different purposes: data acquisition (ETL), data storage (DW server), data processing (application server), and presentation layer (clients).

Data acquisition. Efficient energy management is achievable only if continuous (online) data retrieving on energy consumption is provided. Data retrieving is possible from existing metering instruments, existing information systems and with implementation of new metering instruments.

Existing metering instruments are available for non-electrical power consumption in the case they are equipped with pulse outputs or support supplements with pulse outputs, since data on energy consumption is available over pulse outputs. Pulse outputs are connected

at local data concentrator / communicator. It retrieves information and transfers it into database over serial Ethernet, GPRS, and radio communication.

Not only data retrieving, but data transfer from metering instruments to a central database is of high importance. Cable connection with serial / Ethernet interface to metering centre for data retrieving and storage needs to be established. Metering instruments with pulse outputs can be connected in a comprehensive system based on Wi-Fi LPR radio communicators (batch: C2) and concentrators (C100). Special communicator C2 is equipped with battery (battery life longer than 5 years) and supports connections up to two pulse inputs. Data is transmitted to C100 communicator based on the defined timetable. Communications between C2 and C100 communicators are based on the frequency of 868MHz. Special penetration characteristics support the range of 300 m in the buildings. Data communicator C100 is connected with the database over Ethernet connection.

The energy monitoring information system is expected to support data transmission and integration with different applications, such as Energy Recovery (ER), Supervisory Control and Data Acquisition (SCADA), etc.

Data storage. The data repository of eMIS system is relational data warehouse. Data collected from different sources is stored in fact and dimension tables. Dimension table consists of equipment, location, and sensing devices dimensions. The fact table contains data relating to the climate indicators, indicators concerning the building, and data about energy consumption collected from wired and wireless sensors and meters.

The data warehouse also stores summarized information that varies through time and can easily provide answers to quires such as "Energy consumption of a particular office in a particular building when outside temperature is below 0°C".

Data processing. This layer is in charge of the application server and contains the business logic of the application that incorporates a variety of business models to monitor the energy efficiency of buildings. Among other things, this layer contains the definition of energy efficiency indicators (afore mentioned and described energy efficiency indicators) that allow their proper mapping of the database structure and the corresponding reference data.

The data processing layer generate energy usage graphs and profiles for demand analysis and power-reduction consideration in selectable sampling rates. Itemized electrical bills for departmental allocation and usage verification are also easily created. Another useful function is determining the coincidental peak demand date and time for multiple facilities or loads.

Presentation layer. The presentation layer of the information system was implemented in the form of a web application (Figure 4) that provides insight into energy consumption, enables monitoring of energy efficiency, as well as the automatic creation of reports and data transfer to other systems and institutions.

eMIS functionalities

eMIS, as a comprehensive information system for energy consumption monitoring and controlling, is designed as a Web-based application. The users access the application through a login form and/or certificate. Which

---

[2] From:
http://www.pregled.com/nauka.php?id_nastavak=723&tmpl=nauka_tmpl&tekuca_strana=11, accessed on October 2012.
[3] From:
http://www.gradjevinarstvo.rs/TekstDetaljiURL/Agencija_za_energetsku_efikasnost_%E2%80%93_Energetska_efikasnost_u_zgradarstvu.aspx?ban=820&tekstid=213
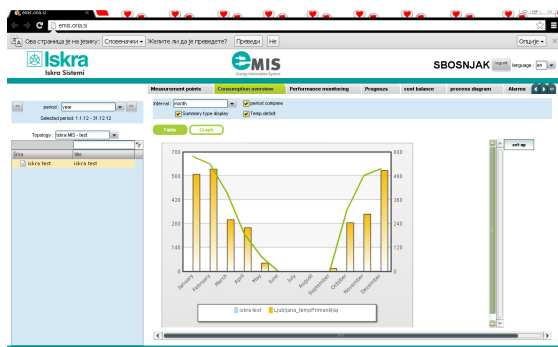
Figure 4.   Illustration of eMIS presentation layer

parts of the application and which data are available depend on the user's authorization.

Prior to commercial application of the eMIS, pilot study was conducted. Pilot application was introduced at two locations, one in Ljubljana Slovenia and the other in Subotica, Serbia. Prototypes included real energy supply and energy efficiency is monitored in a way that meets the needs of the given user, selected for analysis of pilot applications. Pilot buildings were analyzes in terms of the existing power grid, the heating and plumbing system. With the introduction of pilot applications in commercial buildings, experience in the context of quality and performance of the proposed eMIS system was gained. Particularly, end users reviews were collected and analyzed, as well as feedback and suggestions that gave an insight into the strengths of the system and areas of potential and possible improvements and helped to formulate recommendations for the further development of the system. It became apparent that eMIS system must support the profile assessment and energy consumption conditions, optimization of energy consumption that exceeds identified level for the observed energy product and planning (forecasting) of consumption.

Based on the experiences and insights obtained through pilot application construction of e-MIS system was completed. It supports on-line monitoring of energy consumption and energy efficiency assessment not only of buildings as a whole, but also the various monitoring points and key customers. Specifically, the system makes it easy to define the specific consumption, monitoring of energy costs (for different energy products), tracking of targeted energy consumption, alarming service in case of deviation from the trend of consumption and occurrence of infrastructure problems, as well as the monitoring of greenhouse gas emissions. Availability of data in various formats, such as reports, tables, charts, and e-reports on key elements represents one of the main characteristics of eMIS system. Efficient energy management via eMIS system is enabled through continuous collection of data on energy consumption. Data transmission in general is possible from existing measuring instruments, from existing information systems and/or by implementation of new measurement instruments.

Information system consists of three main modules. Module for remote data acquisition verifies the validity and current integration of all relevant data from the above mentioned sources as well as the external data (e.g., weather data), through integrative interface. Module for managing energy efficiency includes algorithms for tracking and allocating the main burden for consumers (heating, ventilation, lighting, etc.), monitoring of energy efficiency compared to conventional consumption, evaluation of indicators for specific energy consumption, correlation of temperature-day, forecast expected consumption and targeting, and monitoring costs. Module

for supply and optimization includes tools for data exchange with energy suppliers: automated readout from measuring devices, instant access to consumption data, consumer profiling, demand forecast, and monitoring of remote parts of the infrastructure. All of the above application modules are fully integrated into a single system.

Topology of measurement points. Measuring points of eMIS system are grouped by energy products, consumers or the location of the measurement. Each measuring point can be described by its attributes and values that are entered and updated through the web interface.

Reading and monitoring of energy consumption. The readings of consumption data refer to any data whose value changes over time or which combines multiple readings. The user has access to read values through simple topology (Figure 5 and 6). In doing so, the criterion by which the data is displayed is specifically set (graphical or table format, daily, weekly or annual level of detail, the comparison with last year's data, etc.).

Energy efficiency monitoring. Elements of monitoring the efficiency of energy consumption are correlations, contributions and specific factors. Correlation module compares the selected energy consumption with measured
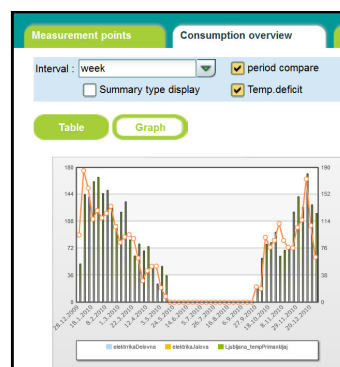
Figure 2.   Graph type presentation of electricity consumption

Figure 3.   Spreadsheet type presentation of water consumption

daily temperatures and indicates the degree of mutual correlation. When using this module, the required observational point i.e. measuring point has to be selected, as well as the limits of the time interval for the observation. Contribution gives graphical representation of participation of individual monitored elements in the total energy consumption during the observed time (Figure 7). Specific factors provide graphical display of specific energy consumption in buildings as an energy benchmark. First, the desired time interval of observation
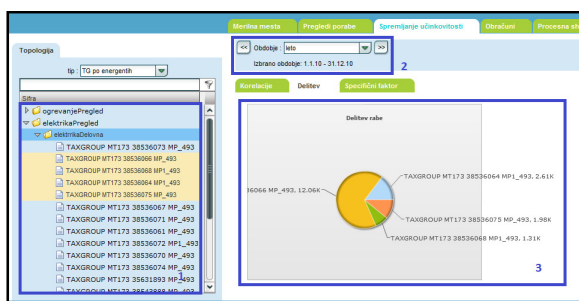
Figure 5. Participation of individual consumers in the total consumption of electricity

is set and the point of observation to display data on energy consumption.

FURTHER RESEARCH POSSIBILITIES

Information available on energy usage by consumers, as well as consumption by individual devices and industrial equipment, can be used to create a basis for the development of Smart grid that is capable of reacting to fluctuations in supply, combining several smaller and medium energy sources and power plants in virtual power plants where energy is more efficiently routed according to user needs. Smart grid should be based on the so-called Internet of Energy concept that represents an innovative approach to power distribution, energy storage, grid monitoring and communication. It will allow units of energy to be transferred when and where it is needed [5].

eMIS system could be expanded with the feature that would connect eMIS with the smart energy sensors that monitor consumption of energy in the whole building and give the user live feedback on the level of their consumption [9, 6], so the awareness of over spenders would risen.

Possible additional improvements refer to system partitioning on the local and cloud intelligence. The design of the eMIS system as a cloud computing service would reduce IT infrastructure costs while adding new functionalities to users. As pointed out in [7], in context of environmental protection and in accordance with the requirements of environmentally sustainable business, cloud computing fits the basic principles, since the IT resources are used more efficiently, and at the same time engaged computers may be physically relocated to other geographical areas where the electricity is more accessible or is obtained from clean and renewable sources e. g. hydropower or solar energy. So, with cloud computing technology utilization optimal allocation of computing resources can be achieved.

Extending eMIS system with the cloud computing technology would bring additional benefits, like notify the customers about the quality of supply (unplanned and planned outages, voltage deviations), promote the rule engine and data mining algorithms as intelligent tools for improving energy and cost efficiency in a user-friendly environment, rise the awareness of the end users for available improvements of energy and cost efficiency, switching off the critical appliances for safety reasons when the house is not occupied, and so on, [11].

One of the considerations refers to data flood caused by acquisition of large amount of raw data from different data sources. The possible resolution that would prevent this from happening is enriching the eMIS system with the flexible data filters and data mining functionalities to manage large amounts of data in an appropriate manner.

CONCLUSION

Starting from the knowledge that a key element in improving the energy efficiency of end users is introduction of cost-effective monitoring system, the focus of this paper is the presentation of e-MIS, as an innovative Web-based application for monitoring of energy consumption and efficiency. Features of the system like simple and reliable usage make the system acceptable for widespread use.

Continuous monitoring and transparent and immediate evaluation of energy efficiency indicators are enabled through components of presented information system: hardware base enables remote collection of data on energy consumption and the corresponding software modules allow continuous monitoring of consumption and evaluation of the effectiveness of energy use (detected consumption) in buildings, as well as management of power delivery and its optimization. It can be concluded that the e-MIS system results in fundamental framework for the operational monitoring of energy efficiency, for optimization of consumption and cost savings, as well as reduction of emissions of greenhouse gases.

Illustrated solution can be set as a service for remote data collection and online data processing (cloud computing concept) for all companies that are unable or unwilling to invest in a computing capacity, infrastructure, software licenses and training of staff, in order to achieve energy efficiency (e.g., small businesses, trade organizations, insurance companies, etc..). Thus, e-MIS can greatly contribute to the implementation of measures for energy conservation policy and sustainable environment through measures of improvement of energy performance in buildings.

e-MIS software solution can be extended in order to be used in other sectors relevant to energy policy and environmental protection: in order to increase return on production and distribution of energy, to minimize the impact of transport on energy consumption, to allow funding and investment in the energy sector, in order to establish and encourage behavior that is characterized by the rational consumption of energy, and to launch a wide action on energy efficiency.

REFERENCES

S. Bosnjak, A. Polic and K. Bogataj, "Energy management information system for energy supply management and optimization (Energetski upravljački informacioni sistem u menadžmentu i optimizaciji snabdevanja energijom)", 17th International Scientific Conference "Strategic Management and Decision Support Systems in Strategic Management", Serbia, 2012, pp. 23-24, ISBN: 978-86-7233-30406.

http://www.sumeteo.info/wxdegreedetail.php?year

Directive on the Energy Performance of Buildings 2010/31/EU

EUROSTAT, Retrieved from: http://epp.eurostat.ec.europa.eu/portal/page/portal/sdi/indicators, 2012.

IERC Internet of Things European Research Cluster, "*The Internet of Things 2012", New Horizons*, published in Halifax, UK 2012, ISBN: 978-0-9553707-9-3.

http://www.kickstarter.com/projects/wattvision/wattvision-the-smart-energy-sensor, accessed on January 15th 2013.

D. Milić, „*Poslovna softverska rešenja u oblaku za mala i srednja preduzeća"*, INFOTEH, March 2011, ISBN 978-99938-624-6-8, Vol. 10, Ref. F-5, p. 922-926.

Proposal for a Directive on energy efficiency and repealing Directives 2004/8/EC and 2006/32/EC

http://www.savantsystems.com/energy_management.aspx, accessed on January 15th 2013.

L. Šereš L., O. Grljević, S. Bošnjak, „*IT Support of Buildings Energy Efficiency Improvement"*, International Conference on Energy Efficiency and Environmental Sustainability, EEES2012, Conference proceedings, ISBN: 978-86-7233-320-6, pp. 55-62.

S. Veleva, V. Glamocanin, V, Davcev and G.K. Papagiannis, "*CLOUDESCO* Cloud computing platform for energy savings and low carbon economy", ICT Proposers' Day, Warsaw 25th September 2012.

J. Nyers, P. Komuves, "Optimum of External Wall Thermal Insulation Thickness using Total Cost Method", EXPRES 2015 Subotica, 7th International Symposium on Exploitation of Renewable Energy Sources and Efficiency. 2015.03.19-2015.03.21. Subotica, pp. 13-17.

Energy demand and consumption investigation of a single family house

Miklos Kassai*

* Budapest University of Technology and Economics/Department of Building Service Engineering and Process,
Budapest, Hungary
kas.miklos@gmail.com

Abstract— **In this research the differences between qualifying calculation methods for determination of building energy performance certification and demands is investigated. On the one hand calculation procedures that were used is the Ministry without Portfolio Decree No. 7/2006 for energy certification and MSZ-140-04 for energy demand calculations (by using WinWatt computer software tool) that are a widely used in the Hungarian practice by designers and experters. Passive House Planning Package (PHPP) is also more and more common used tool in Hungary due to the continuously tightening energy equirements. To see the differences and imperfections between these methods the heating, cooling and ventilation system was designed of a given single family house and the annual energy consumption was investigated with these methologies. To perform the investigation in more detailed three different heating systems were designed. In one case the heat source is a condensing boiler operated with floor heatings. In the other two cases the thermal systems are heat pumps with floor and ceiling heatings. One of the heat pumps is an air-to-water system, the other one is a geothermal heat pump. The advantage of the heat pumps is, that heating, cooling and domestic hot water energy is produced by only one equipment and efficiency. However comparing investment and operating costs for the heat pumps with gas boiler the payback time is very long based on this study. The investment costs, payback periods are investigated for the three different systems evaluating the results also with PHPP and WinWatt tools in this study.**

INTRODUCTION

The energy efficiency of buildings is regulated by the EU acquis [1] and national legislation [2]. By 2018 buildings in the public sector there will be more and more nearly zero-energy (nZEB) and, by 2020, this will apply to all buildings [3]. The definition of a nZEB will be, at least, within the limits of the requirements set for buildings which are currently optimally energy-efficient, including passive houses. A passive house is a proven path that leads to a sustainable building [4], and has been recognized in Europe, in terms of its methodology, almost for two decades [5]. Owing to energy flow optimization, passive houses save 80–90% of space heating energy in comparison with conventional buildings [4]. The energy efficiency of the passive house standard is demonstrated by the large number of passive houses (39,390) that have been built in Europe as of 2012 [6], and their number increases. A passive house [5] requires a maximum of 15 kWh/(m2 year) of useful energy for heating purposes. Low transmission heat loss is achieved by well-insulated and airtight building envelopes without thermal bridges [7]. A passive house has an integrated controlled ventilation system with exhaust air heat recovery, which reduces heat loss due to ventilation [8-10] and provides healthy indoor air quality [11-12]. Heat loss under a peak heating load in the heating season is kept under 10 W/m2 and can be covered by hot air heating [13]. Such houses eliminate the need for conventional heating systems [14]. Heat pumps are increasingly used to generate heat [15, 16]. The evaluation of the energy efficiency of residential buildings through the use of different simulation tools, as well as a partial methodological evaluation for the energy efficiency of individual building components, requires the use of a large number of parameters. This is also true for the PHPP'07 tool, i.e. the Passive House Planning Package – The energy balance and Passive House design tool [17], which had been developed in Europe to provide support to designers in the overall planning of highly energy efficient buildings. Since the use of the tool requires more project data, it cannot, for example, be used in the preliminary design phase for planning a building. Passivhaus Planning Package (PHPP12) is a simplified steady state building simulation tool that is primarily targeted at assisting architects and mechanical engineers in designing Passivhaus buildings [18]. Passive buildings compared to the standard ones require significantly less energy for heating and ventilation, while internal heat gains are almost the same. The energy demand for heating in passive buildings is less than 15 kWh/m2, while for example in new residential in Poland – 60–120 kWh/m2 [19]. Heat gains cover about 20% of whole energy loss in the case of a standard building and up to 65% in a passive house [20]. This fact leads to two important conclusions. Firstly, increasing the heat gains, e.g. by appropriate orientation of windows, may contribute to a significant reduction of energy need for heating [21-23]. Maximization of gains can at the same time cause increase of energy need for cooling, which was confirmed in the article of Enshen [24]. Secondly, a fluctuation of internal heat gains can cause significant change of the internal air temperature and requires specific control strategies. Appropriate control is necessary to obtain good thermal comfort as well as high energy efficiency. Because of it to predict correctly the internal environment conditions in a very low-energy buildings (like passive buildings – nearly zero-energy buildings) and calculate correctly their energy needs, precise building and system models have to be used. What is even more important, much attention should be paid to the appropriate determination of internal heat and moisture gains as well as airflows between building zones, all of which factors are often determined in a simplified way. For example, simplified methodology defined in standard ISO 13790 [25] can be suitable for buildings with standard energy need, but for very low-

energy buildings the methodology has to be more precise. Otherwise real energy performance of buildings can be higher than calculated and energy savings lower than predicted. This aspect is particularly important due to the recast of the Energy Performance of Buildings Directive and implementation of 'nearly zero' energy buildings [26].

The aim of this research was to compare the existing national standards: Decree No. 7/2006 (Degree) based on Energy Performance of Buildings Directive; MSZ-140-04 based on heat loss and heat gain calculation with Passive House Planning Package (PHPP) to evaluate the HVAC energy consumption of a single family house in Hungary. Additionally during the comparison three different HVAC systems were designed to the house: (1) condensing boiler with floor heating; (2) air-to water heat pump with floor heating; ceiling heating and cooling; (3) ground source heat pump with floor heating; ceiling heating and cooling. In each case the house is supplied with fresh air by air-to-air heat recovery ventilation system. Based on the different designed systems the investment costs are determined. Using the existing national standards and PHPP the annual energy consumption of the designed HVAC systems are predicted. By this way the payback time is calculated, the calculation procedures are also compered and differences are investigated.

PHPP AND DECREE NO. 7/2006.

The PHPP qualifying program for passive houses is integrated in Microsoft Excel tables, including 37 worksheets involving even deep details of the topics related to designing passive houses. In Hungary the software PHPP has not spread widely yet, nor has the sizing on the base of that, as the concept of passive house has not become well-known either. In practice generally the requirements of the Decree are seen to be relevant. The Hungarian decree is much more simple, but its result is less detailed than PHPP. In the followings the most important differences between the passive house designer's kit and the Decree No. 7/2006 is introduced. In PHPP designing is restricted by strict energetic limits. There are three criteria that a passive house has to meet:

- required specific heating energy is less than **15** kWh/(m²year), or the required specific heating energy is less than 10 W/m²,
- air tightness n_{50} is less than **0,6** 1/h (in case of pressure difference measured on 50 Pa),
- all required specific prime energy is less than **120** kWh/(m²year).

In the Decree these criteria are not so strict. Such as the air tightness of the whole building is not restricted at all. There are some requirements that are relevant not only for the energetics of the house, but also for the values of the constructing elements, or rather the equipments needed for the operation. There is a criterion for example for the heat transfer coefficients of the building envelope and windows and doors, also there are decrees relevant for building engineering equipments.

The Decree specifies the required value of the overall energy performance as well, and the risk of summer overheating of the buildings. For family houses the prime energy index calculates only with the energy required for the heating and domestic hot water, or if it is also artificially controlled even the energy required for ventilation and cooling is needed.

Maximum value of overall energy performance of residential- and accommodation- type buildings is calculated as follows (A/V: surface / air volume rate of the building) based on the Degree:

A/V < 0,3	E_p = 110 [kWh/(m²year)]
0,3 < A/V < 1,3	E_p = 120 (A/V) + 74[kWh/(m²year)]
A/V > 1,3	E_p = 230 [kWh/(m²year)]

PHPP calculation involves the current consumption of all household equipments beside the energy needs of heating and domestic hot water: all electrical equipments in the building from the washing machine to the laptop, including even lighting. Furtherly the operation household equipments also have to be known and this way precise sizing can be also performed.

PHPP is much more detailed also in energy demand predicting for sizing state than the Hungarian standard MSZ-04-140. Most Hungarian HVAC designers perform heat loss and heat gain calculations using also the software tool WinWatt that works based on this standard.

In PHPP calculation the place, the location of the building and data regarding the climate zone are also very important parameters. Exact lengths and types of the pipes of the HVAC equipments are also needed to perform the calculations. In case of windows and doors it is not enough to indicate whether the layer numbers of the glasses are two or three, but the solar energy transmittance value of glass, the fitting parameters of the frame and the heat bridges are also necessary to be identified. WinWatt is not able to count on the heat bridges for windows and doors.

Another important difference between PHPP and the Decree is that PHPP considers the gross floor space while Decree calculated with net floor space during the heat loss and energy performance calculations. In case of a building with 100 m² net floor space and 50 cm wall thickness the difference in specific value of net heating energy demand is 21%.

DESIGN OF HVAC INTO A PASSIVE HOUSE

Firstly the object was to design the ventilation and the heating system into a passive house in Hungary. There are several solutions for heating the building. The most prevalent methods are the followings nowadays: (1) heating by condensed furnace, (2) heating and cooling with air-to water heat pump, (3) heating and cooling with geothermal heat pump with soil probe. The designed passive house is located in the suburb of Szolnok. The orientation of the single family house is north – south and it is two-storied. Living area of the first ground floor is 138,12 m², and the second floor (upstairs): 77,67 m².

Base of the front wall is Porotherm 38 K brick (38 cm), applied with a heat insulation Baumit of 20 cm. On the attic floor additional heat insulation of 38 cm is applied.

Design of ventilation system

To have a healthy indoor climate and an energy efficient operation, the air-to air heat recovery ventilation and the building structure with good air tightness features are essentials. Ventilation and air-tightness have a strong cause an effect relation. The better the air –tightness of the structure is the more efficient the ventilation is, and the better the air –tightness is, the higher of the need is for sufficient ventilation.

According to observations a single person needs 30 m^3/h of fresh air on average. Due to its size the bedroom on the ground floor needs 60 m^3/h fresh air. In the living room the whole family can stay in the same time, so here a higher air volume flow is needed. Some air exchange is needed also in the dining room, that is in the same air-space as the living room, by this way there is possibility to provide the necessary air-flow.

Because of the moisture formation air extraction in the shower room and wellness is required, 30 m^3/h would be sufficient. In the toilet it is suggested to double the extracted air volume to avoid odors. In the kitchen 60 m^3/h extraction is suggested. Over the cooker a separate exhaust fan was designed to avoid the heat recovery ventilation system spreading odors and to exhaust moisture issued during cooking. The required air volume flow for the ground floor is shown by Table 1.

REQUIRED AIR VOLUME FLOW FOR GROUND FLOOR

Space	Supply Air flow	Exhaust Air flow
	[m^3/h]	[m^3/h]
Dining room	30	0
Kitchen	0	-60
Living room	2x60	0
Wellness	0	-30
Shower room 1	0	-30
Shower room2	0	-30
Bedroom	60	0
Toilet	0	-60
Total:	210	210

To the upstairs 60 m3/h supplied fresh air was designed to the larger bedroom, and 30 m3/h to the two smaller ones. The wardrobe room is big-sized as well, so air change was also designed to here. To the bathroom and toilet the same air volume flow was designed as on the ground floor. Table 2 shows the designed air volume flows into the premises on the upstairs.

REQUIRED AIR VOLUME FLOW FOR UPSTAIRS

Space	Supply Air flow	Exhaust Air flow
	[m^3/h]	[m^3/h]
Bedroom1	60	0
Wardrobe room	30	0
Bedroom2	30	0
Bedroom3	30	0
Bathroom	0	-60
Shower room	0	-30
Toilet	0	-60
Total:	150	150

Summing up the required air volume flows on the ground floor and upstairs the total volume flow of the air is 360 m^3/h.

Design of the three different Heating systems

Heat loss calculation

The transmission heat loss is 4,2 kW and heat loss due to the air filtration is also 4,2 kW. So that the total heat loss of the building is 8,4 kW. Considering the heat recovering ventilation system working by 85% effectiveness air-to air heat exchanger, air filtration heat loss is reduced to 0,77 kW. By this way the total heat loss is 4,97 kW with ventilation system operation.

Heating by condensed furnace

Condensed furnace is the most modern and efficiency gas furnace at the moment, as it has much better efficiency than the conventional furnaces. During its operation it utilizes not only heat coming from burning, but also the heat energy recovered from the water vapor of stack gas. When natural gas burns, its hydrogen joins the oxygen of the air, providing water vapor in the equipment, which has heat energy. In cases of other furnace this energy simply leaves through the chimney. This way using the condensed furnace the gas consumption can be reduced by 20-35 % compared to the conventional gas furnaces [27].

Settling cost is relatively cheap. The price of a condensed furnace is about 800-1000 EUR. Building the heat egress system, floor heating is around 3 225 EUR. Gas connection to the condensed furnace is 330 EUR. All together the total cost to build the system is around 1600 EUR [28].

Heating system with condensed furnace (case 1)

Required heat for sizing is 4,97 kW. In the first case the selected heat-generating equipment is a condensed gas furnace with the type of Vaillant ecoTEC pro VU INT II 246/5-3 unit, that is set on the wall of the machinery room situated on the ground floor. The other part of the heating system is floor heating, whose water supply temperature is 38 °C and water return temperature is 32 °C. Next to the furnace a 25 liter expansion tank with the type of Flamco Flexcon C25 was designed. To the furnace a 300 liter enameled indirect domestic hot water (DHW) tank with the type of CONCEPT SGW(S) was designed. Into the machinery room a 10 loop to the upstairs we set a 5 loop heat manifold are designed. All

15 loops of the floor heating is made of floor heating pipes type of Wavin with 20x2 mm thickness. A temperature sensor is installed into the DHW tank to control the DHW temperature, and another one is placed to the outwall sensing the ambient air temperature to control the heating water temperature generated by the gas boiler. The heating system is also controlled by indoor thermostats placed in the living room, dining room and each of the four bedrooms.

Heating and cooling with air-water heat pump (case 2)

In the second case the heat-generating equipment is an air-to water heat pump with the type of LG Therma V HUN0914, whose heating energy performance is 9 kW. The COP of the air-to water heat pumps decreases significantly in winter coldness, because of it COP values are measured on different temperatures by the manufacturer. The season value of this equipment is 3,43. The other parts of the heating system are floor heating and ceiling heating, whose supply water temperature is 38 °C and return water temperature is 32 °C. A 300 liter DHW tank is connected to the system with other type of VIH RW300. A 5 loop heat manifold designed for floor heating and another 5 loop heat manifold for ceiling heating are designed to the machinery room.

On the upstairs a 5 loop heat manifold is designed for ceiling heating as well, and one loop is branched for floor heating from the supply header pipe. According to cooling demands the heat pump is also suitable for cooling reversing the refrigerant circulation and supplying the ceiling radiant panels with cooling energy by water medium. The controlling of the heating and DHW systems is the same as with gas boiler.

Its settling cost is relatively high. The heat pump itself is about 4840 EUR. Fitting the ceiling and the floor heating is also about 4840 EUR, so the total investment cost is about 9 680 EUR [29].

Heating and cooling with geothermal heat pump with soil probe (case 3)

In this case the heat of the soil is utzilized by soil probes drilled in the soil 100 meter depth vertically. The soil probes provides +5 °C water temperature even from the depth of 10 meters, independently from the seasons. These systems utilizes the heat energy very efficiently.

Through the probes some heat carrier liquid must be recirculated. The liquid is a combination of water and glycol liquor, so that it is antifreeze, and there is no harmful effect to the environment. By this way the heat transfer medium warms up to 5 -7 °C by the time it reaches the surface. The system is also suitable for the passive cooling of the building in summer. Heat uptake capacity of the soil probe is depending on the quality of the soil, and the length of the probe as well. Table 3 shows the heat uptake of the soil probe by meters from the different soil types [30].

SOIL PROBE'S HEAT UPTAKE FROM DIFFERENT SOIL TYPES [30]

Soil type	Heat uptake [W/m]
Guideline values	
Dried wash	20
Rock and waterlogged wash	60
Consolidated rock with good heat conduction features	85
Rock types	
Dried pebble stones, sand	< 20
Waterlogged pebble stones, sand	65 - 80
Strong water flow in pebble stones, sand	80 - 100
Clay, adobe	35 - 50
Sandstone	65 - 80

The investment cost of the system with geothemal heat pump with soil probes is one of the highest comparing with other heating systems. The cost of the heat pump is about 6 450 EUR. Cost of the other part of the heating system is about 4 838 EUR and drilling cost for the probes to the soil is about 4 842 EUR. The total cost of the system is around 16 130 EUR [29].

In the third case the heat-generating equipment is a geothermal heat pump with the type of Vaillant VWS 81/3, whose heating performance is 7,8 kW, its COP is 4,9. Considering the soil conditions in Szolnok, a soil probe of 100 meter length can uptake approximately 3,5 kW of heat energy, that means 2 probes are required to provide the required heating energy demand in sizing state. The two soil probes are designed to be drilled in the back garden in 6 meters distance from each other.

To provide the necessary domestic hot water energy, a 300 liter DHW tank with the type of Vaillant VIH RW300 is connected to the heat pump. The other part of the heating system is the same as described in the second case. In summer passive cooling can be operated when only a water pump circulates the cooling medium from the probes. The controlling system for heating and cooling is the same as described in the other two cases.

Design of HVAC into a passive house

RESULTS

Figure 1 shows the heating energy demand of the designed passive house operated with air-to-air heat recovery ventilation system and with natural ventilation (without heat recovering). The energy demand is calculated with WinWatt (WW) and also with PHPP tools. It can be seen that the two methods give almost the same results. The main difference is, that PHPP needs more detailed input data and it results more reality values.
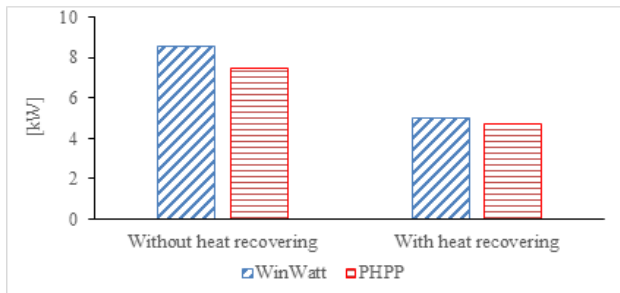
Figure 1. Heating energy demand
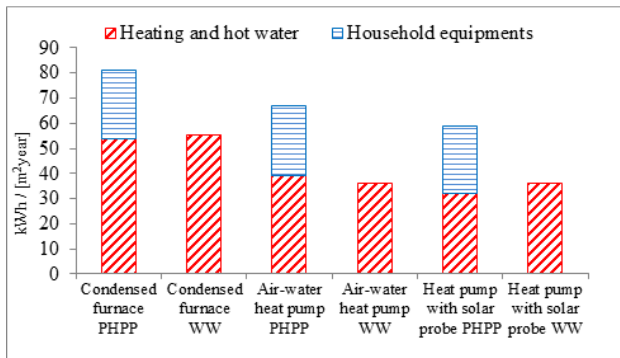
Figure 2. Specific prime energy index

Figure 3. Primer energy index based on EnEV requirements

Figure 2 shows that results of the calculations for the prime energy of heating, DHW and ventilation achieving by the two sofwares are the same. The reason for the difference is, that PHPP is able to calculate with the primary energy need of all electrical equipments, by this way the overall primary energy index can be got.

It is conspicuous, that in the first and third cases the energy consumption calculated by WinWatt is a bit higher, while in the second case a bit lower.

The reason is also the different structure of the two softwares. In PHPP the COP values of the heat pumps can be also given as input data, however WinWatt calculates with average fix COP values independently from quality of the heat pump product [31].

C_k is the electrical heat pump's power factor. Its values for heat step 35/28°C can be seen in Table 4.

POWER FACTOR OF THE HEAT PUMPS [31]

Heat source	Power factor Ck [-]
Water/Water	0,19
Air/Water	0,23
Soil temperature/Water	0,3

The COP is derived from C_k, after its division by 1. Thus WinWatt considers the COP value of air-water heat pump as 3,37; while the value of heat pump with soil probe as 4,34 [30].

According to PHPP the building can qualified as this designed passive house, only in the case of geothermal heat pump with soil probes. Namely the specific prime energy value of a passive has to meet also to the German EnEV requirements (Figure 3) with upper limitation (40 kWh/[m²a]).

CONCLUSIONS

Since the condensed furnace is not suitable for cooling at all, from comfort view heat pump is better choice. It is suitable for heating and cooling as well. Operating the geothermal heat pump with soil probe, also passive cooling can be applied, it means the heat pump itself does not work, only the soil probes provide the cooling energy by a water pump in the cooling period. With this method the cost of operation is very economic, as it can be seen even from the prime energy as well. However the investment costs can be extremely high. From the point of comfort feeling view in this passive house cooling is not necessary, as the proper heat insulation keeps warm outside. In spite of this fact cooling system was also designed as well considering also extreme climate conditions in summer. As the building has low energy needs, it is more reasonable to choose the condensed furnace with higher operational costs, whose settling and fitting is cheaper. As cooling is not really necessary, it is the best and most economical technical solution.

REFERENCES

Directive 2010/31/EU of the European Parliament and of the Council of 19 May 2010 on the energy performance of buildings (recast), *Official Journal of the European Union* L 153/13, 2013.

Regulations on Energy Efficiency in Buildings, *Official Gazette of the Republic of Slovenia*, 93/2008, 47/2009, 52/2010, Available from http://www.uradnilist. si/ pdf/2010/Ur/u2010052.pdf#!/u2010052-pdf. (in Slovenian), 2013.

L. Jisoo, L. Jung-Hun, S. Jungki, J. Su-Gwang, K. Sumin, "Application of PCM thermal energy storage system to reduce building energy consumption" *J Therm Anal Calorim*. 2013;111:279–288.

Passivhaus Institut, Available from http://www.passiv.de/, 2013 (accessed 17.04.2013).

W. Feist, Das Passivhaus–Baustandard der Zukunft?, Protokollband Nr. 12, *Passivhaus Institut*, 1998.

G. Lang, "Study on the Development of Passive House Trends in Europe 2010–2021." Available from

http://www.langconsulting.at/index. php/en/research/32-basic-research/222-trends-2010–2021, 2013 (accessed 17.04.2013).

J. Nyers, L. Kajtar, S. Tomic, A. Nyers, "Investment-savings method for energy-economic optimization of external wall thermal insulation thickness." *Energy and Buildings*. 2014;86:268-274.

L. Kajtar, J. Nyers, J. Szabo, "Dynamic thermal dimensioning of underground spaces" *Energy* 2015;87:361–368.

K.C. Rajnish, C.W. Wen, "A study of an energy efficient building ventilation system." *RoomVent 2011 - 12th International conference on air distribution in rooms*. Trondheim. Juny 19-22. 2011:1-8.

C. Guangyu, A. Hazim, Y. Runming, F. Yunqing, S. Kai, K. Risto, J.Z. Jianshun, "A review of the performance of different ventilation and airflow distribution systems in buildings." *Building and Environment*. 2014;73:171-186.

W. Lihui, B. Xinhui, C. Rui, J.Z. Jianshun, "The synamic thermal comfort index analysis under the air supply vent coupled with the cross-flow." *Procedia Engineering*. 2015;121:544 – 551.

C. Cristiana, N. Ilinca, B. Florin, M. Amina, D. Angel, "Thermal comfort models for indoor spaces and vehicles - Current capabilities and future perspectives." *Renewable and Sustainable Energy Reviews*, 2015;44:304–318.

W. Feist, J. Schnieders, V. Dorer, A. Haas, "Re-inventing air heating: convenient and comfortable within the frame of the passive house concept." *Energy and Buildings*. 2005;37:1186–1203.

J. Schnieders, A. Hermelink, " CEPHEUS results: measurements and occupant's satisfaction provide evidence for passive houses being an option for sustainable building." *Energy Policy*. 2006;34:151–171.

W. Feist, "Neue Passivhaus – Gebäudetechnik mit Wärmepumpen", Protokollband Nr. 26, *Passivhaus Institut*; 2004.

V. Anca-Marina, W. Christopher, C. Ana, A. Natalia-Silvia, B. David, "Estimating the thermal properties of soils and soft rocks for ground source heat pumps installation in Constanta county, Romania" *J Therm Anal Calorim*. 2014;118: 1135-1144.

W. Feist, "PHPP'07. Passive House Planning Package – The energy balance and Passive House design tool", *Passive House Institute*, Darmstadt, Germany; 2007.

W. Feist et al., "Passive House Planning Package 2007: Requirements for Quality Approved Passive Houses. Technical Information PHI-2007/1 (E)", 2nd revised ed., *Passivhaus Institute*. Darmstadt; 2010.

D. Chwieduk, "Prospects for low energy buildings in Poland." *Renewable Energy*. 1999;16:1196–1199.

W. Ebel, "Interne Wärmequellen – Erfahrungen aus dem Passivhaus, Arbeitskreis Kostengünstige Passivhäuser", Protokollband Nr. 5, Energiebilanz undTemperaturen, *Passivhaus Institut*, Darmstadt; 1997.

C. Junghoon, K. Sughwan, P. Kyung-Won, R.L. Dong, J. Jae-Hun, K. Sumin, "Improvement of window thermal performance using aerogel insulation film for building energy saving" *J Therm Anal Calorim*. 2014;116:219–224.

T. Poos, M. Orvos, "Heat- and mass transfer in agitated, co-, or countercurrent,conductive-convective heated drum dryer" *Drying Technology*. 2012;30:1457–1468.

T. Poos, V. Szabo, "Equations of volumetric heat transfer coefficients and mathematical models at rotary drum dryers", *Eurodrying'2015: 5th European Drying Conference*. Budapest, October 21-23. 2015:322-328.

L. Enshen, "Influence of inner heat sources on annual heating and cooling energyconsumption and its relative variation rates (RVRs)" *Building and Environment*. 2005;40:579–586.

Füri, B. Švingál, J.: Some experimental results with ammonia base azeotropic refrigerant R 723 in small heat pump, p. 139 – 142. Proceedings of 7th International Conference on Compressors and Coolants – Compressors 2009, 30. 9.- 2. 10. 2009, Častá - Papiernička, ISBN: 978-80-89376-02-2

Ján Takács, Marek Bukoviansky: Utilization of Geothermal Energy for Residential Sector of the City District Galanta North. EXPRES 2014, pp.82-85, ISBN 978-86-85409-96-7, 2014.

L. Šereš L., O. Grljević, S. Bošnjak, „*IT Support of Buildings Energy Efficiency Improvement",* International Conference on Energy Efficiency and Environmental Sustainability, EEES2012, Conference proceedings, ISBN: 978-86-7233-320-6, pp. 55-62.

ISO 13790. Thermal Performance of Buildings – Calculation of Energy Use for Space Heating and Cooling.

Directive 2010/31/EU of European Parliament and of the Council of 19 May2010 on the energy performance

Condensing boiler, http://www.kondenzacios.com/

http://www.kazanwebaruhaz.hu

http://www.hoszivattyu.arukereso.hu

http://www.sparkheatpump.com

Ministry without Portfolio Decree No. 7/2006 about Determination of Energy Efficiency of Buildings

Energy Aspects of Convective Drying

Orsolya Molnar

Budapest university of Technology and Economics/
Department of Building Services and Process Engineering, Budapest, Hungary
omolnar@mail.bme.hu

Abstract—**Effect of external drying conditions (temperature and humidity of drying gas) on drying kinetics and on energy demand is investigated experimentally at convective drying of gypsum boards in a pilot scale laboratory drying channel. Heat consumption and total energy demand of convective drying is analyzed at different periods of the drying process in function of drying intensity.**

INTRODUCTION

Convective drying of porous materials plays a major role in a lot of industry, e.g. food industry, pharmaceutical industry, mortar and concrete industry, chemical engineering, civil engineering, and soil remediation.

Since drying is one of the most complex and energy-intensive unit operations, it is a process of significant scientific and industrial interests. Analyzing the drying physics and process parameters can finally result not only in improving product quality but improving energy efficiency and reduction of carbon footprint at many industrial applications. Correspondingly some novel aspects of investigation of the drying kinetics are raised in the past decades.

As an extremely energy-intensive unit operation in industry, drying can use about 10-25% of the national energy consumption for industrial processes [1,2]. In an energy intensive industry like heating or drying, improving energy efficiency by 1% could result as much as 10% increase in profit [3]. Therefore, any small improvement in energy efficiency in drying process will lead to a sustainable development to global energy perspective [4].

For analyzing energy issues at convective drying an appropriate material has to be chosen for experimental investigation which can be moistened and dry several times without any damage and shows all the characteristics of capillary porous materials. Gypsum is a handy (user-friendly) non-hygroscopic and non-shrinking capillary-porous material which can be dampened properly to track the whole drying process. Unfortunately research of gypsum board drying is very limited notwithstanding gypsum board production is a typical wet method with intensive convective drying demand [5].

DRAYING KINETICS

Total drying time can be divided into two main parts conventionally where drying kinetics can be characterized by different mechanisms:

1. After a short initial period when the drying rate and temperature of the dried material can either increase or decrease a constant drying rate period (CDRP) can be observed at most porous solids. At this period temperature of the wet material is also constant -approximately the wet bulb temperature- and heat and mass transfer rates are assumed to be controlled by external conditions [6,7,8]. The internal moisture is in liquid phase and its transfer is fast enough to ensure the saturated state of the external surface where evaporation takes place. When internal mass transfer becomes insufficient to compensate the moisture loss on the surface, dry patches are created on this drying gas exposed area, *internal transfer limitations* appear and drying rate starts decreasing and the falling drying rate period (FDRP) starts. In the first part of FDRP internal and external transfer limitations occur simultaneously [9]. Reduction in the drying rate is caused by the progressive reduction of the wet area on the drying gas exposed surface.

2. In the beginning of FDRP internal and external transfer limitations occur simultaneously. Then, in the second part of the (FDRP) the evaporation interface progressively recedes inside the solid in many materials. In this period *internal conditions are supposed to drive* the kinetics [8]. When the drying front reached the bottom or symmetry plane of the dried material the equilibrium drying period starts. At this point there is no liquid phase moisture in the pores anymore and temperature of dried material progressively increases to that of the drying gas.

Hypothesis of a receding evaporation interface can be originated from Sherwood and Luikov and it was a milestone in development of the drying theory. In the receding drying front period three characteristic zones can be observed inside the material: *gas phase layer* under the exposed surface where all pores are dry and vapor molecules are diffusing to the surface in the gas filled pores; *two-phase zone* where there can be found both liquid, and gas filled pores and diffusing vapor molecules from the liquid meniscus as well; and there is a *wet core* where all the pores are filled with liquid. At that kind of porous materials, where the thickness of the two phase zone is comparatively small, the so-called receding front model applies. The receding drying front can be observed particularly at capillary-porous materials and the front's receding velocity is constant according to several experimental results [11,12,13].

However at some common materials such as apple, tomato, silt the CDRP is not obtained, drying takes place totally in the FDRP [14,15,16].

EXPERIMENTAL METHOD

Convective drying process was investigated in a pilot scale laboratory drying channel (Fig. 1.). Velocity of drying air was approximately the same at all measurements (2.2-2.4m/s), drying gas temperature (60-76°C) and relative humidity (2.5-4%) was changed according to Table 1. Dried specimen was handmade gypsum board with the size of 100mm length / 100mm width / 30mm thickness saturated with water. 11 pieces of

Cu-Co thermocouples were built in at the half of total length of the specimen at different depths symmetrically along the thickness (T1 at 1.8mm, T2 at 3.7mm, T3 at 6.7mm, T4 at 9.7mm, T5 at 12.7mm, T6 at 15mm etc.). Both top and bottom surfaces of the board were exposed to the drying gas other parts were closed and insulated. Internal temperature distributions, mass of the drying material and temperature of the drying gas were measured continuously and recorded in every 2 minutes during the whole drying test. Ambient air conditions and the gas velocity were also measured. Characteristic periods of convective drying were distinguished on the basis of measured temperature evolutions.
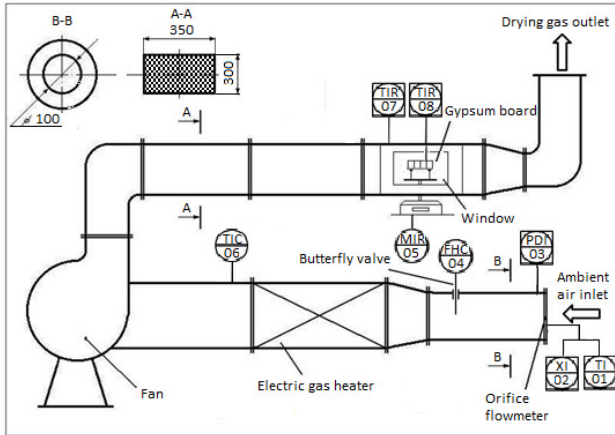
Flow chart of the pilot scale experimental apparatus

INVESTIGATION OF DRYING PERIODS

Characteristic periods of drying can be analyzed on the basis of measured temperature evolutions (Fig. 2.) or internal temperature distributions. In the first part of drying at the constant drying rate period the spatial temperature distribution is homogeneous and it is the wet bulb temperature approximately. After the constant rate period, in the first part of the FDRP where the physically bound internal moisture content starts evaporating, drying rate decreases but spatial temperature distributions are still homogeneous according to measurements. The beginning and the end of receding evaporation front period (P_{front}) can be distinguished easily. When the surface temperature's curve branches from the others (its slope becomes significantly larger than that of the others) drying front starts receding inside the material. Position of front can be followed up by measuring temperatures at different depths of the material. In the dry surface layer temperature distribution is linear with large gradient. In the internal wet core temperature distribution can be considered still homogeneous. When the evaporation front reaches the symmetry plane of the solid, pores run out of liquid phase moisture and core-temperature starts rising in a more progressive way. At this time a breakpoint can be recognized on the symmetry plane's temperature evolution curve.

In the first part of the falling rate period both external and internal transfer limitations are supposed to be relevant. During this period the internal temperature distributions are still homogeneous. Internal limitations are assumed to take over the control where the slope of T evolution curves suddenly increases (Fig. 2.). This is the point where external conditions driven drying (P_I) ends presumably and internal conditions driven drying (P_{II})

starts. From this time progressively larger part of the admitted heat is converted to rise the temperature of dried material while smaller and smaller part of that covers the energy demand of evaporation. This alteration can be observed on the measured temperature evolution curves.
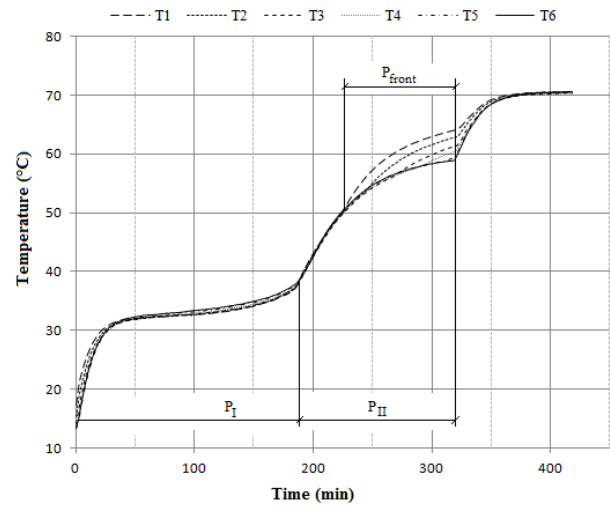
Temperature evolutions at different depth of drying specimen at M1 (T_G=72.6°C)

EFFECT OF EXTERNAL CONDITIONS

Drying kinetics is influenced by external conditions obviously. External conditions can be represented with velocity, temperature and humidity of the drying gas. This paper focuses on the effect of drying gas state only. Influence of gas velocity is not examined.

Four measurements were carried out on the same specimen, two of them (M1, M2) can be considered as high intensity drying and two of them (M3, M4) as lower intensity, mild drying. Velocity of the drying gas was approximately the same in case of all measurements.

Meaning of "drying intensity" is a question and it is defined arbitrary since it is not a commonly used expression. Convective drying is a simultaneous heat and mass transfer process in a flowing gas stream usually. The fact is that merely the Re number is not appropriate for characterization of drying intensity because it considers only the velocity and temperature of the drying gas and cannot provide information about its humidity. Mass flux at drying is the multiplication of the evaporation coefficient (σ - which is a kind of mass transfer coefficient) and the driving force - which is the difference in absolute humidity between the bulk flow of drying gas and the saturation state (Y_S-Y_G). Absolute humidity of drying gas (Y_G) is determined by the ambient state of the air while saturation humidity (Y_S) represents the gas temperature also. Driving force does not concern gas velocity, but in this context it is not relevant. In the CDRP mass flux is constant (N_{const}) and proportional to the driving force, since exposed surface of drying material is saturated:

$$N_{const} = \sigma(Y_S - Y_G) \qquad (1)$$

In FDRP the drying rate (N) is decreasing obviously. Drying rate can be measured easily by measuring the mass evolution (m_w - t) of drying wet material:

$$N = -\frac{1}{A_S}\frac{\Delta m_w}{\Delta t} \qquad (2)$$

In (2) A_S is the exposed surface of the solid where mass transfer takes place.

Constant drying rate - which is an important characteristic of the first, so-called external condition driven period (P_I) -, and receding velocity of the drying front - which is an important characteristic of the second, so-called internal condition driven period (P_{II}) - is examined versus drying intensity. Total drying time and duration of P_I, P_{II} and duration of receding front period (P_{front}) is also analyzed. Periods of P_I, P_{II} and P_{front} are distinguished on the basis of measured temperature evolutions. Information about the specimen, conditions of drying gas and measured data are summarized in Table I.

It can be seen that – contrary to expectations - value of constant drying rate (N_{const}) and the receding velocity of front (v_{front}) both are influenced by external conditions significantly and equally. Namely, increasing the driving force with approximately 30%, N_{const} increases with 38% and v_{front} with 39%.

Total drying time is 31% less at intensive drying than at mild drying unsurprisingly, but lengths of different drying periods (P_I, P_{II}, P_{front}) are also equally correlated with drying intensity similarly to the drying rate and front velocity. Ratio of the length of each individual period to the total drying time is the same regardless of the drying intensity. That is, duration of receding front period is approximately the 30% of total drying time; duration of "external conditions driven drying" period is approximately the 60% of total drying time; and duration of "internal conditions driven drying" period is approximately the 40% of total drying time in case of intensive- or mild drying as well. This means that hypothesis of external and internal transfer limitations seems to be failed. Anyway further investigations should be made on the influence of drying gas velocity and effect of internal conditions such as porosity and pore size distribution as well.

Mass of evaporated moisture can be checked in this respect also. It can be seen that initial mass and moisture content at the beginning of drying process is almost the same at the two intensive drying (M1 and M2) and one of mild drying (M3) measurements (in case of M4 moistening of specimen is not adequate so this measurement is omitted at this examination). This means that moistening conditions were similar at all the three examined measurements. Analyzing moisture content data at the end of P_I and P_{II} it can be seen that wet basis moisture content of the specimen decreased from 40% to 22% in P_I and from 22% to 17% in P_{II} regardless drying intensity. Final mass and final moisture content of dried specimen is almost the same at both analyzed intensive- and mild- drying measurements. This means that material can be dried until the same extent when drying front period ends, despite of the fact that equilibrium moisture content depends on the drying gas humidity according to the sorption isotherm.

	high intensity drying		mild drying	
	M1	M2	M3	M4
"bone dry" mass (g)	290.72	290.72	290.72	290.72
velocity of drying gas (m/s)	2.29	2.43	2.21	2.32
temperature of drying gas (°C)	72.6	76.0	59.8	61.7
rel. humidity of drying gas (%)	2.55	2.50	4.56	4.05
temperature of ambient air (°C)	27.0	23.9	24.3	26.9
rel. humidity of ambient air (%)	24.91	33.85	29.65	24.64
driving force Y_S-Y_G (g/kg)	18.48	19.46	14.39	15.02
constant drying rate (g/m²s)	0.533	0.530	0.346	0.425
receding velocity of front (mm/h)	9.37	9.57	6.72	6.92
duration of P_I (min)	180	194	308	244
duration of P_I (%)	56.25	59.51	62.35	59.22
duration of P_{II} (min)	140	132	186	168
duration of P_{II} (%)	43.75	40.49	37.65	40.78
duration of P_{front} (min)	96	94	134	130
duration of P_{front} (%)	30.00	28.83	27.12	31.55
total drying time (min)	320	326	494	412
total drying time (%)	100	100	100	100
initial mass at beginning of P_I (g)	480.72	482.28	480.25	465.05
mass at P_I to P_{II} (g)	377.42	374.15	370.13	348.02
final mass at the end of P_{II} (g)	351.62	350.11	349.94	327.53
initial dry basis moisture content (g/g)	0.65355	0.65892	0.65193	0.59965
initial wet basis moisture content (%)	39.50	39.72	39.46	37.49
dry basis moisture content at P_I to P_{II} (g/g)	0.29822	0.28698	0.27315	0.19710
wet basis moisture content at P_I to P_{II} (%)	22.97	22.30	21.45	16.46
final dry basis moisture content (g/g)	0.20948	0.20429	0.2037	0.1266
final wet basis moisture content (%)	17.32	16.96	16.92	11.24

ENERGY DEMAND OF CONVECTIVE DRYING

Heat consumption (j_Q) of the experimental convective drying process can be calculated knowing the specific heat of drying gas at atmospheric pressure (c_{pG}), temperature of drying gas (T_G) and temperature of ambient air (T_a):

$$j_Q = c_{pG} j_{mG} (T_G - T_a) \qquad (3)$$

Mass flow rate of drying gas can be calculated by the velocity (v_G) and density (ρ_G) of that and the cross sectional area of the drying channel (A_{ch}):

$$j_{mG} = v_G \rho_G A_{ch} \qquad (4)$$

Total heat demand of the whole drying process (Q) and that of individual periods (Q_{PI} and Q_{PII}) can be calculated considering drying times (Δt, Δt_{PI}, Δt_{PII}) respectively:

$$Q = j_Q \Delta t, \quad Q_{PI} = j_Q \Delta t_{PI}, \quad Q_{PII} = j_Q \Delta t_{PII} \qquad (5)$$

Specific heat demand of total drying and of P_I and P_{II} periods can be calculated from evaporated masses and can be compared also:

$$q = \frac{Q}{m_{evap}}, \quad q_{PI} = \frac{Q_{PI}}{m_{evapPI}}, \quad q_{PII} = \frac{Q_{PII}}{m_{evapPII}} \qquad (6)$$

Total energy consumption is the sum of heat consumption and energy consumption of air transportation. Since drying gas velocity was approximately the same at all measurements energy consumption of the fan is 4kW at all the time. Energy demand of air conveyance is proportional to the operating time.

Calculated data of heat and energy demands are summarized in Table II.

It can be concluded that heat and energy demand of mild drying is not less at all than that of intensive drying thanks to the longer drying time. It can be calculated that increasing the driving force with 30% results approximately 14% smaller total energy demand at the specific experimental apparatus and this energy saving is realized in the first drying period predominantly.

If there were built in a heat exchanger which recovers the heat content of the exhausted gas and can reduce heat demand of drying with 90%, the total energy saving would be 30%! The 73% of this energy saving still would be realized in the first drying period (P_I) and 23% in the second (P_{II}). This means that increasing the driving force of the simultaneous heat and mass transfer process is much more energy effective in the first period where surface moisture is evaporating and results in only minor energy saving during evaporation of bound moisture.

Regarding the specific energy demand it can be seen that heat demand of evaporating unit mass of moisture is much larger in the second part of the process (P_{II}) than in the first one (P_I) as expected. This means that it is a waste of energy to dry wet materials under the necessary level which is determined by the required product quality. Comparing the specific energy demand of high intensity and low intensity drying it can be seen that high intensity drying requires less specific energy, but cca. 25-25% less at both first and second part of the drying process equally. However increase of driving force is restricted by quality considerations naturally.

TABLE II.
HEAT AND ENERGY DEMAND OF
INTENSIVE (M1, M2) AND MILD (M3, M4) DRYING

	high intensity drying		mild drying	
	M1	M2	M3	M4
heat consumption (kW)	11.11	13.49	8.36	8.59
energy consumption of fan (kW)	4.0	4.0	4.0	4.0
total heat demand of P_I (MJ)	120.0	157.0	154.5	125.8
total energy demand of P_I (MJ)	163.2	203.6	228.4	184.3
total heat demand of P_{II} (MJ)	93.3	106.8	93.3	86.6
total energy demand of P_{II} (MJ)	126.9	138.5	137.9	126.9
total heat demand of drying (MJ)	213.3	263.8	247.8	212.4
total energy demand of drying (MJ)	290.1	342.1	366.3	311.2
specific heat demand of P_I (MJ/g)	1.16	1.19	1.40	1.07
specific energy demand of P_I (MJ/g)	1.58	1.54	2.07	1.57
specific heat demand of P_{II} (MJ/g)	3.62	4.44	4.62	4.22
specific energy demand of P_{II} (MJ/g)	4.92	5.76	6.83	6.19
specific heat demand of drying (MJ/g)	1.65	1.69	1.90	1.54
specific energy demand of drying (MJ/g)	2.25	2.19	2.81	2.26

CONCLUSIONS

External conditions have significant effect on drying kinetics obviously. External conditions (especially temperature and humidity of the drying gas) influence the drying kinetics in the first and second period of the drying process equally. It is proved experimentally that external driving force remains dominant in the second part of drying also where physically bound moisture is evaporating from the pores. Hypothesis of internal and external transport limitations seems to be failed. Though further experimental investigations are necessary to examine the effect of drying gas velocity and internal conditions such as porosity and pore size distribution on the drying kinetics.

Regarding to the energy efficiency experimental investigations presented in this paper prove that increasing the driving force (by increasing the drying gas temperature and / or decreasing the absolute humidity of that) results in decreasing drying time and less total energy demand. Nevertheless majority of the total energy saving is realized in the first part of the drying process where free surface moisture is evaporating. At some common materials where constant drying rate period does not occur and drying takes place in the falling rate period totally, energy saving can be much less than it would be expected.

It can be summarized that in case of those convective drying processes where quality considerations of the dried material do not come about, high intensity drying is preferred to low intensity drying because of shorter drying times (which result larger capacity of the drying equipment) and energy savings. Nevertheless knowing particular drying kinetics of the dried material and internal and external transport mechanisms during the simultaneous heat and mass transfer process is inevitable important at energy calculations and scaling up the specific drying units.

REFERENCES

I.C. Kemp, "Fundamentals of energy analysis of dryers", in E. Tsotsas, A.S. Mujumdar, editors. *Mod. Dry. Technol. – Energy Savings*, Weinheim: Wiley-VCH Verlag GmbH; 2011, pp.1-46.

T. Defraeye, "Advanced computational modelling for drying processes – A review", *Applied Energy*, Vol.131, 2014, pp.323-344.

M. Beedie, "Energy saving – a question of quality?", *Dairy Industries International*, Vol.60(12), 1995, pp.27-29.

C. Kumar, M.A. Karim, M.U.H. Joardder, "Intermittent drying of food products: A critical review", *Journal of Food Engineering*, Vol. 121, 2014, pp.48-57.

T. Defraeye, G. Houvenaghel, J. Carmeliet, D. Derome, "Numerical analysis of convectice drying of gypsum boards", *International Journal of Heat and Mass Transfer*, Vol.55, 2012, pp.2590-2600.

S. A. Giner, "*Influence of Internal and External Resistances to Mass Transfer on the constant drying rate period in high-moisture foods*" Biosystem engineering, Vol.102(1), 2009, pp.90-94.

A. Leonard, S. Blacher, P. Marchot, J. Pirard, M. Crine, "Convective drying of wastewater sludges: influence of air temperature, superficial velocity, and humidity on the kinetics", *Drying Technology*, Vol.23(8), 2005, pp.1667-1679.

N. Prime, Z. Housni, L. Fraikin, A. Leonard, R. Charlier, S. Levasseur, "On Water Transfer and Hydraulic Connection Layer During the Convective Drying of Rigid porous Material", *Transport in Porous Media*, Vol.106, 2015, pp.47-72.

N. Job, F. Sabatier, J-P. Pirard, M. Crine, A. Leonard, "Towards the production of carbon xerogel monoliths by optimizing convective drying conditions", *Carbon*, Vol.44, 2006, pp.2534-2542.

L. Pel, H. Brocken, K. Kopinga, "Determination of moisture diffusivity in porous media using moisture concentration profiles", *International Journal of Heat and Mass Transfer*, Vol.39, 1996, pp.1273-1280.

R, Toei, "Theoretical fundamentals of Drying operation", *Spec. Issue of Drying Technology*, Vol.14(1), 1996.

O. Molnar, "Receding evaporation front and heat transfer coefficient at drying", *PhD thesis*, Budapest University of Technology and Economics, 2005.

B. May, P. Perre, "The importance of considering exchange surface area reduction to exhibit a constant drying flux period in foodstuffs", *Journal of Food Engineering*, Vol.54(4), 2002, pp.271-282.

I. Doymaz, "Air-drying characteristics of tomatoes", *Journal of Food Engineering*, Vol.78, 2007, pp.1291-1297.

P. Gerard, A. Leonard, J. P. Masekanya, R. Charlier, F. Collin," Study of the soil-atmosphere moisture exchanges through convective drying tests in non-isothermal conditions", *Int. J. Numer. Anal. Methods Geomech.*, Vol.34(12), 2010, pp.1297-1320.

The Mechanical Ventilation for Large-Area Buildings of Engineering Industry

Z. Straková, J. Takács

Slovak University of Technology in Bratislava, Faculty of Civil Engineering,
Department of Building Services, Bratislava, Slovak Republic
zuzana.strakova@stuba.sk, jan.takacs@stuba.sk

Abstract **- Our national husbandry belongs among economies with the biggest energy consumption per an inhabitant. Slovak republic consumes for making of product's unit approximately twice more energy than the average in forward European countries. Such a big reserves, that we have to achieve in the area of effective increasing of energy utilization are not possible only by administrative way, but by establishing of new technical solutions into a general practice too. In a part of large-area industry operations, the new technical solution lies in the combination heating system by suspendable radiant panels with ventilation by air handling unit with integrated device for heat recovery, which considerably reduces the operation costs. Paper shows the advantages of this combination described in a computational example, as well as experimental measurements. Every step in the calculations and measurements leads to create an optimal working environment for humans with minimum energy requirement** [1], [3]**.**

INTRODUCTION

A comprehensive attitude has to be taken when creating a work environment in an industrial hall, in a large-area building. It is not only the issue of the heating itself but the way of air supply and air heating as well. The dimensions of halls and the underlying physical laws enable to create zones that are the major factor to choice of heating and ventilation systems. The new technical solution lies in the combination *heating system by suspendable radiant panels* with ventilation by *air handling unit* with *integrated device for heat recovery*, which considerably reduces the operation costs.

Figure 1.   Engineering industrial hall

Every step leads to create an optimal working environment for humans with minimum energy requirement [2].

BASIC ZONES OF ENERGY INTENSITY

Every large-area industry building can be divided into zones, which are characterized by a different temperature of indoor air in the vertical direction of an object. The most important area in terms of object's function is to achieve optimum microclimate conditions in the height of up to 2 m above the floor (see Figure 2). The floor is a part of this zone and significantly influences the thermal comfort. The grown ground beneath the floor reaches a constant temperature of about + 10 °C, which is caused by the extensive accumulation ability of the soil and the constant ground water flow [3].
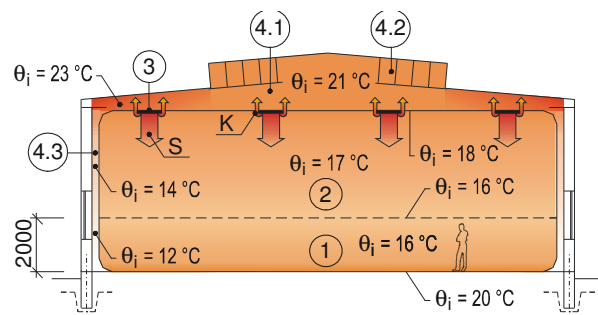
Figure 2.   Indoor air temperature running in radiant heating in the part
under the skylight
1 - zone of residence humans (± 0 to + 2 m), 2 - neutral zone,
3 - suspendable radiant panel, 4 - zone of energy performance,
S – heat transfer by conduction, K - heat transfer by convection

Due to the radiant heating the floor temperature reaches up to 20 °C, which actually makes it secondary heating surface. This is followed by the neutral zone in between 2 m above the floor, which is the height of the suspension of the radiant panels. This zone and temperature achieved do not affect the microclimate conditions in the occupied area. Though, due to the rising air temperatures along the height of the object, it has a significant influence on the energy performance.

The very important zone is the space above the radiant heating surfaces where the indoor air temperature is influenced by the convective component and temperature gradient (see Figure 3). The direct contact with the building encasement – the roof and the skylights, as well

as the walls and windows, causes increased heat loss. The higher the temperature of indoor air in these zones is, the greater the heat loss and energy requirements are.
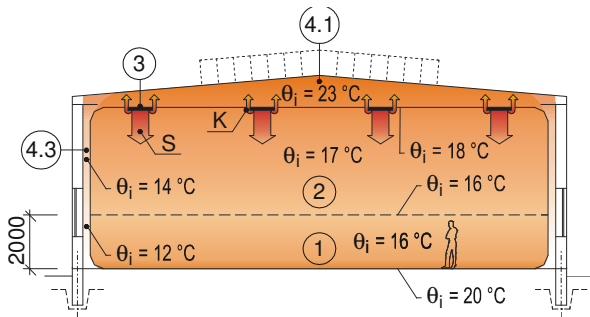
Figure 3. Indoor air temperature running in radiant heating in the part without the skylight
1 - zone of residence humans (± 0 to + 2 m), 2 - neutral zone, 3 - suspendable radiant panel, 4 - zone of energy performance, S – heat transfer by conduction, K - heat transfer by convection

It is therefore necessary to include the above mentioned features of each zone when designing ventilations systems.

COMBINATION OF HEATING WITH MECHANICAL VENTILATION

With regard to the amount of the ventilation air supply, there are two categories of ventilation systems. Ventilation in clean areas, where minimum pollutants occur during the manufacturing process, is so called *hygienic ventilation* with $0,5 \div 1,0$ times/h air exchange. If there is multiple air exchange during the manufacturing process due to the increased amount of pollutants, we talk about *technological ventilation* [4].

A. *The combination of suspendable radiant panels with hygienic ventilation*

The principle of vertical air flow is suitable for hygienic ventilation. It uses the air heat capacity from the neutral zone and the zone of the building's energy consumption. Recuperative unit draws warm air from the roof space through suction elements. Then it brings it through a collecting duct towards recuperation exchanger unit. Ventilation air heated from θ_e = -15 °C to +3 °C is blown by the diffuser into the space. The diffuser vanes settings allow to bring the colder air horizontally into the space bellow the radiant panels. Afterwards it is mixed with the warm air (θ_{ai} = +18 °C) and slowly sinks into the occupied zone, where it reaches the desired temperature θ_i = +16 °C. Increased performance of the radiant panels is required in order to enable thermal energy to reach ventilation air temperature +16 °C in the area of the neutral zone (from the temperature +3 °C). The principle of air supply and its heating fully supports its delivery using the thermal capacity of "the warm pad" under the roof covering.

The values are chosen according to a sample design of ventilation in a large-area building (see Figure 5) with a height of 7,2 m below the roof covering and diffusers mounted in a height of 6,0 m with unit output 920 m³/h. Total air flow rate V is:

$$V = n.V_1 \tag{1}$$
$$V = 5.920 = 4600 \text{ m}^3/\text{h}$$

where:
n is number of diffusers (-),
V_1 is an air flow rate of one diffuser (m³/h).

Air exchange in a building i is:

$$i = \frac{V}{V_b} = \frac{V}{(l.w.h)} \tag{2}$$

$$i = \frac{4600}{(60.18.7,2)} = 0,59 \text{ times/h}$$

where:
V is total air flow rate of diffusers (m³/h),
V_b is object's volume (m³),
l is length (m),
w is width (m),
h is high of object (m).

The basic settings of vanes (see Figure 4) for the outlet temperature θ = + 3 °C to $0° \div 45°$. For temperature +3 °C to +16 °C continuously towards the outlet angle of 60°. The angle of the vane changes with the increasing height of the object, or diffusers' suspension (to 90°). Continuous change of the vanes' settings are controlled by a signal $0 \div 10$ V, depending on the temperature of incoming ventilation air.
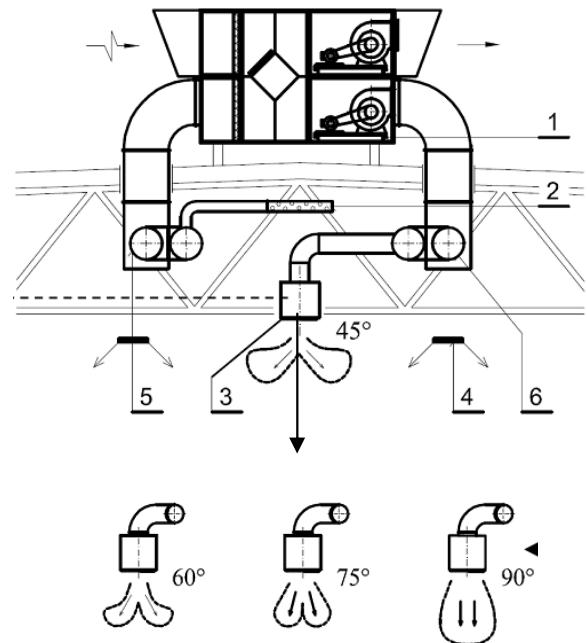
Figure 4. The basic settings of vanes of diffuser $0° \div 90°$
(Note: sign see figure 5)

Another option for hygienic ventilation is a unit with the heat recovery (located on the roof of building) without central air distribution.

These units, among others, are always equipped with effective filtration, heat recovery bypass, adjustable air output and a measurement and control module.

There is a shutter under the ceiling that exhausts the polluted air and at the end of the duct there is a remote controlled nozzle outlet, which supplies the ventilated space with fresh air. After recovery, they can also be equipped with supplementary air heating, but that is not usually necessary when combined with the suspendable radiant panels [5].

Exhaust air inlet has to be placed in the area above radiant panels, in the as highest place as possible. It is clear that the rising warm air flow almost along the entire surface heated by the floor is the basic principle of radiant heating. This is proven by visualization of temperature distribution and air velocity across the entire hall. Obviously, the cooler air falls down in the areas which are mostly cooled by the roof covering. This always happens below the skylights and on the peripheral walls, particularly if they are provided with windows. The fresh air outlet should be placed in the area below the skylight. A vertical flow of supply air is introduced into the natural downward convection below the skylight and then it rises up once again together with the air heated from the floor. The principle of air flow in radiant heating is fully respected and the hall space is perfectly rinsed (see Figure 6). Under certain circumstances, low (outdoor temperature) it may be advantageous to use the outlet and the possible horizontal flow which at a sufficient velocity at the peripheral walls changes into a vertical one, descending downwards to the floor. After its heating by the floor it goes upwards and the hall is being rinsed. (see Figure 7). In both cases, however, it is possible (to a certain outdoor temperature) to operate just with the heat recovery unit, without subsequent reheating of fresh air, because the supply air is reheated not only by induction but also by the so-called secondary heating surfaces.

B. The combination of suspendable radiant panels with technological ventilation

In the manufacturing halls with more pollution, both supply and heating of the ventilation air as well as the removal of contaminated air including its thermal capacity has to be taken into consideration. The combination of radiant heating with ventilation and the related method of creating microclimatic conditions makes it a very efficient technical solution. Radiant heating provides thermal energy by radiating the floor. The air is subsequently heated by the floor and then rises towards roof covering. This principle can be used to deliver fresh air into the working zone. The large-format diffuser are located along the circuit of the heated and vented workshop bringing the heated ventilated air to a temperature of about $1 \div 3$ K, which is lower than the temperature of the indoor air in the space. The discharge rate is $0,3 \div 0,5$ m/s. Its reheating takes place from the warmer part of the floor and machines, and subsequently rises towards the roof covering. The working zone is being filled with fresh air while the pollutants are being removed [6].
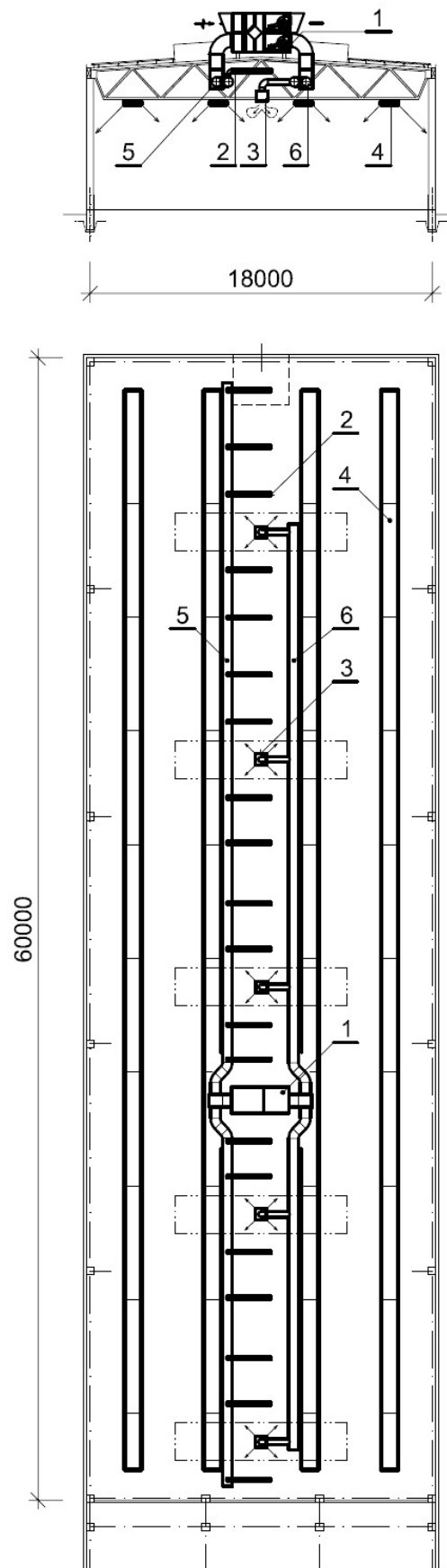
Figure 5.   Large-area building
1 - ventilation heat recovery unit, 2 - exhausting diffuser, 3 - supply diffuser, 4 - suspendable radiant panel, 5 - exhausting air conduit, 6 - supply air conduit

Figure 6   Vertical airflow input

Figure 7   Horizontal airflow input – underceiling flow

A significant advantage of this solution is that the exchange of air for ventilation calculate with the space's height of up to 3,5 m. As a variation, you can use the recovery unit located either on the roof or on one of the front walls.
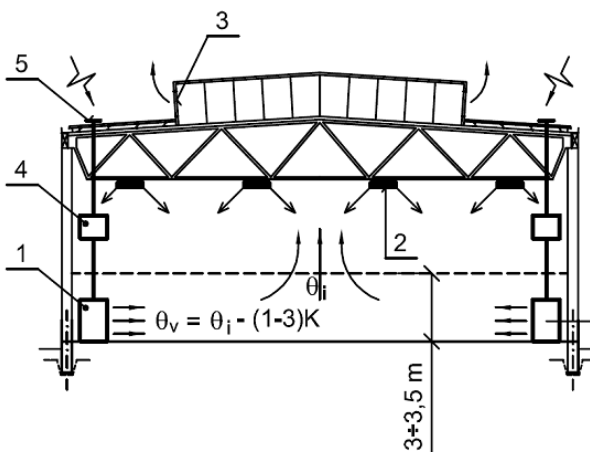
Figure 8.   The principle of ventilation by large-format diffusers
1 – large-format unit, 2 – suspendable radiant panel, 3 – axial fan,
4 – air heater, 5 - outside (fresh) air input

The air of the above mentioned temperature of $1 \div 3$ K, lower than the temperature of the indoor air in the ventilated space, is delivered by the air conduit towards outlets. Its removal takes place in the upper part of the object from the area of so called "warm pad" under the roof covering. This is done by air suction elements via the recovery unit.

In the example presented, a workshop measuring 36 x 18 x 7,2 m was chosen, with required air exchange ventilation 6 times/h and total air flow rate V_1 is:

$$V_1 = i.V_b = i.(l.w.h) \tag{3}$$

$$V_1 = 6.(36.18.7,2) = 27994 \text{ m}^3/\text{h}$$

where:
i is air exchange ventilation (h^{-1}),
V_b is object's volume (m^3),
l is length (m),
w is width (m),
h is high of object (m).

If you take into account only the height up to 3,5 m above the floor, the total air flow rate V_2 will have the value:

$$V_2 = i.V_b = i.(l.w.h) \tag{4}$$

$$V_2 = 6.(36.18.3,5) = 13608 \text{ m}^3/\text{h}$$

where:
i is air exchange ventilation (h^{-1}),
V_b is object's volume (m^3),
l is length (m),
w is width (m),
h is high of object (m).

The ratio of these both total air flows is:

$$\frac{V_2}{V_1} = \frac{13608}{27994} = 0,48 \tag{5}$$

This number accounts for 50 % heat saving needed for heating the ventilation air. This ratio is always determined by the real height of the object.

The control of this combined heating and ventilation system is performed as follows – the performance of radiant panels is controlled by the temperature taken by the spherical sensor. The inlet temperature of the ventilation air falls down in the duct to a constant temperature of about 2 K below the estimated air temperature in radiant heating [7].

EXPERIMENTAL MEASUREMENTS

In according with STN EN ISO 7726 (2001) we had been two experimental measurements in large-area industry object (see Figure 5), which had the task to objectively evaluate the combination of heating system by suspendable radiant panels with ventilation.

In 12 measuring points, randomly distributed in different parts of the whole area of building, was measured following physical parameter:

-    indoor air temperature in the level of the head man, measured at a height of 1,70 m above the floor,

- indoor air temperature in the level of the ankles man, measured at a height of 0,15 m above the floor.

Measurement results are shown in table 1. and table 2.

MEASUREMENT RESULTS OF INDOOR AIR TEMPERATURE IN TWO LEVELS (MEASURING POINT N^0 1-6)

Physical parameter	No.	Measuring point number					
		1	2	3	4	5	6
1. $\theta_{ai, head}$ (°C)	1.	19,8	19,9	19,9	21,2	19,8	19,8
	2.	19,7	19,9	19,8	21,4	19,7	19,8
	3.	20,0	19,8	20,0	21,2	19,8	19,6
2. $\theta_{ai, ankles}$ (°C)	1.	20,4	20,3	20,4	19,3	20,3	18,9
	2.	20,1	19,8	20,2	19,4	20,3	18,7
	3.	19,8	19,9	20,2	19,3	20,5	18,7

TABLE II.
MEASUREMENT RESULTS OF INDOOR AIR TEMPERATURE IN TWO LEVELS (MEASURING POINT N^0 7-12)

Physical parameter	No.	Measuring point number					
		7	8	9	10	11	12
1. $\theta_{ai, head}$ (°C)	1.	21,6	21,3	20,7	24,4	22,8	21,5
	2.	22,0	21,2	20,5	23,9	22,5	21,3
	3.	22,7	21,3	20,7	24,2	22,9	21,3
2. $\theta_{ai, ankles}$ (°C)	1.	19,2	19,3	21,6	22,1	21,3	19,6
	2.	19,0	19,2	21,4	21,9	21,3	19,4
	3.	19,1	19,2	21,7	22,0	21,5	19,5

The following diagram (see Figure 9) illustrates the indoor air temperature running in the work area of human. Difference between the maximum and the minimum value at a particular point is a maximum $\Delta\theta_{ai} = 0,4$ K. The rule according technical norm is maximum 3,0 K.
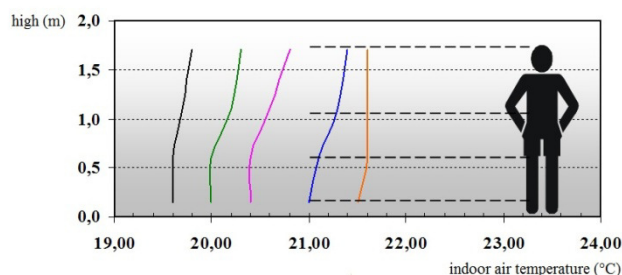
Figure 8.   Vertical temperature gradient of indoor air temperature

Thanks assessment we can confess that the combination of heating system by suspendable radiant panels with ventilation stood as positive in terms of uniformity of thermal conditions in the indoor environment.

CONCLUSION

The described method with vertical ventilation of fresh air supply in combination with radiation heating is particularly advantageous for the ventilation of indoor space to ensure hygienic minimum when $i \leq 1$ times/h. In many cases this may be suitable for air exchange of bigger volume. Those are the areas where the obstacles in the movement of persons could be of issue in reaching stabilized supply. In both cases, it is always necessary to carefully consider the flow velocity in the occupied zone in order not to exceed health standards. Ventilation system with vertical inlet can be applied to less clean premises. However, we have to respect the above mentioned principles when designing and the principle of its parallel run with heating system. The result is a paying system which can be easily operated and does not require a lot of investments. Moreover, it enables to adapt easily to changing operational and technological requirements.

The cooperation between ventilation and heating systems in industry large-area buildings is very important. Design of one system without the other causes an increase in operating costs mainly in energy consumption (electricity, heat, cooling, etc.). And there is not ensured required parameters of indoor living area. Therefore, we as designers should keep in mind the rule about creating an optimal working environment for humans, but at the same time at the lowest possible energy consumption. [2]

REFERENCES

[1] M. Kotrbatý, O. Hojer, Z. Kovářová, *Hospodaření teplem v průmyslu, Nejlevnější energie je energie ušetřena.* (The heat management in industry. The cheapest energy is energy spared). Praha : ČSTZ, 2009. 266 p. ISBN 978-80-86028-41-5.

[2] M. Kotrbatý, J. Seidl, *Průmyslové otopné soustavy.* (The industry heating systems). Praha : STP, 2000. 64 p. ISBN 80-02-01693-9

[3] M. Kotrbatý, Z. Kovářová, *Inteligentní průmyslové haly. Část 1.* (The intelligent industry halls. Part No. 1). 2009. www.tzb-info.cz

[4] M. Kotrbatý, *Inteligentní průmyslové haly. Část 2.* (The intelligent industry halls. Part No. 2). 2010. www.tzb-info.cz

[5] L. Oppl, *Větrání v průmyslu.* (The industry ventilation). Praha : SNTL, 1957. 250 p. ISBN – not specified.

[6] M. Kurčová,: *Energeticky úsporné opatrenia a ich vplyv na vykurovacie telesá.* (Energy-saving measures and their impact on heating units). Bratislava: TZB Haustechnik, 2010, vol. 18, issue 2, 34-36 p.

[7] K. Malinová *Plynovody – legislatíva pre projektovanie a realizáciu.* (Pipelines - Legislation for the design and implementation). In Sanhyga 2014: Proceedings from the 19th Scientific and technical conference with international participation. Piešťany, SR 23.-24.10.2014. Bratislava: SSTP, 2014, 147-150 p. ISBN 978-80-89216-66-6.

[8] L. Kajtár, L. Herczeg, E. Láng: *Examination of influence of CO2 concentration by scientific methods in the laboratory.* 7th International Conference Healthy Buildings 2003. Singapore, 12. 07-11. 2003. pp. 176-181, 2003.

[9] J. Nyers, S. Tomic, A. Nyers: *Economic Optimum of Thermal Insulating Layer for External Wall of Brick.* International J. Acta Polytechnica Hungarica Vol. 11, No. 7, pp. 209-222. 2014

[10] L. Herczeg, T. Hrustinszky, L. Kajtár: *Comfort in closed spaces according to thermal comfort and indoor air quality.* Periodica Polytechnica-Mechanical Engineering 44: (2) pp.249-264. (2000)

Reducing the external costs caused by associated petroleum gas flaring in Serbia

F.E. Kiss*, V.R. Rajović**, N. Maravić* and Đ.P. Petkovič***

* University of Novi Sad/Faculty of Technology, Novi Sad, Serbia
** Serbian Petroleum Industry/Gaspromneft Group, Novi Sad
*** University of Novi Sad/Faculty of Economics, Subotica, Serbia
fkiss@tf.uns.ac.rs; vuk.rajovic@nis.eu; maravic@tf.uns.ac.rs; pegy@ef.uns.ac.rs

Abstract– Flaring of associated petroleum gas (APG) causes considerable environmental damage due to emission of greenhouse gases (GHG) and other pollutants. The goal of this paper is to investigate some technological solutions to reduce the external costs associated with APG released at the Serbian oil fields. Consequential life cycle assessment method and external costs valuation techniques were used to evaluate and compare the external costs associated with three potential APG utilization scenarios: *i)* combustion of APG on flares, *ii)* combustion of APG in heat boilers, and *iii)* combustion of APG in combined heat and electricity generation (CHP) plants. Results have showed that the utilization of APG via CHP plants and heat boilers can provide a significant reduction in global GHG emissions and external costs by displacing marginal production of heat and electricity.

INTRODUCTION

Associated petroleum gas (AGP) is a form of natural gas which is found with deposits of petroleum, either dissolved in the oil or as a gas above the oil in the reservoir [1]. Most common use of APG on site is its combustion on flares. More than 150 billion m^3 of APG is flared annually worldwide [2]. In Serbia around 80 million Sm^3 of APG is released annually (data for 2014) as a waste product from the petroleum extraction industry [3].

Combustion of APG on flares results in greenhouse gas emissions (GHG) such as CO_2, CH_4 and N_2O. It is estimated that APG flaring is responsible for approximately two per cent of global CO_2 emissions [4]. Apart from CO_2 other emissions are released with flaring of APG as well. The emissions of these substances cause considerable damage affecting a wide range of receptors including humans, flora, fauna and materials. Such damages impose costs which are not (or only partially) borne by the producer (i.e. they are not or only partially included in the market prices of the products of oil industry); therefore, they represent external costs [5].

A variety of options are available for reducing externalities, ranging from the development of new technologies for APG utilization, the use of fiscal instruments, or the imposition of emission limits [6]. Main barriers for APG commercialization are mainly low prices on natural gas, long distance between potential buyers and production sites and high capital expenses for APG pipeline [7]. Most efficient utilization technologies are combination of gas processing plants (GPP), dry gas sales and electric power generation [2]. APG combustion in heating boilers on oil fields present common method of APG usage [1].

In the last decade petroleum companies had started to produce heat and electric power simultaneously on oil fields from APG [8]. Combined heat and power (CHP) generation presents innovative solution for increasing energy efficiency and reducing specific fuel consumption [9]. Utilization of APG in CHP plants and heat boilers can reduce the environmental burdens associated with APG combustion since the generated electricity and/or heat could displace electricity and/or heat generated in conventional fossil fuelled power plants or boilers.

In this paper we analyse the potential to reduce the external costs associated with APG by its utilization for electricity and/or heat generation. The goal of this paper is to evaluate and compare the environmental external costs associated with three common APG utilization scenarios: *i)* combustion of APG on flares, *ii)* combustion of APG in heat boilers, and *iii)* combustion of APG in CHP plants. The method follows a life cycle approach and it is limited to the assessment of external costs associated with GHG emissions.

METHOD AND MATERIALS

Data collection and characterisation of APG

Monitoring of APG related material and energy flows was conducted in three year timeline (2012–2014) at four Serbian oil fields (A, B, C and D). The average values of relevant data for APG (chemical composition of APG, lower heating value, LHV and gas density, ρ) are presented in Table 1.

TABLE I.
CHEMICAL COMPOSITION AND CHARACTERISTICS OF APG

Oil field	C_1 [a] (%)	C_2 (%)	C_3 (%)	C_4 (%)	C_{5+} [b] (%)	N_2 (%)	CO_2 (%)	LHV MJ·m⁻³	ρ kg·m⁻³
min	60.1	5.2	0.9	0.1	0.3	0.3	1.8	30.7	0.83
max	69.4	16.3	9.3	2.3	10.2	6.6	21.0	41.7	0.89
avg.	66.1	8.1	4.1	1.1	4.8	4.7	11.1	35.4	0.85

[a] C_x refers to the hydrocarbon with corresponding number of C-atoms
[b] All components higher than C_5 fraction are summed as C_{5+}.

L-1 : Crude oil from oil field
L-2 : Crude oil for further processing
L-3 : Water for further processing
L-4 : Associated petroleum gas for flaring
V-1 : Valve for water regulation
V-2 : Valve for crude oil regulation
P-1 : Pump for water regulation
P-2 : Pump for crude oil regulation
D-1 : Three phase separator
D-2 : Compressor
D-3 : Flaring torch

a)

L-1 : Flow of APG to utilization
L-2 : APG directed to boiler
L-3 : APG directed to flare
L-4 : Cold water returned for re-heat
L-5 : Hot water directed to plate heat exchanger
L-6 : Hot water directed to oil tank heat
L-7 : Cold water directed to plate heat exchanger
C-1 : Compressor 1
C-2 : Compressor 2
V-1: Three edge valve
V-2 : Valve for flaring torch
D-1 : Gas boiler
D-2 : Flaring torch
D-3 : Plate heat exchanger
D-6 and D-7: Fluid pumps
D-4 : Oil tank
D-5 : Heat exchanger on oil tank

b)

L-1 : APG directed to gas engine
L-2 : Electric curent directed to the transformer
L-3 : Flue gases from engine
L-4 : Cooling liquid from engine
L-5 : Cooling liquid from flue gas heat exchanger
L-6 : Flue gases to chimney
L-7 : Flue gases to atmosphere
L-8: Cooling liquid directed to gas engine
L-9: Cooling liquid from plate heat exchanger
L-10 : Cooling liquid to plate heat exchanger
V-1 : Valve for directing APG
D-1 : Internal combustion gas engine
D-2 : Generator
D-3 : Transformer
D-4 : Plate heat exchanger
D-5 : Flue gas heat exchanger

c)

Figure 1. Different APG utilization options: a) flaring, b) generation of heat in boilers, and c) generation of heat and electricity in CHP plant

Description of the APG utilization scenarios

This chapter briefly describes the three alternative APG utilization scenarios investigated in this study: *i)* flaring (S1), *ii)* generation of heat via gas boiler (S2), and *iii)* generation of heat and electricity via CHP plants (S3).

Fig. 1a presents the flowchart of APG flaring on the oil fields. The APG is separated from oil and water and directed via compressor to the water seal drum in which the gas flashing occurs. From the seal drum the APG is directed to the torch where it is flared.

In the second scenario (Fig. 1b) the APG is cooled down using a mixture of hydrofluorocarbon compounds

(HPC) and then directed towards gas boiler to generate heat. If heat is not required the APG is flared according to the process described on Fig. 1a. Thermal efficiency of heat boilers on the Serbian oil fields is 83% and this value is used in this study to calculate the amount of useful heat generated in S2.

In the third scenario (Fig. 1c), after the trace water in APG has condensed in the cooling system, the APG is directed to the internal combustion engine of the CHP plant. APG's chemical energy is converted to electricity and thermal energy in the CHP plants. The net electrical and thermal efficiency of CHP plants installed at oil

fields in Serbia are 42% and 40%, respectively. This means that the overall efficiency of CHP plants is 82%.

Emissions associated with APG combustion

In the combustion processes presented in this research, APG and air (oxidizer) are mixed, in order to form a premixed flame and achieve complete combustion of hydrocarbons from APG. Due to the high combustion efficiency, partial products of combustion are formed in a very low concentrations and therefore are consequently neglected in calculations of external costs. The general reaction for complete combustion of hydrocarbons in APG (Table 1) is discribed by the following equation [10]:

$$M(C_xH_y)kgC_xH_y + \left(x + \frac{y}{1}\right) \times M(O_2)kgO_2 \times \left(x + \frac{y}{1}\right) \\ \times 3.762 \times M(N_2)kgN_2 \\ \rightarrow x \times M(CO_2)kgCO_2 + \frac{y}{2} \\ \times M(H_2O)kgH_2O + \left(x + \frac{y}{4}\right) \times 3.762 \\ \times M(N_2)kgN_2$$

The amount of CO_2, as the only GHG formed and considered in the presented combustion processes, is calculated using the equation (1):

$$m(CO_2) = \frac{mass(C_x)}{100} \times k(C_x) \tag{1}$$

Where coefficient k value (Table 2) depends on the combusted hydrocarbon:

TABLE II.
CALCULATED K VALUES WHICH REFER TO THE CORRESPONDING HYDROCARBON FROM APG

	C_1	C_2	C_3	C_4	C_{5+}
$k(C_x)$	2.75	2.93	3.00	3.03	3.06

The above equations were used to calculate the products of APG combustion in all three scenarios. In scenarios involving heat boilers and CHP plants (S2 and S3) a complete combustion of APG was assumed. In contrast, a combustion efficiency of 98% was assumed for flaring (S1), resulting in venting of 2% of APG, taking into account that flaring can be affected by wind or other atmospheric phenomena resulting in poor air mixing with APG.

Emissions in up- and downstream process

Life cycle GHG emissions were estimated using the life cycle assessment (LCA) method, according to ISO 14040:2006, following the principles of consequential LCA [11]. In this study the APG utilization options are considered as different waste management scenarios. Accordingly, the function is defined as the treatment of APG in environmentally favourable way. The functional unit is defined as 1000 Sm^3 of APG.

In addition to the waste treatment function, the scenarios with heat boiler (S2) and CHP plant (S3) have other functions as well (i.e., electricity and/or heat generation). The ISO 14040:2006 requires that the compared systems fulfil the same function; therefore, the secondary functions should be excluded from the system.

In consequential LCA secondary functions are excluded from the assessment using the substitution method [11] where the multifunctional process is credited with the avoided emissions from the alternative way of producing the secondary co-functions. For example, in S2 the primary function of the system is "waste treatment" while the secondary co-function is "heat generation". It is assumed that the heat generated in S2 will displace heat generated from light fuel oil; therefore, the emissions associated with heat generation from light fuel oil can be subtracted from the emissions released due combustion of APG in heat boilers.

In this study it is assumed that electricity generated in S3 will displace electricity generated in lignite-fuelled power plants in Serbia, whereas the heat generated in S2 and S3 displaces heat generated in industrial boilers fuelled with light fuel oil. GHG emissions associated with the displaced processes are available from the Ecoinvent 3.1 database [12] under the following titles: "Electricity, high voltage {RS}| electricity production, lignite" and "Heat, light fuel oil, at boiler 100kW, non-modulating/CH".

GHG specific damage cost factors

There are many studies which aimed to determine the external costs associated with GHG emissions. Maibach et al. [13] have performed a detailed and comprehensive review of these studies in order to provide estimations on damage costs or avoidance costs associated with GHG emissions. GHG specific damage costs still display a large spread, indicating the high level of uncertainty still attached to this approach. Based on their review Maibach et al. [13] have recommended 25 EUR·Mg^{-1} CO_2 as the central value for the assessment of damage costs associated with climate change. In this study we have adopted this value for the assessment of external costs associated with CO_2 emissions. The damage costs for other GHGs are calculated by multiplying the damage cost factor of CO_2 with the global warming potential factors of CH_4 and N_2O which are 23 and 296, respectively [14]. Therefore, the external costs associated with CH_4 and N_2O emissions are 575 EUR·Mg^{-1} and 7400 EUR·Mg^{-1}, respectively.

The environmental external cost (EC) of specific APG utilization scenario is calculated using (2).

$$EC = \sum_{i=1}^{n} E_i \cdot C_i - \sum_{i=1}^{n} \sum_{z=1}^{m} E_{z,i} \cdot C_i \tag{2}$$

where: E_i is the gross quantity of emission i associated with the specific APG utilization scenario (i.e. before the substitution method is applied); $E_{z,i}$ is the quantity of emission i associated with the provision of equivalent function of the displaced process z; m is the number of

displaced processes; C_i is the damage cost factor for emission i (in EUR·kg^{-1} emission); and n is the number (type) of emissions covered with the analysis.

RESULTS AND DISCUSSION

Table 3 shows material and energy flows associated with the three potential APG utilization options. Values are average for the four oil fields investigated. Since global warming is in the focus of this research the Table contains data merely on GHG emissions. Gross flows refer to total emissions released with combustion of 1000 Sm^3 of APG without considering the benefits from avoided emissions from the displaced process. On the other hand, net results take into account the avoided emissions associated with the displaced processes due to electricity and/or heat production in S2 and S3.

Gross values show similar results for each of the three investigated APG utilization scenarios (from 2015 to 2283 kg CO$_{2eq}$ per 1000 Sm^3 of APG). Gross impacts are the highest for the scenario with the heat boilers (S2) since LCA results also include the GHG emissions associated with the production of electricity used to power circulation pumps, control system etc, which is around 0.0056 kWh per MJ of APG combusted in heat boilers [15]. In this study it was assumed that the auxiliary electricity is supplied by Serbian lignite-fired power plants.

Net values show the results after avoided emissions associated with the displaced processes are subtracted from gross results. Unlike the gross results, the net results show a considerable variation. The inclusion of avoided burdens into the assessment has a significant impact on LCA results. For example, S2 has higher gross global warming impact than S1 (2283 kg CO$_{2eq}$ compared to 2226 kg CO$_{2 eq}$; Table 3), but thanks to its heat output it can replace 30.06 GJ of conventional heat from light fuel oil which provision would cause emission of 2814 kg CO$_{2eq}$ (Table 3). Therefore, the net global warming impacts associated with S2 were estimated at -532 kg CO$_{2eq}$. The negative value means that S2 will not increase the concentration of GHGs in the atmosphere; instead it has the potential to reduce it due to avoided GHG emissions from the displaced process. In S3 the

CHP plant has two energy outputs (14.8 GJ of electricity and 14.2 GJ heat); therefore, the environmental benefits are even more pronounced. The avoided global warming impacts are estimated at 6946 kg CO$_{2eq}$, which gives a net impact of -4932 kg CO$_{2eq}$ per 1000 Sm^3 of APG combusted in CHP plants.

Fig. 2 shows the gross and net external costs caused by GHG emissions released in the life cycle of the tree alternative scenarios. Positive results in waste treatment processes show external costs, i.e. marginal environmental damage, while negative values indicate savings [16]. Therefore, negative value refer to marginal environmental benefit which occurs when external costs associated with the avoided impacts are larger than external costs associated with the waste treatment process.

External costs associated with flaring are estimated at 55.7 EUR per 1000 Sm^3 of APG flared (Fig. 2). This is higher than those resulting from other waste treatment options due to CH$_4$ emissions resulting from partial combustion (see Section C) and the absence of energy recovery. Utilization of APG in heat boilers (S2) and CHP plants (S3) would result in net savings since the external costs associated with the displaced process(es) are higher than the external costs caused by emissions released due to APG combustion (Fig. 2). The net external costs of S2 and S3 were estimated at -13.3 and -123.3 EUR per 1000 Sm^3.

The results on Fig. 2 assume full energy recovery in the case of S2 and S3. In Serbia, high-efficiency CHP plants have a non-discriminatory access to the national electric grid [17]; thus, it is realistic to assume a 100% realization rate for electricity. Full realization of thermal energy is often not possible due to the absence of sufficient and stable local heat demand. Therefore, the assumption that 100% of heat produced in S2 and S3 will displace alternative heat generation process might be too optimistic. Sensitivity analysis has been performed in order to show the sensitivity of S2 and S3 to the potential heat utilization rate. Fig. 3 shows the results of external cost valuation if the rate of heat utilisation is reduced from 100% to 0%.

As shown in Fig. 3 the possibility of heat utilization

TABLE III.

MATERIAL AND ENERGY FLOWS AND EXTERNAL COSTS ASSOCIATED WITH THE THREE APG UTILIZATION SCENARIOS (PER 1000 SM^3 OF APG)

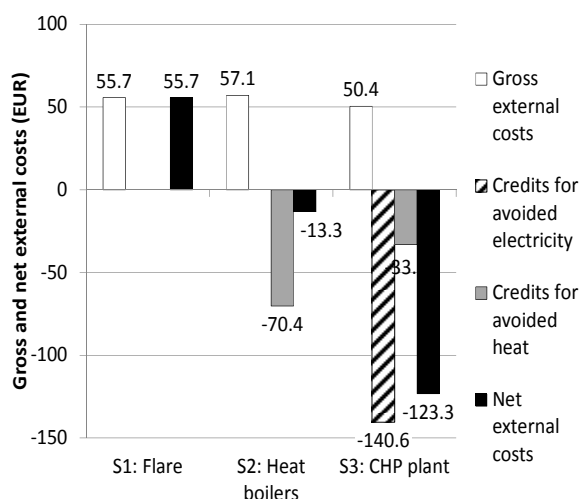| Flows	Unit	S1: Flared*	S2: Heat boilers			S3: CHP plants			
			gross*	DP: heat	net	gross*	DP: electricity	DP: heat	net
Input									
APG	GJ	35.36	35.36	0	35.36	35.36	0	0	35.36
Electricity	GJ	0	0.71	n.a.	n.a.	0	n.a.	n.a.	n.a.
Output									
Electricity	GJ	0	0	0	0	14.85	-14.85	0	0
Heat	GJ	0	30.06	-30.06	0	14.15	0	-14.15	0
Heat (waste)	GJ	35.36	n.a.	n.a.	n.a.	n.a.	n.a.	n.a.	n.a.
GHG emissions									

Figure 2. Gross and net external costs associated with the three alternative APG utilization scenarios (EUR per 1000 Sm^3 of APG)
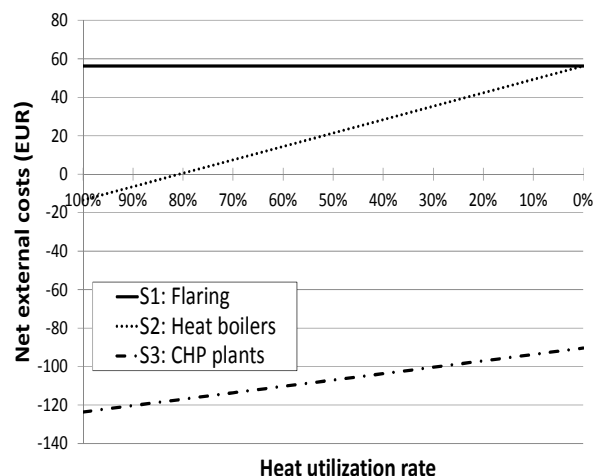

Figure 3. Net external costs of APG utilization depending on the heat utilization rate (EUR per 1000 Sm^3 of APG)

has significant impact on the environmental external costs of S2 and S3. Therefore, this aspect should be considered when making decision on the appropriate APG utilization technology and equipment. Unsurprisingly, the scenario with heat boilers (S2) is much more sensitive to this parameter than the scenario with CHP plants (S3). For example, at 50% utilization rate of heat generated in S2 the net external costs are 21 EUR per 1000 Sm^3 (Fig. 3) which is an increase of 259% compared to the 100% heat utilization rate scenario. On the other hand, in S3 if the heat utilization rate decreases from 100% to 50% the external costs associated with S3 scenario would increase only by 13% (from -123 EUR to -107 EUR; Fig. 3)

It is estimated that around 80 million Sm^3 of APG is released from the Serbian petroleum extraction sites annually [3]. If the total amount of APG is flared this would cause 4.2 million EUR damage due to GHGs released with the combustion of APG. On the other hand, if 100% of APG recovered from Serbian oil fields is used in CHP plants instead of 100% flaring the external costs associated with APG could be reduced by 14 million EUR annually (assuming average heating value of APG and full heat recovery). Even at 0% realization rate for heat, the expected savings are still significant, around 10 million EUR annually.

CONCLUSIONS

Flaring of APG causes considerable environmental damage due to significant amount of greenhouse gases released into the atmosphere. The external costs of flaring were estimated at 55.7 EUR per 1000 Sm^3 of APG. At the investigated Serbian oil fields the average lower heating value of APG was 35.4 MJ·Sm^{-3}. APG can be used as fuel in heat boilers and cogeneration plants. Utilization of APG in heat boilers and cogeneration plants could reduce the global GHG emissions and external costs by displacing marginal production of heat and electricity. Usage of APG in cogeneration plants instead of heat boilers is advantageous from environmental aspect due to

lower external costs. Full utilization of APG in CHP plant could reduce the external costs by 10–14 million EUR annually compared to the 100% flaring scenario.

REFERENCES

R. Tonje Hulbak, "Associated Petroleum Gas in Russia: Reasons for Non-utilization," Fridtjof Nansen Institute, 2010.

Anonymus, "Using Russia's Associated Gas," Prepared for the Global Gas Flaring Reduction Partnership and the World Bank, by PFC ENERGY, 2007.

Anonymus, "Gas Overview," Internal document: Serbian Petroleum Industry, 2014.

M. F. Farina, "Flare Gas Reduction: Recent global trends and policy considerations," General Electric Company, 2011.

M. Holland, and A. Wagner (ed.) "Revealing the costs of air pollution from industrial facilities in Europe" EEA Technical report No 15, 2011.

J. V. Spadaro, and A. Rabl, "External costs of energy: application of the ExternE methodology in France - Final Report," 1998.

M. Ermolovich, Deputy Director for international Energy Cooperation, Russian Gas Society, Interview, October 31st, 2011.

Center for Climate and Energy Solutions. Climate TechBook: Cogeneration/Combined Heat and Power (CHP). Available at: *http://www.c2es.org/docUploads/CogenerationCHP.pdf [11.03.2015]; 2011*

M. A. Rosen, "Reductions in energy and environmental emissions achievable with utility-based cogeneration: simplified illustrations for Ontario," *Appl. Energy*, vol. 61(3), pp. 163–174, 1998.

O. S. Ismail and G. E. Umukoro, "Modelling combustion reactions for gas flaring and its resulting emissions," *J. King Saud Univ. Sc.*, 2014.

T. Ekvall, and B. Weidema, "System boundaries and input data in consequential life cycle inventory analysis," Int. J. Life. Cycle. Assess, vol. 9, pp. 161–171, 2004.

B.P. Weidema, Ch. Bauer, R. Hischier, Ch. Mutel, T. Nemecek, J. Reinhard, C.O. Vadenbo, and G Wernet, "The ecoinvent database: Overview and methodology," Data quality guideline for the ecoinvent database version 3, www.ecoinvent.org 2013.

M. Maibach et al., "Handbook on estimation of external costs in the transport sector," Produced within the study Internalisation Measures and Policies for All external Cost of Transport (IMPACT) Version 1.1, Delft, 2008.

IPCC 2011, "Climate Change 2001: The Scientific Basis. Contribution of Working Group I to the Third Assessment Report of the Intergovernmental Panel on Climate Change," Cambridge

University Press, Cambridge, United Kingdom and New York, NY, USA, 2001.

N. Jungbluth, "Erdöl. Sachbilanzen von Energiesystemen, " Final report No. 6 ecoinvent data v2.0.; vol. 6. Swiss Centre for LCI, PSI. Dübendorf and Villigen, CH. 2007.

O. Parkes, P. Lettieri, and I. D. L. Bogle, "Life cycle assessment of integrated waste management systems for alternative legacy scenarios of the London Olympic Park," *Waste Manage*, vol. 40, pp. 157–166, 2015.

M. Tešić, F. Kiss, and Z. Zavargo, "Renewable energy policy in the Republic of Serbia," *Renew Sust Energ Rev*, vol. 15(1), pp. 752–758. 2011.

J. Nyers, P. Komuves, "Optimum of External Wall Thermal Insulation Thickness using Total Cost Method", EXPRES 2015 Subotica, 7th International Symposium on Exploitation of Renewable Energy Sources and Efficiency. 2015.03.19-2015.03.21. Subotica, pp. 13-17.

Possibility Cooperation of Space Heating System with Heat Pump

Kurčová, M. * Ehrenwald, P. *

* Slovak University of Technology in Bratislava, Faculty of Civil Engineering, Department of Building Services, Slovakia

e-mail: maria.kurcova@stuba.sk, pavel.ehrenwald@stuba.sk

Abstract – **Operation of space heating systems heat pumps (HP) must cover changing heating needs - must adapt to the immediate loads. Therefore is required regulation his performance. If compressor is not secured, supply to condenser more refrigerant, than cannot condense it. Coming to the increase of pressure in condenser and subsequently increase also temperature of condensation. The role of regulation is adaptation of refrigerant flow immediately to the condenser load.**

*Key words* **– heat pump, heating system**

I. INTRODUCTION

In operation of space heating systems heat pumps (HP) may be cover variable heat needs – must be adapt instantaneous loads. Therefore is necessary control of their performance. If compressor is not secured, supply to condenser more refrigerant, than cannot condense it. Coming to the increase of pressure in condenser and subsequently increase also temperature of condensation. The role of regulation is adaptation of refrigerant flow immediately to the condenser load.

II. DUAL POSITION REGULATION

Heat pumps with piston compressors with heating capacity from 10 until 25 kW many times are possible to regulate only with dual position regulation mode. The frequency of switching depends on permission of regulated quantity and of accumulation ability of space heating system. Regarding of compressor life cycle, switching will be not very frequently.

Trouble appears especially at heat pumps type air - water. At low loads needed heat flux in condenser rapidly decrease, whereas heat flux in evaporator increase consequently of higher temperature of atmospheric air. Compressor will switch on short-timed and long-timed switch of, that adapt to requested heat needed. For eliminate this disadvantage recommend mainly at low loads arrange a compensation vessel. His function is to separate heat offer of HP from heat need for space heating of building. In compensation vessel is possible to accumulate a part of heat, produced in heat pump. Periods of switch on and switch out are elongated. From point of view of hydraulic, this separation has advantage in that, changing of flow in heating system not influence of condenser operation.

The regulation in this case realized across temperature girth. Beyond compensation vessel temperature observe also temperature of returned water to the HP. In case that return temperature rise over adjusted, requested value, occur the turn off HP. Circulating pump of space heating system though operate continuously whereby, compensation vessel as a result take away of heat flow is chilled. In case of decrease of temperature in vessel, HP switch on and again heated the compensation vessel (*Fig. 1*).
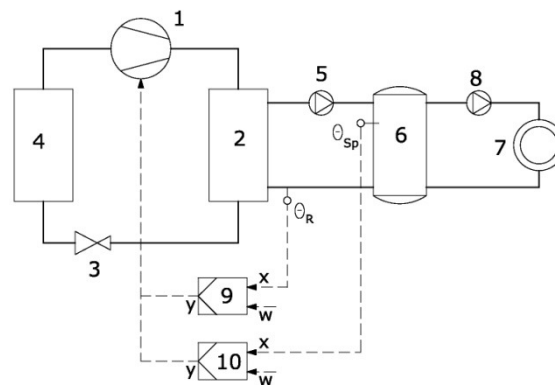
Regulation circuit (dual position regulation)
1-compresor, 2-condenser, 3-expansion valve, 4-evaporator, 5-loading pump, 6-compensation vessel, 7-consumer, 8-circulatimg pump, 9, 10- dual position regulation

III. REGULATION OF EVAPORATOR

Feeding of required quantity of refrigerant, what evaporator capable evaporate, provide expansion (portioning) valve. Function of expansion valve that limited refrigeration flow into the evaporator. If in the evaporator a refrigerant inlet less than it is needed, pressures in evaporator decrease and across expansion valve extend refrigerant flow.

When refrigerant mostly measure evaporated a from evaporator output, the thermostat initiate further open of expansion valve. Converse the expansion valve close, if evaporation on the exit from evaporator is not finish. Instead of thermostatic regulation of expansion valve now use expansion valves with electronic handle. HP in common case is controlled with thermostatic principle of (*Fig. 2*). If pressure in evaporator come down requested value, the expansion valve open and dosage the refrigerant.
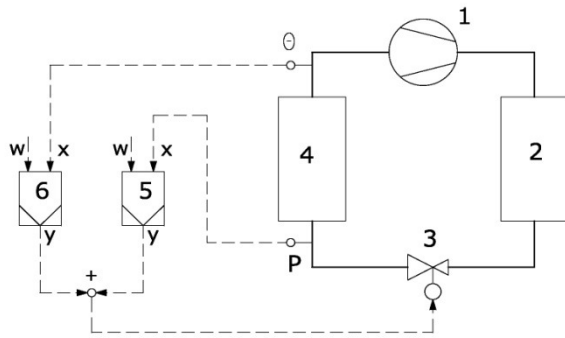
Regulation of evaporator
1-compressor, 2-condense, 3-expansion valve, 4-evaporator,
5-pressure regulator, 6-temperature regulator

IV. KOMPLEX REGULATION OF HEAT PUMP

On the *Fig. 3* represetn a scheme of complex regulation of HP type air – water, what maybe take for consider whole satisfide.
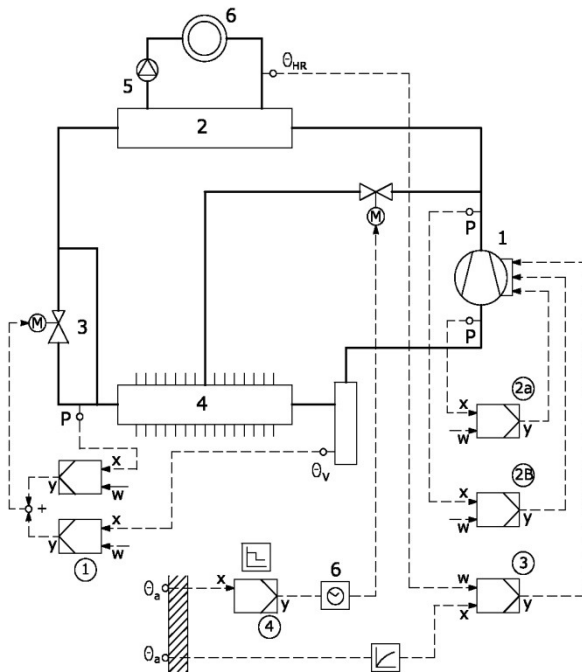
Scheme of regulation heat pump type air - water
1-compresor, 2-condenser, 3-expansion valve, 4-evaporator,
5-ciculation pump, 6-consumer, M-servomotor, θ_V-superheating temperature in compressor suck in, θ_a-external temperature, θ_{HR}-temperature of backwards heating water; regulation circuits: (1) expansion valve with thermostat and pressure compensation, (2a) low pressure guard, (2b) high pressure guard,
(3) performance regulator (4)equipment for defrost with hot gases

There are realized following regulation, respectively control circuits:

- Regulation of evaporator wijh expansion valve with thermostat and pressure compensation, in expansion in capilar tube damper the vibrations.
- Low or high pressure guard. Inmany cases on water

side is added water flow guard, especially in cases of HP water- water.

- Dual position regulator, for regulationof performance. Regulated quantity is temperature of backwards heating water.
- From adjusting external temperature (ffor example +3 °C) through switching clock evaporator is periodical defrosted with hot refrigerant gases.

V. HEAT PUMP AS A MONOVALENT HEAT SOURCE FOR FLOOR HEATING SYSTEM

Heat transmission to the heated space realized with whole area of floor. Heating pipelines are situated in plaster layer, or in the floorpanel structure and are components of closed heating circuit connect to the condenser of heat pump. Floor heating system, thanks his large heat transfer spaces is designate for lowtemperature operation. Low supply temperature give ideal condition of heat pumps high coefficient of performance.

Regulation properties of floor space heating systems, however are not problem free. Heting pipes installed to the floor, at first delver heat to the plaster layer. When this layer may be thickness of 10 – 15 cm, present great heat capacity. At rapid changet of heat load in space, influence of solar radiation, large quantity of people, etc., heat flow stick up for break down, as if further intake of heat across piping completely shut off.

So-called effect of floor heating self-regulation affect operate again. If inmean thermal load (external temperature around 0 °C and surface temperatureof floor is between 22 and 25 °C) growing the temperature in space on quantitiy of floor temperature or higher, breaking any heat flux to this space. But if required lower temperatures, for example in the night, it is impossible to reach rapidly changes of space temperature. From hygienic occasion, surface temperature of floor don't pass value of 27 °C.
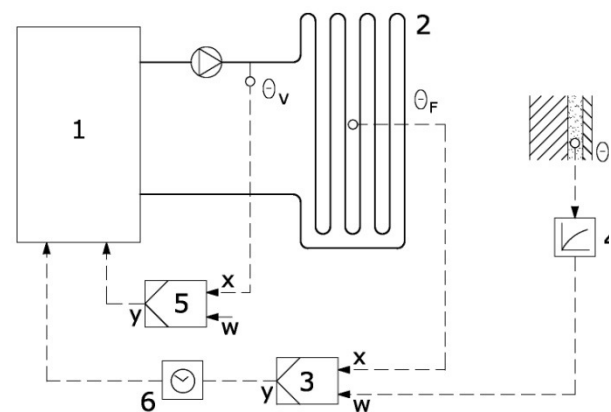
Regulation of heated water temperature according
of external temperature
1-heat pump, 2-floor heating system, 3-temperature regulation,
4-adjusting of demanded quantitiy according of heating curve,
5-limiter of maximal temperature, 6-control device of operation period,
θ_F-floor temperature, θ_a-external temperature, θ_V-temperature of supplied heating water

For solution these requirement weil tried regulation of heating water temperature depending on exterior temperature (*Fig. 4*). Measures temperatures of heating water on supply or backwards twig of space heating circuit and also in floor (sensor of remainder heat). Senzor of meterological conditions, follow main disturbing quantitiy – the external temperature. Excepting temperature of outdoor air, solar radiation and wind speed, also temperature of walls and the thermal inertia of building, have fundmental influence for heat need of building.. Senzor will be integrated into building condtruction of external wall.

On the basis of heating curve, his inclination depend mainly from building construction, in case start of space heating system, e. g. at 15 °C of external temperature, switch on the heat pump, until temperature of heating water achieved required value, e. g. 25 °C. In according with accumulation kapacity of building, it is possible adjust temperature of heated space and freqvency of compressor switchin:

- Beginning of regulation, - beginning point of heating curve,
- Temperature of heating water – shift of heating curve,
- Influence of external temperature – adjusting slope of heating curve.

Each od three caces removing requested value of dual position regulator, whose manages switch in or switch out of heat pump. Temporaly contactor (protective switch of heatpump lifetime) secure that, heat pump will switch on or switch out no fewer than 3 intul 6 minits period. Maximum temperature of heating water guard regulator limitation of maximum.Thereby is possible defend overrun maximally available temperature of floor, eventually maximall temperature in condenser.

Floor space heating systems have large accumulation capacity. Space hating with heat pump is possible operate discontinous also without compensating store receiver, e. g. with break in heating a terme daily three time 2 hour. And even no occcur sensible decrease of heat comfort in space hating area.

VI. CONCLUSION

Performance regulation of HP with discontinous compressor operation control, we noted above, applies at greater arrangements, as are multi pistons compressors or parallel ordering compressors operate in cascade. In first group in cylinders use adjustable stroske sucking and discharge valves or direct cloes-up of sucking pipes. In second group, compressors will switch on or switch out in successive steps according to neded load. Nevertheles after certain number of operating hours, automatically cyclical change order of compressor operation. In bigger application, where needed accurately dosing heat to the consumer system, advantageous choise continous heat pump performance regulation – control of compressor regulation by frequency converter. It is exacting investment, but these solution may be yield widely operating savins and enhancing heat comfort.

Above regulations modes from wiew instruments at present time adequate character of gigital regulation. Are programable with adjusting parameters across web applications in PC or by touch on LCD display, whose are heat pump component. Guaranted simple handling, comprehensible command and enable implenetation between heat sourcesand and heat consumer defining priority application. Self-evidence is also now, self-diagnostic or possibility of distance diagnostic across webserver.

REFERENCES

C. F. Müller, Regelungs- und Steuerungstechnik in der Versorgungstechnik. Heidelberg, 2002.

VALTER, J. Regulace v praxi. BEN, Praha, 2010.

FÜRI, B. Practical experiences with multi-compressor refrigeration systems, Proceedings of 6th International Conference on Compressors and Coolants – Compressors 2006, 27. - 29. 9. 2006, Častá – Papiernička, p. 158– 161. ISBN 80-968986-5-5

FÜRI, B. ŠVINGÁL, J. Some experimental results with ammonia base azeotropic refrigerant R 723 in small heat pump, p. 139 – 142. Proceedings of 7th International Conference on Compressors and Coolants – Compressors 2009, 30. 9.- 2. 10. 2009, Častá - Papiernička, ISBN: 978-80-89376-02-2

J. Nyers, L. Nyers: "Monitoring of heat pumps". 'Studies in Computational Intelligence', Springer's book series, ISBN 978-3-642-15220-7 Vol. pp. 243, 573-581, Heiderberg, Germany. 2009.

J. Nyers, A. Nyers: "COP of Heating-Cooling System with Heat Pump" IEEE International Symposium "EXPRES 2011." Proceedings, ISBN 978-1-4577-0095-8, pp.17-21, Subotica, Serbia. 11-12 03. 2011.

L. Herczeg, T. Hrustinszky, L. Kajtár: Comfort in closed spaces according to thermal comfort and indoor air quality. Periodica Polytechnica-Mechanical Engineering 44: (2) pp.249-264. (2000)

L. Kajtár, L. Herczeg, E. Láng: Examination of influence of CO2 concentration by scientific methods in the laboratory. 7th International Conference Healthy Buildings 2003. Singapore, 12. 07-11. 2003. pp. 176-181, 2003.

J. Nyers, L. Garbai, A. Nyers: A modified mathematical model of heat pump's condenser for analytical optimization. International J. Energy. Vol. 80, pp. 706-714, 2015.

Magyar Zoltán, Garbai László, Jasper Andor Risk-based determination of heat demand for central and district heating by a probability theory approach ENERGY AND BUILDINGS 110: pp. 387-395. (2016)

Nyers J., Nyers A.: "Hydraulic Analysis of Heat Pump's Heating Circuit using Mathematical Model". 9rd IEEE ICCC International Conference" Proceedings-USB, pp 349-353, Tihany, Hungary. 04-08. 07. 2013. ISBN 978-1-4799-0061-9

Effect of air-diffuser' offset ratio on draught comfort in a slot-ventilated room

Balázs Both*, Zoltán Szánthó**

* First author, Budapest University of Technology and Economics/Building Service and Process Engineering, Budapest, Hungary

** Second author, Budapest University of Technology and Economics/Building Service and Process Engineering, Budapest, Hungary

* both@epget.bme.hu
** szantho@epget.bme.hu

Abstract—**Slot-ventilated rooms are widely used in comfort type HVAC (stands for Heating, Ventilation, Air Conditioning) systems. Location of the slot air-diffuser is an important designing parameter of room air distribution in ventilation systems. Offset ratio (OR) of the slot-diffuser is the non-dimensional horizontal distance between the wall and the air inlet. This OR value can influence room airflow characteristics including draught comfort. In this article effect of various offset ratios was investigated on room's draught comfort. The investigations included air velocity and temperature measurements and the measured data were evaluated using statistical methods.**

INTRODUCTION AND THEORETICAL BACKGROUND

People spend most of their life in closed spaces so it is important to provide acceptable air microclimate parameters. Air velocity, turbulence intensity and air temperature – like the most important microclimate parameters – effect the draught comfort in rooms [1]. Slot-ventilated rooms like e.g. offices are widely used in HVAC designing practice. In these ventilated spaces usually a linear slot diffuser is commonly used as air inlet. This diffuser is usually located next to a wall surface as shown in Fig. 1. The main advantage of such slot diffuser placement is that supply air is injected outside of the occupied zone of the room. As a result the draught risk can be decreased in the space [2], [3].

On Fig. 1 it can be seen that supply air flows out from the slot diffuser and a negatively pressurized recirculation zone appears between the supplied air jet and the wall. Then the Coanda-effect appears and the injected air jet bends towards the wall and adheres to the surface at the attachment point. After this, the injected air jet flows along the wall surface and then ventilates the room. The vertical distance between air inlet and the attachment point is the attachment distance (y_a) which can influence room airflow [4], [5].

The horizontal distance between the slot diffuser and the wall surface is h, so the offset ratio (OR) of the diffuser is:

$$OR = h/s_0, \text{ m/m.} \tag{1}$$
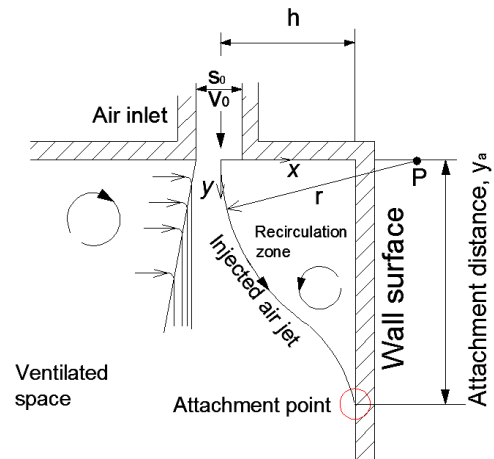
Figure 1. Sketch of the injected air jet into the room

Fig. 2 shows a simple sketch of the slot ventilated room. The injected air jet, which is the primary airflow induces secondary airflows in the room. These primary and secondary airflows make an air distribution system in the room [2].
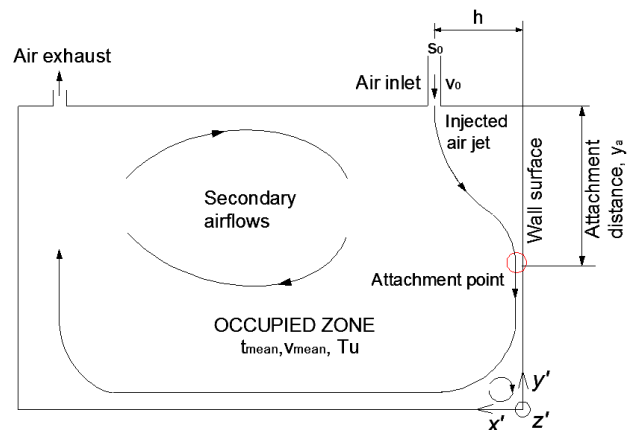
Figure 2. Sketch of the slot-ventilated room

The inlet (or slot) Reynolds-number can be calculated using the inlet air velocity magnitude (v_0), slot width (s_0) and the kinematic viscosity of the injected air ($v_0 = 1.5*10^{-5}$ m²/s on 20 °C):

$$Re_0 = (v_0*s_0)/v_0. \tag{2}$$

The previously defined OR and Re_0 are important inlet parameters of room air distribution design. These

55

parameters effect air velocity and temperature distribution in ventilated rooms. It is a well-known fact that air velocity is a time-dependent quantity which has an average (v_{mean}) and a fluctuating value (v_{RMS}, where RMS stands for Root Mean Square) around the average. Using the average and RMS velocity components, turbulence intensity of the airflow can be calculated [6]:

$$Tu = (v_{RMS}/v_{mean})*100 \%. \qquad (3)$$

Average air velocity, turbulence intensity and temperature (t_{mean}) are the main features of draught comfort in rooms. The most common and internationally accepted model to predict draught comfort in rooms in Europe is Fanger's draught model – or DR model. This model is based on a calculated DR (Draught Rate) number, which is a semi-empirical formula and describes draught comfort in the room [6].

$$DR = (34-t_{mean})*(v_{mean}-0.05)^{0.62}*(0.37*Tu*v_{mean}+3.17), \%. \qquad (4)$$

Note that equation (4) can be valid for one point in the room, or it can be used for the whole room. According to standard CR 1752:2000 [s1] the occupied zone of the ventilated room can be categorized from the aspect of draught comfort. Category A is the best (DR ≤ 15 %) and it is followed by category B (15 < DR ≤ 20 %) and finally category C (20 < DR ≤ 25 %).

Considering the previous statements, it is important to predict air velocity, turbulence intensity and DR in the room to describe draught comfort. Several researchers have investigated draught comfort in the past decades. The most accepted and well-known researches of draught comfort in closed spaces come from Fanger et al [1], [6], [7]. They have investigated the main parameters of draught comfort like air velocity, turbulence intensity and air temperature in whole rooms. The investigation were based on experimental methods including measurements in rooms. The exact type of the applied room air distribution – especially the slot-ventilated room air distribution – was not considered in these researches. They have only made the difference between displacement and mixing ventilation systems. T. Magyar, R. Goda et al. [2], [3], [8], [9], [10] took experimental and numerical investigations on slot-ventilated rooms to describe draught comfort. Cao [11], Rohdin and Moshfegh [12] used experimental method and numerical simulation to model room airflow. Moureh and Flick [13], [14] also took experimental and numerical researches in slot-ventilated rooms. All of the previously introduced authors investigated room airflow in the occupied zone of the ventilated space. In most of these investigations inlet Reynolds-number was the changing parameter.

Some researchers like Nozaki et al. [4], [15], Nasr and Lai [5], Rathore and Das [16] only investigated injected air jets and their attachment process near the air inlet and did not consider the airflow inside the room. In these researches inlet aspect ratio, offset ratio and Reynolds-number were the changing parameters.

Based on recent literature review it is obvious that most of the researchers investigated air inlet and room airflow separately and did not consider the effect of air diffuser' offset ratio on room airflow and draught comfort;

INVESTIGATION AIMS

The primary aim of the current investigation is to predict the effect of air diffuser' offset ratio on a slot-ventilated room's draught comfort. In order to achieve this primary aim it is needed to investigate the average values of air velocity and turbulence intensity in the room. These turbulent parameters play an important role in designing indoor air comfort and room air distribution. DR number can be calculated by measuring air velocity and temperature and then qualification of the room's draught comfort can be made according to standard CR 1752:2000 [s1].

Each problem in engineering sciences can be solved in three ways: with analytical, experimental and numerical methods. Based on recent literature review the analytical solution method is too complicated and requires too much time because of the 3D feature of room airflow. In this article the experimental method was chosen.

EXPERIMENTAL METHOD

Air velocity and temperature measurements were taken in a full-scale test room (office-model) in the Ventilation Laboratory of Budapest University of Technology and Economics. Average air velocity was measured in the air inlet with a hot-wire anemometer and then the inlet Reynolds-number was calculated using equation (2). All of the measurements were done according to the relevant standards [s2], [s3], [s4] [s5]. Offset ratio (OR) of the slot diffuser was the changing parameter during the measurements.

The measurements were took in four relevant heights in the occupied zone of the room according to standard EN ISO 7726 [s4]: ankle level (0.1 m from floor), knee level (0.6 m from floor) and head level of sitting (1.1 m from floor) and standing persons (1.7 m from floor). At each level 29 measurements points were used, which means 116 measurement points in the whole occupied zone. Air velocity ($v_{mean,i}$) and temperature ($t_{mean,i}$) were measured by omni-directional hot sphere probes at the relevant point (i) in each height. The sampling frequency of each probe was 3 Hz and the applied sampling time was 200 seconds according to the relevant standards [s4], [s5]. Using the measured data turbulence intensity and DR number could be calculated with equations (3) and (4). Basic area of the test room was 3*3 m and the nominal height was 2.8 m. Main direction of the air injection and exhaust was vertical.

Main boundary conditions for the measurements were:
- Isothermal air injection;
- Steady-state condition;
- Applied slot-Reynolds-number was $Re_0 = 2500$;
- Nominal length of the slot-diffuser was $L_0 = 1000$ mm;
- Nominal width of the diffuser was $s_0 = 12$ mm;
- Applied offset ratio range was OR = 5÷30;
- Basic area of the test room was 9 m^2;
- Interior height of the room was 2.8 m.

Measured data were evaluated using mathematical statistical methods [17].

Average air velocity could be calculated in each measurement height, using the measured values in 29 points:

$$v_{mean} = 1/n * \Sigma v_{mean,i, \, i \, = \, 1...29} \qquad (5)$$

Based on equation (5), there are four average air velocities at the four heights at each offset ratio. Changing of average air velocity is plotted on Fig. 3 as a function of inlet offset ratio (OR). Average air velocity was found to be constant at ankle level based on the Abbe and general regression tests at probability level 95 %. Expected value of the average air velocity at ankle level is 0.230 m/s and confidence intervals on different probability levels are:

$$P(0.222 \leq v_{mean}, \, m/s \leq 0.238) = 0.90 \qquad (6)$$
$$P(0.221 \leq v_{mean}, \, m/s \leq 0.239) = 0.95 \qquad (7)$$
$$P(0.218 \leq v_{mean}, \, m/s \leq 0.242) = 0.99 \qquad (8)$$

At the other three measurement heights, above ankle level, average air velocity was increasing linearly as OR was higher. Correlation square between the measured data is above 0.90, which means an acceptable linear connection [17].
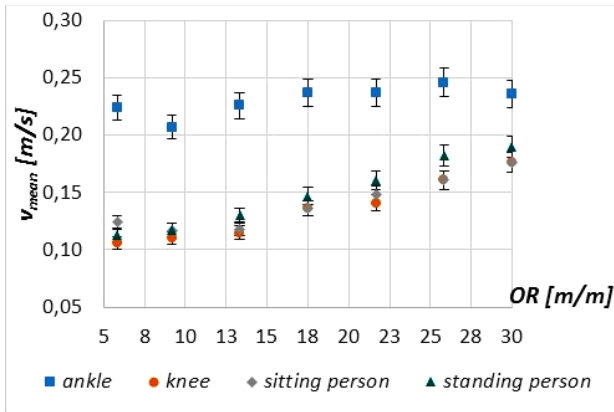

Figure 3. Average air velocity at the four heights as a function of inlet offset ratio (OR), $Re_0 = 2500$, $L_0 = 1000$ mm, $s_0 = 12$ mm

Average air velocities in the four relevant heights at a certain offset ratio are plotted on Fig. 4. It is obvious that at ankle level are higher air velocities than in the other three heights. Main reason of this tendency is the airflow characteristic of the slot-ventilated room. Due to Fig. 2 primary air flows on the floor while in the middle of the room are secondary airflows, induced by the primary airflow. In the primary airflow there are always higher air velocities than in the secondary flow. Average air velocity range is about two times higher at knee, sitting and standing person's head levels than at knee level. This range is between 0.20 and 0.25 m/s at ankle level and between 0.10 and 0.18 at the other three levels, considering the measurement uncertainty, which is 5 % according to the applied probes.
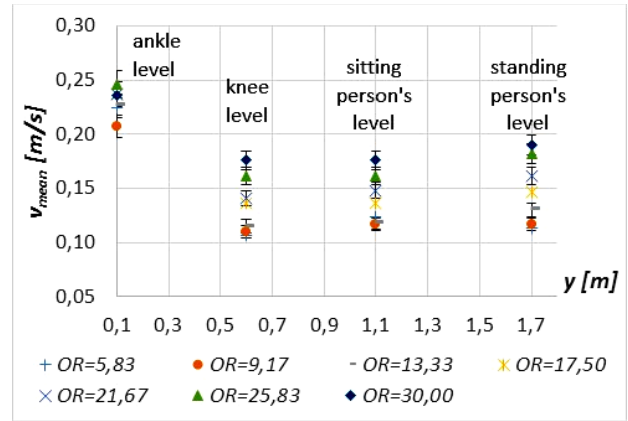
Figure 4. Average air velocities at the four heights, $Re_0 = 2500$, $L_0 = 1000$ mm, $s_0 = 12$ mm

Average turbulence intensity was calculated in each measurement height, using the measured values in 29 points:

$$Tu_{mean} = 1/n * \Sigma Tu_{i, \, i \, = \, 1...29} \qquad (9)$$

This average Tu was determined at all measurement heights and was found to be constant at ankle level at p=95 % with an expected value Tu = 27 %. Confidence intervals on different probability levels are:

$$P(26.7 \leq Tu_{mean}, \, \% \leq 27.3) = 0.90 \qquad (10)$$
$$P(26.6 \leq Tu_{mean}, \, \% \leq 27.4) = 0.95 \qquad (11)$$
$$P(26.5 \leq Tu_{mean}, \, \% \leq 27.5) = 0.99 \qquad (12)$$

At the other levels the turbulence intensity is increasing as OR becomes higher. Main reason of this increasing is that there are bigger recirculation zones between the wall and the injected air jet if the slot diffuser is further away from the wall (OR is higher). In bigger recirculation zones turbulence intensity is also higher [1], [5], [6].

Average turbulence intensity intervals at the four levels are in Table I. At ankle level is the lowest average turbulence intensity, which is constant. At the other three heights, size of the average turbulence intensity range is almost the same in the range of OR = 5÷30.

TABLE I.
AVERAGE TURBULENCE INTENSITIES AT THE FOUR HEIGHTS, IN THE RANGE OF OR = 5÷30

Ankle level (0.1 m from floor	Knee level (0.6 m from floor)	Head level of sitting person (1.1 m from floor)	Head level of standing person (1.7 m from floor)
27 % constant	33÷41 %	34÷41 %	34÷37 %

Fig. 5 contains the relative frequency of the measured turbulence intensity in the whole occupied zone at different offset ratios. According to relevant standards, Tu = 40 % average turbulence intensity is used for draught comfort design calculations in mixing ventilation. It is obvious that most of the measured turbulence intensities – in 116 measurement points – are less, than 40 % at all offset ratios. E. g. at OR = 5.83, 82 % of the measured turbulence intensities are less, then 40 %, while 18 % of the measured turbulence intensities are higher, than 40 %.

Figure 5. Relative frequency of the measured turbulence intensities in the whole occupied zone at different offset ratios, $Re_0 = 2500$, $L_0 = 1000$ mm, $s_0 = 12$ mm
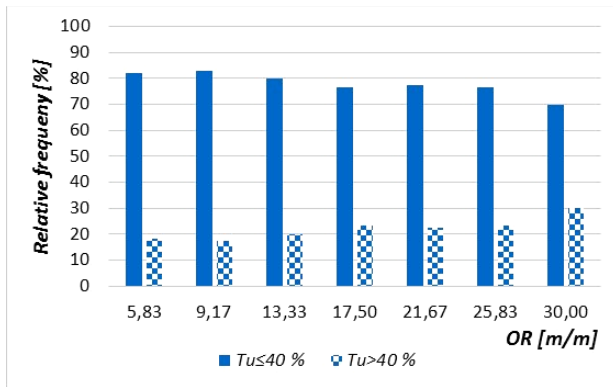
EFFECT OF OFFSET RATIO (OR) ON DRAUGHT COMFORT

DR (Draught Rate) number is a widely used and accepted value in Europe to describe draught comfort in ventilated rooms. According to equation (4), DR number was calculated at each measurement point. These values were averaged at ankle, sitting, standing person's head levels and in the whole occupied zone. Changing of the average DR can be seen on Fig. 6 at different offset ratios.
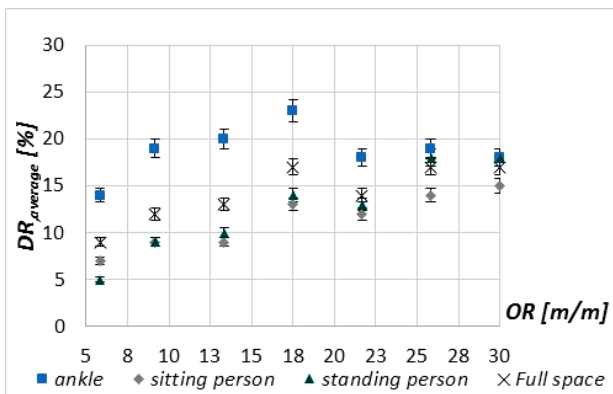

Figure 6. Average DR values at different offset ratios, $Re_0 = 2500$, $L_0 = 1000$ mm, $s_0 = 12$ mm

Abbe and general regression tests were applied to analyze measured data. DR was found to be constant at ankle level at probability level 95 % with an expected value DR = 19 %. Confidence intervals on different probability levels are:

$$P(17.3 \leq DR, \% \leq 20.7) = 0.90 \qquad (13)$$
$$P(17.0 \leq DR, \% \leq 21.0) = 0.95 \qquad (14)$$
$$P(16.4 \leq DR, \% \leq 21.6) = 0.99 \qquad (15)$$

At sitting, standing person's head levels and in the whole occupied zone DR was increasing linearly as a function of OR. Average DR numbers are between 15 and 25 % at ankle level, which results category B and C in draught comfort, according to standard CR 1752:2000 [s1]. At the other heights and in the whole occupied zone average DR is between 5 and 20 %, which results category A and B in draught comfort of the investigated model room.

CONCLUSIONS AND SUMMARY

In this article a slot-ventilated model room's draught comfort was investigated experimentally, considering the effect of air diffuser's offset ratio. Air velocity and temperature measurements were taken in the room and measured data were evaluated with statistical methods. Based on the measured values, turbulence intensity of the airflow and DR (Draught Rate) number were calculated, so draught comfort of the room could be described.

Average air velocity was found to be constant at ankle level, however, at the other three measurement heights, average air velocity was increasing linearly as OR was higher. At ankle level were higher air velocities than in the other three heights according to the airflow characteristic of the slot-ventilated room. Average air velocity range was about two times higher at knee, sitting and standing person's head levels than at knee level.

Average Tu was found to be constant at ankle level, while at the other levels the turbulence intensity was increasing as OR became higher. At ankle level was the lowest average turbulence intensity, which was constant. At the other three heights, size of the average turbulence intensity range was almost the same in the range of OR = 5÷30. Most of the measured turbulence intensities – in 116 measurement points – were less, than 40 % (suggested by relevant standards) at all offset ratios.

DR was found to be constant at ankle level, but at sitting, standing person's head levels and in the whole occupied zone DR was increasing linearly as a function of OR. Average DR numbers resulted comfort categories A and B above ankle level and C at the ankle level of the investigated model room.

REFERENCES

P. O. Fanger and N. K. Christensen, "Perception of draught in ventilated spaces." *Ergonomics*, 1986; 29:2, pp. 215-235.

T. Magyar, "Helyiségek légvezetési rendszerei és a hőérzeti méretezés kapcsolata." *Ventilation Symposium*, Budapest, May 1993, pp. 16 – 43. Budapest University of Technology and Economics.

T. Magyar and R. Goda, "Laboratory modeling of tangential air supply system." *Periodica Polytechnica Ser. Mech. Eng.* Vol. 44, No. 2, pp. 207–215 (2000).

T. Nozaki, K. Hatta, M. Nakashima and H. Matsumura, "Attachment flow issuing from a finite width nozzle." *Bull JSME*, vol. 22, 1979, pp. 340 – 347.

A. Nasr and J. C. S. Lai, "A turbulent plane offset jet with small offset ratio." *Experiments in Fluids* 24, Springer-Verlag 1998, pp. 47 – 57.

P. O. Fanger, A. K. Melikov and H. Hanzawa, "Air turbulence and sensation of draught." *Energy and Buildings*, 12 (1988), pp. 21-39.

H. Hanzawa, A. K. Melikow and P. O. Fanger, "Airflow characteristics in the occupied zone of ventilated spaces." *ASHRAE Trans.*, Vol. 93, Part 1, 1987, pp. 524-539.

T. Magyar, "Qualification of the occupied zones of different types of air supply systems on the basis of measurements." *Periodica Polytechnica* vol. 44, No. 2, pp. 217-227 (2000).

R. Goda, "Measurement and Simulation of Air Velocity in the Test Room with Slot Ventilation." *In: Clima2010: Sustainable Energy Use in Building*. Antalya, Turkey, 2010.05.09-2010.05.12. Antalya: Paper R6-TS46-PP03.

R. Goda, "Turbulence intensity and air velocity characteristics in a slot ventilated space." *Periodica Polytechnica-Mechanical Engineering* 58:(1) 2014, pp. 1-6. DOI: 10.3311/PPme.7154

G. Cao, M. Sivukari, J. Kurnitski and M. Ruponen, "PIV measurement of the attached plane jet velocity field at a high turbulence intensity level in a room." *International Journal of Heat and Fluid Flow* 31 (2010), pp. 897–908.

P. Rohdin and B. Moshfegh, "Numerical modelling of industrial indoor environments: A comparison between different turbulence models and supply systems supported by field measurements." *Building and Environment* 46 (2011), pp. 2365-2374.

J. Moureh and D. Flick, "Airflow characteristics within a slot-ventilated enclosure." *International Journal of Heat and Fluid Flow* 26 (2005), pp. 12–24.

J. Moureh and D. Flick, "Wall air–jet characteristics and airflow patterns within a slot ventilated enclosure." *International Journal of Thermal Sciences* 42 (2003), pp. 703–711.

T. Nozaki, "Attachment flow issuing from a finite width nozzle (report 4: Effects of aspect ratio of the nozzle)." *Bulletin of the JSME*, Vol. 26, No. 221, November 1983, pp. 1884 – 1890.

S. K. Rathore and M. K. Das, "Comparison of two low-Reynolds number turbulence models for fluid flow study of wall bounded jets." *International Journal of Heat and Mass Transfer* 61, 2013, pp. 365 – 380.

S. Kemény and A. Deák, "Kísérletek tervezése és értékelése." *Műszaki Könyvkiadó*, Budapest, Hungary, 2000. ISBN 963 16 3073 0.

L. Herczeg, T. Hrustinszky, L. Kajtár: Comfort in closed spaces according to thermal comfort and indoor air quality. Periodica Polytechnica-Mechanical Engineering 44: (2) pp.249-264. (2000)

RELEVANT STANDARDS

[s1] CR 1752:2000. Ventilation for buildings. Design criteria for the indoor environment.

[s2] EN ISO 5167-1:2003. Measurement of fluid flow by means of pressure differential devices inserted in circular cross-section conduits running full -Part 1: General principles and requirements.

[s3] EN 24006:2002. Measurement of fluid flow in closed conduits.

[s4] EN ISO 7726. Ergonomics of the thermal environment- Instruments for measuring physical quantities.

[s5] ASHRAE. 1992. ANSI/ASHRAE Standard 55-1992, Thermal Environmental Conditions for Human Occupancy, Atlanta: American Society of Heating, Refrigerating, and Air-conditioning Engineers, Inc., USA.

[s6] EN 13779:2007. Ventilation for non-residential buildings. Performance requirements for ventilation and room-conditioning systems.

Determination of gasket load drop at large size welding neck flange joints operating at medium high temperature

A. Nagy[*] and B. Dudinszky[*]

[*]Department of Building Services and Process Engineering, Faculty of Mechanical Engineering,
Budapest University of Technology and Economics, Budapest, Hungary
drnagyandras@freemail.hu, dudinszky@vegyelgep.bme.hu

Abstract— **this paper investigates the development of loosening at flange joints owing to creep and relaxation of gaskets at medium high temperature. The model presented here is able to describe the interaction of gasket and flange addition to the viscoelastic behavior of non-metallic gasket. The time-dependent material characteristics of the investigated gasket [5] were determined by standard tests whilst the reliability and preciseness of the derived equations are proved by test results. The paper deals with the dimensioning of flange joints on leak tightness operating at medium high temperatures.**

I. INTRODUCTION
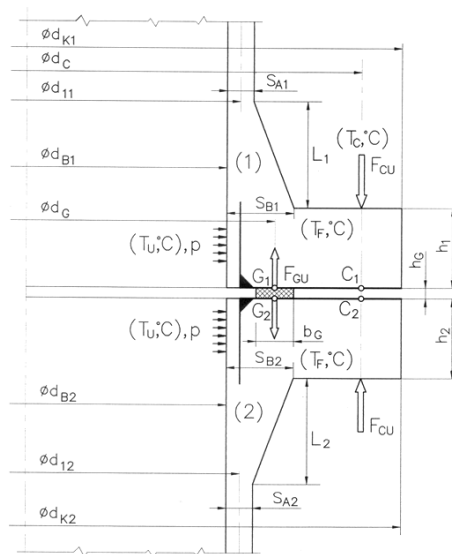
Figure 1. Sketch of the investigated flange joint

The reduction of gasket load at flange joints operating at medium-high temperature is mainly due to loosening effects that arise from internal pressure and additional external moments and forces [3] as well as from creep and relaxation of the non-metallic gasket materials. This drop in gasket load arising from the internal pressure and external loads is discussed in the literature by linear and non-linear gasket model [4].

The only difficulty in determining the residual gasket load under pressurized condition is the time-dependent creep and relaxation of non-metallic gasket.

There was significant work done already in the 1950's to determine, by means of test, the time-dependent characteristics of gasket [1], [2]. At that time a test method suitable to determine the long term load carrying capacity of gasket had been invented and standardized, and this method is still in use [7], [8]. The strength characteristics determined by this way cannot be regarded as pure material characteristics of the gasket, because this is influenced by the interaction between the bolted joint and the gasket. Thus the previous mentioned test method is suitable to compare different gasket material.

II. ANALITICAL MODEL OF FLANGE JOINT

The model presented here enables the mentioned standardized method to determined the true characteristics of the gasket materials. Using the newly developed model and applying the mentioned test method, the time dependent characteristics (that is creep and relaxation of gasket material) can be predicted at any arbitrary joint.

The basic assumption of the model presenting the correlation of acting loads and caused displacements are the follows:

Heat acting of the flange joints comes only from the medium to be sealed, characterized by its pressure p and temperature T_U.

The effect of the yield strength reduction and the change of elasticity modulus owing to the temperature increment both at flange and bolts can be neglected.

Creep and relaxation at flange and at bolts can also be neglected, so the rotational spring stiffness of flange as well as spring stiffness of bolts are independent from time and from displacements.

Another underlying assumption of the model is that during equalization of temperatures among different elements of the flange joint internal forces and stresses are generated by the different heat expansion not influencing the creep and relaxation of gasket, therefore the two phenomena can be investigated independently from each other.

At flange joint presented in this Fig. 1, the displacements caused by simultaneous heat and mechanical loads and the changes of internal forces [4], [6] will happen according to the Fig. 2, shows.
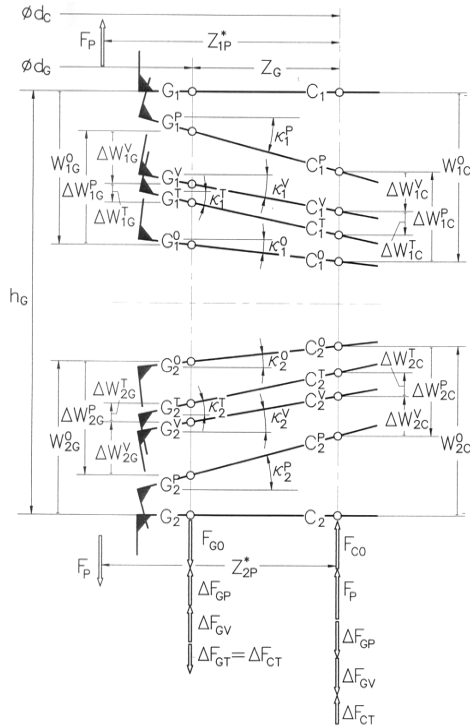
Figure 2. Displacements and changes of internal forces owing to the simultaneous heat and mechanical loads

In this figure the displacements ΔW and angular displacements κ can be seen which are together responsible for the reduction of gasket load. The flanges themselves are replaced by corner rigid skeletons, having K_1 and K_2 rotational spring stiffness. As the figure shows both the displacements and angular displacements and gasket load drop can be divided into parts and they can be investigated separately from each other.

In this figure ΔF_{GP} mean the gasket load drop arising from the pressure induced header end load F_P and ΔF_{GV} is the unknown gasket load drop caused by creep and relaxation of the gasket.

In order to investigate the loosening effect caused by gasket relaxation, the gasket should be modelled and the interaction of gasket and flange should be analysed. To create its viscoelastic model, the typical non-linear characteristics of non-metallic gasket materials should be taken into consideration, as well as the fact that during the standardized relaxation test of frequently applied gasket materials non-zero residual compression stress appears.

The developed rheological analogue model which is the basis of further investigations can be seen in the next Fig. 3.
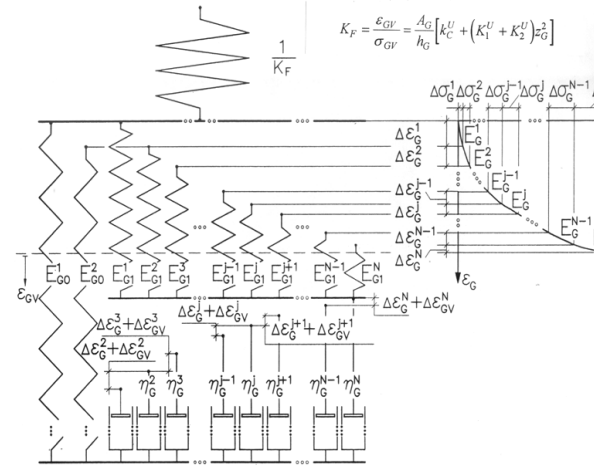
Figure 3. Rheological analogue model of flange joint

As the figure shows the model fulfils both requirements. The non-linear characteristics of the gasket are produced by the springs of the elementary Maxwell-model connected in parallel, and the interaction of gasket and flange is symbolized by the spring connected to the gasket model having the modulus K_F calculated from this equation (1) where A_G is the surface area while h_G is the thickness of the gasket, k_C^U is the spring stiffness of bolts.

$$K_F = \frac{\varepsilon_{GV}}{\sigma_{GV}} = \frac{A_G}{h_G}\left[k_C^U + \left(K_1^U + K_2^U\right)z_G^2\right] \tag{1}$$

This figure presents the state belonging to the σ_G^N starting compression stress. The determination of the total decrease of gasket load originated from the relaxation of the gasket is possible only in several steps using the equations belonging to the different linearized ranges of the compression characteristic curve.
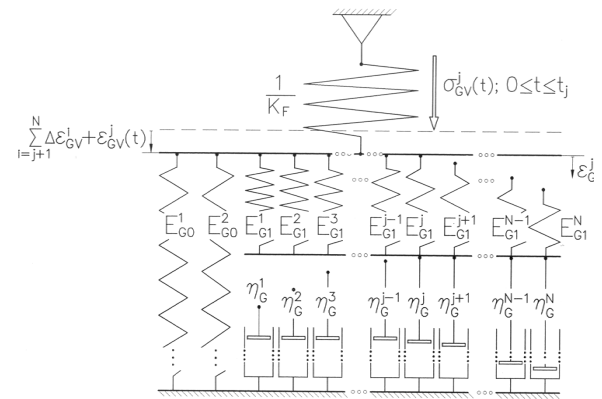
Figure 4. The range j. of the relaxation process

The Fig. 4, shows the range j. of the loosening process. In this range the gasket compression stress can be expressed as a function of time with the following differential equation (2).

$$\frac{1 + K_F E_G^j}{\sum_{i=1}^{j} E_{G1}^i} \cdot \frac{d^2\sigma_{GV}^j}{dt^2} + \frac{1 + K_F\left(E_{G0}^1 + E_{G0}^2\right)}{\sum_{i=j}^{N} \eta_G^i} \cdot \frac{d\sigma_{GV}^j}{dt} = 0 \tag{2}$$

Its solution regarding the boundary conditions is:

$$\sigma_{GV}^j(t) = \sigma_G^N - \frac{\sum_{i=1+j}^N \left(E_G^i - E_{G0}^1 - E_{G0}^2\right)\Delta\varepsilon_G^i}{1 + K_F\left(E_{G0}^1 + E_{G0}^2\right)} -$$

$$-\frac{\sum_{i=1}^j E_{G1}^i\varepsilon_G^j}{1 + K_F\left(E_{G0}^1 + E_{G0}^2\right)}\left[1 - \exp\left(\lambda_2^j t\right)\right] \tag{3}$$

where $\varepsilon_G^j = \sum_{i=1}^j \Delta\varepsilon_G^i$ means the total compressions of

the gasket and the coefficient λ_2^j can be calculated from this equation (4).

$$\lambda_2^j = -\frac{\sum_{i=1}^j E_{G1}^i\left[1 + K_F\left(E_{G0}^1 + E_{G0}^2\right)\right]}{\sum_{i=j}^N \eta_G^i\left(1 + K_F \cdot E_G^j\right)} \tag{4}$$

The actual range of validity for this function is a short time period $0 \le t \le t_j$ where its upper limit is determined by equation (5).

$$t_j = -\frac{\sum_{i=j}^N \eta_G^i\left(1 + K_F E_G^j\right)}{\sum_{i=1}^j E_{G1}^i\left[1 + K_F\left(E_{G0}^1 + E_{G0}^2\right)\right]}\ln\frac{\varepsilon_G^{j-1}}{\varepsilon_G^j} \tag{5}$$

The relaxation and creep of the gasket occurring during this time period can be calculated using these equation:

$$\Delta\sigma_{GV}^j = \frac{\sum_{i=1}^j E_{G1}^i\Delta\varepsilon_G^j}{1 + K_F\left(E_{G0}^1 + E_{G0}^2\right)} \tag{6}$$

$$\Delta\varepsilon_{GV}^j = \varepsilon_{GV}^j\left(t_j\right) = K_F\Delta\sigma_{GV}^j \tag{7}$$

The resultant relaxation and creep of the gasket considering the total loosening process can be calculated by this way and finally the following equations (8), (9) can be obtained.

$$\Delta\sigma_{GV}^{\inf(N)} = \sum_{j=1}^N\Delta\sigma_{GV}^j = \frac{\sum_{j=1}^N\sum_{i=1}^j E_{G1}^i\Delta\varepsilon_G^j}{1 + K_F\left(E_{G0}^1 + E_{G0}^2\right)} \tag{8}$$

$$\Delta\varepsilon_{GV}^{\inf(N)} = \sum_{j=1}^N\Delta\varepsilon_{GV}^j = K_F\Delta\sigma_{GV}^{\inf(N)} \tag{9}$$

The characteristics of springs and viscous fluid elements can be determined according to the following consideration.

The values of characteristics of viscous fluid element gives the required continuity of the resultant relaxation curve.

$$\left(\frac{d\sigma_{GV}^j}{dt}\right)_{t=t_j} = \left(\frac{d\sigma_{GV}^{j-1}}{dt}\right)_{t=0} \tag{10}$$

Substituting ranges of the relaxation curve after simplifying the following recursive formulae can be found.

$$\sum_{i=j-1}^N \eta_G^i = \frac{1 + K_F E_G^j}{1 + K_F E_G^{j-1}}\left(\frac{\sum_{i=1}^{j-1} E_{G1}^i}{\sum_{i=1}^j E_{G1}^i}\right)^2 \sum_{i=j}^N \eta_G^i \tag{11}$$

The factor of viscous fluid element at the beginning as well as spring constants can be determined by tests. These tests give the compression stress-strain characteristic curve that is to be applied parallel to the standardized long term load carrying capacity test of the gasket which can be determined by the earlier mentioned test method.

Knowing these test results the searched characteristics of the model can be calculated using equations (12), (13), (14).

$$E_{G0}^1 + E_{G0}^2 = \frac{E_G^2\Delta\varepsilon_G^2 - \left(\Delta\hat\sigma_{GV}^{\inf(2)} - \Delta\hat\sigma_{GV}^{\inf(1)}\right)}{\Delta\varepsilon_G^2 + \hat K_F\left(\Delta\hat\sigma_{GV}^{\inf(2)} - \Delta\hat\sigma_{GV}^{\inf(1)}\right)} \tag{12}$$

$$E_{G0}^1 = E_G^1 - \frac{\Delta\hat\sigma_{GV}^{\inf(1)}}{\Delta\varepsilon_G^1}\left[\frac{\Delta\varepsilon_G^2\left(1 + \hat K_F E_G^2\right)}{\Delta\varepsilon_G^2 + \hat K_F\left(\Delta\hat\sigma_{GV}^{\inf(2)} - \Delta\hat\sigma_{GV}^{\inf(1)}\right)}\right] \tag{13}$$

$$\eta_G^N = -\frac{\left(\sum_{i=1}^N E_{G1}^i\right)^2\varepsilon_G^N}{1 + \hat K_F E_G^N}\left[\left(\frac{d\hat\sigma_{GV}}{dt}\right)_{t=0}\right]^{-1} \tag{14}$$

where $\hat K_F$ assign the relative modulus of the testing device and $\Delta\hat\sigma_{GV}$ symbolise the measured resultant relaxation.

III.   TEST AND CALCULATED RESULT

Several experiments were carried out to prove the reliability and applicability of the viscoelastic model. First several thicknesses of gaskets from different manufacturers were investigated to determine characteristics of the gasket materials including the time dependent properties.

Figure 5. ZWICK-type universal tensile machine

ZWICK type universal tensile machine equipped with programmecontrolled heating Fig. 5, was used to determine stress-strain characteristics while the time-dependent properties were determined by BOSSER-type standardized test device Fig. 6.

Figure 6. BOSSER-type standardized test device

Using the test results, the coefficient for elasticity and viscous fluid can already be numerically calculated. Knowing the characteristics of the model and choosing different values for pretightenings the calculation can be carried out.

The calculation refer to a joint having equal stiffness to the standardized test device used for determination of the time dependent characteristics, so the test device gives a possibility to directly check the preciseness of the model.

The measured and calculated values of resultant relaxation can be seen in the following figures.

The Fig. 7, show the changes of calculated and measured resultant relaxation at $250\,^{0}C$ in the function of pretightenings of different gaskets with equal 2.0 mm thickness. In this figure the continuous curves present the measured results while the dashed curves show the calculated values.Fig. 8, show the calculated and measured values of it at $250\,^{0}C$ for different thickness of IT-type gasket material as a function of pretightening.
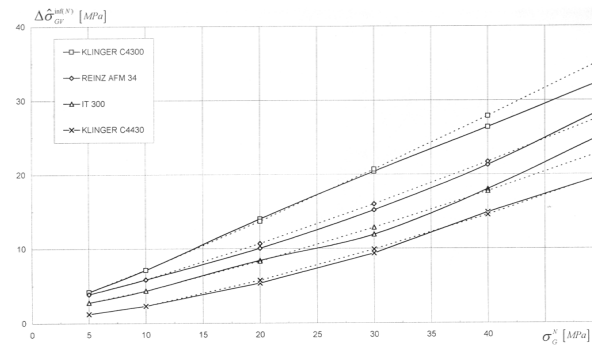
Figure 7.Measured and calculatedresultantrelaxationsas a function of pretighteningatdifferenttypes of *hg = 2 mm*thickgasketat*250 °C*
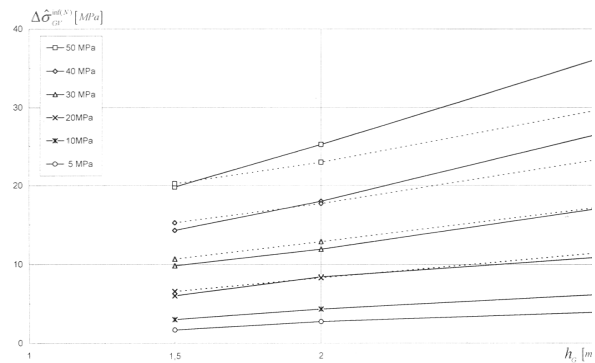
Figure 8.Measured and calculated resultant relaxations at **IT300** gaskets of several thicknesses as a function of pretightening at

250 °C

During the experiments the time-dependence of the relaxation process taking place in the test device was also recorded. The next two figures Fig. 9, 10, shows the calculated and measured relaxation curves belonging to gaskets made of REINZ and IT 300 materials with 2.0 mm thickness.
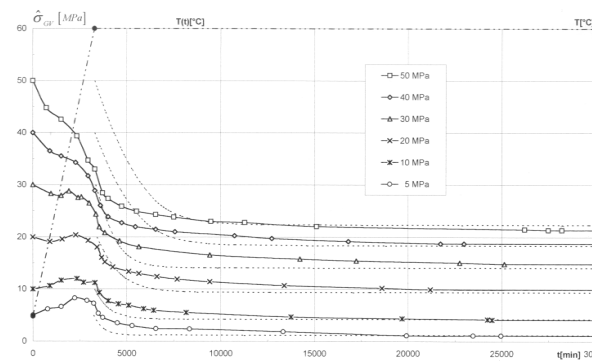
Figure 9. Process of relaxation at *250 °C* of **REINZ AFM34** type gaskets having *hg = 2 mm* thickness and pretightened at different values

The test proved that independently of the type of gasket, the ideal exponential losses characteristic of relaxations could appear only inthe range of heat-keeping period. Increasing pretightening in the range of heating up lead to the pressure losses on the gasket growing bigger and bigger and they incline from exponential one.This is the reason why at the beginning of the heat keeping period the calculated and measured results differ.
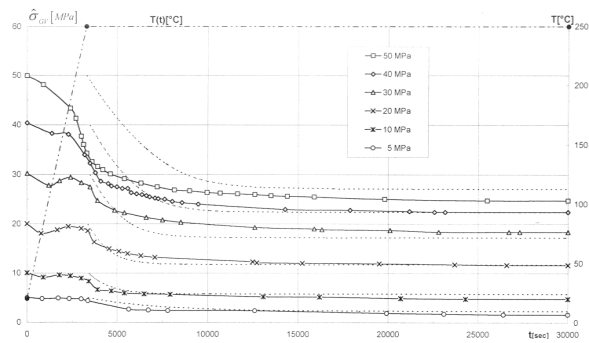
Figure 10. Process of relaxation at *250 °C* of **IT300** type gaskets having *hg = 2 mm* thickness and pretightened at different values
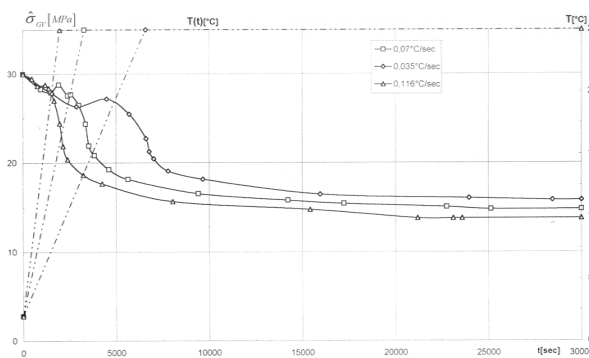
Figure 11. Effect of heating-up velocity on relaxation process

Fig. 11, represents the effect of the heating-up velocity on relaxation in the range of heat-keeping. There are three different relaxation curves representing three different heating-up velocities. This test were carried out on 2. 0 mm thickness REINZ-type gasket at $250^{0}C$ and the pretightenings was 30 Mpa. As the figure show there is no significant effect of heating-up velocity on the total gasket pressure losses, as significant changes (three times bigger) in heating-up velocity during the test resulted in pressure losses differing slightly from each other.
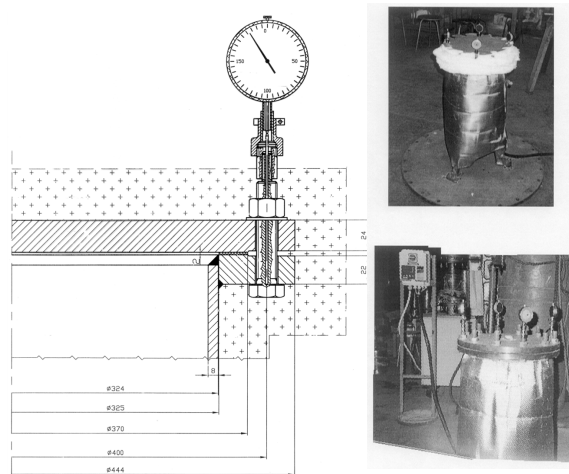
Figure 12. Sketch of the test device

To testify the effect of geometrical size on the preciseness of developed rheological analogue model, an automatically heated test device was manufactured which can be seen in Fig. 12.
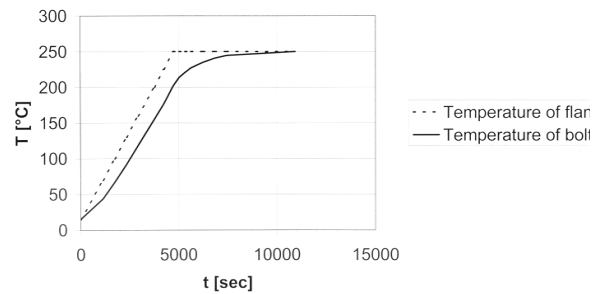
Figure 13. Temperature of flange and bolts along the heating-up period

As the figure shows the decrease of gasket surface pressure was recorded by measuring four bolts elongation around the circumference.

During the test to keep the required $250^{0}C$ temperature inside the vessel a 40 mm thick isolation was used along the whole body.

The following figures(Fig. 13-17,) show the measured and calculated results referring to three different type 2.0 mm thick gaskets.
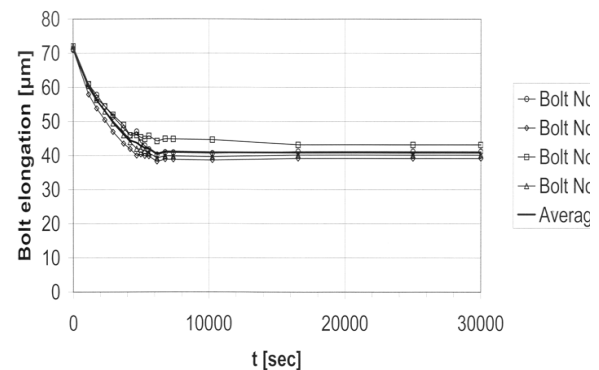
Figure 14. Measuredelongation of boltsat*250 °C*crefferingto**REINZ AFM 34**

OnFig. 13, the dashed line shows the program controlled temperature of flange ring near to the gasket while the continuous curve presents the temperature of the centre of bolts recorded by contact thermometer.
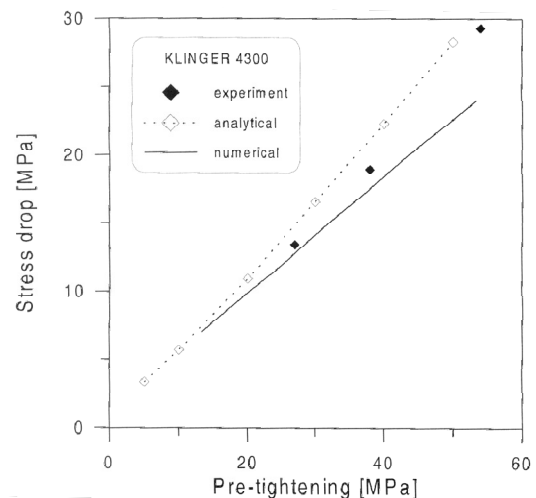
Figure 15. Total gasketsurfacepressuredrop (**KLINGER 4300**)

64

On Fig. 14, a typical measured bolts elongation can be seen in the function of time referring to the REINZ AFM type gasket. The thin curves shows the measured values while the thick presents the calculated average. Considering this figure it can be stated that the difference among bolt elongations are not to much less than 10% of the average. Measuring the bolt elongation we can calculate the changes of gasket surface pressure. Finally in the last three figures (Fig. 15-17,) the comparison of calculated and measured results can be seen.
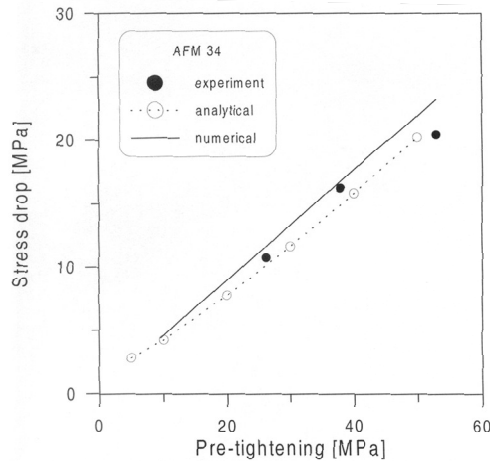
Figure 16. Total gasket surface pressure drop (**REINZ AFM 34**)
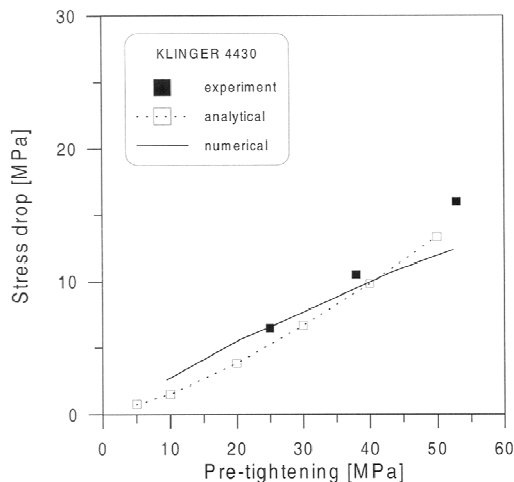
Figure 17. Total gasket surface pressure drop (**KLINGER 4430**)

In these figures the total gasket surface pressure drop can be seen in the function of pretightenings. The single symbols show the experimental, while the continuous and dashed curves present the calculated values by analytical and FEM model.

IV. CONCLUSION

The results of presented theoretical and experimental investigations allow the following statements.

Results calculated according to the developed model and test concerning gasket relaxation in case of thickness less than 3.0 mm and pretightening less than 40 Mpa show good correlations.

The effect of gasket stress drop during the heating-up period causes significant differences at the beginning of investigations between the calculated and measured relaxation curves in case of pretightening by more than 20 Mpa.

Concerning the future the developed model should be extended considering by taking the creep and relaxation of flanges and bolts into account.

REFERENCES

[1] S. Schwaigerel, and E. Krageloch, Prüfung von Weichdichtungen. BWK 1952, 4, 404-407.
[2] A. E. Johnson, Creep and relaxation of metals at elevated temperatures. Engineering, 1949, 168, 237-245.
[3] H. J. Bernhard, Flange theory and the revised Standard B. S.10: 1962-flanges and bolting for pipes, valves and fittings Proc. Int. ech E., 1963, 178, 107-131.
[4] A. Nagy: Determination of the Gasket Load Drop at Large Size Welding Neck Flange Joints in the Case of Nonlinear Gasket Model. Int. J. Pres. Ves. & Piping. 67 (1996) 243-248.
[5] A. Nagy: Time Depending Characteristics of Gasket at Flange Joints. Int. J. Pres. Ves. & Piping. (1997).
[6] L. Varga, A. Nagy: Optimale Form und neue Analyse von Flanschkonstruktionen. Konstruktion 49, H. (1997).
[7] DIN 52913 Druchstandversuch an IT Dichtungsplatten (1990).
[8] BS 7531: 1992 Specification for Compressed Non-Asbestos Fibre Jointing. Appendix B.

Determination of evaporation rate at free water surface

T. Poós*, E. Varju*

*Department of Building Services and Process Engineering, Faculty of Mechanical Engineering,
Budapest University of Technology and Economics, Budapest, Hungary
poos@mail.bme.hu,varjuevelin93@gmail.com

Abstract– **There are many industrial facilities with free surface water reservoir for different technological purposes. On the free surface heat transfer and diffusion occur, whereby the vapor diffuses into the ambient air. Therefore, the water loss should be replaced. There are many empirical correlations for calculating the quantity of the evaporated water which methods largely differ from each other. The evaporation rate can be determined by the newly assembled experimental apparatus and measurement method.During the measurement the velocity and the temperature of the ambient air, the temperature of the evaporating liquid can be varied.The evaporation rate can be calculated upon the measured and recorded data.**

INTRODUCTION

In the contact surface of a free water surface with air, heat- and mass transfer process occurs [1], [2], when from the saturated surface of water vapor diffuses to the unsaturated air. This phenomenon is called evaporation and is shown in Fig. 1. Diffusion occurs because of the temperature-based driving forces at the first two cases and because of the humidity-based driving forces at the third case. At the fourth case the temperature is lower than the dew point, that is why condensation occurs. These four cases can be described by the following equations [3].
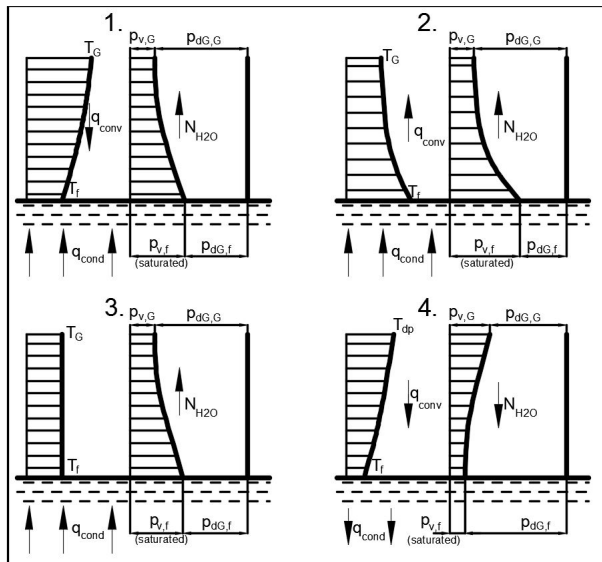
Figure 1. Partial pressure difference and temperature-based driving forces at the four cases of liquid evaporation

The temperature-based driving force between the water surface and the unsaturated air can cause heat flux, which can be given by the heat flux density:

$$q_{conv} = \alpha \left| T_f - T_a \right|. \tag{1}$$

The vapor from the water surface diffuses to the unsaturated air, which can be described by the molecular evaporation rate:

$$N_{H2O} = k_G M_{H2O} \left(p_{v,f} - p_{v,G} \right). \tag{2}$$

The evaporation rate in terms of temperature-based driving forces, Sartori[4] established three different cases. This theory can be supplemented to four categories, where the evaporation rate can be written to the different cases:

$$1: N_{H2O} = \frac{q_{conv} + q_{cond}}{r_{H2O}}, if\ T_G > T_f; \tag{3}$$

$$2: N_{H2O} = \frac{q_{cond} - q_{conv}}{r_{H2O}}, i\ T_G < T_f; \tag{4}$$

$$3: N_{H2O} = \sigma \left(Y_f - Y_G \right), if\ T_G = T_f; \tag{5}$$

$$4: N_{H2O} < 0\ (condensation), if\ T_{dp} > T_f. \tag{6}$$

Evaporation from free liquid surface occurs commonly in everyday-life and industrial processes e.g. open air reservoirs, pools and swimming pools. There are two mechanisms of the air movement: forced convection by ventilation indoor or by wind outdoor, or natural convection based on concentration difference. Evaporation intensity can differ in case of still or rippling surfaces. A number of publications discuss the measurement of surface evaporation; their results are based on experiments.

Based on the experiments, correlations to best describe the phenomenon were identified by regression analysis; in general, they can be applied only in limited conditions. According to special sources, Dalton was the first in 1802 to discuss the issue and to describe the problem of evaporation byempirical hydrodynamic approximation. He concluded that the intensity of evaporation is proportionate to the partial pressure difference of the liquid surface and the main stream of air and the velocity of air flow.

In 1918 the correlation proposed by Willis Carrier [5] is mostly applied to water surface evaporation based on laboratory experiments, then Himus and Hinchley [6] in 1924 examined evaporation in wind tunnel.In 1931measurements results of Rohwer [7] completed achievement of Carrier, who published his research results[8] in book entitled Fan Engineering in 1949. Powell [9] created a correlation for evaporation due to forced convection in 1940.

In 1966, the WMO conference [10] published a volume, where several correlations were proposed for evaporation rate. Kohler and Parmele [11] determined equation of evaporation rate for natural convection in1967.

There are many experimental results for evaporation from a swimming pool, like McMillan (1971) [12], Ryan and Harleman (1973) [13], Czarneczki (1978) [14] Govindand Sodha(1983) [15], Szeicz and McMonagle (1983) [16] achieved significant results in this area.

An another research field is the heat loss of a solar pond through evaporation, where Kishore and Joshi (1984) [17], Subhakar and Murthy (1993) [18], Alagao et al. (1994) [19] determined the evaporation rate.

Sartori (1989) [20] created an equation depending on laminar, transitional and turbulent range.

Hahne and Kübler (1994) [21] made experiments on two outdoor swimming pools to determine the evaporation loss and checked several empirical correlations due to experiments, then based on the results created their own equation to describe the process more accurate. Similar measurements performed Molineaux et al. (1994) [22] based on results of Watmuff et al. (1977) [23] and Smith et al. (1994) [24] too.

Pauken (1999) [25] examined evaporation in wind tunnel in case of a heated tank, then proposed a correlation, that can be used for natural and forced convection too.

Tang and Etzion (2004) [26] performed their measurements outdoor on an open and a covered shallow pools, but their results are correct only for small water surfaces.

Moghiman and Jodat (2007) [27] dealt with evaporation at moving air above indoor swimming pools, where their experiments were made in a test chamber, therefore to create a connection between evaporation rate and airflow rate.

Bower and Saylor (2009) [28] examined the connection between Sherwood and Rayleigh number. Data were collected from a set of water tanks undergoing natural convection-driven evaporation. These data were reduced to a dimensionless mass transfer coefficient for evaporation.

Shah (2012) [29] worked out a measurement method, which can be used for swimming pools, other pools with quiet water surface and pools for nuclear fuels to determine the evaporation rate of water.

Raimundo et al. (2014) [30] examined the connection between evaporation of heated water surface and parameters of air stream at forced convection.

Kunmar and Arakeri (2015) [31] investigated natural convection at heated tank, where the tank on the top and as well at the bottom could be heated. Based on the results they made a connection between Sherwood and Rayleigh number.

Table I contains the correlations of evaporation rate, which were mentioned earlier.

The listed equations are valid in various interval (different gas and liquid temperature, surface area) and conditions (natural or forced convection), which reduces their usefulness. In addition, these equations are correct only for water, but in the industry there are several cases, where other, volatile components (e.g. ethanol used for cleaning, boric acid solution in power plant) can evaporated to the ambient. By exceeding concrete concentration environmental and health standards can be broken.To know the phenomenon of evaporation is important to environmental and health areas, but to energy recovery technologies too [32]. In this paper measurement

TABLE II.
EQUATIONS OF EVAPORATION RATE

Ref. Nr.	Equations
6	$N = 10^{-9}(64.58 + 28.06 v_G)(p_{v,f} - \varphi p_{v,G})$
7	$N = (0.0850 + 0.0508 v_G)\dfrac{p_{v,f} - \varphi p_{v,G}}{r_{H2O}}$
8	$N = (0.088403 + 0.001296 v_G)\dfrac{p_{v,f} - \varphi p_{v,G}}{r_{H2O}}$
9	$N = 9.86 \cdot 10^{-8}(p_{v,f} - p_{v,G})\dfrac{(v_G L)^{0.65}}{L}$
10	$N = 0.0372 v_G \dfrac{p_{v,f} - \varphi p_{v,G}}{r_{H2O}}$
11	$N = \rho_{H2O}(0.181 + 0.00236\overline{v_G})(p_{v,f} - \varphi p_{v,G})$
12	$N = (0.0360 + 0.0250 v_G)\dfrac{p_w - \varphi p_G}{h_w}$
13	$N = (0.027(T_{wvir} - T_{Gvir})^{1/3} + 0.031 v_G)\dfrac{p_{v,f} - \varphi p_{v,G}}{r_{H2O}}$
14	$N = (0.05053 + 0.06683 v_G)\dfrac{p_{v,f} - \varphi p_{v,G}}{r_{H2O}}$
15	$N = (0.0741 + 0.0494 v_G)\dfrac{p_{v,f} - \varphi p_{v,G}}{r_{H2O}}$
16	$N = \dfrac{\rho_G c_p}{\gamma}(p_{v,f} - p_{v,G})\dfrac{\left(\ln\left(\frac{z}{z_0}\right)\right)^2}{v_G r_{H2O}\kappa}$
17	$N = (5.7 + 3.8 v_G)\dfrac{M_{H2O}}{M_G}\dfrac{p_{v,f} - \varphi p_{v,G}}{P c_{H2O}}$
18	$N = \left[(T_f - T_G) + \dfrac{(T_f + 237)(p_{v,f} - \varphi p_{v,G})}{268900 - p_{v,f}}\right]^{1/3}\dfrac{0.0144(p_{v,f} - \varphi p_{v,G})}{r_{H2O}}$
19	$N = (0.074 + 0.040 v_G)\dfrac{p_{v,f} - \varphi p_{v,G}}{r_{H2O}}$
20	$N = (0.00407 L^{-0,2}0.0 v_G^{0.8})\dfrac{p_{v,f} - \varphi p_{v,G}}{P}$
21	$N = (0.0803 + 0.0583 v_G)\dfrac{p_{v,f} - \varphi p_{v,G}}{r_{H2O}}$
22	$N = \dfrac{3.1 + 2.1 v_G}{c_G}\dfrac{M_{H2O}}{M_G}\dfrac{p_{v,f}}{p_{v,f} + p_{v,G}}$
23	$N = \dfrac{2.8 + 3.0 v_G}{c_G}\dfrac{M_{H2O}}{M_G}\dfrac{p_{v,f}}{p_{v,f} + p_{v,G}}$
24	$N = (0.0888 + 0.0783 v_G)\dfrac{p_{v,f} - \varphi p_{v,G}}{r_{H2O}}$
25	$N = (74.0 + 97.97 v_G + 24.91 v_G^2)(p_{v,f} - p_{v,G})^{(1.22 - 0.19 v_G + 0.038 v_G^2)}$
26	$N = (0.2253 + 0.24644 v_G)\dfrac{(p_{v,f} - \varphi p_{v,G})^{0.82}}{r_{H2O}}$
27	$N = (0.0038 + 0.1356 v_G)(p_{v,f} - \varphi p_{v,G})^{(-1.255 v_G^3 + 2.182 v_G^2 - 1.362 v_G + 1.377)}$
28	$Sh = 0.230 Sc^{1/3}Ra^{0.321}$
29	$N = 0.00972 \rho_{H2O}(\rho_G - \rho_{H2O})^{1/3}(Y_f - Y_G)$
30	$N = 10^{-9}(37.17 + 32.19 v_G)(p_{v,f} - \varphi p_{v,G})$
31	$Sh = 0.264 Ra^{0.292}$

results and evaporation rates are presented for the first and second categories.

EXPERIMENTAL APPARATUS AND METHODS

Experimental apparatus

During the measurements of evaporation was used the equipment that is found at the Department of Building Services and Process Engineering. The piping and instrumentation diagram is shown in Fig. 2.

For the movement of air is used a centrifugal fan (type: NVH50) (P-101-01) that is driven by an electric motor (maximum rotational speed 2890 1/min) (type: VZ32/2)

made by EVIG. The suction section begins with an orifice flow meter (O-101-01) on a 200 mm diameter pipe. A U-tube manometer measures the pressure difference on the orifice flow meter. The air velocity is adjustable by using a frequency converter and a butterfly valve (V-101-01). For air heating is used an electric heater (type: Thermo-Team LF-36, accuracy: 0.5 °C) (H-101-01), that has 21 kW regulated and 9+6 kW fixed performance. In the evaporation section (E-102-01) can be found the thermovessel(type: Grant GLS Aqua 12 Plus) (T-102-01), which contains the liquid used for evaporation.The temperature of liquid can be adjusted between ambient temperature and 99 °C (accuracy: 0.1 °C). Its maximum volume is 5 dm³ and the evaporating surface is 325 mm x300 mm.The thermo vessel and the scales below it are on a manually adjustable elevator (L-102-01). By modifying the height of elevator the water surface of the thermo vessel can be approximate to the bottom of the air tunnel. The humid gas leaves the system through the chimney (F-102-01) to the ambient.

Instrumentation and methods

The measurement begins by filling with water the thermo vessel, then the setting of accurate temperature of liquid (TRC-102-01) occurs by turning on the heating. Laterturning on the fan with a given rotational speed (SIC-101-01), the required temperature of air (TIC-101-01) can be modified by the electric heater. Before starting the measurement, the apparatus shall be run empty until the stationary state is reached – stabilized values measured by the thermometers. The flow rate can be modified by the butterfly valve (FIC-101-01), and be determinedfrom the pressure difference (PDI-101-01), that is measured at the orifice flor meter. Before the measurement the evaporated water has to be compensated, until the water surface get aligned with the bottom of the air tunnel. At the beginning of the measurement the temperature (TR-101-01) and the humidity (XR-101-01) of ambient is determined. Registration of evaporation properties occurs by a data logger (type: Ahlborn Almemo 2590-9). The mass of evaporated water (WR-102-01) by a scales (accuracy: 1 g), the surface temperature of water (TR-102-02) by an infrared thermometer (type: AMiR 7842), that is above the

thermo vessel and the temperature of the gas (TR-102-01) is measured by a T-type thermometer. The measured values are registered with minute sampling by self-developed software. The measurement periods last minimum for two hours.

During measurements the ambient and gas properties and the weight of the water vessel were collected. Based on measurements results, evaporation rate can be specified in the knowledge of the quantity of moisture, is leaving the surface in a time interval:

$$N_{H2O} = -\frac{dm_{H2O}}{dt} \cdot \frac{1}{A}. \tag{7}$$

RESULTS

The summary of measurements results is shown in Table II, where the first and second cases were investigated. The results are demonstrated by the air velocity. During measurements the air velocity, temperature, humidity and water characteristic temperature were constant. The varying parameter was only the weight of water. It can be determined the weight decrease of the water by fitting a lineal to the plotted points (dm_{H2O}/dt).

TABLE III.
SUMMARY OF MEASUREMENTS RESULTS

v_G	T_G	Y_G	dm_{H2O}/dt	T_{H2O}	T_f	$Y_{f,sat}$	N_{H2O}
m/s	°C	g_{H2O}/kg_{dG}	g/s	°C	°C	g_{H2O}/kg_{dG}	kg/(m²h)
	50,0	3,5	-0,0144	30,0	27,9	25,9	0,531
0,6	50,1	5,1	-0,0263	40,0	38,0	41,6	0,970
	50,1	5,1	-0,0509	50,0	47,6	70,8	1,879
	50,0	5,7	-0,0763	59,9	57,4	126,3	2,819
	49,9	5,8	-0,0207	29,9	27,6	25,5	0,763
1,1	50,0	5,3	-0,0381	40,0	37,2	39,9	1,406
	50,1	6,5	-0,0634	50,0	46,7	67,2	2,340
	50,0	5,6	-0,1100	60,0	56,1	117,0	4,061
	49,9	3,7	-0,0323	30,0	27,3	25,2	1,191
1,8	50,0	4,0	-0,0509	40,0	36,5	38,5	1,879
	50,0	5,8	-0,0891	50,0	45,8	63,6	3,291
	50,1	5,6	-0,1486	60,0	54,8	107,9	5,488
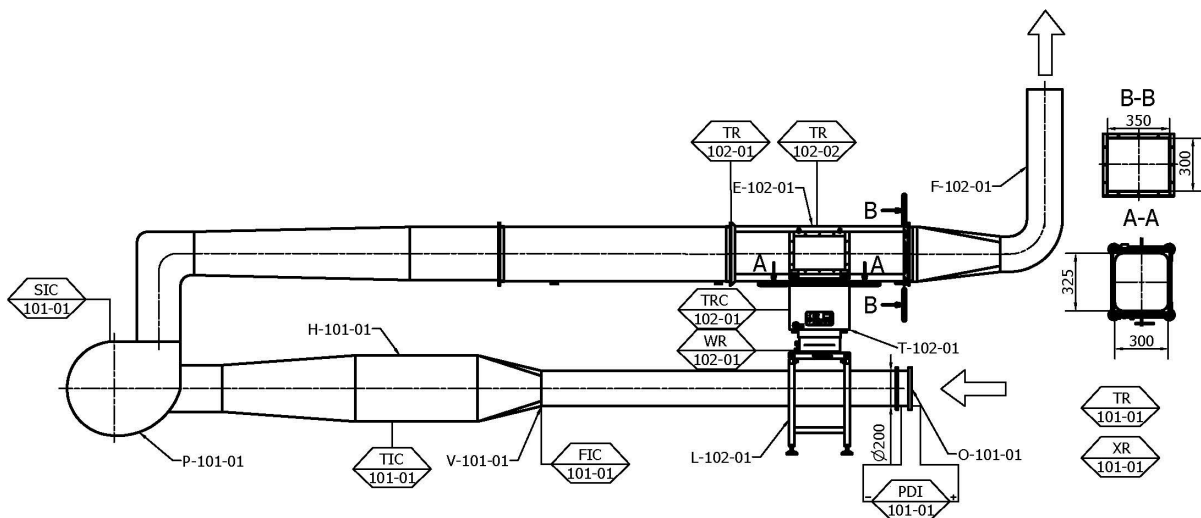
Figure 2. Instrumented flow diagram of the measurement equipment
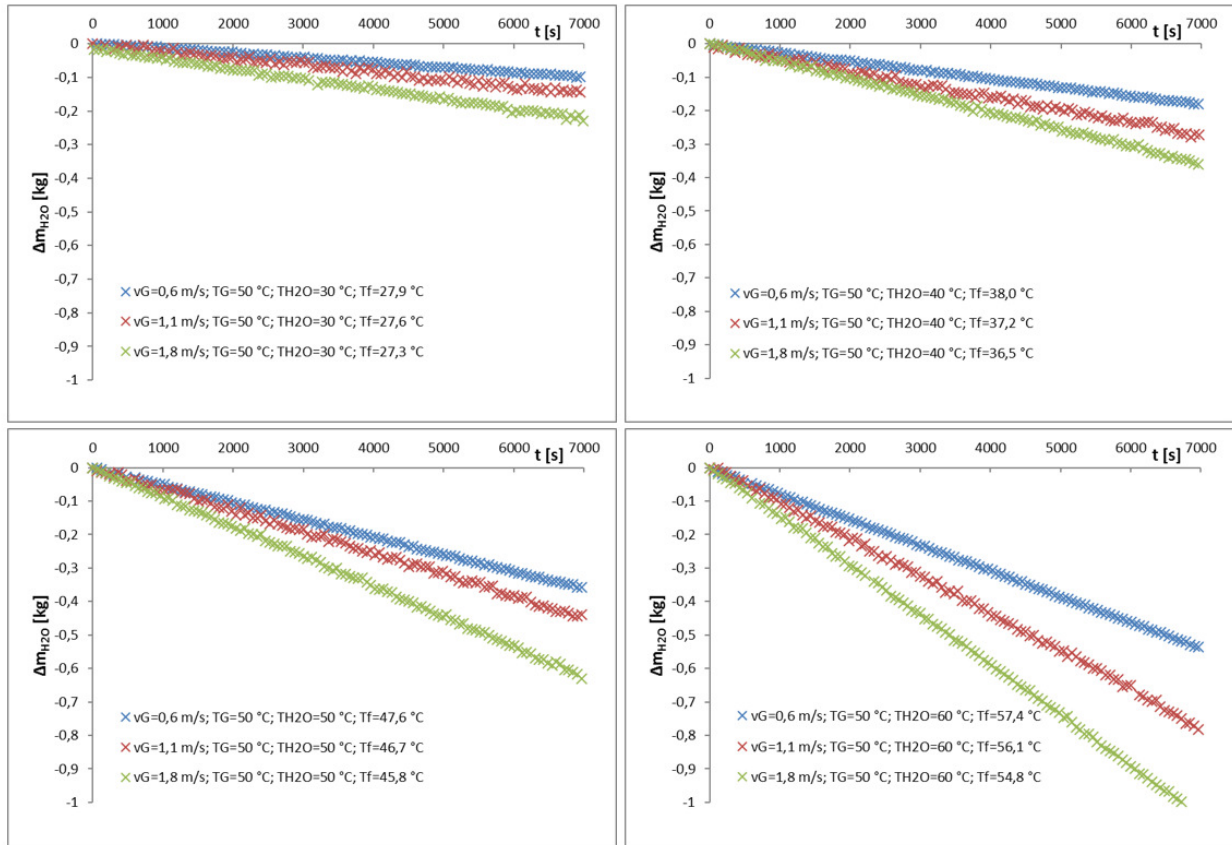
Figure 3. The weight of evaporated water at different temperature-based driving forces in function of time

During measurements water is being evaporated at different air flow rate and liquid temperature. Three cases were investigated at constant air temperature:the water temperature is higher, the air and liquid temperature are equal, the water temperature is lower than the air temperature.In all three cases, the measurements were done at three different air velocities. The weight of evaporated water in function of time is shown in Fig 3. On the diagrams can be clearly seen the effect of the water temperature and the air velocity on the evaporation rate.

The evaporation rate from the measurements results in function of Reynolds-number is shown in Fig. 4. The same temperature-based driving forces are plotted in the same colour, which for can be fitted a trend line. In order
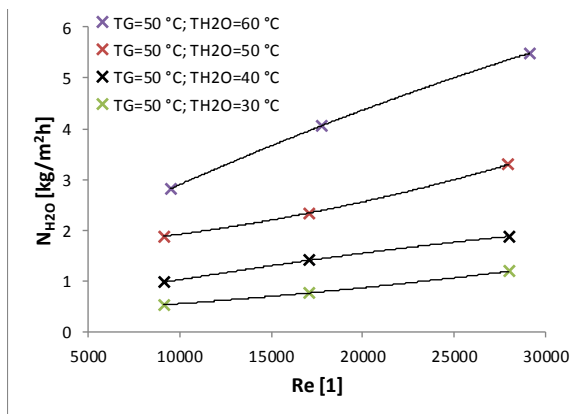
Figure 4. The evaporation rate at different temperature-based

to determine the equations of the trend lines more measurements are needed.

CONCLUSIONS

In the course of our work, evaporation from a liquid surface was examined based on laboratory measurements. In this paper, a critical review on several well-known equations employed for the calculation of evaporation rate from free water surfaces has been carried out. Both empirical and theoretical working formulas have been analysed. Since up to now there was not consensus on which equations were better to employ, a large scattering of evaporation rates has resulted.

A measurement method has been developed and a measurement station has been established for testing heated fluid vessel, suitable for identifying evaporation processes increased by heat sources in the course forced convection. The velocity and the temperature of the humid gas and the temperature of the liquid can be regulated in a wide interval. Therefore, the tests were investigated not only in natural evaporation, but helping with heated liquid too. In the cases examined, evaporation was not only consequent upon environ-mental impacts, but it was also assisted by the heat source of the liquid. This case has

been discussed deficiently by literature on the description and calculation of evaporation.

Our equipment is suitable to research the first, second and third evaporation categories, which appears the evaporation in traditional sense. Measurements were carried out for two cases: the temperature of the gas is higher than the liquid's, and for the opposite case. The measurement objectives are to determine vapor evaporation in various flow conditions, and to calculate the evaporation coefficient. The measurement results are plotted on diagrams. Our future plan is to establish an equation system, which can describe the phenomenon of evaporation in wide range of interpretation, taking into account the different categories.

NOMENCLATURE

A	Surface of heat- and mass transfer	m^2
c	Specific heat	J/(kg°C)
k_G	Mass transfer coefficient with partial pressure difference	mol/Ns
L	Characteristic length	m
m	Mass	kg
M	Molecular weight	kg/mol
N	Evaporation rate	$kg/(m^2 s)$
p	Pressure	Pa
P	Total pressure	Pa
q	Heat flow density	W/m^2
r	Latent heat of vaporization	J/kg
Ra	Rayleigh-number	1
Re	Reynolds-number	1
Sc	Schmidt-number, υ_G/D	1
Sh	Sherwood-number, $k_c L/D$	1
T	Temperature	°C
t	Time	s
v	Velocity	m/s
Y	Absolute humidity of gas on dry basis	kg_{H2O}/kg_{dG}
z	Height above ground level	m
z_0	Roughness length for water	m
α	Heat transfer coefficient	$W/(m^2°C)$
ρ	Density	kg/m^3
φ	Relative humidity	1
γ	Psychrometric constant, $\gamma=66$	Pa/K

Subscripts

amb	*Ambient*
cond	*Conductive*
conv	*Convective*
dG	*Dry gas*
dp	*Dew point*
f	*Water surface*
G	*Humid gas*
H2O	*Water*
v	*Vapor*
vir	*Virtual*
'	*Modified*

REFERENCES

[1] S. Szentgyörgyi, K. Molnár and M. Parti, Transzportfolyamatok, Budapest: Tankönyvkiadó, 1986.

[2] E. R. Treybal, Mass-transfer operations, vol. Third Edition, USA: McGraw-Hill Company, 1981.

[3] T. Poós and V. Szabó, "Párolgási sebesség fűtött folyadék szabad felszínéről," in *International Engineering Symposium at Bánki*, Budapest, 2013.

[4] E. Sartori, "A critical review on equations employed for the calculation of the evaporation rate from free water surfaces," *Solar Energy 68-1,* pp. 77-89, 2000.

[5] W. H. Carrier, "The temperature of evaporation," *ASHVE Transaction 24,* pp. 25-50, 1918.

[6] W. G. Himus and W. J. Hinchley, "The effect of a current of air on the rate of evaporation of water below the boiling point," *Journal of the Society of Chemical Industry 43-34,* pp. 840-845, 1924.

[7] C. Rohwer, "Evaporation from free water surfaces," *U.S. Dept. Agric., Tech.Bull 271,* p. 96, 1931.

[8] H. W. Carrier, Fan Engineering 5th ed., Buffalo, NY: Buffalo Forge Co., 1949.

[9] W. R. Powell, "Evaporation of water from saturated surfaces," *Engineering 150,* pp. 238, 239, 278-280, 1940.

[10] WMO, "Measurement and estimation of evaporation and evapotranspiration 83," 1966.

[11] A. M. Kohler and H. l. Parmele, "Generalized estimates of free-water evaporation," *Water Resour 3,* pp. 997-1005, 1967.

[12] W. McMillan, "Heat dispersal - Lake Trawsfynydd cooling studies," pp. 41-80, 1971.

[13] P. Ryan and D. J. Harleman, "An analytical and experimental study of transient cooling pond behavior," *Technical Report 161,* 1973.

[14] T. J. Czarneczki, "Swimming pool heating by solar energy," *Technical Report 19,* 1978.

[15] M. Govind and S. M. Sodha, "Thermal model of solar swimming pools," *Energy Conv. 23-3,* pp. 171-175, 1983.

[16] G. Szeiz and C. R. McMonagle, "The heat balance of urban swimming pools," *Solar Energy 30-3,* pp. 247-259, 1983.

[17] N. V. V. Kishore and V. Joshi, "A practical collector efficiency equation for non-conventing solar ponds," *Solar Energy 33-5,* pp. 391-395, 1984.

[18] D. Subhakar and S. S. Murthy, "Saturated solar ponds: 1. Simulation procedure," *Solar Energy 50-3,* pp. 275-282, 1993.

[19] B. F. Alagao, A. Akbarzadeh and W. P. Johnson, "The design, construction and initial operation of a closed-cycle, salt-gradient solar pond," *Solar Energy 53-4,* pp. 391-395, 1994.

[20] E. Sartori, "A mathematical model for predicting heat and mass transfer from a free water surface," *ISES Solar world Congress,* pp. 3160-3164, 1989.

[21] E. Hahne and R. Kübler, "Monitoring and simulation of the thermal performances of solar heated outdoor swimming pools," *Solar Energy 53-1,* pp. 9-19, 1994.

[22] B. Molineaux, B. Lachal and O. Guisan, "Thermal analysis of five outdoor swimming pools heated by unglazed solar collectors," *Solar Energy 53-1,* pp. 21-26, 1994.

[23] H. J. Watmuff, S. W. W. Charters and D. Proctor, "Solar wind induced external coefficients for solar collectors," *COMPLES 2,* p. 56, 1977.

[24] C. C. Smith, G. Lof and R. Jones, "Measurement and analysis of evaporation from an inactive outdoor swimming pool," *Solar Energy 53-1,* pp. 3-7, 1994.

[25] M. T. Pauken, "An experimental investigation of combined turbulent free and forced evaporation," *Experimental Thermal and Fluid Science 18,* pp. 334-340, 1999.

[26] R. Tang and Y. Etzion, "Comparative studies on the water evaporation rate from a wetted surface and that from a free water surface," *Building and Environment 39,* pp. 77-86, 2004.

[27] M. Moghiman and A. Jodat, "Effect of Air Velocity on Water Evaporation Rate in Indoor Swimming Pools," *Iranian Journal of Mechanical Engineering 8-1,* 2007.

[28] M. S. Bower and R. J. Saylor, "A study of the Sherwood-Rayleigh relation for water undergoing natural convection-driven evaporation," *International Journal of Thermal Sciences 52,* pp. 3055-3063, 2009.

[29] M. M. Shah, "Improved method for calculating evaporation from indoor water pools," *Energy and Buildings 49,* pp. 306-309, 2012.

[30] A. M. Raimundo, A. R. Gaspar, V. M. Oliveira and D. A. Quintela, "Wind tunnel measurements and numerical simulations of water evaporation in forced convection airflow," *International Journal of Thermal Sciences 86,* pp. 28-40, 2014.

[31] N. Kunmar and H. J. Arakeri, "Natural Convection Driven Evaporation from a water surface," *Procedia IUTAM 15,* pp. 108-115, 2015.

[32] M. Kassai, N. R. Mohammad and S. J. Carey, "A developed procedure to predict annual heating energy by heat and energy recovery technologies in different climate European countries," *Energy and Buildings 109,* pp. 267-273, 2015.

Application of volumetric heat transfer coefficient on fluidized bed dryers

T. Poós[*] and V. Szabó[*]

[*]Department of Building Services and Process Engineering, Faculty of Mechanical Engineering,
Budapest University of Technology and Economics, Budapest, Hungary
poos@mail.bme.hu, szabo.viktor@mail.bme.hu

Abstract – The input parameters of mathematical models are the heat transfer coefficient functions to describe the process of fluidized bed drying. Determining the contact surface of particles includes a number of uncertainties. The purpose of our work is to apply the volumetric heat transfer coefficient to create the criterial equations. During our work the results of the review of literature data are compared with our measurements.

Keywords: fluidized bed dryer, heat- and mass transfer, criterial equation, volumetric heat transfer coefficient

INTRODUCTION

Fluidized bed dryers are widely used in the food and chemical industry to dry wet particles fast and effectively [1]. Some mathematical models are applied in the literature for describing the method of fluidized bed drying [2]. These models involves the solution of differential equation systems. The models are suitable to describe the temperature and moisture content distribution of the material and gas along the length of the dryer, and in the function of drying time. Furthermore, using these models the main parameters of the equipment can be specified without measurements. It is important to know the heat - and the mass transfer process during the drying and to apply sufficiently accurate thermal models describe the process to determine device parameters [3-4]. The input parameters of the mathematical models are the heat transfer coefficient equations beside the geometry and drying characteristics. The heat transfer coefficient equations are criterial equations, which can be determined by measurements. Modelling of fluidized bed dryers require the knowledge of heat transfer coefficient between gas and solid particles. Measuring the heat- and mass transfer surface of the fluidized material has a lot of difficulties. Determining the contact surface of particles includes a number of uncertainty due the irregular surface of particles, the size standard deviation, and the not ideal contact between gas and material. Using volumetric heat transfer coefficient and modified dimensionless numbers for the mathematical models are good possibilities describe the drying process of wet particles [5]. The purpose of our work is to apply the volumetric heat transfer coefficient for fluidized bed drying that eliminates the mentioned uncertainties in the heat transfer area. The results from the literature are compared with the results of our measurements.

METHODS

Volumetric heat transfer coefficient

A pilot plant fluidized bed dryer device was developed to examine the phenomenon of fluidization, the simultaneous heat- and mass transfer during drying of particles and it makes possible to evaluate the volumetric heat transfer coefficient. We presented the device, the measuring method and the results during our prevouis works [6]. Some kind of grains were dried with varied operating parameters during our experiments.

Due the mentioned difficulities, a parameter can be given to characterise the contact surface, which depends on the geometry of the dryer, the properties of contact between gas and particles, and the hold-up of materials. This parameter is the volumetric interfacial surface area [7]:

$$a = \frac{A_{cont}}{V_{d,sta}} = \frac{A_{cont}}{A_d L_{sta}},\qquad(1)$$

where A_{cont} is the contact surface of materials, $V_{d,sta}$ is the volume of the dryer, where the particles staying, A_d is the surface of dryer, L_{sta} is the static height of particles. Fig. 1. shows the detail of the fluidized bed dryer presented the gas- and material flow, the main properties of gas and material, and the position of drying particles during the operation.

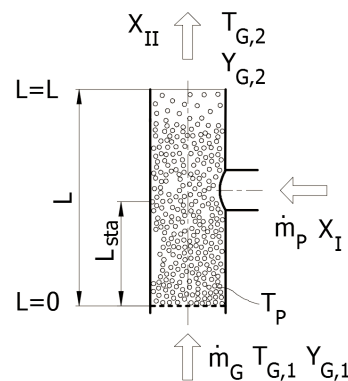Figure 1. Sketch of the dryers section is showing the position of fluidized particles and the properties of material- and gas flow

The mass balance equation shows the connection between the amount of evaporated water from the material and the amount of humidity taken by the drying gas during the drying process:

$$\int_{t=0}^{t=t} \dot{m}_G(Y_{G,2} - Y_{G,1})dt = \int_{X=X_I}^{X=X_{II}} m_{dP}dX,\qquad(2)$$

where $\dot{m}_G$ is the mass flow of drying gas, $Y_{G,1}$ is the absolute humidity of gas at the inlet point of dryer, $Y_{G,2}$ is the absolute humidity of gas at the outlet point of dryier, m_{dP} is the mass of dry particles, ΔX is the moisture content decrease of the material in time Δt. The heat balance equation shows the total heat flow between the particles and the drying gas. The total heat flow can be separated the heat flow for heating up the particles ($Q_{heating}$) and the heat flow from evaporation (Q_{evap}):

$$\dot{Q}_{total} = \dot{Q}_{heating} + \dot{Q}_{evap}. \qquad (3)$$

At the constant drying rate period the heating up process is negligible, because the surface tempeature of materials is constant and it tends to the wet bulb temperature. The total heat flow using the mass balance equation (2):

$$\dot{Q}_{total} = \frac{m_{dP}\Delta X}{\Delta t} r_{H2O} = \dot{m}_G(Y_{G,2} - Y_{G,1})r_{H2O}, \qquad (4)$$

where r_{H2O} is the latent heat of evaporation. The convective heat flow according to Newton:

$$\dot{Q}_{total} = \alpha A_{cont}(\overline{T}_G - T_P), \qquad (5)$$

where $\overline{T}_G$ is the average of inlet and outlet gas temperature, T_P is the temperature of the surface of particles. Combining Eqs. (4) and (5):

$$\alpha A_{cont}(\overline{T}_G - T_P) = \dot{m}_G(Y_{G,2} - Y_{G,1})r_{H2O}. \qquad (6)$$

The volumetric heat transfer coefficient obtained from Eqs. (1) and (6) in the constant drying rate period:

$$\alpha a = \frac{\dot{m}_G(Y_{G,2} - Y_{G,1})r_{H2O}}{(\overline{T}_G - T_P)A_d L_{sta}}. \qquad (7)$$

The main advantage of using the volumetric heat coefficient is, that the correlation (7) contains easily calculable parameters with less uncertainties. It means, that calculating this value the real shape and the amount of the particles in the dryer, and the properties of gas-material contact, so the surface area of the particles is unconserned.

The Reynolds- and the modified Nusselt-numbers are the components of the criterial equations for modelling fluidized bed drying:

$$Re = \frac{v_G \cdot d_p}{v_G} \qquad Nu' = \frac{\alpha a \cdot d_P{}^2}{\lambda_G}. \qquad (8)$$

Summary of the dimensionless equations from the literature

In the literature there are several $Nu=f(Re)$ equations using to characterize the heat transfer between solids and drying gas. Equations from literature were summerised in Table 1, which are valid in the case of fluidized bed drying. The plots of the listed $Nu=f(Re)$ equations from the literature are represented in Fig. 2. The general ascertainment of these studies is, that the basis of the dimensionless equations is the heat transfer coefficient between gas and material.

The heat transfer coefficient can be calculated with making some approximations, like to assume that the geometry of particles is sphere, and the contact between gas and material is ideal. These mean, that during the drying each particle are in contact with the drying gas, on its whole surface. With these assumptions, knowing the total number of particles in the drying chamber, the contact surface of material can be determined (6).

It can be stated, that these equations differ significantly each other due the inaccuracy of determining the contact surface. We revised the measurements results of literature data available, and evaluated the volumetric heat transfer coefficient from them.

Review of literature data

During our work we revised the measurements data from some literature sources. The calculations can be applied only those studies, where the dimensionless equations with their scopes were published, and the measurement conditions and the specifications of the particles were published as well. Other important condition was during the review, that the studies dealt with the case of drying, and the criterial equations are valid on the constant drying rate period. Usually there were lack of measured data available, so the heat transfer coefficient was calculated using iteration. During the

Ref.	Equations	Scope
Heertjes [8]	$\alpha = 7.427Re^{0.78}$	$8.8 < Re < 52.3$
Kettelring [9]	$Nu = 0.0135Re^{1.3}$	$9 < Re < 55$
Kumaresan [10]	$5.6493 \cdot 10^{-5}Re^{1.537}$	$30 < Re < 70$ and $0.0106 < Nu < 0.298$
Alvarez [11]	$Nu = 2.41 \cdot 10^{-4}Re^{1.733}$	$80 < Re < 250$
Alvarez [11]	$Nu = 8.24 \cdot 10^{-4}Re^{1.635}$	$80 < Re < 250$
Ciesielczyk [12]	$Nu = 0.106Re \cdot Ar^{0.047}\left(\frac{L}{d_p}\right)^{-0.083} \varphi^{1.21}$	$3.61 < Re < 125.9$ and $1.24 \cdot 10^2 < Ar < 1.14 \cdot 10^5$ $121 < \frac{L}{d_p} < 705$ and $1.14 < \varphi < 1.81$
Ranz [13]	$Nu = 2 + 1.8Re^{0.5}Pr^{0.33}$	$100 < Re$
Roy [14]	$Nu = 0.0205Re^{1.2876}Pr^{0.33}$	$1 \leq Re \leq 10^3$
Fedorov [15]	$Nu = 1.63 \cdot 10^{-2}Ar^{0.549}Re^{0.41}\left(\frac{L}{d_p}\right)^{-0.24}$	$2 \cdot 10^3 < Ar < 7.5 \cdot 10^5$ $20 < Re < 100$
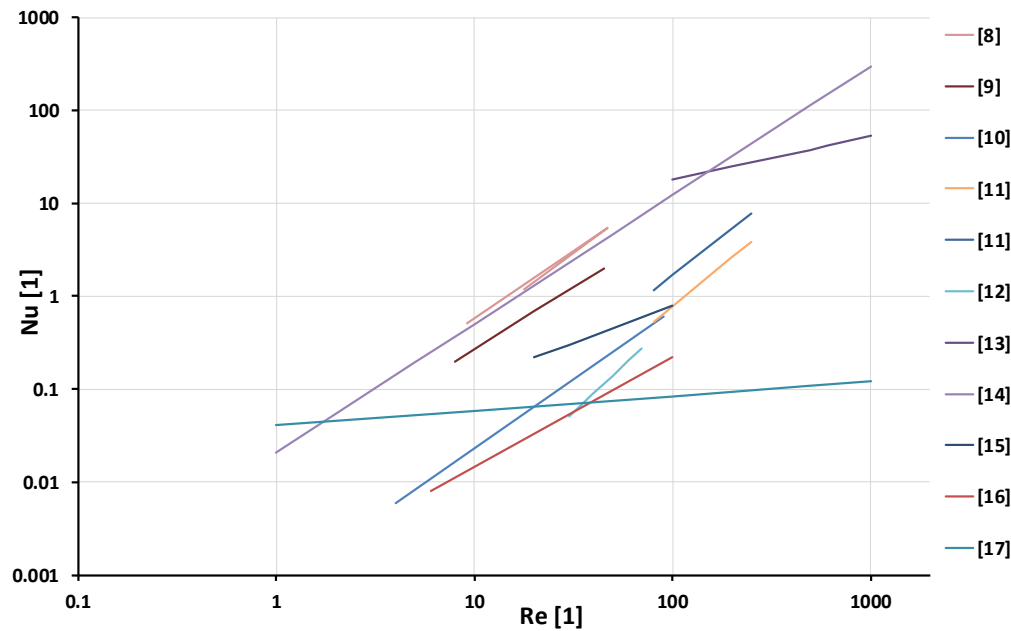
review the heat transfer coefficient and the volumetric heat transfer coefficient were evaluated.

Knowing the *Nu=f(Re)* equations, and its scopes, the heat transfer coefficient can be calculated with iteration. The iteration steps are the following:

1st step: The Reynolds-number was calculated from the measured data. The absent data were set up to an optional value.

2nd step: The value Nu_{crit} was evaluated from the criterial equation with using the Reynolds-number.

3rd step: The heat transfer coefficient was calculated (6) from the given, or adjusted parameters.

4th step: Calculating $Nu_{calc} = \dfrac{\alpha \cdot d_P}{\lambda_G}$.

The method iteration is complete, when the deviation between Nu_{calc} and Nu_{crit} is less than 1%
$$\left| \frac{Nu_{crit} - Nu_{calc}}{Nu_{calc}} \right| < 0.01.$$

After the iteration of heat transfer coefficient every important operation parameters are known. Using Eq. (7) the volumetric heat transfer coefficient can be calculated, than the modified Nusselt-number (8) can be evaluated.

Kumaresan et al. [10] carried on experiments in the constant drying rate period on a fluidized bed dryer in batch operation. The diameter of the experimental apparatus was *55 mm*, the height was *435 mm*. The particles used for the experiments were ammonium-chloride with particle diameter between *0.495 ÷ 0.912 mm*, the velocity of inlet air *1.136 ÷ 1.391 m/s*, the range of its temperature *60 ÷ 75 °C*, the initial moisture content *0.04 ÷ 0.06 kg_{H2O}/kg_{dP}*, and the mass of the fluidized particles varied in the range *0.09 ÷ 0.13 kg*. The equation for determining the heat transfer coefficient is:

$$Nu_{Kumaresan} = 5.649 \cdot 10^{-6} Re^{1.997}, \qquad (9)$$

Eq. (9) is valid $30 < Re < 70$ and $0.0106 < Nu < 0.298$.

Alvarez et al. [11] used two different types of materials for their pilot-plant fluidized bed drying experiments:

soya meal, sawdust and fish meal. The velocity of drying gas ranged between *2.8 ÷ 3 m/s*, the inlet temperature was *65 ÷ 105 °C*. The dimensionless correlation using the measurement data of soya meal:

$$Nu_{soya\,meal,Alvarez} = 2.41 \cdot 10^{-4} Re^{1.753}, \qquad (10)$$

$$Nu_{sawdust,Alvarez} = 8.24 \cdot 10^{-4} Re^{1.655}, \qquad (11)$$

Eq. (10) and (11) are valid on $80 < Re < 250$.

Ciesielczyk et al. [12] used in their experiments Polytetrafluoro-ethylene, ammonium sulphate, sand and silica gel. 208 measurements were performed, from these 97 measurements are suitable to study the falling drying rate period as well. Particle sizes ranged from *0.339 ÷ 1.24 mm*, the inlet temperature *333 K* and *363 K*, static bed height between *150 mm* and *240 mm*, air velocity from *0.2 ÷ 1.8 m/s*. The initial moisture content of materials was constant in every measurements. The criterial equation for Nu-Re correlation is:

$$Nu_{Ciesielczyk} = 0.106 Re Ar^{0.0437} \left(\frac{L_{sta}}{d_{1P}} \right) \Phi^{1.12}, \qquad (12)$$

Eq. (12) is valid: $3.61 < Re < 125.9$ and $1.24 \cdot 10^3 < Ar < 1.14 \cdot 10^5$ and $121 < \frac{L}{d_P} < 705$ and $1.14 < \Phi < 1.81$.

Figure 3. Comparison of dimensionless equations from [10-12]
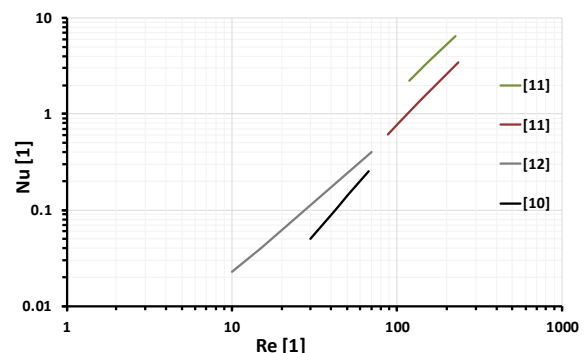
RESULTS

Fig. 3. shows the mentioned *Nu=f(Re)* dimensionless equations (9)-(12) from the literature with their scopes [10-12], where the measurement conditions were known. There are many other *Nu=f(Re)* functions located in the literature, but the calculations could be done only on the mentioned publications due the lack of the measurement data.

Fig. 4. shows the converted measurement points from literature with our results evaluated from the measurements. The revised data using modified Nu'-Re equations show better fit compared to the original values. The results show proper conformity with data based on literature and the results of our measurements.
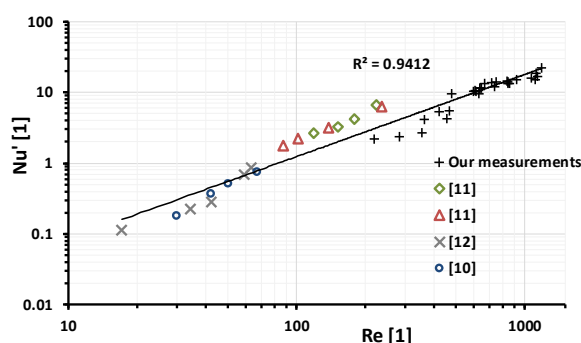
Figure 4.   *Nu' vs Re* correlation of literature cited and our measurements [10-12]

A trendline was fitted to the measurement points, which shows strong correlation. The coefficient of determination to the measurements points is $R^2 = 0.9412$. Using volumetric heat transfer coefficient and modified Nusselt-number the margin of error can be reduced.

CONCLUSION

The purpose of our work is to introduce the volumetric heat transfer coefficient for fluidized bed drying, which eliminates the uncertainties the determination of the heat transfer surface between gas and particles. Modified *Nu'=f(Re)* equation shows proper correlation between the results of the measurements in the literature, and the results of our measurements. The goal of our work is a new method for scaling up fluidized bed dryers using volumetric heat transfer coefficient.

ACKNOWLEDGMENT

REFERENCES

[1]   A. S. Mujumdar, „Heat Transfer in Fluidized Beds – An Overview," *Special Topic in ME6204 Convective Heat Transfer, ME Department,* NUS, 2010.

[2]   J. S. Walton, R. L.Olson, and O. Levenspiel, "Gas-Solid Film Coefficients of Heat Transfer in Fluidized Coal Beds*,*" *Ind. Chem. Eng.* vol. 44, pp. 1474-1480, 1952.

[3]   M. Kassai and C. J. Simonson, "Performance investigation of liquid-to-air membrane energy exchanger under low solution/air heat capacity rates ratio conditions," *Building Services Engineering Research & Technology.* vol. 36. n. 5. pp. 535-545, 2015.

[4]   M. Kassai, G. Ge and C. J. Simonson, "Dehumidification performance investigation of liquid-to-air membrane energy exchanger system," *Thermal Science.* DOI: 10.2298/TSCI140816129K (*Accapted article*), 2014.

[5]   T. Poós and M. Örvös, "Heat- and mass transfer in agitated co-or countercurrent, conductive-convective heated drum dryer," *Drying Technology*, vol. 30. n. 13. pp. 1457-1468, 2012.

[6]   M. Örvös, V. Szabó and T. Poós, "Volumetric heat transfer coefficient for modelling the fluidized bed dryers," *5th European Drying Conference*, ISBN: 978-963-9970-62-5, pp. 296-303, 2015.

[7]   R. E. Treybal, *Mass-transfer operations,* 3rd edition, McGraw-Hill Company, New York, 1981.

[8]   P. M. Heertjes and S. W. McKibbins, "The partial coefficient of heat transfer in a drying fluidized bed", *Chem. Eng Sci.* vol. 5, pp. 161-167, 1956.

[9]   K. N. Kettelring, E. L. Manderfield and J. M. Smith, "Heat and Mass Transfer in Fluidized System"*, Chem. Eng. Progr.* vol. 46, pp. 139, 1950.

[10]   R. Kumaresan and T. Viruthagiri, "Simultaneous heat and mass transfer studies in drying ammonium chloride in a batch-fluidized bed dryer," *Indian Journal of Chemical Technology*, vol. 13. n. 5. pp. 440-447, 2006.

[11]   P. Alverez and C. Shene, "Experimental study of the heat and mass transfer during drying in a fluidized bed dryer," Drying Technology, vol. 14. n. 3-4. pp. 701-718, 1996.

[12]   W. Ciesielczyk and M. Mrowiec, "The method of decreasing the number of experiments needed to design a fluidized bed drying," *Inz. Chem. I Proc.,* vol. 4. n. 12. pp. 551-567. 1991.

[13]   W. E. Ranz and W. R. Marshall, "Evaporation of drops," *Chem. Eng. Progr.* vol. 48. n. 3. pp. 141-146, 1952.

[14]   P. Roy, M. Vashishtha, R. Khanna and D. Subbarao, "Heat and mass transfer study in fluidized bed granulation—Prediction of entry length", *Particuology*, vol. 7. n. 3. pp. 215-219, 2009.

[15]   J. M. Fiedorov, "Teorija I rascziot prociessa suszki wo wzwiesziennom stoje," *Goseniergaizdat*, Minsk, 1976.

[16]   S. Jan-Fou, P. G. Romankow, and P. G. Raszkowska, *Zurnal. Prikl. Chimii,* vol. 3, pp. 530, 1962.

[17]   J. Khorshidi, H. Davari and F. Dehbozorgi, "Model Making for Heat Transfer in a Fluidized Bed Dryer", *Journal of Basic and Applied Scientific Research*, vol. 1, n. 10, pp. 1732-1738, 2011.

[18]   J. Nyers, L. Garbai, A. Nyers: A modified mathematical model of heat pump's condenser for analytical optimization. International J. Energy. Vol. 80, pp. 706-714, 2015. (IF 4.844)

Expected thermal comfort in underground spaces

János Szabó*, László Kajtár*

* Budapest University of Technology and Economics, Department of Building Service and Process Engineering,
Budapest, Hungary
kajtar@epgep.bme.hu
szaboj@epgep.bme.hu

Abstract — **In this paper a method is presented for dimensioning underground spaces in terms of heat transfer characteristics and thermal comfort. The accurate dynamic determination of the average energy demand of an underground space is difficult because the soil surrounding the rooms is a semi-infinite space and its temperature varies in annual cycles. The dynamic physical and mathematical model with initial and boundary conditions have been developed. Within the procedure of mathematical modelling the heat transfer properties, the heat comfort model and the simulation algorithm of underground spaces have been created. The obtained simulation results are presented in diagrams in favour of the quick sizing of the required heating and cooling performance of underground spaces. The presented diagrams can be used in an effective manner also for the calculation of thermal comfort in underground spaces.**

Keywords: PMV, PPD, underground space, simulation, modelling

INTRODUCTION

The history of underground spaces suitable for human occupancy coincides with the history of humans. These residential spaces provide shelter against hot weather, storms and nomadic roving tribes. Examples can be found in almost all continents: in Tunisia, China, Ghana, America and Turkey. The constant temperature of 8-12°C in underground spaces provides reliable protection against both cold winter and hot summer [1], [2], [3].

Urban development today cannot be imagined without underground spaces. Many spaces with different functions are built underground, including not only parking lots, but also shopping malls, exhibition halls and service facilities. Office buildings, shopping centres can also have levels below the ground floor [4], [5], [6].

An important feature of underground spaces is the higher protection against the climatic influences. The soil temperature follows the external changes with phase delay and with significant attenuation. As a result, the heating and the cooling thermal loads are remarkably lower. A pleasant thermal comfort can be ensured with less energy in underground spaces [7], [8], [9].

An underground space is not bordered by walls, but with semi-infinite spaces. This has to be considered when developing the physical model. The soil temperature varies in annual cycles. The development of physical and mathematical models necessarily requires simplifying assumption. Different methods can be found in the international literature for determining the heating and cooling capacities. Measurement results are also available regarding the heat transfer properties and thermal comfort

in operating underground spaces. In this paper the dimensioning model is presented and a solution method is proposed for the determination of heating and cooling performance, supply air properties and thermal comfort parameters. The developed method can be used for the spaces located underground.

Sizing methods of underground spaces can be found in the literature of the 1950s. The starting points of these methodologies are steady state equations [10]. Sizing methods can be found for dynamic processes of the warm-up period and providing constant temperature. Design methods approximate time-varying boundary conditions of the heat conduction differential equation with time constant boundary conditions of the first and second kind.

In scientific literature combined analysis of heating, cooling energy demand and thermal comfort is not to be found. In contrast with the above mentioned results of scientific literature research, we applied time-varying boundary condition of the third kind which correspond to the real process. A new software tool for the numerical simulation was developed in the framework of study. The results obtained by the method were presented in general diagrams.

The primary aim of investigation was to develop the dimensioning method which is suitable for determining time dependent changes in the required performances for heating and air handling processes in underground spaces.

In addition, the parameters of thermal comfort can be calculated based on the obtained temperature, humidity of
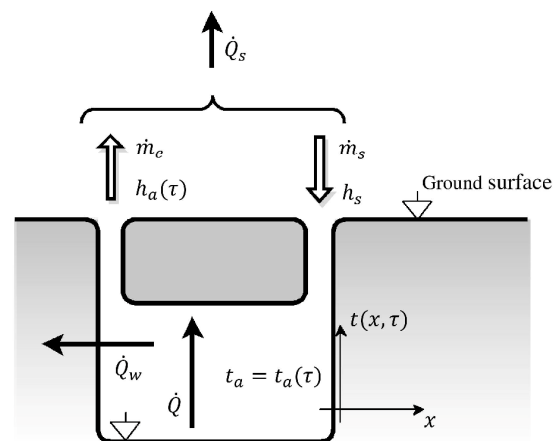

Figure 1.   Underground spaces with energy sources, heat fluxes, system parameters and working mediums (air and soil)

air and wall surface temperature in the underground space. In this way, it is possible already during the dimensioning

process to determine the most important indicators of the thermal comfort, the values of *PMV* and *PPD* [11], [12].

PHYSICAL MODEL

The physical model of an underground space consists of ventilation, heating-cooling system and the soil surrounding the underground space.

Working mediums are the mass of moist air and surrounding soil. Still, important components of this system are the heat fluxes and the parameters of the system, see Fig. 1.

DYNAMIC MATHEMATICAL MODEL

The mathematical model of an underground space describes the heat balance of the underground space including the ventilation and heating-cooling demand, internal thermal load, and the heat flux through the wall. The analysed thermal events in the underground space happen in the space and in the time, therefore their mathematical description is possible with partial differential equations. The leading partial differential equation has been obtained on the basis of the heat balance of the underground space [13]. The heat conduction through the soil mass over the time domain is described by Fourier's parabolic partial differential equation. The convection heat transfer from the air to the wall of the underground space is defined by integrating the differential equation.

The dynamic heat balance equation

The heat balance of the underground space means the increment of the sum of heat fluxes, which equals the increment of the air enthalpy filling underground space (1).

$$\left[\dot{Q} - \dot{Q}_w(\tau) - \dot{Q}_s(\tau)\right]d\tau = c_{p,a} \cdot \rho_a \cdot V \cdot dt_a \quad (1)$$

Where:

The internal heat load includes human, light, electrical equipment components and also mechanical cooling and heating loads.

$$\dot{Q} = \dot{Q}_h + \dot{Q}_l + \dot{Q}_e + \dot{Q}_{h,c} \quad (2)$$

Convective heat transfer from the air to the wall:

$$\dot{Q}_w(\tau) = \int_A \alpha \cdot [t_a(\tau) - t(x,\tau)|_{x=0}] \cdot dA \quad (3)$$

The heat capacity of ventilation is the supply air enthalpy increment:

$$\dot{Q}_s(\tau) = \dot{m}_S \cdot [h_a(\tau) - h_s] \quad (4)$$

The dynamic heat transfer through the soil

The dynamic heat transfer through the soil is described by one dimension Fourier partial differential equation of the heat conduction equation (5), as seen Fig. 2 [14], [15]:

$$\frac{\partial t(x,\tau)}{\partial \tau} = a \cdot \frac{\partial^2 t(x,\tau)}{\partial x^2} \quad (5)$$

Boundary conditions:

$$\textbf{at } x = 0 ; \; -\lambda \cdot \frac{\partial t(0,\tau)}{\partial x} + \alpha \cdot [t_a(\tau) - t(0,\tau)] = 0 \; (6)$$

$$\textbf{at } x = \infty ; \; t(\infty,\tau) = const. \quad (7)$$

Initial condition:

$$\textbf{at } \tau = 0 ; \; t(x,0) = t_a(0) = const. \quad (8)$$

DYNAMIC MATHEMATICAL MODEL

The partial differential equation (5) is easier to solve, if in the conditional equations (6), (7) and (8) the constants equal zero. This means, shifting the zero point of the temperature scale to the initial soil or air temperature. The transformed coordinate axis of temperature is distinguished by a comma (Fig. 2).

One type of the equations, which satisfies the one-dimension Fourier partial differential equation of heat conduction (5) is:

$$t = A + Bx + \frac{C}{\sqrt{\tau}} \cdot e^{-\frac{(q-x)^2}{4 \cdot a \cdot \tau}} \quad (9)$$

The constants in the equation above (A, B, C, a, q) can be determined based on the conditional equations.

If the boundary condition varies in time, the differential
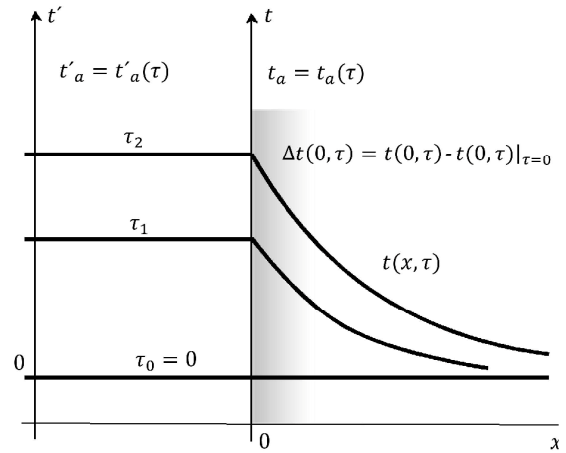
Figure 2.   Temperature distribution of the air, and soil in the semi-infinite space depending on x-coordinate and τ-time

equation of the heat conduction can be solved using Laplace transformation or by the Duhamel's method [16]. The Duhamel's method can be conveniently used when the initial temperature distribution is arbitrary or when the temperature of the surrounding medium (air) depends on time and distance. In this case the temperature of the surrounding medium (air) depends only on time, so the Laplace transformation is preferred [17].

Based on the equations (5), (6), (7), (8) the obtained solution (10) is a convolution integral as a function of time (τ) and distance (x).

In fact, physically, the solution is the modified temperature increment of the soil from the wall surface at time (τ) and distance (x).

The solution is a convolution integral:

$$\Delta t(x, \tau) = \int_0^\tau t_a'(\tau - u) \cdot g(u) \cdot du \quad (10)$$

Where:

$$g(u) = H \cdot \sqrt{\frac{a}{\pi \cdot u}} \cdot e^{-\frac{x^2}{4 \cdot a \cdot u}} - a \cdot H^2 \cdot e^{H \cdot x + a \cdot H^2 \cdot u} \cdot$$

$$erfc\left[\frac{x}{2 \cdot \sqrt{a \cdot u}} + H \cdot \sqrt{a \cdot u}\right] \quad (11)$$

$$H = \frac{\alpha}{\lambda} \quad (12)$$

After substituting the function (11) and (12) in equation (12), we can get the wall surface or modified soil temperature increment. After substituting the before determined wall surface temperature increment in heat balance equation (1) the result is the differential equation of the underground space in the time domain:

$$\frac{dt_a}{d\tau} + k_1 \cdot t_a + k_2 \cdot \left[\int_0^\tau t_a'(\tau - u) \cdot g(u)|_{x=0} \cdot \right.$$

$$\left. du + t(0, \tau)|_{\tau=0}\right] + k_3 = 0 \quad (13)$$

Where:

$$k_1 = \frac{A \cdot \alpha + \dot{m}_s \cdot (c_{p,a} + x_a \cdot c_{p,s})}{c_{p,a} \cdot V \cdot \rho_a} \quad (14)$$

$$k_2 = -\frac{A \cdot \alpha}{c_{p,a} \cdot V \cdot \rho_a} \quad (15)$$

$$k_3 = \frac{\dot{Q} - \dot{m}_s \cdot (x_a \cdot r_0 + h_s)}{c_{p,a} \cdot V \cdot \rho_a} \quad (16)$$

Initial condition:

$$\text{at} \quad \tau = 0 \;;\; t_a(0) = t(x, 0) = const. \quad (17)$$

Comments:

- At the start of heating the soil temperature is considered as resultant temperature. The soil and the air temperature are equal in all points of space.

- The temperatures of various surface parts could be different, if these are justified. Then the heat loss of the wall has to be calculated separately for each part of surface, which should be substituted in the equation (1).

- The absolute humidity of the air in the underground space is included in the constants of equation (13). If the humidity load is not significant, the absolute humidity of the supply air is equal to the room air absolute humidity. This is the usual case for comfort spaces.

- If the absolute humidity of the air varies in time, the variables k_1 and k_3 of equation (13) will also vary in time.

NUMERICAL SOLUTION OF THE MATHEMATICAL MODEL

Equation (13) is an integro-differential equation, which contains convolution integral. The differential equation can be solved by means of finite difference methods. For this purpose, the differential equation (13) was converted into a difference equation. The convergence of the numerical procedure can be ensured if the studied temperature and heat flux are monotonous functions of time and no sudden changes occur. Within the simulation process the optimum time step was accordingly investigated and selected [19].

An algorithm is worked out and a software tool is designed for the numerical solution of differential equation (13). The algorithm of the dimensioning procedure of underground spaces is illustrated in Fig. 3.

Initial values and data for simulation

The dimensions of the studied underground space are: 8 m width, 40 m length and 3 m height.

The thermal sensation of human is influenced by activity and clothing. The base values of these parameters

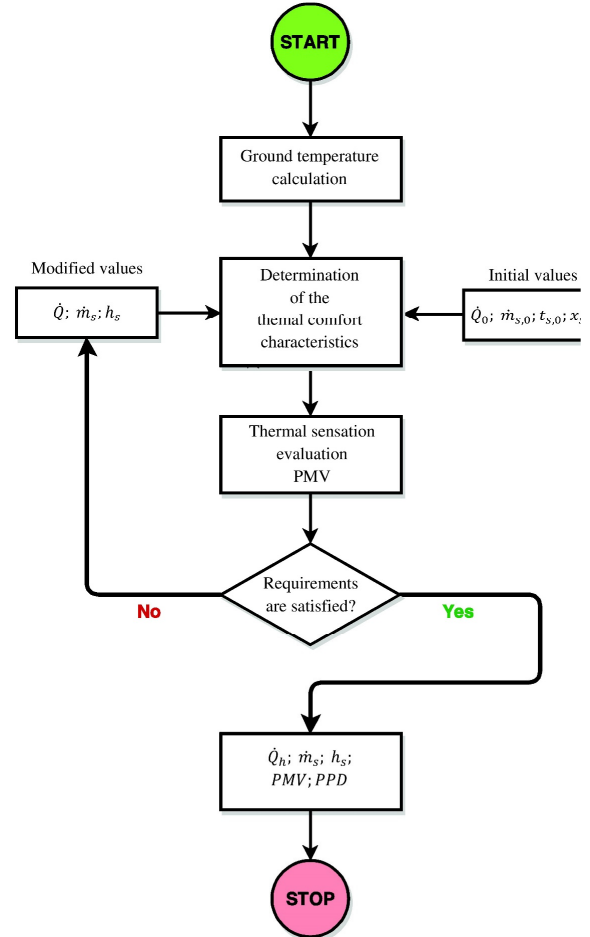Figure 3.   Algorithm for the dynamic thermal dimensioning of an underground space

are:

$$\frac{M}{A_{Du}} = 1[\text{met}] = 58[\text{W/m}^2] \text{ (sedentary activity level)}$$

$$I_{clo} = 1[\text{clo}] = 0.155[\text{m}^2\text{K/W}] \quad \text{(typical working clothes)}$$

Characteristics of the soil:

$\rho = 1\,800$ kg/m³
$\lambda = 1.5$ W/m K
$c = 0.84$ kJ/kg K
$t = t(0, 0) = 12°C$ ($x = 0$, $\tau = 0$)

Reults

In the study, the heat load, the enthalpy of the supply air and the air exchange rate were taken into account. The basic data of the respective versions are shown in Table 1.

	№	(1)	(2)	(3)	(4)	(5)	(6)
Input data	δ ; [cm]	3	0	5	3	3	3
	$\frac{\Sigma \dot{Q}}{V}$; $\left[\frac{W}{m^3}\right]$	17	17	17	48	17	17
	n ; [1/h]	3	3	3	3	6	3
	t_S ; [°C]	24	24	24	24	24	30
	x_S ; [g/kg]	8	8	8	8	8	8
	$t(0,0)$; [°C]	12	12	12	12	12	12
Results	$\dot{Q}_h$; [kW]	10	10	10	30	10	10
	$\dot{Q}_h + \dot{Q}_s$; [kW]	48,1	48,1	48,1	68,1	86,1	52,1
	$\dot{q}_w$; [W/m²]	11,2	19,8	8,9	18,8	10,9	12,9
	PMV ; [-]	0,07	-1,39	0,48	2,20	0,00	0,59

Table 1 also contains the results obtained after 70 hours.

We transferred the results of heat transfer characteristics and the thermal comfort dimensioning process into diagrams. Thermal load and ventilation figures were converted into specific values, so that the results obtained can be used also for dimensioning tasks.

Fig. 4. shows the change of heat flux through the wall of the underground space.

Fig. 5 shows the thermal comfort improvement in the respective cases.

The influence of thermal insulation thickness can be seen in Fig. 6 and Fig. 7 at various air exchange rates (n=1 and 3 1/h) and internal heat load.

The basic values considered for the dimensioning can be reliably used in general cases too. The conclusions summarised can be obtained from the evaluation of the results. Version (1) from the previously presented Table 1. can be considered as a reference.
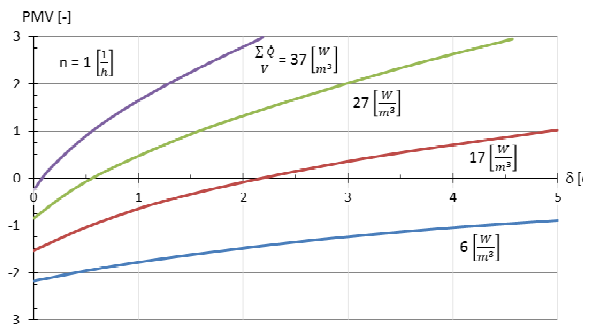
Figure 6.   Influence of the thickness of thermal insulation on the PMV value ($n = 1$ h^{-1}, $\tau = 70$ hour)
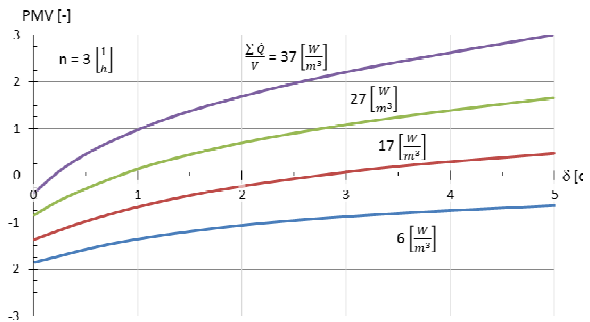
Figure 7.   Influence of the thickness of thermal insulation on the PMV value ($n = 3$ h^{-1}, $\tau = 70$ hour)

Figure 4.   Graphics of the heat fluxes through the wall as a function of time

Figure 5.   Thermal comfort in the underground space ($\tau = 70$ hour)

Discussion

The heat flux through the wall of an underground space can be reduced significantly by the use of a 3 cm thick thermal insulation /Versions (1) and (2)/.

The increase of the thermal insulation thickness over 5 cm (Fig. 6 and Fig. 7) has minor impact, thus not recommended.

If the resultant heat balance (people, lighting, technology) of the underground space does not exceed the value of 15-18 W/m³ and the thermal insulation thickness is at least 3 cm it is not required to use mechanical cooling (Fig. 5).

If thermal insulation of 3 cm thickness is used, then the initial maximum heat loss is reduced to 16 W/m² and after 70 hours it reduced to 13 W/m². (Fig. 4).

If the thickness of the thermal insulation is 5 cm, the heat loss is reduced to 10.5 W/m² (Fig. 4).

CONCLUSIONS

We developed a dimensioning method for underground spaces. The physical model is capable for the analysis of dynamic processes, the temperature change of the wall and the air, as well as the thermal sensation characteristics (*PMV*, *PPD*) determined in the underground space. According to our investigations the thermal comfort characteristics have been considered permanent after 70 hours. From these data we developed generally applicable dimensioning diagrams for sizing underground spaces. These help to determine the required heating power, ventilation air flow, and thermal comfort characteristics. By using a finite-element model we could get more detailed results. However, these results required long time or great software and hardware needs. The applied algorithm and dimensioning charts could give quick and useful results.

Summary of conclusions

- The older scientific literature of dimensioning methods are not suitable for complex calculation of heating, cooling performance and thermal comfort in underground spaces.

- During the investigation of the non-steady state process, the change of air temperature after 70 hours was less than 0.00001°C/s (0.036°C/h).

- Heating and cooling are significantly affected by the internal heat load of the underground space. In case of 15-18 W/m^3 resultant heat balance, it is not required to use mechanical cooling or heating.

- It is recommended to use 3-5 cm thick thermal insulation on the surrounding surfaces of the underground space.

- The supply air flow must be dimensioned according to the required fresh air need. From the energy point of view it is not recommended to increase the temperature and the volume flow of the supply air.

- By assuming heat penetration depth of 3 m on the basis of practical data, the soil volume neglected at the corners is below 10 %, if the circumference of the underground space is more than 85 m.

REFERENCES

[1] Labs, K.: The use of Earth covered Buildings through History. Forth Worth, Texas, The Use of Earth covered Buildings, 1975.

[2] F. Allard, J. Brau, C. Inard, J.M. Pallier, Thermal experiments of full-scale dwelling cells in artificial climatic conditions, Energy and Buildings, Volume 10, Issue 1, February 1987, pp. 49–58.

[3] A. A. Al-Temeemi, D. J. Harris, A guideline for assessing the suitability of earth-sheltered mass-housing in hot-arid climates. Energy and Buildings 36 (2004) 251-260.

[4] Simge Andolsuna, Charles H. Culpa, Jeff Haberla, Michael J. Witte: Energy Plus vs. DOE-2.1e: The effect of ground-coupling on energy use of a code house with basement in a hot-humid climate, Energy and Buildings, Volume 43, Issue 7, July 2011, pp. 1663–1675. DOI: 10.1016/j.enbuild.2011.03.009

[5] K Ip, A Miller: Thermal behaviour of an earth-sheltered autonomous building – The Brighton Earthship, Renewable Energy, 34 (9), 2009, pp. 2037-2043. doi:10.1016/j.renene.2009.02.006

[6] C.A. Balaras, K. Droutsa, E. Dascalaki, S. Kontoyiannidis: Heating Energy Consumption and Resulting Environmental Impact of European Apartment Buildings, Energy & Buildings, 37, pp. 429-442, (2005).

[7] Bligh T: Comparison of energy consumption in earth covered vs. non-earth covered, Forth Worth, Texas, The Use of Earth covered Buildings, 1975

[8] Miquel Casalsa, Marta Gangolellsa, Núria Forcadaa, Marcel Macarullaa, Alberto Girettib: A breakdown of energy consumption in an underground station, Energy and Buildings, Volume 78, August 2014, pp. 89–97. DOI: 10.1016/j.enbuild.2014.04.020

[9] P. Novak: Background document for Rules on efficient use of energy in buildings, July, 2008 (published as Rules, Official Gazette of RS No. 93/08, pp. 12698- 12717)

[10] Macsinszkij V. D.: Teplotehnicseszkie osznovi sztroitelsztva, Moskov, Sztrojizdat, 1980.

[11] Alberto Barbaresi, Daniele Torreggiani, Stefano Benni, Patrizia Tassinari: Underground cellar thermal simulation: Definition of a method for modelling performance assessment based on experimental calibration, Energy and Buildings, Volume 76, 2014, pp. 363–372. DOI: 10.1016/j.enbuild.2014.03.008

[12] Yimin Xiaoa, Xichen Liua, Rongrong Zhangb: Calculation of transient heat transfer through the envelope of an underground cavern using Z-transfer coefficient method, Energy and Buildings Volume 48, 2012, pp. 190–198. DOI: 10.1016/j.enbuild.2012.01.040

[13] L. Kajtár, Thermal comfort dimensioning and results of measurements in underground spaces, Delft, 1992. 5th International Conference on Underground Space and Earth Sheltered Structures. 1992, pp. 636 – 645

[14] H.S. Carslaw, J.C. Jaeger: Conduction of heat in solids, 1959, ISBN: 0198533683

[15] H Gröber, S Erk, U Grigull: Die Grundgesetze der Wärmeübertragung. Berlin - Göttingen Heidelberg, Springer Verlag, 1963.

[16] Konrad Schumacher: On the resolving of linear non autonomous partial functional differential equations, Journal of Differential Equations, Volume 59, Issue 3, 1985, pp. 355–387. DOI: 10.1016/0022-0396(85)90146-9

[17] Oberhettinger F, Badii L: Tables of Laplace transforms, 1973, p. 428 SBN: 978-3-540-06350-6

[18] Miao, XP; Wang, Q; Cheng, BY; Mao, JF: Global optimizing analysis of indoor environment quality parameters in underground space (2005), Indoor Air 2005 (ISBN:978-7-89494-830-4) pp. 2778-2782.

[19] Petráš D, Lulkovičová O, Takács J, Füri B.: Obnoviteľnézdroje energie na vykurovanie. In: Vykurovanie rodinných a bytových domov. Bratislava: Jaga, 2005. pp.193–217, ISBN 80-8076-012-8.

[20] Nyers József, Slavica Tomic, Nyers Arpad: Economic Optimum of Thermal Insulating Layer for External Wall of Brick, ACTA POLYTECHNICA HUNGARICA 11: (7) pp. 209-222. (2014)

[21] M R Nasr, M Kassai, Gg Ge, C J Simonson: Evaluation of defrosting methods for air-to-air heat/energy exchangers on energy consumption of ventilation, Applied Energy. 08/2015; 151. DOI: 10.1016/j.apenergy.2015.04.022

[22] Petráš, Dušan - Lulkovičová, Otília - Takács, Ján - Füri, Belo: Obnoviteľnézdroje energie pre nízkoteplotné systémy. Bratislava : Jaga Group, s.r.o., 2009. 221 s. ISBN 978-80-8076-075-5

[23] T. Poós, M. Örvös, L. (2013) Legeza Development and Thermal Modeling of a New Construction Biomass Dryer, DRYING TECHNOLOGY 31:(16) pp. 1919-1929.

[24] Nyers J, Nyers A: Investigation of Heat Pump Condenser Performance in Heating Process of Buildings using a Steady-State Mathematical Model, ENERGY AND BUILDINGS 75: pp. 523-530. (2014)

[25] Nyers J, Garbai L, Nyers A: Analysis of Heat Pump's Condenser Performance by means of Mathematical Model, ACTA POLYTECHNICA HUNGARICA 11:(3) pp. 139-152. (2014)

[26] M. Kassai, C. J Simonson: Performance investigation of liquid-to-air membrane energy exchanger under low solution/air heat capacity rates ratio conditions. Building services engineering research & technology 36:(5) pp. 535-545. (2015)

Analysis of steady states in district heating systems

László Garbai, Andor Jasper,

Department of Building Service and Process Engineering, Budapest University of Technology and Economics, Hungary

garbai@epgep.bme.hu

jasper@epgep.bme.hu

Abstract - **This article studies heat balance in district heating systems. It provides a calculation model for the heat balance in a district heating system in case of various operating parameters – primaryand secondary mass flow, primary and secondary forward water temperatures – and for internal temperatures in buildings in case of given external meteorological features.In our study, district heating system parameters are deemed to be known and given, so it is about an existing district heating system.In our surveys, a so-called heat power transmission coefficient is introduced, which is a new calculation formula and can be used for determining the heat power to be transferred from the heat source to the internal space of the building, which obviously exits as loss through delimiting walls.**

NOMENCLATURE

$\dot{Q}$	heat power,
k	heat transmission coefficient,
A	surface,
$\dot{m}$	mass flow,
t	temperature,
t_b	interior temperature,
t_k	ambient temperature,
ϕ	Bosnjakovic coefficient,
W	heat capacity flow rate.

Subscripts:

FMCS	heat exchanger,
Lakás	apartment,
rad	radiator,
1	primary system,
2	secondary system.

I. INTRODUCTION

Public utility networks play highly important roles in the life of settlements, with the most complex technology represented by district heating systems. District heating is an important branch of energetic both in Europe and in Hungary. District heating systems are highly asset-intensive; they are costly in terms of investment and operation; at the same time, they play a major role in energetic because they provide premises and opportunities for the cogeneration of thermal and electric energy, as well as an ideal option for the utilization of renewable and for compliance with EU energy policy directives. 650,000 apartments built in the past few decades mostly by prefabricated building methods are supplied with district heating.

A major practical problem of district heating system operation is to calculate the heat balance of a district heating system by taking variable operational parameters into account. Our study further presents, for system components, the energy balance equations, heat transfer and heat exchanger equations for steady states, and use them for obtaining the heat power transmission coefficient to demonstrate heat balance in the district heating system.

II. HEAT BALANCE IN A DISTRICT HEATING SYSTEM WHEN THE HEAT EXCHANGER EQUATION IS LINEARIZED

A simple and explicit solution is obtained by the linearization of the heat exchanger equation, the error of which is negligible in most cases. The arithmetic mean temperature difference is used in the solution, rather than logarithmic mean temperature Δt_k. The basic equations are shown below.

Heat delivery in the primary system:

$$\frac{\dot{Q}}{\dot{m}_1 c_1} = t'_1 - t''_1.$$

(2.1)

Heat power of the heat exchanger for heating in the heat center:

$$\frac{2\dot{Q}}{(kA)_{FHCS}} = t'_1 + t''_1 - (t'_2 + t''_2)$$

(2.2)

Heat power of the radiator in the apartment:

$$\frac{\dot{Q}}{(kA)_{rad}} = \frac{t'_2 + t''_2}{2} - t_b$$

(2.3)

Heat loss in the apartment:

$$\frac{\dot{Q}}{(kA)_{lakás}} = t_b - t_k$$

(2.4)

By aggregating equations Error! Reference source not found. and (2.2):

$$\frac{\dot{Q}}{\dot{m}_1 c_1} + \frac{2\dot{Q}}{(kA)_{FHCS}} = 2t'_1 - (t'_2 + t''_2)$$

(2.5)

By aggregating equations (2.3) and Error! Reference source not found.:

$$\frac{\dot{Q}}{(kA)_{rad}} + \frac{\dot{Q}}{(kA)_{lakás}} = \frac{t'_2 + t''_2}{2} - t_k$$

(2.6)

After rearrangement:

$$\frac{\dot{Q}}{\dot{m}_1 c_1} + \frac{2\dot{Q}}{(kA)_{FHCS}} + \frac{2\dot{Q}}{(kA)_{rad}} + \frac{2\dot{Q}}{(kA)_{lakás}}$$
$$= 2t'_1 - 2t_k$$

. (2.7)

Developed for $\dot{Q}$:

$$\dot{Q} = \frac{1}{\frac{1}{\dot{m}_1 c_1} + \frac{2}{(kA)_{FHCS}} + \frac{2}{(kA)_{rad}} + \frac{2}{(kA)_{lakás}}} \cdot$$
$$\cdot (2t'_1 - 2t_k)$$

. (2.8)

The heat power transmission coefficient from the equation above:

$$k = \frac{1}{\frac{1}{2\dot{m}_1 c_1} + \frac{1}{(kA)_{FHCS}} + \frac{1}{(kA)_{rad}} + \frac{1}{(kA)_{lakás}}}$$

.(2.9)

III. HEAT BALANCE IN A DISTRICT HEATING SYSTEM WHEN THE HEAT EXCHANGER EQUATION IS NOT LINEARIZED

The Bosnjakovic coefficient [2]:

$$\phi = \frac{t'_1 - t''_1}{t'_1 - t'_2} = \phi \left(\frac{kF}{\dot{W}_1}, \frac{\dot{W}_1}{\dot{W}_2} \right)$$
.

(2.10)

Using the Bosnjakovic coefficient, omitting development:

$$k = \frac{1}{\frac{1}{(kA)_{rad}} + \frac{1}{(kA)_{lakás}} + \frac{1}{\dot{m}_1 \cdot c \cdot \phi} - \frac{1}{2 \cdot \dot{m}_2 \cdot c}}$$
.

(2.11)

Also taking into consideration the temperature dependence of the heat transmission coefficient of the radiator:

$$k$$
$$= \frac{1}{\frac{1}{(kA)_{lakás}} + \frac{1}{\dot{m}_1 \cdot c \cdot \phi} + \left(\frac{1}{kA}\right)^{\frac{1}{1+M}} \cdot Q^{\frac{1}{1+M}-1} - \frac{1}{2 \cdot \dot{m}_2 \cdot c}}$$
.

(2.12)

Heat transmission only for the primary system:

$$\dot{Q} \left[\frac{1}{2\dot{m}_1 c_1} + \frac{1}{(kA)_{HCS}} + \frac{1}{2\dot{m}_2 C} \right] = t'_1 - t''_2$$
.

(2.13)

Heat transmission only for the secondary system:

$$\dot{Q} \left[\frac{1}{2\dot{m}_2 c_1} + \frac{1}{(kA)_{rad}} + \frac{1}{(kA)_{lakás}} \right] = t'_2 - t_k$$
.

(2.14)

The Bosnjakovic coefficient is used for linking linear and non-linear problem management. More specifically, this way the non-linear problem is also

basically solved because the application of the non-linear heat exchanger equation can be dispensed with.

The heat power transmission coefficient – in a certain sense, analogous with the heat transmission coefficient applied for composite wall structures – makes it possible to calculate changing modes of operation with an extremely simple calculation: the heat power possible to be transferred to the heated space, subject to diverse input parameters. This way, the air temperature produced can be calculated.

IV. SUMMARY

In our study, a calculation formula was developed for examining heat balance in the entire district heating system, using the energy balance equations to be stated for district heating system components. This calculation formula makes it possible to determine the heat balance of heated buildings by adjusting various circulation parameters, and thereby the air temperature produced in the living space of the building. The calculation formula includes heat transfer properties in the primary and secondary systems, heat exchanger data, the thermodynamic features of the structures delimiting the building, and the heat transmission parameters of the heat exchanger. Very simple calculations can be used this way to study the impact of operating parameter modifications. This calculation formula can be used for the survey of both centralized and decentralized district heating systems, also including cases when consumers are not concentrated into a single consumption point, but they are detached geographically.

REFERENCES

[1]   Garbai, L.: District heating (in hungarian), 2012. ISBN: 978-963-279-739-7

[2]   Környey, T.: Heat transmission (in Hungarian) Műegyetemi Kiadó, Budapest, 1999.

[3]   Magyar, Z. – Petitjean, R.:Energy Saving of District Heated Flats from the Recondition of the Heating System in Hungary, ASHRAE Transactions 108 Part 2, 2002, pp. 575-579.

[4]   Harmati, N., Folic, R., Magyar, Z.: Energy performance modelling and heat recovery unit efficiency assessment of an office building, Thermal Science International Scientific Journal, 2015. http://thermal science.vinca.rs/online-first/1363,

DOI:10.2298/TSCI140311102H

[5]   Szanthó, Z.: Determining the optimal schedule of district heating, Periodica Politechnica Ser. Mech. Eng. VOL.44 No. 2. Pp.285-300. (2000.)

[6]   Nyers J., Nyers A.: "Hydraulic Analysis of Heat Pump's Heating Circuit using Mathematical Model". 9rd IEEE ICCC International Conference"

Proceedings-USB, pp 349-353, Tihany, Hungary. 04-08. 07. 2013. ISBN 978-1-4799-0061-9

[7]   J. Nyers, L. Garbai, A. Nyers: A modified mathematical model of heat pump's condenser for analytical optimization. International J. Energy. Vol. 80, pp. 706-714, 2015. (IF 4.844)

Examination of a Transpired Solar Air Collector System for Ventilation Air and DHW Heating

B. Bokor*, L. Kajtár*

*Budapest University of Technology and Economics (BME) / Department of Building Service and Process Engineering, Budapest, Hungary

bokor@epgep.bme.hu and kajtar@epgep.bme.hu

Abstract — **Solar thermal systems have become wide-spread all over Europe, as the energy consumption of buildings is getting a more and more frequently discussed environmental issue. The majority of the systems use water or water-glycol solution as heat transfer medium. Solar collectors that warm up air directly are still a novelty to Central-European countries, although in North America they have already proven their suitability in building service engineering systems. In our paper we describe the build-up and operational principle of unglazed, transpired solar air heaters (UTCs) and present the summer operation of a system we are currently measuring on a shopping centre near Budapest, Hungary. As in summer not much heated air is needed in the building, the hot air streams through an air-to-water heat exchanger, by the use of which the solar heat is utilised for domestic hot water preheating. The temperatures reached by the collector, as well as the water temperature rise are shown for two weeks, as less and a sunnier one over the course of summer 2015. We compare the temperature curves to the weekly curves of global and diffuse radiation measured on a horizontal surface.**

INTRODUCTION

Since the European Union committed itself to the 20/20/20 targets in its Energy Efficiency Plan of 2011, many environmentally friendly HVAC systems have been installed all over Europe, also in Hungary. Solar radiation offers a predictable source of renewable energy which can be broadly utilised in building service engineering. Alongside the commonly known solar pool heaters, flat plate and vacuum tube collectors the yet not widespread solar air heaters can also be flexibly inserted into both new and existing systems. Their simple construction makes low first costs possible and their operation remains very reliable. UTCs have been shown to reach an economic payback of between 2 and 10 years. [1] They use air as heat transfer medium which provides for many advantages, though its specific heat capacity is considerably lower than that of water. Air does not freeze at sub-zero temperatures, so there is no need of costly anti-freeze solutions. Regarding the summer operation, surplus heat doesn't damage the system in case of longer stagnation periods. However, in an efficient system "surplus heat" is an unknown term, as it is being utilised for some other demands. The transpired solar collector system of the shopping centre near Budapest is a good example for energy efficient design, as it supplies not only the ventilation system, but domestic hot water production, too.

UNGLAZED TRANSPIRED SOLAR COLLECTORS

The build-up of an unglazed transpired collector (UTC) can be seen in figure 1. A dark, corrugated metal shield, which is evenly perforated over its surface, is fixed onto a building's façade in a given distance. This metal shield is the absorber. Outdoor air transpires the absorber, rises in the gap and finally a fan forwards it to the ventilation system of the building.

Figure 1 Build-up of a façade-mounted UTC [12]

One could easily think that in the lack of transparent glazing the thermal performance of a UTC depends very much on actual weather conditions. However, this is not the case. A thin layer of warm air develops at the outside of the absorber, which is being sucked in through the perforations, as figure 2 shows. The suction stabilises the boundary layer on the absorber, making the effect of wind on the heat production negligible. [2] While rising up in the gap between absorber and building façade (also called plenum), the air gets heated further. This means that both sides of the absorber take an active part in the heat transfer process. Furthermore, the convectional losses of the building envelope can be regained on the surfaces where the air heaters are installed. As detailed in [3], capillary tubes can be installed on the back plate to provide the system with warm air, even during hours of no solar radiation.

Cladding a building's façade with absorber shields that heat up under solar radiation would not only mean heat gain in winter, but also additional heat load in summer. Due to the UTCs perforated construction, the air can circumvent in the plenum, entering on lower perforations and exiting through higher ones. In this case the air handling units (AHU) are obviously supplied with air through a bypass and suck outdoor air at ambient temperature.
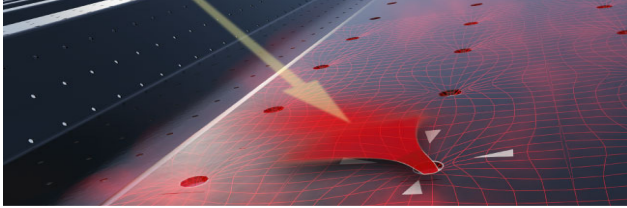

Figure 2 The very stable, warm boundary layer is being sucked into the plenum [13]

However, the surplus heat that comes to be on the UTC can be utilised even in summer months. Using an air-to-water heat exchanger we can preheat domestic cold water and save energy in the domestic hot water (DHW) production process. Solar based DHW production for collectors using liquid as heat transfer medium is discussed in [4], [5] and [6]. In this paper we approach solar DHW production with the use of the UTC.

From the 3rd June 2015 we have been continuously measuring the UTC system of a shopping centre in Maglód, Hungary, in which the surplus heat from the collector supplies a DHW preheater. Our aim is to get to know the yearly amount of energy the system delivers, as well as the heat exchange properties between the UTC and the domestic water system.

DESCRIPTION OF THE MEASURED SYSTEM

The town Maglód, where the measured system is to be found, is located in the Budapest metropolitan area, 28 km south-east from the centre of the capital. The shopping centre is of 28 862 m^2 gross area, the vast majority of which is a hypermarket, but at the entrance there are many individual shops, too. Both the south-east and the south-west façade of the building are equipped with a UTC of the Canadian manufacturer SolarWall.

Figure 3 SolarWall UTC on the South-West facade of the shopping centre

The architectural features of the shopping centre are especially advantageous for the use of a UTC. The façade has a low glazing proportion, meaning the solar heat gain

of the building without UTC would be low. This is why warehouses, assembly halls and other industrial buildings are very much suitable for the set-up of a UTC system on their facades. Eryener and Akhan describe the performance examination of a transpired solar collector installation of a Turkish manufacturing building in [6]. For our investigation we have chosen the one located on the south-west façade (see figure 3), as this one supplies the air-to-water heat exchanger for DHW production, too. The area of the UTC is 366 m^2 through which the air is drawn to four air handling units and one air-to-water heat exchanger. Each AHU supplies systems for different purposes of the shopping centre, such as

- offices,
- kitchen,
- bakery,
- and changing rooms.

Also we have chosen the AHU of the bakery for our measurements besides the heat exchanger. This one is 24/7 in operation as the ovens and other gas consumers require fresh air for operational and safety reasons at all times. The AHUs of offices and changing rooms operate based on a time programme, whereas that of the kitchen is not in use. It is important to choose the AHU which is always in operation, because measurement at those with no suction would result in too high temperatures that would not represent valuable results. The air handling units are installed on the roof of the building close to the top of the UTC.

As the "inlet air" enters the UTC through perforations evenly spread on its entire surface, we assume that the inlet temperature is equal to the ambient temperature. We measure the ambient temperature on a shaded place close to the collector. The temperature after the UTC is measured in the air duct connecting the UTC with the bakery's AHU.

For the investigation of the DHW preheating with the UTC we measure air temperatures in the air duct connecting the UTC with the air-to-water heat exchanger, after the heat exchanger, as well as water temperatures before and after the heat exchanger.

Due to space limitations in the current article we present only the temperature curves before and after the UTC and the water temperatures before and after the air-to-water heat exchanger.

RESULTS

The solar radiation onto a horizontal surface has been measured on the roof of Budapest University of Technology and Economics, building "D". Based on the data of the Hungarian Meteorological Office for the examined time period we can state that the temperature and solar radiation properties of the two locations were the same. The following two diagrams (figures 4 and 5) show that the week between 22/06/2015 and 28/06/2015 was cloudier than the following one from the 29/06/2015 to 05/07/2015.

In figure 4 it is clearly visible that on many days, especially on Tuesday 23/06/2015 the global radiation hardly exceeds the diffuse radiation as a result of cloudy weather. The peaks result from higher measured values which have come to be as the sun lit the pyranometer between clouds for a short time.
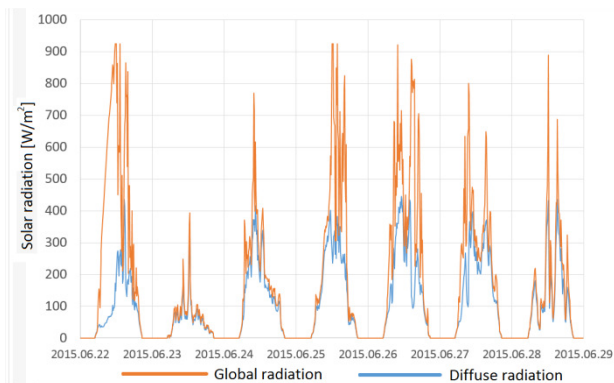
Figure 4 Global and diffuse radiation on a horizontal surface from 22/06/2015 to 28/06/2015

In contrast, the week shown in figure 5 was much sunnier. The most illustrative days of sunny weather with a remarkable amount of direct radiation are the last three days of the week, where the daily run of global radiation is hardly disturbed by any clouds.
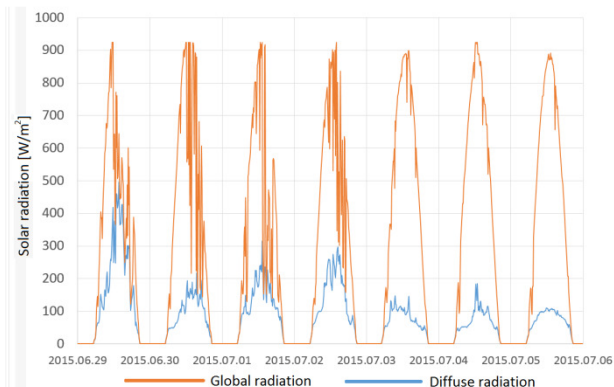
Figure 5 Global and diffuse radiation on a horizontal surface from 29/06/2015 to 05/07/2015

Figure 6 shows the temperature rise on the SolarWall UTC during the week with less solar radiation. Visibly on rather cloudy days, such as the Tuesday 23/06/2015 the collector could hardly heat the outdoor air higher than by 3 K. However, on less but still cloudy days (e.g. Friday 26/06/2015) the air reached higher temperatures by max. 14.4 K after the UTC.
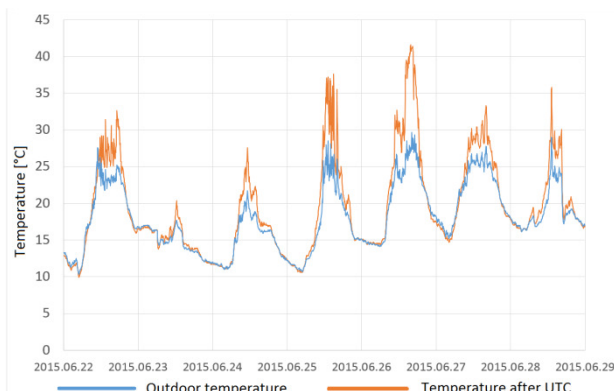
Figure 6 Air temperature rise on the UTC from 22/06/2015 to 28/06/2015

Over the course of the following sunnier week (see figure 7) temperature rose in a much higher amount, reaching almost 50 °C on Sunday. On this day the temperature rose on the UTC by a maximum of 12.2 K. In general, based on figure 7 we can state that the UTC produced a daily maximum temperature rise of 10 K from Tuesday to Sunday (30/06/2015-05/07/2015), days with clear summer weather.
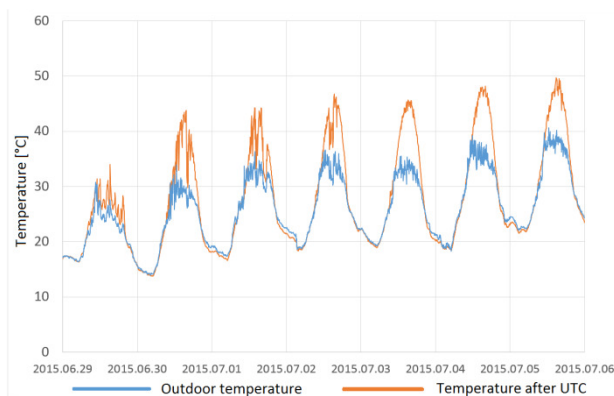
Figure 7 Air temperature rise on the UTC from 29/06/2015 to 05/07/2015

However, high air temperature such as 50 °C is not to be led into the ventilation system of the shopping centre during summer time. With the use of an air-to-water heat exchanger the surplus heat of the UTC can be utilised for DHW preheating. The effect of this can be seen on figures 8 and 9.

Although the week shown in figure 8 had cloudy weather, the UTC was able to rise the temperature of water remarkably, though to a smaller extent than during the sunny week (figure 9). Comparing figures 6 and 8 one can observe that on the cloudy Tuesday (23/06/2015) the low radiation has a minimal effect on the air's temperature rise, but not much on that of water.
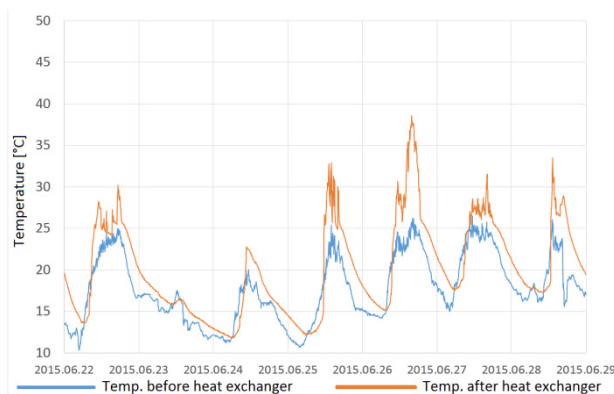
Figure 8 Temperature rise in DHW preheating from 22/06/2015 to 28/06/2015

The fact that water temperature after the heat exchanger is still higher than before, can be explained with the outdoor air temperature remaining higher than water temperature before the heat exchanger. This phenomenon can be observed every night: the warmer outdoor air has a certain heating effect on water, in spite of no solar radiation.

Figure 9 shows that over the sunny week with typical summer weather, the effect of the air-to-water DHW preheater is remarkable. On Sunday 05/07/2015 the water temperature rose by a maximum of more than 10 K.
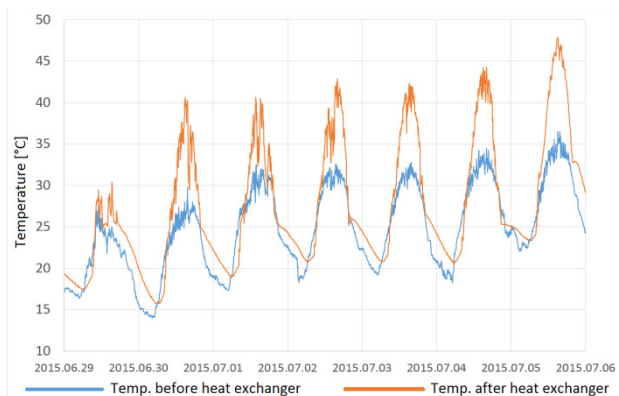
9. Figure Temperature rise in DHW preheating from 29/06/2015 to 05/07/2015

CONCLUSIONS

The results show that the unglazed transpired solar collector on the SW façade of the shopping centre in Maglód is able to reach remarkably high temperatures in summer. However, the air conditioning system of a building is not in any need of hot air in summer, so the heat which comes to be on the collector needs to find an alternative use to be exploited. In the examined shopping centre this heat is utilised in the domestic hot water production over an air-to-water heat exchanger. Results show, that the air temperatures were risen by a maximum of 14 K in sunny periods, while in cloudy days the air reached about 3 K on the collector. The surplus heat of the UTC could preheat water by a reliable 10 K temperature rise in sunny weather and 2 K on cloudy days. Comparing figures 7 and 9 we can observe that the rise of air and water temperatures follow each other over the course of certain days, showing that water preheating is a sensible use of the UTC's surplus heat.

REFERENCES

[1] Hall R, Wang X, Ogden R, Elghali L: Transpired Solar Collectors for Ventilation Air Heating – Proceedings of the Institution of Civil Engineers pp 101-110, 2011

[2] Kutscher CF: An Investigation of Heat Transfer for Air Flow through Low Porosity Perforated Plates. Doctoral thesis, University of Colorado, 1992

[3] Eryener D, Akhan H: Theoretical and Experimental Investigation of Perforated Solar Air Collector Coupled to a Capillary Radiant Heating System. Proceedings of 9th International Conference on Heat Transfer, Fluid Mechanics and Thermodynamics. Malta, 2012

[4] Horváth M, Kassai-Szoó D, Csoknyai T: Solar Energy Potential of Roofs on Urban Level based on Building Typology. Energy and Buildings 111: pp. 278-289. (2016)

[5] Horváth M, Csoknyai T: Maximal and Optimal DHW Production with Solar Collecotrs for Single Family Houses. EXPRES 2015 Subotica, 7th International Symposium on Exploitation of Renewable Energy Sources and Efficiency. Subotica, Serbia, 2015

[6] Horváth M, Hrabovszky-Horváth S, Csoknyai T: Parametric Analysis of Solar Hot Water Production in "Commie-block" Buildings. Energy (IYCE), 2015 5th International Youth Conference on. Pisa, Italy, 2015

[7] Eryener D, Akhan H: The Performance of First Transpired Solar Collecotr Installation in Turkey. Energy Procedia, International Conference on Solar Heating and Cooling for Buildings and Industry SHC 2015

[8] Bokor B, Kajtár L: Solar Air Heaters – New Opportunities in Solar Thermal Energy Use. In proceedings of Vykurovanie 2015, pp 453-460. Stará Lubovna, 2015

[9] Petráš D, Lulkovičová O, Takács J, Füri B.: Obnoviteľnézdroje energie na vykurovanie. In: Vykurovanie rodinných a bytových domov. Bratislava: Jaga, 2005. p. 193 – 217, ISBN 80-8076-012-8.

[10] Petráš D, Lulkovičová O, Takács J, Füri B: Obnoviteľné zdroje energie pre nízkoteplotné systémy. Bratislava: Jaga Group, s.r.o., 2009. 221 s. ISBN 978-80-8076-075-5

[11] Takács J, Lulkovičová O, Füri B: Helyzetkép a megújuló energiaforrások hasznosítasi lehetöségeiről Szlovákiában In: Magyar Épületgépészet. - ISSN 1215-9913. – vol. 57, 12 (2008), s. 24-27

[12] Nyers J, Tomic S, Nyers Á: Economic Optimum of Thermal Insulating Layer for External Wall of Brick, Acta Polytechnica Hungarica 11: (7) pp. 209-222.

[13] http://www.cabuildingproducts.co.uk/

[14] http://www.matrixairheating.com/

Design and Simulation of a Solar Dish Concentrator with Spiral-Coil Smooth Thermal Absorber

Saša R. Pavlović[*], Velimir P. Stefanović[*], Evangelos Bellos[**]

[*] University of Niš, Faculty of Mechanical Engineering, Department for Energetics and Process technique, Aleksandra Medvedeva 14 Street, 18000 Niš, Serbia
[**]National Technical University of Athens, School of Mechanical Engineering, Thermal energy department, Athens, Zografou, Greece
Corresponding author: saledoca@gmail.com

Abstract- The efficient conversion of solar radiation into heat at high temperature levels requires a use of concentrating solar collectors. The goal of this paper is to present the optical and thermal analysis of a parabolic dish concentrator with a spiral coil receiver.The parabolic dish reflector consists of 11 curvilinear trapezoidal reflective petals constructed byPMMA with silvered mirror layerand has a diameter of 3.8 m, while its focal distance is 2.26m. This collector designed with commercial software Solidworks and simulated, optically and thermally in its Flow Simulation Studio. The optical analysis proved that the ideal position of the absorber is at 2.1m from the reflector in order to maximize the optical efficiency and to create a more uniform heat flux over the absorber. In thermal part of the analysis, the energetic efficiency was calculated approximately 65%, while the exergetic efficiency is varied from 4% to 15% according to the water inlet temperature. Moreover,other important parameters as the heat flux and temperature distribution over the absorber are presented. The pressure drop of the absorber coil calculated at 0.07bar, an acceptable value that was validated with the theoretical one.

Keywords: Solar dish reflector, spiral-coil absorber, optical analysis, thermal analysis, Solidworks

I. INTRODUCTION

Energy consumption has increasing rate worldwide because of the new trends in lifestyle. With threats of global warming and increased energy cost, the use of renewable and sustainable energy sources is becoming more and more popular. Solar energy is the most abundant and its usage is the more widespread. Solar collectors are heat exchanger devices which capture the incident solar irradiation and transform a part of this to useful heat. This heat is given to a working fluid in order to be transferred to the load or to the storage device. The temperature level of the working fluid is determines its exergy flow which is also a crucial parameters flow medium and high temperature applications. In order to increase the temperature of the working fluid and its exergy rate, concentrating collectors are used in many applications.

The solar thermal collectors have been widely used to concentrate solar radiation and convert it into medium-high temperature thermal processes. Low cost, two axis tracking solar dish with flat mirror system's (Solarux CSP) design and its advantages are described in this paper.In this paper, it has been focusing on air-conditioning, heating, and producing electricity by using Solarux CSP. The aim of this invention is to use planar mirrors instead of parabolic mirrors in order to recuce cost and design a system that can be manufactured easily, can be constructed on every kind of terrain (rocky, plain etc.) and can be used by third world countries[1,2] The solar concentrating collectors operate by focusing incident solar radiation onto a small area known as the focal area. Many classes of concentrating collectors are available, each with different concentrating ratios and maximum absorber temperature, depending on the type of application. Generally, solar thermal utilization can be categorized into low- temperature solar concentrating system and high temperature solar thermal systems. The low temperature solar systems, which may not involve sunlight concentration, have lower conversion efficiency. The high temperature solar thermal systems, which require sunlight concentration, have higher conversion efficiency [3,4]. Pavlovic et al. [5] presented a mathematical and physical model of the new offset type parabolic concentrator and a numerical procedure for predicting its optical performance. The designed parabolic concentrator is a low cost solar concentrator for medium temperature applications. The same researchers [6] developed mathematical model of solar parabolic dish concentrator based on square flat facets applied to polygeneration system.

Traditionally, the optical analysis of solar concentrators has been carried out by means of computer ray-trace programs. This method for calculating the optical performance is fast and accurate but assumes that the radiation source is a uniform disk. Imhamed M. Saleh Ali et al. [7] have presented study that aims to develop a 3-D static solar concentrator that can be used as low cost and low energy substitute. Their goal was to design solar concentrator for production of portable hot water in rural India. They used the ray tracing software for evaluation of the optical performance of a static 3-D Elliptical Hyperboloid Concentrator (EHC). Optimization of the concentrator profile and geometry is carried out to improve the overall performance of system. Kaushika and Reddy [8] used satellite dish of 2.405 m in diameter with aluminium frame as a reflector to reduce the weight of the structure and cost of the solar system. In their solar system the average temperature of water vapor was 300[0]C, when the absorber was placed at the focal point. Cost of their system was US$ 950. El Ouederni et al. [9] was testing

parabolic concentrator of 2.2 m in diameter with reflecting coefficient 0.85. Average temperature in their system was 380⁰C. Y.Rafeeu and M.Z.Z.AbKadir [10] have presented simple exercise in designing, building and testing small laboratory scale parabolic concentrators. They made two dishes from acrylonitrile butadiene styrene and one from stainless steel. Three experimental models with various geometrical sizes and diameters were used to analyze the effect of geometry on a solar irradiation. Zhiqiang Liu et al. [11] presented a procedure to design a facet concentrator for a laboratory-scale research on medium – temperature solar concentrator. Quianjun et al. [12] have investigated on the photo – thermal conversion efficiency in order to improve the cost effectiveness of the solar system. They used the Monte Carlo ray tracing method for calculating the radiation flux distribution on the receiver and the ANSYS Fluent for calculation of radiation and convection heat transfer mechanisms. Their results show that outlet water temperature and energy input linearly increase with increasing direct normal irradiation, but energy output non-linearly increases with increasing direct normal irradiation. Their results also show that the maximum energy efficiency is 52.12% when the direct normal irradiation is 800 W/m^2. Eswaramoorthy and Shanmugam [13] have investigated the thermal efficiency of solar cooker with the diameter of the parabola equal to 3.56 m and the parabolic concentrator surface area of 10.53 m^2. Their results show that the thermal efficiency of the system was found to be 60%. K.S. Reddy et al. [14] has experimentally investigated 20 m^2 solar parabolic dish collector in order to study its performance with the modified cavity receiver. The average value of the overall heat loss coefficient was found to be about 356 W/m^2. K. Jones and Wang [15] computed the flux distribution on a cylindrical receiver of parabolic dish concentrator using geometric optics method. The parameters such as concentrator surface errors, pointing offset errors and finite sunshape were considered in the geometric optics method. Thakkar et al. [16] have investigated possible use of parabolic dish collector in process industries. They presented performance assessment mathematical model for heating application using thermal oil. R. Blázquez et al. [17] describes optical test for the DS1 (parabolic Stirling dish) prototype carried out by CTAER. The aim of this investigation was to characterize the DS1 prototype optical parameters. For this purpose the real and the theoretical flux distribution was calculated on a target placed at the focal plane. The theoretical flux distribution was obtained by photogrammetry technique and ray tracing tools; the real flux distribution was measured by photographic flux mapping technique of lunar images. The results comparison showed that the dish surface had an average optical error of 2.5 mrad and an estimated spillage value of 7%, for this geometry. Zhigang et al. [18] have predicted of the radiation flux distributions of the concentrator - receiver system by Monte Carlo ray tracing. The ray-tracing method was first validated by experiment, then the radiation flux profiles on the solar receiver surface for faceted real concentrator and ideal paraboloidal concentrator, irradiated by Xe-arc lamps and real sun, for different aperture positions and receiver shapes are analyzed, respectively. The resulted radiation flux profiles are subsequently transferred to a CFD code as boundary conditions to numerically simulate the fluid flow and conjugate heat transfer in the receiver cavity by coupling the radiation, natural convection and heat conduction together. Pavlovic et al. [19] presented optical design and ray tracing analysis of solar dish concentrator composed of 12 curvilinear trapezoidal reflective facets made from solar mirror with silvered coating layer. The goal of this paper was to present optical design of a low-tech solar concentrator that can be used as a potentially low-cost tool for laboratory-scale research on the medium temperature thermal processes, cooling, industrial processes, polygeneration systems etc. Shuai, Y. et al. [20] The Monte-Carlo ray-tracing method is applied and coupled with optical properties to predict radiation performance of dish solar concentrator/cavity receiver systems. The effects of sun shape and surface slope error have been studied and the corresponding probability models are introduced in this paper. Based on the concept of equivalent radiation flux, an upside-down pear cavity receiver is proposed in view of directional attributes of focal flux

In this paper authors, after conducting large number of numerical simulations and various geometrical configurations of the receiver, accepted the spiral type of the solar receiver. The first step of the analysis includes an optical optimization in order to predict the distance between reflector and spiral coil. The next part is the determination of the energetic and exergetic efficiency of the collector for a range of water inlet temperature. Other important parameters are presents with diagrams and figures from the simulation tool, which is Solidworks flow simulation studio. More specifically the temperature over the absorber and inside the water is given. The heat flux distribution over the down part of the absorber and along the spiral is presented. The pressure drop between inlet and outlet and the velocity of the water in every location are presented. By giving all these information, the problem is fully analyzed and the operation is explained with many details. The next figures shows.

II. GEOMETRICAL MODEL OF SOLAR PARABOLIC DISH CONCENTRATOR

In this paragraph, the model description is presented. Figures of the designed system are given (Figures 1-4) and the basic parameters of the geometric parameters of the system are shown in table1. The ideal optical configuration for the parabolic concentrator is a continuous paraboloidal mirror (shown on Figure 1), which is very expensive to fabricate, and it costs escalating rapidly with aperture area. A continuous parabolic dish surface can be approximated by a discrete surface consisting of 11 curvilinear trapezoidal reflective petals situated in a single parabolic frame (shown on Figure 2), dramatically reducing the system cost, while still allowing for concentration ratios at a level suitable for a wide range of medium to high temperature applications. Dimensions of reflecting surface in solar dish concentrator are determined by desired power at maximum levels of irect normal radiation and efficiency of collector conversion.
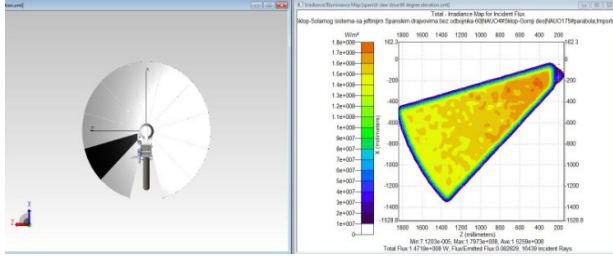
Fig. 1.Incident flux distribution on the lower left reflective petal of parabolic solar concentrator
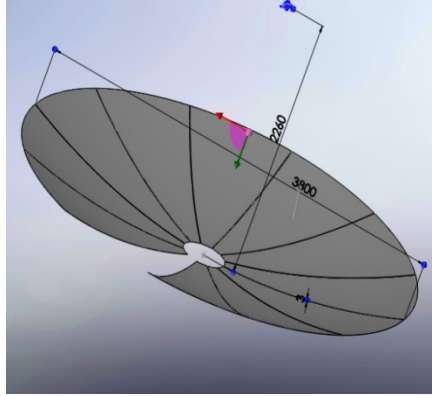

Fig. 2. CAD model of solar parabolic concentrator with dimensions D = 3800 mm, f = 2260 mm

Mathematical representation of solar parabolic dish concentrator is paraboloid that can be represented as a surface obtained by rotating parabola around axis, which is shown on Fig. 1. Our model of parabolic concentrator is designed with 11 curvilinear trapezoidal reflective petals. Mathematical representation of the reflective petal can be presented as the parabola segment shown in Figure 3. On Figure 4 is presented one curvilinear trapezoidal reflective petal, which is made from the PMMA (polymethyl methacrylate) with special reflective coating. Thickness of the petal is 3 mm.
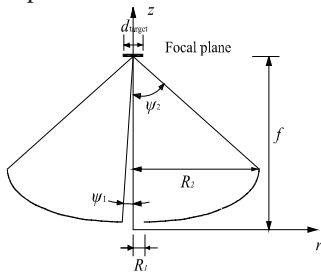

Fig. 3. Drawing of truncated parabola used to construct a truncated circular paraboloid
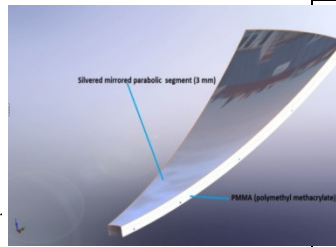
Fig. 4. Trapezoidal reflective facet concentrator – segmented mirrored petal

Usually paraboloids that are used in solar collectors have rim angles from 10 degrees up to 90 degrees. The paraboloid with small rim angles have the focal point and receiver at large distance from the surface of the concentrator. Paraboloids with rim angle smaller than 50^0 (our parabolic solar concentrator has the rim angle Ψ_{rim} = 45.6^0) are used for cavity receivers while paraboloids with large rim angles are most appropriate for the external volumetric receivers (central receiver solar systems).

Focal diameter ratio of our solar concentration system is 0.59. The model of solar parabolic concentrator (Figures 5 and 6) is very complex and has a large number of elements that ensure proper positioning of the system at any point of time. This model of solar parabolic dish concentrator provides to maximum concentration of solar radiation in the receiver at any point of time with minimal optical losses of incident radiation. On figures are presented CAD renderings of our system, which is under construction. After finishing construction of the system we shall continue with the experimental verification of the system in the solar accredited laboratory of Faculty of Mechanical Engineering in Nis.

Fig. 5. 3D CAD rendering model of thermal solar concentrating system
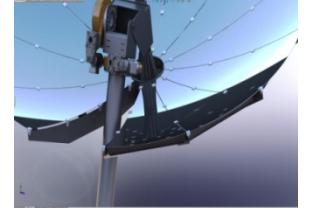
Fig. 6. Mirrored segmented parabolic concentrator

Design parameters of the solar parabolic dish concentrator are shown in Table 1. The table gives analytical determination of every parameter because there are many geometric characteristics in the designed model. It is essential to state that the receiver has a spiral coil shape with a smooth geometry.

TABLE I. DESIGN PARAMETERS OF THE SOLAR PARABOLIC DISH CONCENTRATOR

Parameters	Numerical Value	Unit
Concentrator aperture diameter	3.8	[m]
Collector aperture diameter (A_a)	10.28	[m^2]
Surface area of parabolic dish	21.39	[m^2]
Focal-diameter ratio (f/D)	0.6	[-]
Direct beam radiation (G_b)	800	[W/m^2]
Receiver diameter (dr)	0.4	[m]
Reflectivity of segmented petals)	0.88	[-]
Focal distance (f)	2.26	[m]
R_1	0.2	[m]
CR_g	37.1	[-]
CR_{opt}	35.6	[-]
R_2	1.9	[m]
Ψ	45.6	[^{0}]
Depth of the concentrator	0.399	[m]

III. COMPUTATIONAL DOMAIN AND SIMULATION

The examined model is given in figure 7. The reflector and the absorber are shown in this figure because these are the two parts of the computational domain. The solar rays are also given in this figure. Figure 8 shows only the coil geometry. The inlet of the flow is the point "A" in Figure

8 and the outlet is the point "B" in the same Figure. The vacuum in the reflector is made for the bracket of the coil. Only these two parts are used in the simulation in order to make a simpler model.
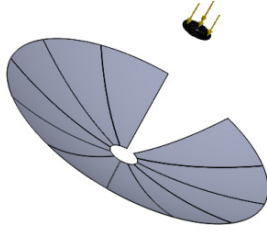
Fig.7. Examined model in Solidworks flow simulation environment
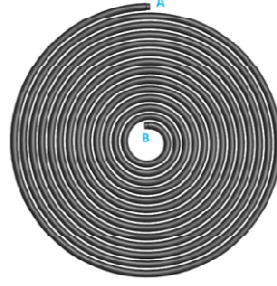
Fig.8. The absorber coil shape. Point A is the inlet and B the outlet of the flow

Solidworks flow simulation studio combines optical and thermal analysis together and for this reason is ideal for this kind of simulation. The next tables give the main parameters of the simulation. Typical values were used in order to simulate conditions similar to the reality [21]. The environment temperature has assumed to be 10°C in order to simulate difficult ambient conditions with high heat losses.

TABLE II. SIMULATION PARAMETERS

Title	Parameter	Value
Mass flow rate	m	0.04kg/s
Solar beam radiation	G_b	800W/m²
Reflectance	ρ	0.88
Absorbance	α	0.8
Emittance	ε_r	0.1
Ambient temperature	T_{am}	10ºC
Air-receiver convection coefficient	h_{air}	10 W/m²K

In the flow simulation studio, the user has to determine the simulation conditions. First of all an internal analysis was selected because the water flows inside the tube. After this part the user selects that there is conduction in solids and the existence of solar irradiation. The radiation is selected to be constant and vertical to the aperture of the reflector. After this part the material was selected. Copper is selected for the absorber and a special mirror material for the reflector. Water is the working fluid that selected in this simulation. The mesh of the model was created by Solidworks with emphasis in fluid cells refinement.

The next important step is the boundary conditions determinations. In the inlet of water the flow mass rate and the uniform temperature were selected. After this, the static pressure in the outlet of the tube was stet to be environmental. The last boundary condition is the heat convection between the coil outer surface and the environment. It is important to say that for determining a different operating condition, the water inlet temperature was changed in the proper boundary condition. After this step, the radiation surfaces were selected. The reflector was set to be a symmetrical surface in order to reflect the rays. Also, in the ray trace method the reflections were set to be forward. For the outer coil surface, new radiation surfaces were created by setting the suitable emissivity and absorbance.

The last part is the set of the proper goals. The global fluid and solid temperature levels selected as the first goals, because these goals helps the program to converge better. Moreover, the bulk average temperature in the outlet of the coil was selected as a goal. Furthermore, the solar energy captured by the coil was selected as goal, a goal that is very useful for the optical optimization. Finally, the mean coil temperature was selected as a goal. By changing the inlet temperature of the water, the collector was examined in various operating conditions. Also, by changing the distance between the coil and the reflector, the optical analyses were done.

Other collector types have been also analyzed with Solidworks flow simulation studio. A flat plate collector [26] and a evacuated tube collector [27] have been analyzed with focus on the thermal part of the analysis. A parabolic trough collector [28] have analyzed optical and thermally with very good results.

In this section, the basic equations that used for analyzing the results are presented. These equations are related to thermal, optical and exergetic efficiency of the collector.

The useful energy is calculated by equation (1), if the water outlet temperature is known:

$$Q_u = m \cdot c_p \cdot (T_{out} - T_{in}) \tag{1}$$

The total available solar radiation is calculated as:

$$Q_s = A_a \cdot G_b \tag{2}$$

The thermal efficiency is given by equation (3):

$$\eta_{th} = \frac{Q_u}{Q_s} \tag{3}$$

The optical efficiency is calculated through the goal of coil absorbed solar radiation:

$$\eta_{opt} = \frac{Q_{abs}}{Q_s} \tag{4}$$

The absorbed solar energy from the receiver is given by the next equation:

$$Q_{abs} = \eta_{opt} \cdot Q_s \tag{5}$$

The exergetic efficiency is calculated from equation (6):

$$\eta_{ex} = \frac{E_u}{E_s} \tag{6}$$

The exergy output is given by the next equation [22-23]:

$$E_u = \dot{m} \cdot c_p \cdot \left[(T_{out} - T_{in}) - T_{am} \cdot \ln\left(\frac{T_{out}}{T_{in}}\right) \right] \tag{7}$$

The useful exergy from the working fluid is the useful heat diminished by the entropy generation of the process. This is the maximum possible work that can be produced, if this heat is the source of a canto cycle.

The solar radiation exergy is given by Petela type [24]:

$$E_s = Q_s \cdot \left[1 - \frac{4}{3} \cdot \left(\frac{T_{am}}{T_{sun}} \right) + \frac{1}{3} \cdot \left(\frac{T_{am}}{T_{sun}} \right)^4 \right] \qquad (8)$$

The sun temperature is selected to be 4350K, which is the 75% of the sun temperature in its outer layer. This is an assumption that has been taken into a great number of studies [25]. Moreover the use of the Petela formula is very discussed issues worldwide because it is difficult to determine the exact available exergy form the sun. Newer models take into consideration other geometrics characteristics of the sun, as the incident angle. Badescu [29] have proposed the use of sun geometric characteristic in order to determine better the exergy of solar radiation. However, the examined collector operates with a full tracking system which minimizes the incident angle and the Petela formula is the proper one for the analysis.

IV. OPTICAL ANALYSIS AND OPTIMIZATION

After the system design, the next step is the optical analysis and optimization of the system. More specifically, it is essential to predict the most suitable geometry for maximizing the solar energy utilization. An optimization is useful in order to predict the optimum distance between the coil and the absorber. By locating the coil in the focal point of the dish, all the solar rays will be concentrated there something that is not the preferable. The reason is because the solar radiation should be concentrated in all the part of the coil in order to heat all the water inside it and to be captured by a better way. So, the coil was placed closer to the reflector in order to create a more uniform heat flux distribution and to maximize the intercept factor. Figure 9 shows the optimization of this distance. The intercept factor γ is fully connected with the optical efficiency by the next equation:

$$\eta_{opt} = \gamma \cdot \rho \cdot \alpha \qquad (9)$$

Where ρ is the reflectivity of the mirror and α absorbance of the coil.
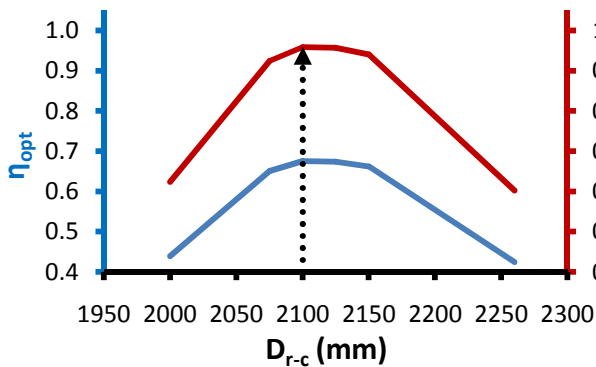
Fig.9. Optimization of the coil-reflector distance

Figure 3 proves that the optimum distance is 2100mm, lower than the focal length. In this distance the intercept factor is 0.96 and the optical efficiency 0.676. This is a very important result for solar dish collectors. The reflectance (ρ) and the absorbance (a) are kept constant and for this reason the optical efficiency and the intercept

factor are proportional amounts. Figure 4 depicts the heat flux distribution over the down part of the coil. The maximum heat flux is observed close to the center but no to the center. The reason for this result is explained to the distance optimization. By locating the coil closer to the reflector, the rays are not concentrated in the center, but in all over the geometry. This situation creates a more uniform distribution and faces the problems of very high values in the center of the solar dish absorber. Another interesting result is the lower heat flux concentration in a circular sector, something that explained by the missing part of the reflector in the respective region.

Figure 11 shows the heat flux distribution along the coil line. In the region 0-5m, the heat flux intensity has a constant increasing rate and in the region 5-8m this increasing rate in getting greater. After this point, the heat flux intensity makes a maximum point and after this point is decreasing. The maximum heat flux is close to the end, but about some centimeters before. More specifically, the total coil length is about 9 meters and the maximum heat flux is in 8.32m. Moreover, figure 12 shows the heat flux distribution as a function of the radius R from the center. The results are similar to them from figure 11. It is essential to state that every point of the spiral has a different radius and for this reason the line in figure 12 is continuous. This design creates a more uniform distribution close to the center. If all the solar energy delivered to one point, then the material would be faced problems and the water will not utilizes all this energy. It is essential to state that the region of the coil which is over the vacuum in the reflector has lower het flux intensity, something very logical.
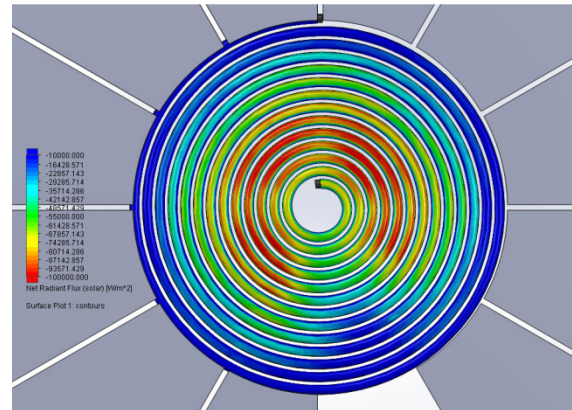
Fig.10. Heat flux distribution of absorbed solar energy in the down part of the absorber
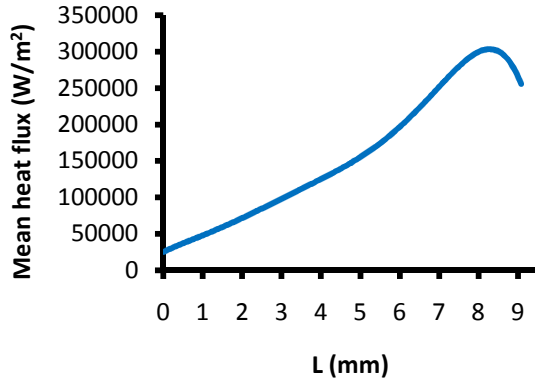
Fig. 11. Mean heat flux absorbed along the helix
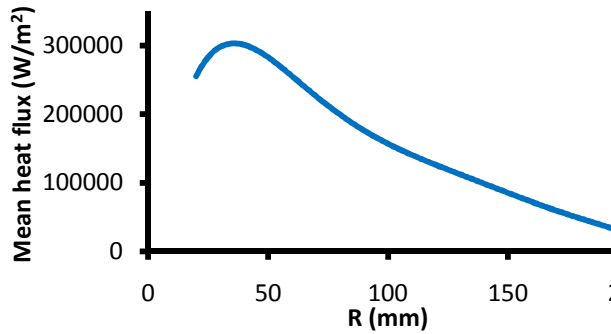
Fig. 12. Mean heat flux absorbed as a function of the distance from the center

V. ENERGETIC PERFORMANCE OF THE COLLECTOR

The collector efficiency is depended by the operating conditions and especially by the water inlet temperature. Moreover, the exergetic efficiency of the collector is an important parameter, especially when the useful heat is used for high temperature applications. In this paragraph the thermal efficiency and the exergetic efficiency of the collector are presented and analyzed. Figure 13 shows these parameters as a function of the parameter $(T_{in}-T_{am})/G_b$, a usual parameter for expressing the collector efficiency.
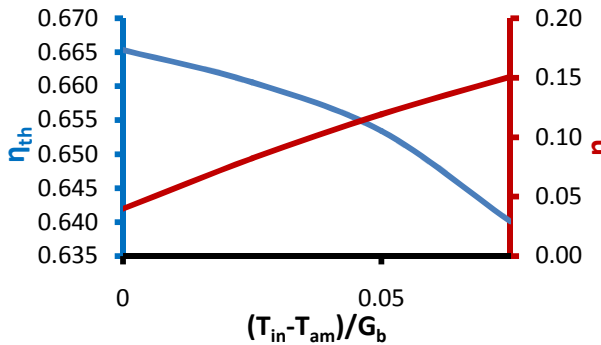
Fig.13. Thermal and exergy efficiency of the collector

From the above figure it is obvious that the thermal efficiency is not very affected by the inlet temperature. More specifically, for inlet temperature equal to ambient temperature at 10^oC, the thermal efficiency is 66.5% and for water inlet temperature equal to 70^oC the efficiency decreases only 2.5%. On the other hand the exergetic efficiency has a great increase, from 4% to 15% when the water inlet temperature varies from 10^oC to 70^oC. The

next equations are the approximation of thermal efficiency (equation 10) and exergetic efficiency (equation 11) with least square method.

$$\eta_{th} = 0.6651 - 0.0755 \cdot \left(\frac{T_{in}-T_{am}}{G_b}\right) - 3.4173 \cdot \left(\frac{T_{in}-T_{am}}{G_b}\right)^2 \quad (10)$$

$$\eta_{ex} = 0.0398 + 1.8051 \cdot \left(\frac{T_{in}-T_{am}}{G_b}\right) - 4.3757 \cdot \left(\frac{T_{in}-T_{am}}{G_b}\right) \quad (11)$$

The next figures show the temperature distribution in the absorber and in the fluid. In all these figures the water inlet temperate has assumed to be 50^oC. Figure 14 shows the temperature of the coil and of the fluid along the spiral coil. It is obvious that the temperature is getting greater and the difference between the solid temperature and the fluid temperature has an increasing rate. The reason for this phenomenon is the increasing rate of heat flux closer to the end of the coil. Figure 15 gives respective results as figure 14. In figure 14 the mean temperature in every place along the coil is given, while in figure 15 the exact temperature distribution over the down part of the coil is given. Figure 16 presents a horizontal cross section with the water temperature. The temperature difference in the water is about 34K from inlet to the outlet, while the absorber temperature reaches 93^oC, an acceptable temperature value. By analyzing these three figures together (14,15,16) the results shows to be similar and to be validated to each other, something very important for the strength of the presented method.
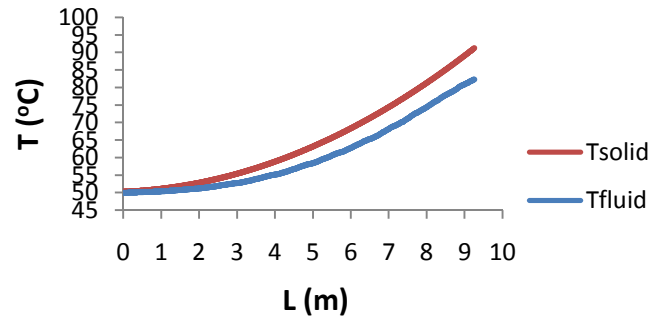
Fig. 14. Mean fluid and absorber temperature along the helix
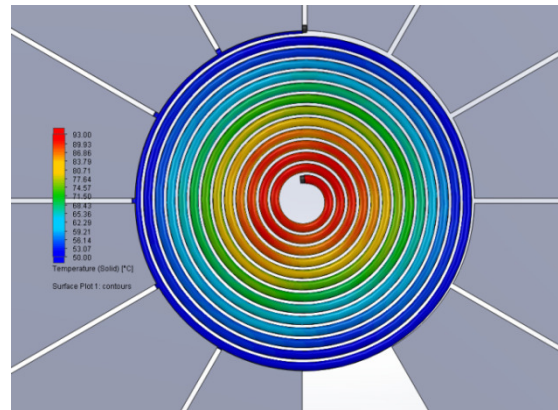
Fig.15. Absorber temperature in the down part
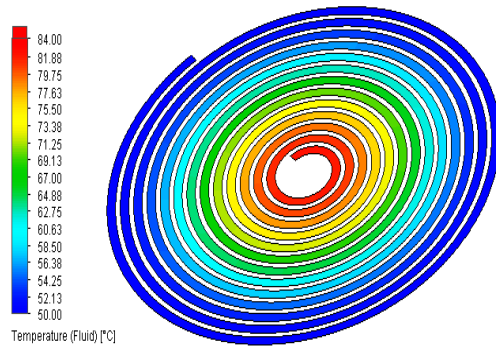
Fig. 16. Water temperature distribution in a horizontal cut in the middle of the tube

Figure 17 shows the fluid temperature in vertical cross sections. It is obvious that the water is getting warmer while it is closer to the center of the helix. Figure 18 gives the exact fluid temperature distribution in the outlet of the coil. The water is warmer in the down part of the tube, because the solar radiation is concentrated in this part. The total temperature deviation is about 2K across this vertical cross section, a value that is not high. These results prove that temperature in a cross section can be assumed uniform with an error of about 1K.
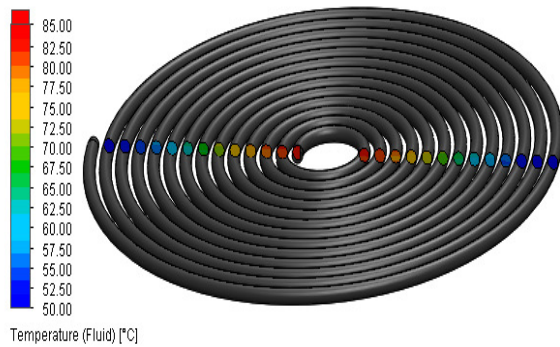
Fig. 17. Water temperature distribution in cross sections
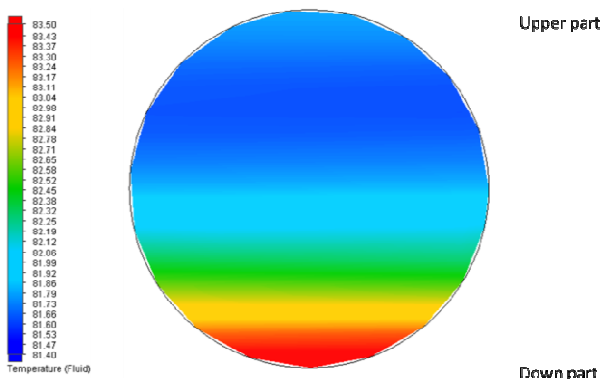
Fig.18. Water temperature distribution in the cross section of the outlet. The upper part of the figure presents the hotter down part of the coil
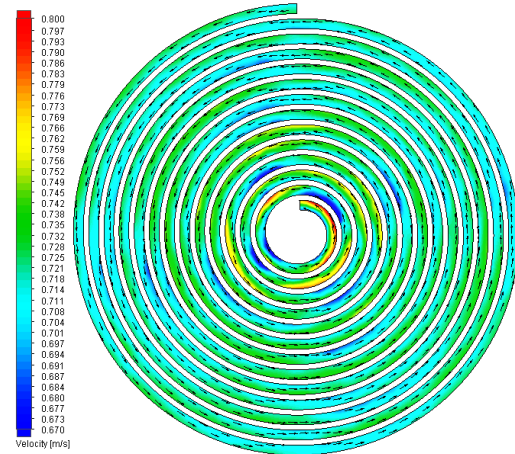
Fig. 19. Water velocity in a horizontal cut in the middle of the tube

Figure 19 shows the velocity of the water inside the tube. This parameter varies from 0.6m/s to 0.8m/s. While the water flows inside the tube, its velocity is getting greater in its right side, because this part has greater rotating velocity. This phenomenon is more intense closer to the center, where the flow rotation is greater.

The last figure gives the pressure drop in the spiral coil. While the water goes closer to the exit (cross sections closer to the center), its pressure is getting lower because of energy losses. The total pressure drop is about 0.07bar and a circulator is needed in order to cover this pressure drop. The pressure drop is a very important parameter because of the high length of the absorber. In every design, this parameter is taken into consideration because the energy consumption in circulator may add a great operation cost in the system.
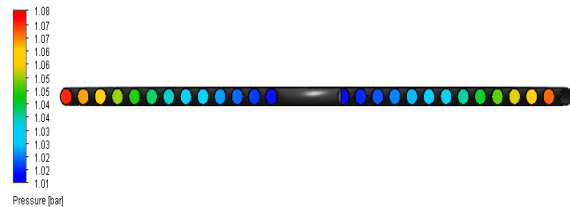
Fig. 20. Fluid pressure distribution in cross sections of the coil

CONCLUSIONS

In this study an innovative and low-cost solar dish receiver with a spiral coil absorber is analyzed optically and thermally. First of all the model was designed in Solidworks and after was simulated in its flow simulation studio. The optical analysis proved that the optimum distance between reflector and coil is 2100mm, lower than 2260mm which is the focal length. This result leads to maximum intercept factor and to a more uniform heat flux distribution.

The energetic analysis proved that the collector performs well in great range of operating conditions. Its exergetic efficiency is getting greater with the higher inlet water temperature, a result which makes this collector ideal for higher temperature applications as solar cooling, electricity production and polygeneration in buildings. Analytical approximations for thermal and exergetic efficiencies are presented in the text.

In the deeper analysis of the collector, the heat flux is maximum close to the center but not in the center. More specifically, the total helix length is 9m and the maximum heat flux is in the region close to 8.32m. On the other hand, the temperature of the coil is maximum in the end of the coil. Moreover, the pressure drop along the spiral coil is calculated at 0.07bar, an acceptable value that indicated the use of a small circulator in the system.

For further work, thermal oil or air can be tested in order to operate this collector in higher temperature levels. In this analysis water was tested as working fluid, because it is the more usual fluid for thermal processes.

REFERENCES

[1] Evren M. Toygar, Tufan Bayram, Oğuzhan Daş, Ali Demir *The design and development of solar flat mirror (Solarux) system*, Renewable and Sustainable Energy Reviews 54, 1278-1284 (2016)

[2] Kalogirou, S., Potenal of solar industrial process heat applications, Applied Energy2003;76: 337–361

[3] Amit, J., Tuyet, V., Rajeev, M., & Susheel, K.M.,Optimizing the Cost and Performance of Parabolic Trough Solar Plants with Thermal Energy Storage in India, Environmental Progress 1999;32:824-829

[4] Abutayeh, M., Goswami, D.Y., & Stefanakos, K.E. Solar thermal power plant simulation, Environmental Progress 2013;32:417-424

[5] Pavlovic, S., Vasiljevic, D., Stefanovic, V., Stamenkovic, Z., Ayed, S., Optical Model and Numerical Simulation of the New Offset Type Parabolic Concentrator with Two Types of Solar Receivers, Facta Universitatis, Series: Mechanical Engineering 2015;13:169-180

[6] Pavlovic, S., Stefanovic, V., Suljkovic S., Optical Modeling of Solar Dish Thermal Concentrator Based on Square Flat Facets, Thermal Science 2014;989-998

[7] Imhamed M. Saleh Ali, Tadhg S., O'Donovan, K.S. Reddy, Tapas K. Mallick, "An Optical Analysis of a Static 3-D Solar Concentrator, Solar Energy, 88, (2013), pp. 57-70

[8] N.D.Kaushika, K.S.Reddy, Performance of Low Cost Solar Paraboloidal Dish Steam Generating, Energy Conversion & Management 2000;41,713-726

[9] A.R.El. Ouederni, M. Ben Salah, F.Askri and F. Aloui, Experimental Sstudy of a Parabolic Solar Concentrator, Revue des Renouvelables 2009;12:395-404.

[10] Rafeeu, M.Z.A.AbKadir, Thermal Performance of Parabolic Concentrators Under Malysian Environment,: A case study, Renewable and Sustainable Energy Reviews 2012;16: 3826-3835.

[11] Zhiqiang, L, Justin, L., Wojciech, L., Optical Design of a Flat Solar Concentrator, Solar Energy 2012;86:1962-1966.

[12] Qianjun, M., Ming, X., Yong, S., Yuan, Y., Study on Solar Photo-Thermal Conversion Efficiency of a Solar Parabolic Dish System, Environmental progress & Sustainable energy 2013;33:1438-1444.

[13] Eswaramoorthy, M. & Shanmugam, S. The Thermal Performance of a Low Cost Solar Parabolic Dish Collector for Process Heat, Energy Source, Part A 2012;34:1731-1736

[14] Reddy, K.S., Kumar, S.N., Veershetty, G., Experimental Performance Investigation of Modified Cavity Receiver With Fuzzy Focal Solar Dish Concentrator, Renewable Energy 2015;74:148-157

[15] Jones, P.D., Wang, L., Concentration Distributions in Cylindrical Receiver/Paraboloidal Dish Concentrator Systems, Solar Energy 1995;54:115-123

[16] Takkar, Vanita., Doshi, A., Rana, A., Performance Analysis Methodology for Parabolic Dish Solar Concentrators for Process Heating Using Thermic Fluid, Journal of Mechanical and Civil Engineering 2015;12:101-114.

[17] Blázquez, R., Carballo, J., Cadiz, P., Frasquet, M., et al. Optical Test of the DS1 Prototype Concentrating Surface Enegy Procedia (2015);69:41-49.

[18] Zhigang Li, Dawei Tang, Jinglong Du, Tie Li., Study on the Radiation Flux and Temperature Distributions of the Concentrator - Receiver System in a Solar Dish/Stirling Power Facility, Applied Thermal Engineering, 31, (2011), pp. 1780- 1789.

[19] Pavlovic,S., Vasiljevic,D., Stefanovic, V., Optical Design of a Solar Parabolic Thermal Concentrator Based on Trapezoidal Reflective Petals, ICAT "2014, Proceedings, International Conference on Advances Technology & Sciences, Antalya, Turkey, August 12-15, 2014, pp. 1166 – 1171

[20] Shuai, Y., Xia, X.L., & Tan, H.P. Radiation Performance of Dish Solar Concentrator Cavity/Receiver Systems, Solar Energy 2008;(82):13–21.

[21] Duffie JA, Beckman WA. Solar engineering of thermal processes. 2nd ed. New York: Wiley Interscience; 1991.

[22] Kotas, T.J. The Exergy Method of Thermal Plant Analysis; Krieger Publish Company: Malabar, FL, USA, 1995.

[23] Bejan, A. Advanced Engineering Thermodynamics; Wiley Interscience: New York, NY, USA, 1988.

[24] R. Petela, Exergy analysis of solar radiation, (Chapter 2), in: N. Enteria, A. Akbarzadeh (Eds.), Solar Thermal Sciences and Engineering Applications, CRC Press, Taylor & Francis Group, 2013.

[25] S. Kalogirou, Solar Energy Engineering, edited by Soteris A. Kalogirou, Academic Press, Boston, 2009

[26] E. Bellos, C. Tzivanidis, D. Korres, K. A. Antonopoulos, Thermal analysis of a flat plate collector with Solidworks and determination of convection heat coefficient between water and absorber, ECOS Conference 2015, Pau, France

[27] E. Bellos, C. Tzivanidis, K. A. Antonopoulos, Thermal performance of a direct-flow coaxial evacuated tube with solidworks flow simulation, 6th International Conference on "Experiments/Process/System Modelling/Simulation/Optimization, Athens, 8-11 July, 2015

[28] Thermal and optical efficiency investigation of a parabolic trough collector C. Tzivanidis, E. Bellos, D. Korres, K.A. Antonopoulos, G. Mitsopoulos Case Studies in Thermal Engineering 2015;6c:226-237

[29] V. Badescu, Maximum reversible work extraction from a blackbody radiation reservoir. Way to closing the old controversy, Europhys. Lett. 2015;109:40008

[30] J. Nyers, L. Kajtar .S. Tomic, A. Nyers, "Investment-savings method for energy-economic optimization of external wall thermal insulation thickness." *Energy and Buildings*, 2015;86:268-274.

[31] L. Kajtar, J. Nyers, J. Szabo, "Dynamic thermal dimensioning of underground spaces" *Energy* 2015;87:361–368.

[32] L. Herczeg, T. Hrustinszky, L. Kajtár: Comfort in closed spaces according to thermal comfort and indoor air quality. Periodica Polytechnica-Mechanical Engineering 44: (2) pp.249-264. (2000)

[33] M. Kassai, C. J Simonson: Performance investigation of liquid-to-air membrane energy exchanger under low solution/air heat capacity rates ratio conditions. Building services engineering research & technology 36:(5) pp. 535-545. (2015)

[34] Magyar Zoltán, Garbai László, Jasper Andor Risk-based determination of heat demand for central and district heating by a probability theory approach ENERGY AND BUILDINGS 110: pp. 387-395. (2016)

Effects of Industrial Symbiosis on Company's Energy Efficiency and Renewable Energy Use

Slavica Tomić*, Dragana Delić**

*University of Novi Sad/Faculty of Economics, Subotica, Serbia
**University of Novi Sad/Faculty of Economics, Subotica, Serbia
tomics@ef.uns.ac.rs, delicd@ef.uns.ac.rs

Abstract - **Manufacturing activities account for around one-third of the world's total final energy consumption. When energy prices are low and relatively stable, and energy costs represent only a small part of total production costs, energy as an input factor within the industrial production process had low or even zero priority for corporate management. This is about to change. A number of environmental megatrends are likely to converge and to transform manufacturing activities in the future. These trends will lead to economic and environmental efficiency and sustainability becoming central to company's resilience and competitiveness. Increased competition for raw materials and energy put pressure on the natural resources (which resulted in price increase) and has potentially significant effects on future company's growth and success. Improvement of resource productivity and energy efficiency through industrial symbiosis (by-products and waste become energy resources) could yield significant economic and environmental benefits for company.**

Keywords: **industrial symbiosis, energy efficiency, renewable energy**

I. INTRODUCTION

Continued economic growth and development and technological progress put significant pressure on environment and have negative consequences on global supplies of resources. A number of environmental megatrends in the form of climate change, population growth, urbanization, accumulation of waste, increased competition for energy, demand for land, water, and materials, will require major shifts in the way business (industry) operate [1, pp.19]. The challenges (for industry) are huge and complex: they involve a multitude of concepts and disciplines, ranging from resource efficiency to innovative business models. In the face of these challenges, the reactive trends (possible responses) by business (industry) could be: the increasing use of mechanisms to "price" the impact of production on the environment, higher sustainability standards around the impact and efficiency of production, zero waste strategy (concept), closed loop or circular (business) model, industrial symbiosis, eco-industrial parks, and etc. The one of main ideas behind those concepts is that companies should use waste and/or by-product as inputs in order to maximize resource (material and energy) efficiency and minimize pressure on virgin resources.

II. CIRCULARITY AND RESOURCE EFFICIENCY

Efficiency means the relationship between the results achieved and the resources employed. The need for even more efficient utilization of resources is coming more and more sharply into focus in business, in research and in politics. A crucial question is what options do companies have to reduce not only costs but also the use of resources and emissions, by exploiting more efficient technologies, solutions, practices. There is a need to reduce the quantity of resources used whilst increasing production output, and therefore to improve the productivity of resources. This means manufacturing as much as possible from the use of a given quantity of raw materials and energy. Instead of "maximum profit (gain) from the minimum of capital there is a need to achieve maximum profit from the minimum of resources" [2, pp.4].

Manufacturing is directly related to natural resources and immediately affected by their diminishment. Therefore, the future of production will need a reduction of the environmental impacts associated with resource use and reduction of the associated economic costs and risks to business. Production systems which create products-output, while using less material and energy inputs represents sustainable manufacturing systems. The objective of resource efficient manufacturing is to improve manufacturing productivity whilst inputting less raw material, water and energy. Greater resource efficiency has been pursued broadly in industry and advances have been made, largely because efficient use of resources has significant financial benefits which in competitive markets have always been a priority. Though often framed as a "green" objective, this can equally be understood as a significant increase in multi-factor productivity. According to McKinsey Global Institute report [3] "there is an opportunity to achieve a resource productivity revolution comparable with the progress made on labour productivity during the 20th century". According to the report, resource productivity could meet up to 30 percent of the global demand for natural resources until 2030.Market forces alone are unlikely to generate sufficient progress in material and energy productivity within a critical mass of manufacturing activities, at least until scarcity of those inputs reaches a stage which is disruptive to the economy as a whole, and resource-intensive industries in particular.

Industrial sustainability or sustainable industrial systems imply circularity (circular, closed-loop model), which keeps materials within the system of production and use, rather than discarding them, i.e.:

- reuse, remanufacturing, refurbishment and recycling;
- synergetic business relationships for better use (utilization) of by-products and waste (industrial symbiosis);
- industrial clustering for decarbonization, etc.

Circularity (or circular, closed-loop, cradle-to-cradle strategy) is an approach which stands in contrast to the "linear", traditional production and consumption (take-make-dispose) pattern, and involves the joining up of the value chain so that end-of-life products are reused as inputs, and waste is utilized as a resource wherever possible. By associating both ends of a linear value chain, the chain can be joined up either with other value chains, forming networks of industrial symbiosis, or with itself, meaning that whatever waste, by-products or heat there is in a process must be exploited rationally in a different manufacturing process. Within circular industrial (eco) systems, organizations (companies) utilize each other's material and energy flows including wastes and by-products to reduce the systems virgin material and energy input as well as the waste emission output from the system as a whole. In addition to the improvements achieved to date in the sphere of recycling, it is increasingly a matter of integrating resource cycles within process chains and within production generally. The use of recycling materials from production waste makes a significant contribution to improving energy efficiency. This contribution results predominantly from the distinctly lower use of energy required for the production of secondary material. In the ideal situation, recyclable material from production can be utilized further without, for example, energy-intensive melting processes or similar, thus further improving energy efficiency. There is a large potential in metal processing, especially in the area of sheet metal and stamping waste. For example, up to 60 % of metal sheets used in automobile production end up as production waste [4, pp.12].Also, according to the research [5], chemical and metallurgical companies intensively reuse by-products in their internal processes - the chemical companies are able to capture their by-products and find economical means to convert them into marketable products or they were used in another step of the production process.

Although companies have clear incentives to be efficient within their own core processes, by-products, waste, surplus energy frequently occur. This raises the possibility of synergetic collaborations to make use of these resources as inputs in a different processes (within the same or among different companies), through concepts such as industrial symbiosis. Industrial symbiosis represents an association between two or more industrial facilities or companies in which waste or by-products of one become the raw materials (inputs) for another with the aim to manage the flow of resources through socio-economic systems with a view to optimizing their use. Hence, industrial symbiosis involves identification and development of relationships that would not "naturally" occur. This can result in economic benefits such as the generation of new revenue (additional sales of by-products or waste), saving on

waste treatment expenses or landfill taxes (costs savings) and the more efficient use of resources. Additionally, industrial symbiosis collaborations can generate positive externalities which the system as a whole benefits from. These include not only the benefits of greater material efficiency, such as resilience against resource insecurity and environmental benefits (landfill diversion, CO_2 reduction, raw material saved...), but also high levels of (cross-sectoral) innovation and knowledge spillovers [6, pp. 99].

National Industrial Symbiosis Programme (NISP) in UK, example of industrial symbiosis best practice, generated a good return on public investment of £5-£9 of value for every £1 put in. Calculations of reductions in water and material use, CO_2 emissions and waste going to landfill show that this occurred at a cost of less than £1 per tonne. The results achieved through NISP provide a robust evidence base to support the role of industrial symbiosis in helping businesses improve efficiency and profitability, competitiveness and better environmental performances. Between April 2005 and March 2013, due to collaboration in form of industrial symbiosis (supported by NISP), 45 million tonnes of materials were recovered and reused, industrial carbon emissions was reduced by 39 million tonnes, 71 million tonnes of industrial water was saved, £1.1 billion cost savings achieved, £1.4 billion generated in additional sales[7].

Industrial clustering for decarbonisation is the integration between industrial sites to deliver energy savings. It can reduce emissions by optimizing the use of resources (waste or by-products) - such as CO_2 from one process to be used beneficially by another process, while costs are shared, heat is used wisely and other benefits increase [8].Waste heat recovery can bring further energy efficiency benefits through re-use of low grade heat by other heat users outside of the sector producing that waste heat. Clustering is a long-term, gradual option that requires new or replacement plants to be encouraged to locate where clustering benefits can be realized, and existing plants to maximize local opportunities. The barriers to clustering are generally related to organizational collaboration and include the perceived risk of becoming reliant on a partner who may not be present in the long term.

III.   INDUSTRIAL   SYMBIOSIS,   ENERGY EFFICIENCY AND RENEWABLE ENERGY USE

Resource efficiency, particularly energy efficiency is very important in manufacturing activities, since manufacturing accounts for around one-third of the world's total final energy consumption [9].   Better industrial energy efficiency, first and foremost the efficiency of the manufacturing processes at the core of industry is the most effective lever available to curb industrial energy consumption. Growing numbers of companies are seeing energy efficiency as a key part of their efforts to promote sustainability and promoting energy efficiency in their supply chains to meet their own sustainability commitments.

When energy prices are low and relatively stable, and energy costs represent only a small part of total production costs, energy as an input factor within the industrial production process had low or even zero priority for corporate management. In those conditions,

energy costs are in most cases only treated as overhead rather than as a cost category for which managers were directly accountable for. This situation has changed with the considerably rising of energy sourcing prices within the last decade. As a result, the number of companies addressing energy-related issues has risen in recent years and increasing activity concerning energy management can be determined in business practice. Industrial companies have seemed to realize that energy management can be an effective lever for enhancing their production systems and operations towards improved energy efficiency and thereby reducing energy use and related costs. One of the ways to improve energy efficiency and renewable energy use in manufacturing is through industrial symbiosis, which can contribute to less final energy consumption and better economic and environmental performances of companies. Selected examples of internal and external industrial symbiosis in food and beverage production companies (Nestle, Strauss Adriatic, Carlsberg, and British Sugar) will illustrate how by-products and production waste (leftovers) could be turn into energy (resources).

A. *Nestlé*

Anaerobic digestion system at Nestlé's factory (Fawdon, the North East of England) is turning chocolate and sugar confectionery waste from the site's manufacturing processes into renewable energy. Rejected chocolates and sweets which are not suitable for sale or reprocessing (and which would otherwise be disposed of externally), along with waste residues such as starch and sugar are broken down in to small pieces. This mixture is then partially dissolved using the waste liquids from the site's cleaning processes to create a 'chocolate soup' which is then fed into an airtight tank where anaerobic digestion occurs. Almost 10% of the site's overall energy needs (heat and power) is met by burning the biogas which is the primary by-product of anaerobic digestion. As a result of the heat and power generated from the biogas, factory's greenhouse gas emissions are expected to fall by about 10%. Set up at a cost of CHF 4.7 million, the anaerobic digestion system isn't cheap; but due to the cost savings it has generated, the investment is expected to take around four years to pay off. The factory's anaerobic digestion converts about four tonnes of solid waste and 200,000 liters of liquid waste a day, making the site that have now achieved zero waste for disposal status. Also, in 22 Nescafé factories, the spent coffee grounds and discarded coconut shells resulting from the manufacturing process are used as a source of renewable energy (fuel) [9, 10, and 11].

B. *Strauss Adriatic*

Company Strauss Adriatic uses coffee chaff (which has always been treated as a waste) as fuel (biomass) to heat complete production and administrative facilities of its plant in Serbia. The plant in Serbia annually produces 140 tonnes of coffee chaff briquettes, which is enough for 3 months of heating. The boiler room is designed to burn other kinds of biomass as well, so that the rest of the heating fuel can always be chosen in accordance with the market trends. The total value of the investment is EUR 120, 000, but annual savings are estimated at between 65,00 and 90,000 Euros thanks to huge financial savings (the use of coffee chaff cuts heating costs)[4].Aside from being cost efficient, the use of coffee chaff briquettes as a fuel is also eco-efficient because it solves the problem of waste disposal since the coffee chaff is a by-product of the coffee processing process, and as such it used to represent a waste. One kilogram of coffee chaff briquettes has the energy value of 13,500-14,000 KJ, while the energy value of wood briquettes amounts to 17-18,000 per kilogram (classical energy value of biomass ranges from 11,000 to 20,000 KJ per kilogram and is considered a usable source of energy). Analyses focused on gases released during the combustion process, showed that the emission of harmful gases is no bigger than when any other form of biomass is combusted. What remains after the coffee chaff combustion is ash which can be used as an additive in the cement industry.

C. *Carlsberg*

Circularity is becoming a more integrated part of brewing operations, too. Waste and by-products from the brewing process provide excellent opportunities for re-use. Many of Carlsberg's breweries are re-using and recycling close to 100 percent of their total solid waste and by-products. Examples include brewer's grains sold as animal feed and the recovery of methane from the anaerobic digestion of wastewater to produce renewable energy for use at breweries. Carlsberg often applies anaerobic treatment technologies that recover organic carbon to produce biogas, which is a source of renewable and clean energy. In total, 5.2% of heating energy comes from renewable energy sources. Company currently operates 15 biogas-recovery wastewater plants, which produce and use over 9.5 million cubic meters of biogas - energy enough to heat 11,000 European homes [13, 14].

D. *British Sugar*

The core product of the company British Sugar is sugar. But, company employs a number of methods and uses by-products and production waste to minimize energy consumption, maximize (energy) efficiency and diversify business. British Sugar factory in Wessington developed and installed system to capture biogas from the effluent treatment plant and use it as a supplementary renewable fuel. The project increases energy efficiency, reduces fossil fuel consumption and provides CO_2 emissions savings of around 2,000 tonnes per annum. Thereafter, fermentation/distillation plant producing up to 55,000 tonnes of bioethanol per year. This is used as a renewable fuel to blend with petrol.

Company also uses combustion gases (which traditionally go to the chimney) and recovered heat from CHP plant to grow tomatoes in glasshouse (over 140 million tomatoes annually).This provides heating and CO_2 which is essential to promote plant growth. More than two hundred and forty milesof piping carries hot water from the factory's Combined Heat and Power (CHP) plant around the glasshouse, to maintain the temperatures which suit tomato plants. This hot water would otherwise be destined for cooling towers, so the scheme ensures that the heat is used productively. Another benefit is the productive use of waste carbon

---

dioxide from the factory, which tomatoes use during photosynthesis. At Corner ways, carbon dioxide (a by-product from the CHP boiler) is pumped into the enormous glasshouse to be absorbed by the plants, rather than vented into the atmosphere as waste emissions[5].

IV. CONCLUSION

The long-term environmental constraints on the world's ecosystem pose specific challenges for the industry (manufacturing sector).The circumstances in which manufacturers will have to operate in future will be very different. The closed energy and material loops was believed to entail a promising way in which future industrial systems could be designed so that the negative environmental impact from industrial operations could be *close* to zero. Uncertain supply of resources and worries over the environmental and social effects of greenhouse gases emissions, have lead companies to focus on how the use of by-products and waste as energy, through industrial symbiosis, can be optimized. While also serving environmental objectives, focus on productivity gains through energy and resource efficiency should equally be regarded as an economic priority.

REFERENCES

[1] Industrial Evolution - Making British Manufacturing Sustainable, Manufacturing Commission, 2015. Available at :

[2] http://www.policyconnect.org.uk/apmg/sites/site_apmg/files/industrial_evolution_final_single-paged.pdf

[3] Energy Efficiency in Production: Future Action Fields, Fraunhofer Institutes, Available at:

[4] http://www.iwu.fraunhofer.de/content/dam/iwu/en/documents/EffPro_en.pdf

[5] Resource Revolution: Meeting the World's Energy, Materials, Food and Water Needs, McKinsey Global Institute, 2011. Available at :

[6] http://www.mckinsey.com/business-functions/sustainability-and-resource-productivity/our-insights/resource-revolution

[7] http://www.iwu.fraunhofer.de/content/dam/iwu/en/documents/EffPro_en.pdf

[8] Uncovering Industrial Symbiosis in Tianjin Region, China, Center for Industrial Ecology Yale University, USA. Available at http://cie.research.yale.edu/sites/default/files/Tianjin%20IS%20Spring%202008.pdf

[9] http://www.policyconnect.org.uk/apmg/sites/site_apmg/files/industrial_evolution_final_single-paged.pdf

[10] http://www.nispnetwork.com/about-nisp/a-proven-track-record

[11] Industrial Decarbonisation &Energy Efficiency Roadmaps to 2050, Cross-sector Summary, 2015. Available at:

[12] https://www.gov.uk/government/uploads/system/uploads/attachment_data/file/419912/Cross_Sector_Summary_Report.pdf

[13] Intelligent manufacturing: Targeting better energy efficiency. Economist Intelligence Unit report, 2013. Available at: https://library.e.abb.com/public/a30ca06a25eee52bc1257bf000319c43/EE_EIU_2013%20v2.pdf

[14] http://www.nestle.com/media/newsandfeatures/nestle-factory-fawdon-uk-candy-waste-reduction

[15] http://storage.nestle.com/nestle-society-full-2014/files/assets/common/downloads/publication.pdf

[16] http://www.nestle.com/asset

[17] lbrary/Documents/Library/Documents/Corporate_Social_Responsibility/2011-CSV_environmentalsustainability.pdf

[18] http://www.carlsberggroup.com/investor/downloadcentre/Documents/CSR%20Reports/Carlsberg_Group_CSR_Report_2014.pdf

[19] [1]http://www.britishsugar.co.uk/Environmental.aspx

[20] http://www.carlsberggroup.com/csr/stories/Pages/Turningwasteintoresources

[21] M. R. Chertow, "Uncovering" Industrial Symbiosis, Journal of Industrial Ecology, Vol. 11, Issue 1, pp. 11–30, 2007.

[22] M. Martin, N. Svensson, M. Eklund, "Who gets the benefits? An approach for assessing the environmental performance of industrial symbiosis", Journal of Cleaner Production Vol. 98, pp. 263–271,2015.

[23] L. Šereš L., O. Grljević, S. Bošnjak, „IT Support of Buildings Energy Efficiency Improvement", International Conference on Energy Efficiency and Environmental Sustainability, EEES2012, Conference proceedings, ISBN: 978-86-7233-320-6, pp. 55-62.

Analysis of ventilation heat losses in case of refurbished buildings

Imre Arany, Ferenc Kalmár

University of Debrecen, Department of Building Services and Building Engineering, Debrecen, Hungary
imigold@freemail.hu; fkalmar@eng.unideb.hu

Abstract—**Energy saving in the building sector is one of the most important issues. In European countries severe requirements were established related to the overall heat transfer coefficients of the building envelope. Transmission heat losses are drastically reduced and the air tightness of the building envelope is extremely high. However, the fresh air must be provided to the occupants, otherwise health problems may occur. Controlled ventilation with heat recovery can be assured only by installing mechanical ventilation systems. Nevertheless, the heat demand of the ventilation can be higher after refurbishment, than it was initially. In this paper the calculation procedures of the fresh air demands are presented and the effects of the refurbishments on the ventilation heat losses are illustrated by a case study.**

INTRODUCTION

According to Directive 2002/91/EC, buildings, accounts for more than 40 % of final energy consumption in the Community and is expanding, [1]. This trend will lead to higher carbon dioxide emissions in this sector. The Directive 2010/31/EU highlights that measures to improve further the energy performance of buildings should take into account climatic and local conditions as well as indoor climate environment and cost-effectiveness. According to this Directive as of 31 December 2020 new buildings in the EU will have to consume 'nearly zero' energy and the used energy will be 'to a very large extent' from renewable sources. In Hungary there were different national projects launched in order to help the owners of houses or flats or local governments to enhance the energy characteristics of buildings. In each of these programs one of the main indicators was the decrease of energy demand after refurbishment of the building envelope and its energy supply system. For a typical detached house with average thermal characteristics of the envelope, in central European countries heating represents between 70-80 % of its energy need. Proper insulation of the opaque building elements can be done either by inorganic fibrous materials or by organic foamy materials. However, the physical properties of these insulating materials are influenced by the building technology and meteorological conditions, so in the energy calculations appropriate thermal characteristics have to be taken into account, [2, 3, 4, 5]. In order to determine the optimal thermal insulation layer thickness for a building envelope, different methods have been developed, [6, 7, 8]. In Hungary the Regulation in force established the requirement related to the overall heat transfer coefficient of the external walls to 0.24 $W/m^2 \cdot K$. Triple glazed windows with low emissivity coatings and inert gases (argon, krypton) can reduce considerably the transmission heat loss trough these building elements. The window frame is an important part of a fenestration product. The glazing spacer and the location of the spacer in the frame may influence the thermal performance of the window. Normal window frames consisting of only wood, PVC, Al or wood/Al. Thereby the overall heat transfer coefficient values of these windows is larger than 0.80 $W/m^2 \cdot K$.

Existing buildings are characterized by low air tightness and relatively high air leakage. This air leakage is driven by differential pressures across the building envelope due to the combined effects of stack, external wind and mechanical ventilation systems. Jokisalo et al. studied the building leakage, infiltration, and energy performance analyses for Finnish detached houses, [9]. According to their results, infiltration causes about 15–30% of the energy use of space heating including ventilation in the typical Finnish detached house. According to Kalamees the typical air leakage places in the studied houses were: the junction of the ceiling/floor with the external wall, the junction of the separating walls with the external wall, penetrations of the electrical and plumbing installations through the air barrier systems, penetrations of the chimney and ventilation ducts through the air barrier systems, leakage around and through electrical sockets and switches, and leakage around and through windows and doors, [10]. Chan et al. analyzed more than 70,000 air leakage measurements in houses across the United States, [11]. Based on a classification tree analysis, they found that the year built and floor area are the two most significant predictors of leakage area: older and smaller houses tend to have higher normalized leakage areas than newer and larger ones. It is clear that after a thermal refurbishment of a building the infiltration will decrease considerably. This side effect of the additional thermal insulation of opaque building elements and windows change respectively, is advantageous from the point of view of heat demand, but creates new commitments from the ventilation point of view.

In building there are different sources of water vapor and the moisture content can rise to risky values, if the necessary air change is not assured continuously. Before refurbishment air leakage of a building, in most of cases "provided" a fresh air flow rate, which kept the absolute humidity of the indoor air under the critical value. After thermal refurbishment, if no mechanical ventilation is installed, mould appeared on the inner surface of the junctions of different building elements. Of course, the occupants can open the windows to change the air in a room, but the energy issues does not encourage the owners to open the windows as frequent as it would be needed on one hand, occupants can endure quite high CO_2 concentrations. Installing mechanical ventilation systems

the investment costs can grow considerably. Furthermore operating and maintenance costs have to be taken into account. In this paper the heat demand is analyzed in case of building refurbishments, taking into account the fresh air demand calculated using different requirements established in standards or Regulations.

VENTILATION RATE DEMAND IN BUILDINGS

The pollution sources in a building are the occupants and their activities, materials in the building, including furnishing, carpets household chemicals and the ventilation or air conditioning system. Many pollution sources emit hundreds or thousands of chemicals, but usually in small quantities, [12]. The sensory pollution load on the air is caused by those pollution sources having impact on the perceived air quality. The sensory pollution load in a space may be found by adding the loads caused by all the different pollution sources in a space.

The air quality may not be the same throughout a ventilated space. What really counts for the occupants is the air quality in the breathing zone. The air distribution type has the most important impact on the indoor air quality. This is expressed by the ventilation effectiveness, [12]:

$$\varepsilon_v = \frac{c_e - c_s}{c_i - c_s}. \qquad (1)$$

where: ε_v – is the ventilation effectiveness; c_e – is the pollution concentration in the exhaust air; c_s – is the pollution concentration in the supply-air; c_i – is the pollution concentration in the breathing zone.

The required ventilation rate for comfort can be calculated from the equation, [12]:

$$\dot{V}_c = 10 \frac{G_c}{C_{c,i} - C_{c,0}} \frac{1}{\varepsilon_v}. \qquad (2)$$

where: G_c – is the sensory pollution load, [olf]; $C_{c,i}$ – is the desired indoor air quality, [decipol]; $C_{c,0}$ – is the perceived outdoor air quality at air intake, [decipol].

The ventilation rate required from a health point of view is calculated using equation (3), [12]:

$$\dot{V}_c = \frac{G_h}{C_{h,i} - C_{h,0}} \frac{1}{\varepsilon_v}. \qquad (3)$$

where: G_h – is the pollution load of a chemical, [μg/s]; $C_{h,i}$ – is the guideline value of a chemical, [μg/l]; $C_{c,0}$ – is the outdoor concentration of a chemical at air intake, [μg/l].

In CR 1752 the required ventilation rates are given for different building categories taking into account both the minimum ventilation rate for occupants only ($\dot{v}_p$) and the additional ventilation for building ($\dot{v}_B$). The sum of the ventilation rates give the fresh air needed for ventilation, [13].

$$\dot{V}_{tot} = N\dot{v}_p + A\dot{v}_B. \qquad (4)$$

where: $\dot{V}_{tot}$ - is the total ventilation rate of the room, [l/s]; N – is the number of persons in the room; A – room floor area, [m^2].

CR 1752 classifies the buildings into three categories (A, B, C) and gives the $\dot{v}_B$ values for low-polluting and non low-polluting buildings. In case of a department store the minimum ventilation rate for occupants is 2.1, 1.5 and 0.9 l/s·m^2, for A, B and C building category respectively. The $\dot{v}_B$ values for low-polluting building are: 2.0, 1.4, and 0.8 l/s·m^2, for A, B and C building category respectively. Meanwhile, for non low-polluting building, the $\dot{v}_B$ values are 3.0, 2.1, 1.2 l/s·m^2, for A, B and C building category respectively. Thus, important differences will appear between the required total ventilation rates, depending on the building category.

A building is called low polluting or very low polluting, when the majority of building materials used for finishing the interior surfaces meet the national or international criteria of low-polluting or very low polluting materials, [13]. EN 15251:2007 classifies the buildings into three categories (I, II, III) and gives the $\dot{v}_B$ values for very low-polluting, low-polluting and non low-polluting buildings. In case of very low polluted building the $\dot{v}_B$ values are: 1.0, 0.7 and 0.4 l/s·m^2, for I, II and III building category respectively. For low-polluting and non low-polluting buildings the proposed values are similar to the values required by CR 1752. It can be observed, that the requirement is three times higher in case of non low polluting building in comparison with a very low polluting building. This will lead to significant differences between the calculated ventilation rates of buildings.

According to the Hungarian Regulation the required fresh air flow rate supplied in a closed space depends on the physical demand level of performed work. In case of intellectual (sedentary) work, 30 m^3/h pro person ventilation rate have to be introduced in the room, while in case of light, medium, heavy work the requirement is: 30 m^3/h pro person, 40 m^3/h pro person and 50 m^3/h pro person, respectively, [14].

Desired ventilation rate can be calculated based on the heat and moisture load of the space. When determining the cooling load, all internal heat gains (occupants, lighting, electronic equipments, technologies) and the solar gains have to be taken into account. The ventilation rate demand is calculated as the ratio between the cooling load of the closed space and the difference between the indoor air enthalpy and supply-air enthalpy. When determining moisture load of a closed space all water vapor sources have to be taken into account: occupants, water surfaces, plants, cooking, washing, drying, etc. In this case, the required ventilation rate can be determined as the ratio between the water vapor load of the closed space and the difference between the absolute humidity of the indoor air and absolute humidity of supply-air.

The established ventilation rate is the basic information in the design of mechanical ventilation systems. All the elements (ducts, fans, filters, humidifiers, heat exchangers, air terminal devices, etc.) are chosen, based on the

ventilation rate. Thus, the design value of the ventilation rate demand influences both the investment and operational costs of the ventilation system.

In the following a case study will be presented illustrating the effects of the ventilation rate demand calculation, in case of a building refurbishment.

CASE STUDY

The analyzed building is a two levels furniture store built in 1996, having a net floor area of 751 m^2 in total. The external walls were built from brick with vertical holes, the floor is laid directly on the ground and the attic is unheated. The second floor is on the mansard. The windows and roof windows are double glazed, with an overall heat transfer coefficient of 3.0 W/m^2·K. The overall heat transfer coefficient of the entrance door is 3.5 W/m^2·K, of external walls 0.84 W/m^2·K, 0.294 W/m^2·K of the mansard roof and of the floor is 0.334 W/m^2·K. In the building there is no mechanical ventilation system. The heat demand for ventilation was calculated for and air change rate of 0.8 h^{-1}. At −15 °C external design temperature, the heat demand of the building is 42481 W (Table I.).

TABLE I.
HEAT DEMAND OF THE ANALYZED BUILDING

ROOM	NET FLOOR AREA, [m^2]	INDOOR AIR TEMPERATURE, [°C]	HEAT DEMAND, [W]
EXHIBITION ROOM 1.	319.3	20	18610
LOBBY	12.37	17	1569
OFFICE	11.31	22	1650
BOILER ROOM	5.22	16	376
STAIRCASE	17.66	18	3119
TOILET	1.2	16	−48
STORE-ROOM	12.37	16	1160
WC	1.73	16	138
EXHIBITION ROOM 2.	345.1	20	14538
EXHIBITION ROOM 3.	12.37	20	711
DRESSING ROOM	12.37	19	658

The assumed air change rate practically represents a ventilation rate of about 1502 m^3/h. This amount of fresh air would be enough for about 38 persons being at the same time in the building (assuming 40 m^3/h·person the fresh air demand). Practice has shown that simultaneously max. 20 persons are usually in the analyzed building.

According to the Building Energy Performance Regulation in force, if the analyzed building would be refurbished and the refurbishment would be partially supported by the State, the requirements related to the overall heat transfer coefficients of the refurbished envelope are: 0.24 W/m^2·K (external wall); 0.3 W/m^2·K (floor); 1.15 W/m^2·K (windows); 1.45 W/m^2·K (entrance door); 0.17 W/m^2·K (mansard roof), 1.25 W/m^2·K (roof windows) [16]. For external walls graphite-enhanced expanded polystyrene was used as additional thermal insulation (9 cm) and at the roof 10 cm thick PUR foam boards. Along the basement 9 cm extruded polystyrene was assumed.

The new overall heat transfer coefficient values of the building elements are shown in Table II.

TABLE II.
OVERALL HEAT TRANSFER COEFFICIENTS OF REFURBISHED BUILDING ENVELOPE

BUILDING ELEMENT	ORIGINAL U VALUE, [W/ m^2·K]	NEW U VALUE, [W/ m^2·K]
EXTERNAL WALL	0.840	0.234
FLOOR	0.334	0.217
ROOF	0.294	0.161
WINDOWS	3.0	1.0
ROOF WINDOWS	3.0	1.2
ENTRANCE DOOR	3.0	1.31

Using the new heat transfer coefficient values and keeping the original air change rate, the new heat demand values were calculated (Table III.).

TABLE III.
HEAT DEMAND OF THE REFURBISHED BUILDING

ROOM	HEAT DEMAND, [W]	REDUCTION OF HEAT DEMAND, [%]
EXHIBITION ROOM 1.	12114	34.9
LOBBY	783	50.1
OFFICE	818	50.4
BOILER ROOM	152	59.6
STAIRCASE	1697	45.6
TOILET	−48	0
STORE-ROOM	607	47.7
WC	38	72.5
EXHIBITION ROOM 2.	11494	20.9
EXHIBITION ROOM 3.	436	38.7
DRESSING ROOM	438	33.4

After thermal refurbishment of the building envelope the total heat demand decreased to 28529 W. This means a reduction with 32.8% of the heat demand. However, after refurbishment was assumed the same air change rate.

Let us see, what will happen with the heat demand of the building, if mechanical ventilation would be installed after refurbishment.

According to EN 15251:2007 (department store, II. category), the 7 m^2/person should be taken into account. This means practically 107 persons in the store! The ventilation rate demand, calculated based on the floor area $\dot{V}_{tot}$ will be 2.9 m^3·h·m^2 (2178 m^3/h).

The pollution load in the building is approximately 338 olf. Assuming the desired indoor air quality 1.4 decipol; and the perceived outdoor air quality at air intake, 0.1 decipol, the ventilation rate demand will be 9692.3 m^3/h. The ventilation effectiveness was considered 0.9.

According to the Hungarian Regulation, the specific flow rate might be considered 40 m^3/h·person, which means 4280 m^3/h (even with 107 persons in the store).

Certainly, when the ventilation system is designed, the highest ventilation rate demand has to be taken into account. This means an air change rate value after refurbishment of 5.16 h^{-1}. Naturally, the ventilation system operating time is not the whole day (open hours are between 9:00 am and 17 pm). However, in the period when the store is closed an air change rate of 0.3 h^{-1} should be take into account (considering high air tightness of the refurbished building). Assuming that in the mechanical ventilation system a heat exchanger is built-in with a mean heat recovery efficiency 0.73, the heat

demand of the refurbished building was recalculated. The new values are shown in Table IV.

TABLE IV.
HEAT DEMAND OF THE REFURBISHED BUILDING, CALCULATING THE VENTILATION RATE DEMAND BASED ON IAQ

ROOM	HEAT DEMAND, [W]
EXHIBITION ROOM 1.	18629
LOBBY	1015
OFFICE	1063
BOILER ROOM	273
STAIRCASE	2405
TOILET	−26
STORE-ROOM	832
WC	69
EXHIBITION ROOM 2.	18168
EXHIBITION ROOM 3.	637
DRESSING ROOM	670

As it could be observed, the heat demand of some rooms increased, even though heat recuperator was taken into account.
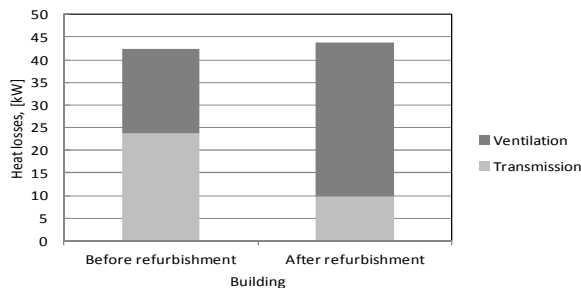
Heat losses of the analyzed building

CONCLUSIONS

Nowadays energy saving is one of the most important priority in the building sector. Existing building stock is the biggest energy consumer in most European countries.

It is obvious that existing buildings should be refurbished from energy pint of view. However, should not be forgotten that, not only the energy requirements became stricter, but also the comfort requirements increased. Buildings are built to assure healthy and comfortable environment to the occupants.

Usually, after a deep refurbishment of the building envelope, important energy savings are expected. Nevertheless, requirements related especially to the fresh air flow rate may lead to an increase of the ventilation heat losses and the expected energy savings will not be met. It was proved that, without properly designed ventilation system CO_2 concentration can increase considerably in closed spaces, [16, 17, 18]. Consequently, controlled mechanical ventilation has to be installed in case of building refurbishments to avoid health related complains.

REFERENCES

[1] EC Directive, (2010). "Directive 2010/31/EU of the European Parliament and of the Council of 19 May 2010 on the energy performance of buildings (recast)." Official Journal of the European Communities, L 153/13, 18.6.2010, Brussels.

[2] Á. Lakatos, "Moisture induced changes in the building physics parameters of insulation materials", Science and Technology for the Built Environment 21:(9) pp. 1-13. (2016).

[3] Á. Lakatos, I. Csáky, F. Kalmár, "Thermal conductivity measurements with different methods: a procedure for the estimation of the retardation time", Materials and Structures 48:(5) pp. 1343-1353. (2015).

[4] F. Szodrai, Á. Lakatos, "Simulations of the Changes of the Heating Energy Demand and Transmission Losses of Buildings in Central European Climate: Combination of Experiments and Simulations", International Review Of Applied Sciences And Engineering 6:(2) pp. 129-139. (2015).

[5] Á. Lakatos, "Comparison of the thermal properties of different insulating materials", Advanced Materials Research 899: pp. 381-386. (2014).

[6] F. Kalmár, "Energy analysis of building thermal insulation", Proceedings of 11th Conference for Building Physics, Dresden, 26-30 September 2002, p.103-112

[7] A. Bolattürk, "Determination of optimum insulation thickness for building walls with respect to various fuels and climate zones in Turkey", Applied Thermal Engineering 26 (2006) 1301–1309.

[8] J. Nyers, P. Komuves, "Optimum of External Wall Thermal Insulation Thickness using Total Cost Method", EXPRES 2015 Subotica, 7th International Symposium on Exploitation of Renewable Energy Sources and Efficiency. 2015.03.19-2015.03.21. Subotica, pp. 13-17.

[9] J. Jokisalo, J. Kurnitski, M. Korpi, T. Kalamees, J. Vinha, "Building leakage, infiltration, and energy performance analyses for Finnish detached houses", Building and Environment 44 (2009) 377– 387.

[10] T. Kalamees, "Air tightness and air leakages of new lightweight single-family detached houses in Estonia", Building and Environment 42 (2007) 2369–2377.

[11] W. R. Chan, W. W. Nazaroff, Ph. N. Price, M. D. Sohn, A. J. Gadgil, "Analyzing a database of residential air leakage in the United States", Atmospheric Environment 39 (2005) 3445–3455.

[12] CR 1752: 1998, Ventilation for buildings – Design criteria for the indoor environment, CEN Report.

[13] EN 15251–2007: Indoor environmental input parameters for design and assessment of energy performance of buildings addressing indoor air quality, thermal environment, lighting and acoustics.

[14] 3/2002. (II. 8.) SzCsM-EüM együttes rendelet a munkahelyek munkavédelmi követelményeinek minimális szintjéről.

[15] 20/2014. (III. 7.) BM rendelet, Az épületek energetikai jellemzőinek meghatározásáról szóló 7/2006. (V. 24.) TNM rendelet módosításáról.

[16] I. Csáki, "Szellőztetés hatása a széndioxid koncentrációra lakóépületekben", 15th Building Services, Mechanical and Building Industry Days, Debrecen, 2009.10.15-2009.10.16., pp. 115-122.

[17] I. Csáki, "Szennyező anyagok a belső környezet levegőjében", I. Alpok-Adria Passzívház Konferencia – Pécs, 2009.09.04-2009.09.05., pp. 357-359.

[18] L. Herczeg, "Irodaterek belső levegő minőségének értékelése: A szén-dioxid koncentráció hatása az ember közérzetére és az irodai munka teljesítményére", Magyar Épületgépészet LVIII:(5) pp. 3-7. (2009)

[19] F. Kalmár, Á. Nagy, "Szén-dioxid-koncentráció alakulásának vizsgálata egy oktatási épületben", Magyar Installateur, 1, 2016, pp. 39-42.

[20] L. Kajtár, L. Herczeg, E. Láng: Examination of influence of CO2 concentration by scientific methods in the laboratory. 7th International Conference Healthy Buildings 2003. Singapore, 12. 07-11. 2003. pp. 176-181, 2003.

[21] L. Herczeg, T. Hrustinszky, L. Kajtár: Comfort in closed spaces according to thermal comfort and indoor air quality. Periodica Polytechnica-Mechanical Engineering 44: (2) pp.249-264. (2000)

[22] J. Nyers, L. Nyers: "Monitoring of heat pumps". 'Studies in Computational Intelligence', Springer's book series, ISBN 978-3-642-15220-7 Vol. pp. 243, 573-581, Heiderberg, Germany. 2009.

Energy Inefficiency of the Republic of Serbia as a Barrier to Future Energy Development

A. Boljević* and M. Strugar Jelača*

* Faculty of Economics in Subotica/Department of Management, Subotica, Serbia

aboljevic@ef.uns.ac.rs; m.strugar.jelaca@ef.uns.ac.rs

Abstract — **Modern trends in the area of energy efficiency have opened a number of issues, as whether developing countries (the Republic of Serbia being one of them) are ready to enter into this process of transformation and the new industrial era. In order to answer that question, we formulated the goal of the research which is reflected in the analysis of the energy potential of the Republic of Serbia, its utilization and efficiency levels. A detailed and systematic analysis of various theoretical frames and industrial reports identified the reasons for the low energy efficiency of Serbia at macro and micro levels, which represents a key barrier to securing energy and ecologically sustainable environment of our country. The lack of government initiatives or financial instruments for encouraging renewable energy, as well as accumulated and unresolved political and economic problems are just some of the barriers at macro level, while on micro level a large number of organizations in Serbia have problems with: high costs of heating and electricity, old plants, boilers that are not working at their full capacities and a range of other problems. Despite the current unfavorable energy balance, a small number of organizations is opting for change, because change itself is unknown, it carries a great risk and financial investments.**

With regard to the situation identified in this field and considering the awareness of our society, process of energy efficiency growth and switching to renewable sources would be time consuming, followed by the need to implement radical and systemic changes at the state level and organizational system level, which would produce effects in the future. Measures in the shortest possible time frame are suggested in order to minimize the negative effects due to poor energy efficiency and primary use of conventional sources of energy, taking into account the existing situation and constraints, so this could yield positive effects and ensure environmental protection.

Key words: energy inefficiency, barriers, eco technology

INTRODUCTION

One of the most important global topics in scientific, political and business circles is providing energy efficiency in order to achieve the same or even greater benefit while using less energy and simultaneously ensuring economic, social and environmental sustainability. The growing demand for energy, which a large number of countries encounter, and taking into account economic and environmental effects, focuses on defining the measures of stimulating growth of country's energy efficiency, along with adhering to the concept of sustainable development and environmental protection. All this leads to formation of a post-fossil energy age that promotes finding new sources of power and new efficiencies with breakthrough technologies.

As we are witnessing it today, the energy market is facing much more challenges: limitation of fossil fuel reserves, increase in population, dearth of energy security, economic and urbanization growth [1]. Increasing research in that area point to a rapid downward trend of world reserves of conventional sources of energy and the need to go towards larger exploitation of renewable energy sources. It is believed that natural resources scarcity will lead to an increase in price of non-renewable resources, which will place renewable resources progressively on the business agenda of industries [2], enabling long term sustainability through realization of set of benefits shown on Fig. 1.
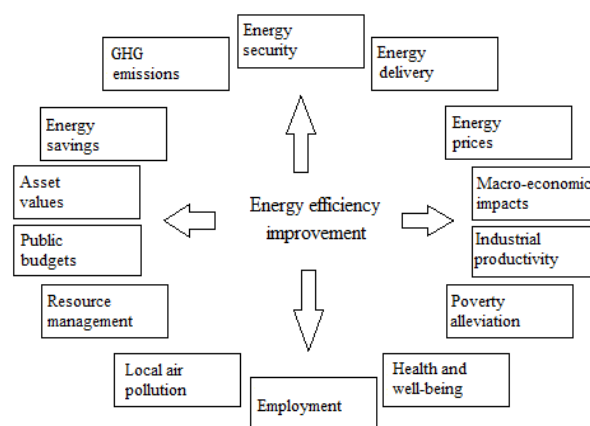
Figure 1. The multiple benefits of energy efficiency improvements [3]

In order to realize multiple benefits of energy efficiency, there is growing attention on the new sources of power and new efficiencies with breakthrough technologies that need to be found to step into the so-called post-fossil energy age. That would include lower cost of production, distribution and continuous operation, as well as smooth transition from nuclear energy, natural gas and biomass to solar, wind, and hydropower [4]. Although many are unprepared to handle the transformation, in the coming years there will be a new marketplace environment and fresh challenges in the form of transforming the entire industry [5]. Particularly in developing countries, where our country is listed, there is a gap between theoretical aims and objectives in this field on the one hand and practical realization of the same on the other. Despite present focus on increasing

investment into renewable energy while promoting new strategies for energy efficiency, in practice there is lack of implementation of the same, which leads to the conclusion that this industry is still characterized by focus on the planning phase with minimal involvement in implementation phase and the absence of practical benefits. On the territory of the Republic of Serbia situation in this area is very unfavorable because the percentage of utilization of renewable energy sources is at low level, with modest prospects for future improvement.

Global trends in energy efficiency and current situation in our country in this field have influenced the formulation of the basic objective of this paper that is aimed at identifying the reasons of economic inefficiency as present barrier to greater use of renewable energy sources. We have focused on two stages in this research; first, literature reviews from reputed academic journals and industry articles, and second, qualitative research used to identify various sources of energy inefficiency in the Republic of Serbia.

The paper is organized as follows: the second section describes energy situation and its utilization at the terriotory of the Republic of Serbia, the third section discusses and elaborates reasons of energy inefficiency in our country, the fourth identifies measures for establishing ecologically healthier environment, while the last one is the conclusion.

ENERGY SITUATION AND ITS UTILIZATION IN THE TERRITORY OF THE REPUBLIC OF SERBIA

"Serbia is rich in sources of "clean" energy from nature, solar energy, wind, rivers, geothermal sources and biomass, of which it currently uses 33% of the available technical potential for achieving the estimated objective for 2020." [6]. The greatest potential of renewable energy sources is biomass 49%, in large hydroelectric power plants 27%, solar energy 13%, wind energy 4%, geothermal energy 4% and 3% in small hydroelectric power plants [7]. The potentials of Serbia in renewable energy sources are amounted to about 4 million tonnes of oil equivalent (toe), of which biomass takes 2.68 million toe, solar energy has a potential of 640 000 toe, small hydropower plants of 440 000 toe, geothermal energy 185 000 toe and wind energy 160 000 toe. However, there is insufficient use of the potential that Serbia has, particularly in the field of hydropotential and biomass.

Currently, the aforementioned energy potential from renewable sources in the territory of the Republic of Serbia is not sufficiently utilized, and from the future's viewpoint it cannot be used effectively unless there is a clear political vision in this area, along with scientific and technological support. Political instability and a series of economic problems in domestic market that require state intervention slowed down the development of an adequate institutional framework in the field of renewable energy sources and raising awareness about the importance of using them. In order to overcome negative effects of political and economic developments in our country, which also have bad influence on energy efficiency, it is necessary to place an accent on harmonization of external and internal factors affecting this area in the future. One of the vital external forces for growth and development of renewable energy are governments' regulatory and budgetary support in consistent manner, while the internal forces refer to those inside the industry that are formulated by business strategy, technology adoption, skilled workers etc. [8, p. 1369]. From the perspective of energy efficiency in renewable sources, it is of utmost urgency to identify the steps aimed at establishment of enabling external and internal environment, so we could keep the pace with the global trends and requirements.

REASONS FOR ENERGY INEFFICIENCY OF THE REPUBLIC OF SERBIA – BARRIERS AT MACRO AND MICRO LEVEL

The main obstacle for creation of an energy efficient environment of our country is low awareness of both the state and its population about the importance and the treatment of such environment as a concept of negligible economic importance, which is inconsistent with the understanding of prominent economists worldwide. Unsustainable use of energy, together with limited supply of energy leads to slow economic growth and even negative levels of economic indicators [9]. Our energy intensity and energy productivity are far below the average values of these indicators in the EU [10], which indicates to the need for the Republic of Serbia to encourage changes in the energy use primarily at macro level and also at micro level. The need for change in this area at macro level is indispensable, as evidenced by the data of the International Energy Agency [3, p. 19], which indicates that 2/3 of the energy resources will remain unutilized until 2037 if policies and procedures in this field do not change.

There are numerous reasons of energy inefficiency in the Republic of Serbia:

• mentioned political issues and public policy that allows subsidizing the industry by taxpayers through provision of cheap energy with minimal investments and instruments to help in the use of renewable energy sources;

• social factors;

• industrial sector with lack of attention paid to energy efficiency investment opportunities by stakeholders in both private and government sectors, causing a growing technological gap in the territory of the Republic of Serbia from the perspective of poor application of energy efficient technologies.

Insufficient state incentives for investment into purchase of new energy-efficient plants caused utilization of the old ones that still use lignite as a fuel. On the other hand, the European Union's objective is to provide 20 % of its energy consumption from renewable energy sources [11], along with reducing fossil energy consumption and the consequent emission of green house gases [12]. Despite initiatives at the European Union level, Serbia has a high level of greenhouse gases emission, as evidenced by the fact that from the perspective of carbon dioxide emission per capita in 2013 Serbia was ranked fifth out of 36 countries in Europe. Another reason for the high CO_2 emissions in our country is under-representation of the need to control emissions of CO_2 in political circles and the absence of government subsidies for green energy [13, p. 4]. According to the "Doha Amendment to the Kyoto Protocol" to the United Nations Framework Convention to Climate Change, it commits countries to 18% reduction (from 1990. levels) of green house gases by 2020 [14]. Globally, there is a growing

concern about emissions of Green House Gas and consequent climate change, therefore renewable energy sources have become more attractive options for power generation [15, p. 763], while in the territory of the Republic of Serbia even in 2015 the situation has not been better from the perspective of utilization of renewable energy, because it lacked about 1,000 megawatts of electricity, which was again produced from lignite. All this is caused by high consumption of primary energy per unit of GDP in Serbia, which is 15 percent higher than the world average and nearly twice as high compared to the European members of the OECD [16]. As Wilkins summarises it, such increase in energy demand in developing countries highlights and emphasizes the urgent need for renewable, sustainable, affordable and environmentally sound energy systems [17].

Another reason that leads to the energy inefficiency of our country is the fact that the price of electricity is at a very low level, because it is on average 6 to 7 times cheaper than in the countries of the European Union, which leads to a small interest of both businesses and individuals for investing in more energy-efficient forms of energy. From their point, savings from using renewable energy sources are minimal compared to today's way of using electricity as a final energy, while from the perspective of economists it is evident that releasing some of the resources that are spent on energy could increase the disposable income that can continue to be invested into industrial sector. Social factors play a significant role, in terms of lack of population's awareness about the limitations and negative consequences of non-renewable energy resources, as well as distrust of both citizens and businesses in renewable energy sources, since investments in renewable energy require large costs in the present for greater and invaluable future benefit. Many potential customers are giving more importance to keep the initial low costs rather than to minimize the operating costs . Population's indifference towards the use of renewable energy stems from lack of knowledge and exposure to renewable energy in rural areas, and lack of easy access to information on the latest technologies, which results in uncertainty about the quality of new technologies [19]. Based on that, for the developing countries those technologies (which had not been used in their context before) had been more expensive and also presented more risk than the existing technologies [20]. Advocating the preceding viewpoint may lead to difficulties in business expansion in this area in the near future and so financial investment in the renewable energy business and its growth in the future may also be affected [8]. In order to minimize the probability of occurrence of the previous scenario, some of the proposed measures are to be implemented, namely: the development of knowledge management processes, either internal or external information sharing to sort out the problems of talent shortages and the lack of societal awareness [8, p. 1370]. Furthermore, education and information dissemination related to renewable energy must include everything, from resource studies and education about various renewable technologies to training and information about available government incentives and support systems [15, p. 766].

At present, there is a lack of sufficient government incentive schemes as well as financing mechanisms to promote the adoption of renewable and sustainable energy technologies by businesses and industries [18]. Our country needs to formulate and promote a legal framework which will foster the creation of so-called green environment and induce the organizations to act accordingly. The need for such measures is necessary because the current uncertainties that the entrepreneurs involved perceive will greatly affect their innovation decisions and can prevent them from engaging in innovation projects aimed at developing and implementing emerging renewable energy technologies [8, p. 1378]. There should be emphasis on providing a set of financial incentives of different forms (subsidy, tax exemption, low interest loan, long-term credit, and specific funds for grid connected projects in rural/mountainous areas) [15, p. 766].

In addition to initiatives at macro level, it is necessary to encourage the initiative at micro level through development and application of new energy-efficient technologies that can be seen as a form of green or eco-innovation at the level of our organization, which is of great importance, representing a vision of sustainable innovation. Together with the aforementioned types of innovation application by large, financially strong and market-dominant organizational systems, it is necessary to encourage small and medium-sized organizations that want to keep up with the green way of doing business in cooperation and connection to large organizations with possibilities of joint investments in renewable energy and green technology. In this way the essential flow of information and knowledge at the organization level would be provided, which should also be encouraged at the state-organization level, science-economy level and vice versa. The current situation in our organizations reflects a low level of expertise in the field of energy efficiency and renewables, due to the lack of adequate guidance and technical support for operators [21] as well as poor 'information flow and communication', which are some of the greatest barriers to technology transfer experienced in industry [15, p. 766].

MEASURES FOR ESTABLISHING ENVIRONMENTALLY HEALTHIER ENVIRONMENT

Inefficient use of energy sources, ongoing reliance on conventional energy sources and minimal use of renewable energy sources has led to poor environmental situation in our country, which points to the need for proposing measures with the aim of overcoming the same.

One of the greatest threats to disrupted ecological environment in our country is transport sector, which is responsible for 30% of CO_2 emissions, and given the average age of cars, namely 13 years, the average fuel consumption per 100 kilometers is 10 liters. Since the European Commission carried out an initiative to reduce greenhouse gas emissions within the transport sector, emphasis is placed on using biofuels and bio liquids which will provide GHG emission reduction of at least 35%. Looking at the trend of using biofuels in the period from 2007 to 2013, there is a significant progress that has led to three times higher production in 2013 compared to 2007. However, comparing to neighboring EU member states, biofuels consumption in Serbia is significantly

lower here than in Hungary, Romania and Bulgaria, while it is higher than in Croatia (Table 1.).

Country	2007	2008	2009	2010	2011	2012	2013
Bulgaria	0,147	0,147	0,221	0,846	0,699	3,496	3,496
Croatia	0,110	0,147	0,328	0,110	0,164	1,526	1,526
Hungary	1,2	6,892	7,079	7,317	6,934	6,531	6,062
Romania	1,693	2,061	1,690	4,753	7,761	9,126	9,126
Serbia	0,980	1,961	2,941	2,941	2,941	2,941	2,941

At the national level it is necessary to encourage the use of biofuels and bio liquids in parallel with prescribed sustainability criteria while sourcing, producing and using biofuels and bio liquids in accordance with the Renewable Energy Directive (2009/28/EC). Making such procedure will enable financial support from the EU to the organizations that adhere to these procedures, as well as the ability to export the same to the EU market. One needs to go a step further by promoting the use of methodology for calculating the reduction of GHG emissions due to utilization of biofuels in transport, which would allow savings of GHG emissions in January 2017 at the amount of 50%, while for January 2018 expected savings could rise to 60%. State's commitment is inevitable at macro level for environmental protection with minimal GHG emissions and promotion of utilizing renewable energy sources, which will encourage formation of green or eco-industry, one of the most dynamic sectors in the European Union with a strong tendency of growth. However, positive effects of the proposed measures at macro level will fail if the companies in this and other sectors do not recognize the need for more energy-efficient way of doing business.

At the organization level, the need for more energy-efficient and environmentally responsible business should be carried out by potentiating green innovation as the vision of sustainable innovation with the aim of diagnosis, monitoring, reduction or prevention of environmental problems [22]. In the future, transformation of traditional business should be ensured towards green business which would lead to minimization of technology gap that exists in the territory of the Republic of Serbia due to utilization of energy-inefficient technologies. This transformation is important because organizations are one of the major participants whose current way of doing business led to poor environmental situation. Application of green business concept would make organizations become more environmentally responsible, and in the new era of green economy they would be more likely to achieve competitive advantage. Deteriorating ecological image in the world is caused by global warming, major environmental pollution, excessive waste, lack of natural resources, and it stimulates the development and utilization of green technologies which should enable implementation of sustainable development and thus protect the environment and solve accumulated environmental problems. Countries around the world should encourage investment into research and development of these types of technologies, which represent the innovation trend. So far, countries that invest the most into the development of green technology are Japan, the United States and Germany [23]. Today, most organizations in the world tend towards implementation of green technologies, application of green materials in order to create the so-called green profile of their products [24], which directly provides new market opportunities. Organizations that implement green innovation invent new techniques, methods and processes in order to eliminate negative environmental impacts. Some economists believe that organizations that invest in green business concept and application of green technologies lead to positive social effects, but that the financial effect of that action is absent. For these reasons, although the green innovations together with green technologies represent an innovative trend to be pursued, a large number of organizations is not motivated to invest into research and development of green innovation due to absence of income. The above mentioned situation occurs also in the industrial sector of Serbia, because this kind of technology is still considered to be financially ineffective. However, a number of economists believe that its use does not lack financial effects, but tends to increase competitiveness of an organization, and therefore secures better financial position. They believe that green technologies are leading to a win-win situation with economic and environmental benefits [25, p. 422]. Organizations that find themselves in a win-win position lead to positive effects for directly or indirectly involved parties in the process of doing business. In addition to the positive effects that an organization has at micro level, there is realization of positive effects on macro level through benefits for all members of society.

Given the whole society's benefit from the development and application of green innovation, both in the field of management and technology, organizations in our country should work together on their research and development in order to achieve greater effects. The need for joint action stems from two reasons. Primarily, today's organizations are still inexperienced in coping with environmental problems, because there are no organizations that possess the ability to develop and implement eco-innovation processes and products [25, p. 423]. On the other hand, common development and application of eco-innovation solves environmental problems. Organizations in the field of green business need to establish cooperation with the government, intellectual institutions, suppliers, customers, competitors' organizations and industry associations [26, p. 413], in order to achieve a synergetic effect in the context of environmental protection. Interaction and coordination of all participants is indispensable in order to achieve the desired effects of application of the concept of eco-innovation and green business, as their implementation alone does not lead to a win-win situation and prosperity of the market.

CONCLUSION

Various barriers to adopting energy efficiency and sustainable energy technologies in Serbia have been identified from the literature review and expert opinions in detail. The main obstacle for creation of an energy efficient environment in our country is poor awareness of both the state and its population of the importance and the treatment of this concept as the one that has negligible economic importance. From the aspect of the country, there is a lack of sufficient government incentives

schemes or financing mechanisms to promote the adoption of renewable or sustainable energy technologies. From the perspective of the population, there is insufficient awareness of their limitations and negative consequences of non-renewable energy resources, as well as distrust of both citizens and businesses about renewable energy sources, since investments into renewable energy requires large costs at present for a higher and invaluable benefit in the future. Previously mentioned barriers of energy efficiency lead to a bad situation in Serbia, caused by frequent false directing of Serbia towards investment in unsustainable systems which will lead to major negative effects on the environment, climate change and long-term development of the country. Therefore, this paper may play an important role in understanding various barriers and help in better utilization of energy potential of the Republic of Serbia, as well as removal of the mentioned barriers in order to adopt sustainable energy technologies more effectively and efficiently.

Currently underutilized renewable energy potential of the Republic of Serbia directs political public to formulate a clear vision in the field of energy efficiency, through setting up an adequate institutional framework that will allow the alignment of external and internal factors affecting this area and their positive effects in practice. It is necessary to implement planning in the field of energy efficiency, where an important role is played by the scientific community which should point to the world trends in this area, as well as the state that sets the energy development strategy, desired objectives and the proposed actions in the function of achieving global benchmarks. Synthesis of the planning phase and implementation phase is indispensable in order to ensure the transformation of the desired goals into practical results as soon as possible by establishing cooperation with the business sector of our country at the levels: Knowledge Management Process, Intellectual Capital Maintenance and Performance Measurement. In this way, essential flow of information and knowledge would be provided at the levels organization-organization, organization-state, science-economy and vice versa. In the business sector the emphasis should be placed on transition from traditional to green business that supports the use of new energy efficient technologies, minimizes emission of CO_2 and allows application of concept of sustainable development. If the state promotes energy and environmentally responsible behaviour of its population and such activities of all participants in its economy, there will be a synergy effect of positive benefits in this area, and a win-win situation for all participants, both at present and in the future.

REFERENCES

[1] Z. Abdmouleh, R. Alammari, and A. Gastli. "Review of Policies Encouraging Renewable Energy Integration & Best Practices", Renewable and Sustainable Energy Reviews, 45, pp. 249–62, 2015.

[2] G. Svensson, "Aspects of Sustainable Supply Chain Management: Conceptual Framework and Empirical Example", *Supply Chain Management: An International Journal* , vol. 12, no. 4, pp. 262–6, 2007.

[3] IEA. *Capturing the Multiple Benefits of Energy Efficiency*, France:OECD/IEA, 2014.

[4] K. W. Guo, "Green Nanotechnology of Trends in Future Energy: A Review", International Journal of Energy Research, vol. 36, no. 1, pp. 1-7, 2012.

[5] B. Meckley. *The Value of Smarter Energy IBM Center for Applied Insights Industry Champion for Energy and Utilities*, pp.8–10, 2011.

[6] Ministarstvo, *Energetska politika Republike Srbije prema OIE*, http://www.energetskiportal.rs/ministarstvo/, Referenced at January 05, 2016.

[7] M. Tešić, F. Kiss, and Z. Zavarago, Z. "Renewable Energy Policy in the Republic of Serbia", *Renewable and Sustainable Energy Reviews*, vol. 15, no. 1, pp. 752-758, 2011.

[8] A. Seetharaman, L. L. Sandanaraj, K. Moorthy, and A. S. Saravanan, "Enterprise Framework for Renewable Energy", *Renewable and Sustainable Energy Reviews*, vol. 54, pp. 1368–1381, 2016.

[9] C. Wolfram, O. Shelef, and P. J. Gertler, "How Will Energy Demand Develop in the Developing World", *National Bureau of Economic Research*, No. w17747, 2012. http://www.nber.org/papers/w17747, Referenced at January 10, 2016.

[10] D. Kragulj and M, Porežanin, *"The Importance of Energy Sector for the Revitalization of Serbian Economy"*, in Proceedings of the X Conference of businessmen and scientists: Innovative operative management solutions for revitalization of the economy of Serbia, SPIN No. 15, University of Belgrade, Faculty of Organizational Sciences, pp. 232-238, 2015. ("*Značaj energetike za revitalizaciju privrede Srbije*", X Skup privrednika i naučnika: Inovativna rešenja operacionog menadžmenta za revitalizaciju privrede Srbije, Zbornik radova SPIN 15, Univerzitet u Beogradu, Fakultet organizacionih nauka, str. 232-238, 2015.)

[11] European Commission. *Renewable energy*, 2013. http://ec.europa.eu/energy/renewables/index_en.htm, Referenced at December 20, 2015.

[12] A. Menegaki and K. Tsagarakis, "Rich Enough to Go Renewable, but too Early to Leave Fossil Energy?", *Renewable and Sustainable Energy Reviews*, 41, pp. 1465–1477, 2015.

[13] B. Presnall, "A Little attention for the Great Possibilities", *Economist: Alternative energy of Serbia*, p. 4, 2010. ("Malo pažnje za velike mogućnosti", *Ekonomeast: Alternativna energija Srbije*, p. 4, 2010.)

[14] United Nations, *Doha amendment to the Kyoto protocol*. http://unfccc.int/files/kyoto_protocol/application/pdf/kp_doha_am endment_english.pdf, Referenced at December 20, 2015.

[15] S. Luthra, S. Kumar, D. Garg, and A. Haleem, "Barriers to Renewable/Sustainable Energy Technologies Adoption: Indian Perspective", *Renewable and Sustainable Energy Reviews* , 41, pp. 762–776, 2015.

[16] Government of the Republic of Serbia, *Energy Development Strategy of the Republic of Serbia to 2025 with Projections till 2030*, 2014. (Narodna skupština R. Srbije, *Strategija razvoja energetike Republike Srbije do 2025. godine sa projekcijama do 2030. godine*, 2014.)

[17] Wilkins G. *Technology Transfer for Renewable Energy*. India: CRC Press Ltd, 2012.

[18] S. Reddy and J. P. Painuly, "Diffusion of Renewable Energy Technologies –Barriers and Stakeholders' Perspectives", *Renewable Energy*, vol. 29, no. 9, pp. 1431–47, 2004.

[19] M. Kennedy and B. Basu, "Overcoming Barriers to Low Carbon Technology Transfer and Deployment: An Exploration of the Impact of Projects in Developing and Emerging Economies", *Renewable and Sustainable Energy Review*, 26, pp. 685–93, 2013.

[20] M. Suzuki, "What are the Roles of National and International Institutions to Overcome Barriers in Diffusing Clean Energy Technologies in Asia? Matching Barriers in Technology Diffusion with the Roles of Institutions", in *Environmental Change and Sustainability,* Chapter 7, S. Silvern and Young, S.*,* Croatia: Intech, 2013, pp. 185-214.

[21] S. Rand, B. David, G. Brunori, A. C. Dockès, M. FischlerM, and A. Guillaumin, *WP4: Environmental Technologies Synthesis Report*, April 2008.

[22] J. Hemmelskamp, "Environmental Policy Instruments and their Effects on Innovation", *European Planning Studies*, vol. 5, no. 2, pp.177-94, 1997.

[23] OECD. *Science, Technology and Industry Scoreboard 2013: Innovation for Growth*, Paris: OECD, 2013.

[24] B. Bigliardi and M. Bertolini, "Green Innovation Management: Theory and Practice", *European Journal of Innovation Management*, vol. 15, no. 4, 2012.

[25] J. Doran and G. Ryan, "Regulation and Firm Perception, Eco-innovation and Firm Performance", *European Journal of Innovation Management*, vol.15, no.4, pp. 421-441, 2012.

[26] M. Yarahmadi and G. P. Higgins, "Motivations Towards Environmental Innovation: A Conceptual Framework for Multiparty Cooperation", *European Journal of Innovation Management*, vol. 15, no. 4, pp. 400-420, 2012.

[27] J. Nyers, S. Tomic, A. Nyers: Economic Optimum of Thermal Insulating Layer for External Wall of Brick. International J. Acta Polytechnica Hungarica Vol. 11, No. 7, pp. 209-222. 2014.

Analysis of solar thermal energy system in Slovakia

Diana Kováčová

Slovak University of Technology, Faculty of Civil Engineering, Department of Building Services, Radlinského 11, 810 05 Bratislava, Slovakia

diana.kovacova@gmail.com

Abstract- **This contribution is aimed at assessing the operation of solar energy system during summer in residential building situated in Bratislava, Slovakia. In apartment building, heat transfer medium temperature was measured at the inlet and outlet of solar collectors, also the flow of the heat transfer medium in solar collectors, flow of the hot water, temperature in the storage tanks, intensity of solar radiation and outside temperature at minute intervals.**

The results point out, that solar coverage factor, is strongly dependent on the daily domestic hot water consumption profile, and also, indicate the necessity of instalation of additional heat source.

I. INTRODUCTION

Solar thermal collectors represent one of the most widely used technologies for heat production from renewable energy sources[1].Installation of solar collectors in houses is more and more popular than installation of solar collectors in residential buildings. In the context of the Europe-wide trend towards energy-neutral buildings, we believe, that we are on the threshold of developing the solar systems in residential buildings [2].

The application of solar systems in buildings contributes to the improvement of energy performance of buildings, along with the optimization of operating costs for the production of thermal energy. Norm EN15316-4-3 [3] refers to the energy efficiency and influence of thermal solar systems.

II. SOLAR ENERGY SYSTEM

The subject of investigation is a multifunctional residential building. Inhabiting, 120 people in 58 apartments on 11 floors. This residential building has 22 flat plate solar collectors KS 2000 TLP in one row connect to the series, oriented to the southwest on the roof of the building. The slope of the solar collectors is 45°, the absorption area of the collectors is 40.04 m^2 and efficiencyis80 %. These flat plate solar collectors are used only to supply hot water in the house. There are hot water tank with volume 1 000 l and accumulation tank of hot water from solar collectors with volume 1 000 l. Preparation of hot water is implemented in a way fast heat plate heat exchanger in the absence of sunlight.

III. EXPERIMENTAL MEASUREMENT

The purpose of the experimental measurement was to find the evaluation of the energy generated and supplied, and also efficiency of the solar system.

A. Selected results of the experimental measurements

For the purposes of experimental measurement performed were used ultrasonic flow meter Portasonic 9000, ultrasonic flow meter Portasonic 7000, ultrasonic flow meter DTFX, Monitoring central COMET MS5D, temperature probes, Pyranometer CMP3, external temperature detektor.

B. Hot water consumption

Hot water consumption was from 6,0to 6,93 m^3/day Figure 1what is 50 to 57,5 l for a person a day,in the residential building. The biggest hot water usage was between 7:00 a.m. and 8:00 a.m. during weekdays, while the lowest was between 2:00 a.m. and 4:00 a.m. During the weekend, the biggest hot water usage was from 9:00 a.m. to 11:00 a.m., while the lowest was between 2:00 a.m. and 3:00 a.m.
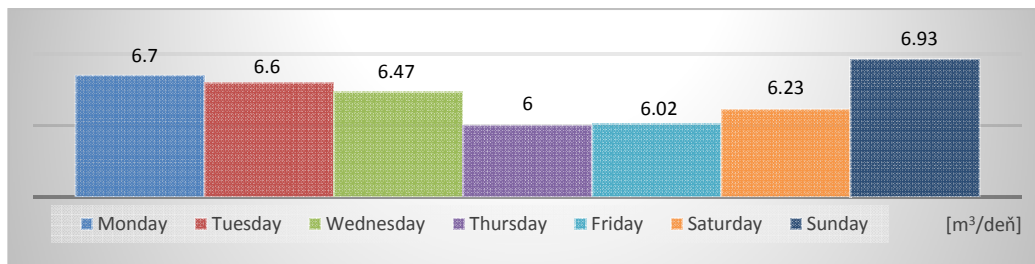
Fig.1 Hot water consumption in residential building

C. Average temperature in solar energy system

The average temperature from 3rd to 7th of July 2015 is tepresets on Figure 2. The temperature of the heat transfer medium at the inlet to collectors is directly proportional and affects the temperature of the heat transfer medium at the outlet. The temperature of hot water tank is increasing during the night, because the residential building has hot water 24 hours during the day and there is no big water consumption during the night.
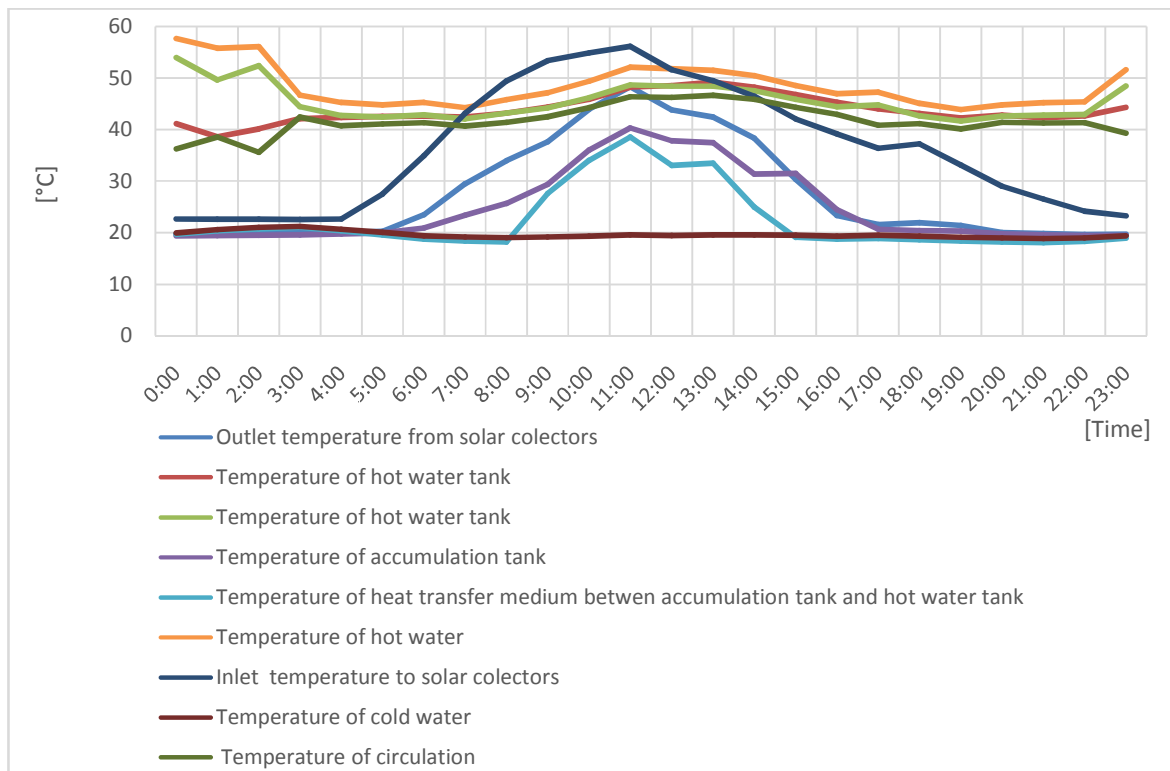
Fig. 2 Average temperature in solar energy system from 3rd to 7th of July 2015

The temperature of the heat transfer medium at the outlet of the collectors ranged from 32.6 °C to 52.7 °C,external temperature ranged from 20.5 °C to 33.6 °C and the maximum intensity of solar radiation during day reached 748.5 W/m^2 from 8:00 a.m. to 5:00 p.m.   The lowest intensity of solar radiation 215.5 W/m^2 was on 7th of July, when despite the cloudy weather temperature of the heat carrier amounted to 51.7 ° C, whereas it is also influenced by the exterior temperature, which on that day was 33.6 ° C.

D. Energy supplied by solar collectors and the amount of energy take at apartment building

Performance and efficiency of a solar collector is determined by the optical and thermal characteristics.

The amount of energy supplied by solar collectors and the amount of energy used from boiler room shows Figure 3.
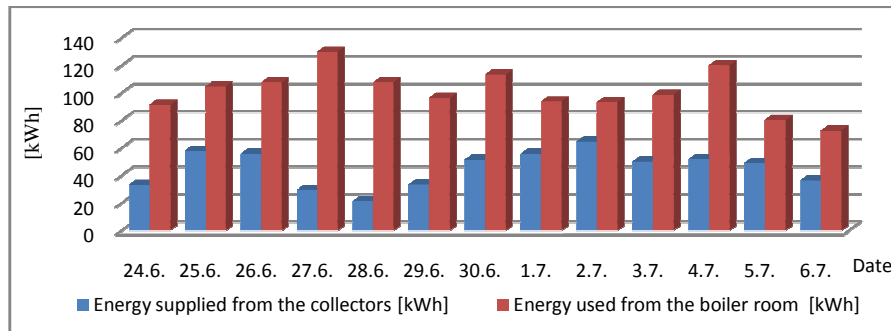

Fig. 3 Energy balance of solar collectors

An average of the energy supplied from the collectors is 45.3 kWh/day **Table 1.**The amount of energy used from the boiler room is approximately 96.9 kW/day **Table 2**. During the experimental measurement the efficiency average achieved daily of the collectors was from 54 %to 77 %.Table 1 shows average day values of the solar energy system and climatic conditions at the time from 8:00 a.m. to 5:00 p.m.

TABLE 1.
ENERGY SUPPLIED FROM SOLAR ENERGY SYSTEM

Date	The fow of the heat transfer medium m	Inlet temperature from solar collectors Θ_v	Outlet temperature from solar collectors Θ_p	Energy supplied by solar collectors Q_{sol}	Exterior temperature Θ_e	Intensity of solar radiation I	Efficiency η_{sol}
	(l)	(°C)	(°C)	(kW)	(°C)	(W/m^2)	(%)
24.6.	2131.60	27.10	45.02	40.91	20.53	526.43	62.30
25.6.	3104.34	35.24	52.69	58.01	21.42	690.00	60.40
26.6.	3352.50	36.42	52.00	55.94	24.68	687.00	62.94
27.6.	1866.84	21.40	36.10	29.39	23.20	440.00	72.43
28.6.	1630.56	20.40	32.60	21.31	21.76	350.00	71.87
29.6.	1990.62	22.40	32.80	22.17	22.17	520.00	73.73
30.6.	3269.94	35.30	50.00	51.48	26.80	660.00	65.59
1.7.	3293.10	33.90	49.70	55.73	27.20	645.00	66.42
2.7.	3997.38	28.53	40.30	50.40	28.93	580.00	74.33
3.7.	3627.36	33.67	46.63	50.35	29.09	676.25	70.19
4.7.	3285.24	37.70	51.70	49.26	31.03	660.10	67.57
5.7.	3268.38	35.28	50.60	53.63	33.64	622.73	71.04
6.7.	3973.00	38.38	49.28	46.38	33.01	582.30	68.85
7.7.	3530.63	34.68	48.32	51.03	29.96	651.27	69.39

TABLE 2.

112

ENERGY SUPPLIED FROM SOLAR ENERGY SYSTEM

Date	Flow of the heat carrier substance	Temperature of hot water	Temperature of the cold water	Energy supplied
	m	Θ_{sv}	Θ_{sv}	Q_{sol}
	(l)	(°C)	(°C)	(kW)
24.6.	3000	44.87	18.70	91.30
25.6.	3100	47.69	18.62	104.81
26.6.	3200	47.67	18.73	107.69
27.6.	4400	45.14	18.02	138.78
28.6.	3400	45.36	18.11	107.76
29.6.	3100	45.02	18.27	96.44
30.6.	3400	47.10	18.43	113.37
1.7.	2800	47.32	18.52	93.79
2.7.	2900	46.00	18.30	93.42
3.7.	2900	48.27	18.98	98.77
4.7.	3500	48.93	19.43	120.09
5.7.	2300	48.90	19.30	79.18
6.7.	2200	48.01	19.66	72.55
7.7.	2100	51.37	19.73	77.27

Outlet temperature from solar collectors is considerably effected by intensity of solar radiation. The solar energy system does not achieve high temperature on the outlet from solar collectors, because the system is undersize.

Temperature of cold water is approximately 18 °C, because cold water is affected by ambient temperature in boiler room which reaches 28 °C.

CONCLUSION

Quality solar collectors can achieve energy with very good efficiency, but it is the correct applicatirons of complete solar system thatdecides the total efficiency.

Residential building requieres subsidiary source for preparing hot water during summer, because collectors are designed to cover only 30 % of needs during the summer. This building has the solar energy system under sized and the system requires additional solar collectors and higher volume of the accumulation tanks.

ACKNOWLEDGMENT

REFERENCES

[1] SCIUTO, S.: Solar control: an integrated approach to solar control techniques, World Renewable Energy Congress V, Renewable energy Energy Efficiency, Policy and theEnvironment, 1998, s. 368-378.

[2] Ricci, M., Bocci., E., Michelangeli, E., Micangeli, A., Villarini, M., Naso, V.: Experimental Tests of Solar Collectors Prototypes Systems. In. Energy Procedia, Volume 82, December 2015, Pages 744–751, ISSN: 1876-6102

[3] MATUŠKA, T. Solární soustavy pro bytovédomy. Grada Publishing, a. s., 2010. 136 s. ISBN 978-80-247-3503-0

[4] EN 15316-4-3 Vykurovacie systémy v budovách. Metóda výpočtu energetických požiadaviek systému a účinností systému. Časť 4-3: Systémy výroby tepla, tepelné solárne systémy, 2013. s. 44

[5] FAN, J., JIVAN-SHAH, L., FURBO, S.: Flow Distribution in a Solar Collector Panel with Horizontally Inclined 1944–1948 Absorber Strips, In Solar Energy, 81 (2007), ISSN 0038- -092X

[6] Mghouchi, T. Ajzoul, A. El Bouardi: Prediction of daily solar radiation intensity by day of the year in twenty-four cities of Morocco, In. Renewable and Sustainable Energy Reviews, November 2015, Pages 823 – 831 s., ISSN: 1364-0321

[7] Li, H., Ma, W., Wang X., Lian, Y. Estimating monthly average daily diffuse solar radiation with multiple predictors: A case study. Renew Energy, Volume 36, Issue 7, July 2011

[8] SANCHEZ, M., MARTINEZ, I., RINCON, E., DURAN, M.: Design and Thermal-optic Analysis of an Ultra-solar Concentrator. In Energy Procedia, Volume 57, 2014, Pages 311–320, ISSN 1876-6102

[9] Bojanowski, S., Vrieling, A., Skidmore, A. K.: A comparison of data sources for creating a long-term time series of daily gridded solar adiation for Europe, In. Solar Energy 99 (2014), 152-171 s., Impact Factor: 3.47

[10] Evrendilek, F., Ertekin, C., 2008. Assessing solar radiation models using multiple variables over Turkey. Clim. Dynam. 31, 131–149

[11] MATUŠKA, T. Solární zařízení v příkladech. Grada Publishing, a. s., 2013. 256 s. ISBN 978-80-247-3525-2

[12] PASICHNY, V.: Some aspects of concentrated solar energy technologi calusing, World Renewable Energy Congress V, Renewableenergy Energy Efficiency, Policy and the Environment, 1998, s. 101-105.

[13] MILLER, F., VANDOME, A., MC BREWSTER, J.: Passive Solar Building Design: Passive solar building design, Sun path, Building insulation, Day lighting, Solar water heating, Passive house, Solar energy, Low-energy house, Zero-energy building, Alpha script Publishing, 2009.

[14] L. Herczeg, T. Hrustinszky, L. Kajtár: Comfort in closed spaces according to thermal comfort and indoor air quality. Periodica Polytechnica-Mechanical Engineering 44: (2) pp.249-264. (2000)

[15] J. Nyers, S. Tomic, A. Nyers: Economic Optimum of Thermal Insulating Layer for External Wall of Brick. International J. Acta Polytechnica Hungarica Vol. 11, No. 7, pp. 209-222. 2014.

Use of ABC in Paper Recycling Firm

Ivana Medved, PhD*, Sunčica Milutinović, PhD**

* University of Novi Sad, Faculty of Economics, Subotica, Serbia,
** University of Novi Sad, Faculty of Economics, Subotica, Serbia
ivana@ef.uns.ac.rs, suncica@ef.uns.ac.rs

Abstract — **Traditional and modern methods and techniques of cost accounting can fulfill the requirements of environmental management. The work was carried out as a brief practical study of the possibilities of use activity based costing (ABC) as modern cost accounting system for the purpose of environmental management accounting (EMA). The aim of the study was to test the usefullness of ABC in the case of paper recycling firm. Current problems of work, examined in terms of modern cost accounting technique, were in the findings for the problem of costs justification and measurement utility in environmental management accounting.**

INTRODUCTION

Environmental degradation is causing numerous economic and social consequences. It's possible that impacts of environmental degradation, will be difficult or even impossible to eliminate in future. Potential problems that threaten the environment, and thus endanger, directly and/or indirectly, human health and the functioning and survival of companies can be observe and solve from many different aspects. Investors and managers should pay attention to the importance of ecological management. Companies that have any environmental problem will not have a long-term perspective of sustainable development.

Inclusion of conservation or/and recovery of the environmental costs in the production process is called ecological (sustainable) production system. Environmental management is a skill of managing different levels of organizational systems (businesses, local government, state, etc.) through the control of risks that threatens the survival of these systems, or through the control of pollution and troubleshooting the impact of human beings on the environment [11].

Eco-management (environmental management) is a special concept of business management or enterprising management activities toward the acquisition of knowledge and practices to achieve the objectives in terms of survival of an organizational (business) systems in terms of the quality of its functioning [9].

The key factors that are essential for the implementation of major environmental projects and business improvement, especially for the purpose of sustainable development are:
1) education and information in order to increase environmental awareness;
2) regulations of the state in the form of legislation in the field of environmental protection, and control of implementation thereof;
3) the development of techniques and technologies in the field of environment (environmental technologies, waste, etc.);
4) quantitative indicators in favor of environmental projects measured by the ratio of costs and benefits with informational support of the accounting and especially of the cost accounting.

Projects of ecological management imposes new targets in front of the world economy, and in front of the managers in companies. Projects that minimize harm to the environment and contribute to the establishment of a controlled business environment require additional (working, research) time and additional investment (finances and knowledge). Consequently, the financial reporting is more complex and set new requirements from accounting, and in particular from cost accounting in terms of costing the environmental protection. It also refers to the importance of improving financial reporting in order to meet specific eco-management business decision-making.

In considering the application of ecological, "green" technology to reduce waste (emissions, waste water, solid waste), the possibilities of saving energy or recycling waste, the problem of measuring and presenting the realized benefits or costs incurred are always current.

In addition, it is important to emphasize that there is not always a full commitment to the protection of the environment (because it means less profit) but not a totally neglecting sustainable development (because it means endangering the future market position and reduce raw material) [12].

In this regard, among other things, accounting, both at the macro and micro level, as a information system should contribute to awareness of the investments in environmental protection, the manner of their systematization, responsibilities and effects of these investments. Costing, with the application of modern concepts and techniques for calculating the costs of environmental damage and environmental protection and the recognition of specific activities to which it relates, it is necessary to set up a way to provide timely, high-quality content and information basis to all internal and external stakeholders. Identification of the costs of environmental protection and the costs of the environmental improvement is important to determine the amount of these costs, but also to make decisions regarding investment in the protection and preservation of the environment. Economic experts like accountants should provide such information.

COST ACCOUNTING IN FUNCTION OF ECO-MANAGEMENT

Environmental cost are impacts incurred by society, an organization, or an individual resulting from activities that

affect environmental quality; these impacts can be expressed in:

a) monetary terms and

b) non-monetary terms.

They include any such cost, direct or less tangible, with short- or long-term financial consequences for the firm. Those costs are often not tracked by or are hidden in overhead accounts within traditional management accounting systems, but they can be a significant component of a firm's overall cost structure [5].

Investors and government representatives are interested in:

a) amount of costs of pollution (environmental damage) or amount of costs of reducing environmental pollution;

b) amount of costs of prevention and protection of environment; and

c) amount of eventual benefits of the (non) use different ways to reduce pollution

which requires the provision of adequate data and information [8].

Part of the accounting information system that provides the identification and preparation of information that occurred in relation to environmental damage and protection is developed from the Environmental – Ecological Accounting, also known as Eco-Accounting i.e. Green Accounting.

Environmental Accounting (EA) is focused on internal management decisions of firm.

EA can be applied at all levels of firm to help make timely information and criticaly business decisions, such as those in Table 1 below [5].

At the level of the firm, in the first place, it is necessary bookkept environmental costs (which are the subject of Environmental Financial Accounting – EFA), and after

TABLE VI.
BUSINESS DECISIONS SUPPORTED BY ENVIRONMENTAL ACCOUNTING

Product Design	Capital Investments
Process Design	Cost Control
Facility Siting	Waste Management
Purchasing	Cost Allocation
Product/Process Costing	Product Retention/mix
Risk/Liability Management	Product Pricing
Strategic Planning	Performance Evaluations
Supplier Selection	Plant Expansion
Environmental Program Justification	

that eco-costs can be directed towards the appropriate centers (areas) of responsibility where the costs incurred as a result of business activities (which is subject of Environmental Management Accounting – EMA).

EA and EMA can be viewed from:

1) the macro level (approach) as the national accounting environment, and

2) the micro level (aspects) of environmental accounting as part of the firm (corporation).

Structure and functioning of EMA is represent in Table 2 below [13].

Environmental cost identification makes possible for the costs to be bookkept and reported. The costs of

TABLE II.
STRUCTURE AND FUNCTIONING OF EMA

Accounting in Monetary Units			Accounting in Physical Units
Conventional Accounting	Environmental Management Accounting		Other Assessment Tools
	MEMA Monetary EMA	PEMA Physical EMA	
DATA ON THE CORPORATE LEVEL			
Conventional bookkeeping	Transition of environmental part from bookkeeping and cost accounting	Material flow balances on the corporate level for mass, energy and water flows	Production planning systems, stock accounting systems
DATA ON THE PROCESS/COST CENTRE AND PRODUCT/COST CARRIER LEVELS			
Cost accounting	Activity based material flow cost accounting	Material flow balances on the process and product levels	Other environmental assessments, measures and evaluation tools
BUSINESS APPLICATION			
Internal use for statistics, indicators, calculating savings, budgeting and investment appraisal	Internal use for statistics, indicators, calculating savings, budgeting and investment appraisal of environmental costs	Internal use for environmental management systems and performance evaluation, benchmarking	Other internal use for cleaner production projects and ecodesign
External financial reporting	External disclosure of environmental expenditures, investments and liabilities	External reporting (EMA-statement, corporate environmental report, sustainability report)	Other external reporting to statistical agencies, local governments, etc.
NATIONAL APPLICATION			
National income accounting by statistical agency	National accounting on investments and annual environmental costs of industry, externalities costing	National resource accounting (material flow balances for countries, regions and sectors)	

environmental damage and protection may have the following characteristics:

1) most commonly they are associated with the manufacturing process or product;

2) they depend on the conditions in which the production process takes place;

3) the problem is their identification and assessment of the their amount;

4) they are not subject of more detailed consideration and inclusion of International Accounting Standards and International Financial Reporting Standards (IAS/IFRS).

EMA, with it's central information basis - cost accounting, is the main source of information for the purpose of identification and managing costs of environmental damage and protection. New techniques and methodology of cost accounting cann't be implemented without planning, measuring, controling and cost analysing. In recent years, there are intensive searches for the most effective cost system to improve measurement and reporting towards enviromental operations and projects. For the purpose of improving information capabilities of EA and EMA, with the traditional costing system is recommended to use modern

costing systems. Some of modern costing systems for EMA are:

(1) Activity based costing (ABC);
(2) Target Costing;
(3) Total Life Cycle Costing;
(4) Attributes Based Costing;
(5) Process Costing;
(6) Value Chain Cost Analysis;
(7) Kaizen Costing and others.

The failure to include eco-costs in financial analyses has the effect of sending the wrong financial signals to managers making process improvement, product mix, pricing, capital budgeting, and other routine decisions. In a increasingly global economy, where labor, materials, and capital costs are likely to converge over time, effective management of environmental costs and performance may become increasingly important in determining corporate winners and corporate laggards [4].

CASE STUDY OF ABC IMPLEMENTATION IN PAPER RECYCLING FIRM

Paper recycling firm has two major products - paper and cardboard, that sells as packaging cardboard, most commonly to printing firms. Both paper and cardboard are produced completely from waste paper. In addition, there is also some waste paper that can no longer be recycled, yet it can be used for other purposes, heating for example.

The first stage of activity based costing, that is responsible for designing the activity, actually implies that the (production) process or project are split into measurable activities or work units [1][2][3].

The monitored process or project must be dividable into activities which are easy to define and qualify [6]. Total cost of activities being carried out will depend on the number according to which activity repeats itself over the monitored time period. An activity is based on numerous factors, many of them concern an firm itself, production process and the relationship between required precision and time needed to prepare costing. Since costs are allocated to activities (which consume resources) it is most important to regularly determine activities in the observed production process. In the paper recycling firm certain activities are identified and presented in the Table 3 below.

The second stage of activity based costing puts emphasis on the importance on recognition of all costs which can be directly allocated to the activities and cost objects. Direct costs are directly allocated to cost objects (the finally cost units – paper and cardboard). Sometimes, certain overhead costs can be directly allocated to a certain activity (when their place of origin, namely the type of activity due to which they rose are obvious). In the observed period, in the paper recycling firm, the following costs are being monitored: direct material costs, direct labour costs, costs for receiving material, costs for machinery preparation, amortization costs, raw material costs, insurance costs, and utilities costs. Direct material and labour costs are directly allocated to paper and cardboard products as an integral part of cost calculation.

The third stage of ABC system application relates to the allocation of resource costs to activities. The bases for such an allocation are activities costs drivers (activity

TABLE III.
DIFFERENT ACTIVITY COST POOLS IN PAPER RECYCLING FIRM

Activity Cost Pool	Activity
Sales Orders	**Establishing Customer Contacts**
	Preparing Orders
	Claims Collection
Production Planning and Preparing	**Production Planning**
	Equipment Purchasing and Maintaining
	Purchasing Raw Materials
Production Process	**Receiving and Sorting Waste**
	Pressing
	Grinding

measures). The activity cost driver is an allocation base to measure resource consumption. Determination of cost driver is the process of establishing specific qualities by which several products trigger off some indirect costs. These are typically displayed by the number of the repeated identical operations (actions) or time necessary to perform certain operation in a specific activity. If a resource is used to perform more than one activity, it is necessary to rely on this resource cost driver to be able to determine what amount from overhead costs of resource needs to be allocated to separate activities. This can be done relying on the first degree cost driver (consuming resources). It's presented in the Table 4 below. Allocating overhead cost to activities is most commonly conducted via percentage-sharing in performing certain activity, which is to be determined according to the time, number of hours, number of actions conducted by the resource application to perform the activity, etc.

The fourth stage of activity based costing comprises of calculating the activity (cost driver) rate. To obtain the activity rate it's necessary to multiply a total of activities

TABLE IV.
DETERMINING THE PAPER-RECYCLING FIRST-DEGREE COST DRIVERS FOR A MONTH'S TIME

Activity Cost Pool	Cost driver	The number of cost drivers for paper	The number of cost drivers for cardboard	A total of cost drivers
Sales Orders	**Order**	**200 orders**	**800 orders**	**1,000 orders**
Plans and preparation of raw materials	**Receiving slips**	**120 receiving slips**	**80 receiving slips**	**200 receiving slips**
Preparation and maintenance of Equipment	**Labour hour**	**56 hours**	**84 hours**	**140 hours**
Production process	**Mechanical hour**	**4.480 hours**	**6.720 hours**	**11.200 hours**
Final product distribution	**Dispatch note**	**200 dispatch**	**800 dispatch**	**1000 dispatc**

costs with a total of activities cost drivers (measured

according to the number the activities repeat themselves or activity duration and others). For example, the production process activity often as the measure of activity (cost driver) is characterized by a small number of mechanical hours. The production process activity rate is obtained when common costs of this particular activity are multiplied by a total of mechanical hours.

The fifth stage of ABC implementation consists of allocating costs to the spending items (paper and cardboard) via the second degree cost allocation, namely the second degree activity cost driver − the activity rate. It's presented in the Table 5 below.

Next stage is to put together data on all activities for each separate product. This implies that activity (cost driver) rate is multiplied by the number of cost driver for each separate product. On the basis of product activity we

TABLE V.
DETERMINATION OF THE ACTIVITY (COST DRIVER) RATE OF PRODUCTION FOR THE PAPER RECYCLING

Activity Cost Pool	A total of Cost drivers	Overhead costs (amortization and insurance)	Activity (Cost Driver) Rate
Production process	**11.200 mechanical hours**	**50.400 RSD**	**4,50 RSD per mechanical hour**

obtained the following information on the products showed in Table 6 below.

The final step to apply ABC is to release final statement for calculated production of total cost. This will enable that each separate product attributed to all overhead costs through the amount of activities (the

TABLE VI.
CALCULATING OVERHEAD COSTS FOR ACTIVITY BASED PRODUCTION PER PRODUCT

Activity Category	Activity (Cost Driver) Rate	Paper		Cardboard	
		Number of Cost Drivers	Cost	Number of Cost Drivers	Cost
Production process	4,50 RSD per mech. hour	4480 mech. hours	20.160 RSD	6720 mech. hours	30.240 RSD

product of the activity rate and the number of cost drivers for that particular product) and also to all costs of direct material and direct labour. The important benefit of using ABC in paper recycling firm is that the indirect costs are more easily allocated to the identified activities compared to traditional costing. Also, ABC allows identification of non-productive activities.

The implementation and application of activity based costing in paper recycling firm depends on:
a) the accuracy of collected financial data (from financial reports) and operational data (from analytical evidence),
b) precision to identify and execute basic stages of activity based costing (that is obligation of accountants),
c) the top management's support, and

d) the building up of a multifunctional expert team to aid the development of this system (all functions or firm's segments have to use information provided by the ABC system).

The potential for paper recycling is enormous since household waste is largely composed of waste paper. It is significant, however, that from sustainable development perspective, recycling different types of waste (as paper, plastics, accumulators, batteries, metal, PET packaging, tins, glass, worn out pneumatic material, organic waste, motor oil, electronic and electrical waste, etc.) is not only important but also economical.

CONCLUSIONS

Enviromental accounting and environmental management accounting aren't new types of accounting, but represent a particular approach for collecting, systematization, recording, and reporting on measures ventures and investments in the environmental management protection. At the macro and micro level of organizational system, EMA should contribute to the awareness of all interested stakeholders in terms of providing information basis for quick and efficient decision-making on investments in environmental protection and timely measured cost of environmental damage and protection. In addition, in order to meet the required information, it's necessary to choose an appropriate cost accounting system (tradional or/and modern), in function of EA or EMA aims. It requires finding and adjustment a methods and techniques of costing, new form and content of the report, in order to meet the growing informational demands of the contemporary approaches to environmental management and enviromental accounting.

In this paper, the case study of recycling paper and cardboard shown a methodological procedure of Activity-Based Costing. ABC as a modern approach to costing, is an upgrade of traditional costing systems. Mainly is used for the purpose of internal business decision-making. The essence of the ABC system is the allocation of costs incurred by spending resources on activities that caused their spending. Implementation of the main phases of ABC in the recycling process, shown that ABC should be used in cost accounting for enviromental protection because of:
- identification of numerous activities included in production process,
- the indirect costs are more easily allocated to the identified activities compared to traditional costing,
- more precise cost are measured for each product, and
- it's possible to identify the productive and non-productive activities.

In fact, it can be concluded that it is necessary, according to circumstances, to explore more detailed the application of different modern management approaches and costing, which should contribute to the quality of information and the efficiency of business decisions in environmental management.

REFERENCES

[1]   Atkinson, R. Kaplan, E. M. Matsumura, M. Young, Management Accounting – Information for Decision-Making and Strategy Execution, 6th edition, *Harlow: Pearson Education Limited*, 2012.

[2]   R. Garrison, E. Noreen, P. Brewer, Managerial Accounting, 11th edition, *New York: McGraw-Hill Irwin*, 2006.

[3]   Glad, H. Becker, Activity-based costing and management, *John Wiley and Sons*, 1997.

[4]   Goodstein, Economics and the Environment, 5th edition, *London: John Wiley and Sons,* 2008.

[5]   R. Graff, E. Reiskin, A. White, K. Bidwell, Snapshots of Environmental Cost Accounting, Tellus Institute, US EPA, 1998.

[6]   D. Hicks, Activity-Based Costing: Making It Work for Small and Mid-Sized Companies, *New York: John Wiley and Sons - Wiley Cost Management Series*, 1999.

[7]   M. Major, „Activity-based costing and management: a critical review“ *Issues in Management Accounting edited by Hopper T., Northcott D., Scapens R. Harlow,* England: Pearson Education Limited, 2007: pp. 155-174

[8]   Medved, „Obračun troškova u projektima zaštite životne sredine“, („Costing in Projects of Environment Protection“ – in Serbian with English abstract), *Subotica: Anali Ekonomskog fakulteta*, 2008: pp. 167-178

[9]   Milenović, Ekološka ekonomija – teorija i primena, („Ecological Economy – theory and practice“ – in Serbian), Niš: Fakultet zaštite na radu, 2000.

[10] Milićević, Strategijsko upravljačko računovodstvo, („Strategic Management Accounting“ – in Serbian), *Beograd: Ekonomski fakultet*, 2003.

[11] N. Počuča, Ekomenadžment u kompanijama, („Ecomanagement in companies“ – in Serbian), *Beograd: Građevinska knjiga*, 2008.

[12] P. Samuelson, W. Nordhaus, Economics, 18th edition, *Yale University: Massachusetts Institute of Technology*, 2005.

[13] United Nations Division for Sustainable Development, “Environmental Management Accounting Procedures and Principles”, *Economics and Social Affairs*, New York: United Nations, 2001.

[14] J. Nyers, L. Kajtar, S. Tomic, A. Nyers, “Investment-savings method for energy-economic optimization of external wall thermal insulation thickness.” *Energy and Buildings*. 2014;86:268-274.
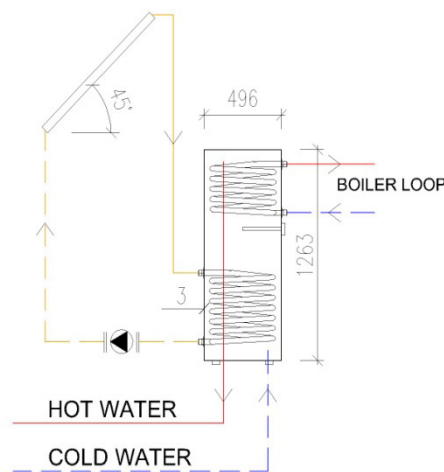
118

Variation of Solar Energy System Components According to its Efficiency

L. Skalík[*]

[*] [#]*Department of Building Services, Slovak University of Technology in Bratislava*
Radlinského 11, 810 05 Bratislava, Slovakia
lukas.skalik@stuba.sk

Abstract — **The energy demand of buildings represents in the balance of heat use and heat consumption of energy complex in the Slovak national economy second largest savings potential. Their complex energy demands is the sum of total investment input to ensure thermal protection and annual operational demands of particular energy systems during their lifetime in building. The application of energy systems based on thermal solar systems reduces energy consumption and operating costs of building for support heating and domestic hot water as well as savings of non-renewable fossil fuels. Well designed thermal solar system depends on many characteristics, i. e. appropriate solar collector area and tank volume, collector tilt and orientation as well as quality of used components. The evaluation of thermal solar system components by calculation software shows how can be the original thermal solar system improved by means of performance. The system performance can be improved of more than 31 % than in given system by changing four thermal solar system parameters such as heat loss coefficient and aperture area of used solar collector, storage tank volume and its height and diameter ratio.**

INTRODUCTION

The aim of paper is to investigate the thermal performance and design of a solar domestic hot water system which is based on given inputs for storage tank and solar collectors.

Use of solar energy gives a chance to save energy due to the installation of the thermal solar systems. Thermal solar systems are used in different countries for many years however there are still a lot of investigations to improve technologies. The comparison of given original thermal solar system and improved thermal solar system is investigated.

ORIGINAL SOLAR DOMESTIC HOT WATER SYSTEM

Dimensions and details of calculated solar heating system are given in Fig. 1. In summer period, system is more efficient than in the winter period, therefore the electric spiral is used during the period without a lot of sun. The solar domestic hot water system consists of solar collector, spiral tank, heat exchanger spiral, back-up energy from electric heating element with power of 2 kW and boiler with power of 15 kW. Storage tank used for solar heating system is spiral tank. All calculations are made by calculation program for spiral tanks "SpiralSol". This software is detailed described in [1]. The type of hot

water tank is bivalent, which is heated both by solar collector and by auxiliary energy supply system. Spiral storage tank and heat exchange spiral are made from steel and its volume is 230 liters. Aperture area of solar collector is 2,78m^2.

Scheme of thermal solar system [4]

Net utilized solar energy was found by using calculation program SpiralSol. The system performance, the yearly solar fraction and the yearly system solar fraction for the solar heating system were found by calculations.

To verify calculations of net utilized solar energy from SpiralSol the equations below are used. Values of tapped energy and auxiliary energy were calculated and taken directly from software.

Net utilized solar energy = tapped energy - auxiliary energy

1678.2 kWh - 895.1 kWh = 783.1 kWh
(1)

System performance = net utilized solar energy - pump energy - control system

783100 Wh - 63.9 Wh - 2 W * 2131.3 h - 1 W * 6628.7h = 772.145 kWh
(2)

Solar fraction = net utilized solar energy / tapped energy

783.1 kWh / 1678.2 kWh * 100 % = 47 %
(3)

119

System solar fraction = system performance / tapped energy

$$772.145 \text{ kWh} / 1678.2 \text{ kWh} * 100 \% = 46 \% \quad (4)$$

RESULTS OF CALCULATIONS FOR ORIGINAL SDHW SYSTEM [4]

| Net utilized solar energy [kWh]	The system performance [kWh]	The yearly solar fraction [%]	The yearly system solar fraction for the solar heating system [%]
783	772	47	46

IMPROVED THERMAL SOLAR SYSTEM

In order to increase energy efficiency and overall performance of thermal solar system, following parameters have been investigated:

- Solar collector:
  - heat loss coefficient;
  - aperture area;
  - tilt and orientation.
- Solar storage tank:
  - tank volume;
  - height / diameter ratio of tank.

Solar Collector Heat Loss Coefficient

High value of the heat loss coefficient at the bottom of the solar collector cover effects in poor behavior of thermal solar systems and high heat losses through the cover of solar collector. In order to improve efficiency of thermal solar systems, applying appropriate insulation with a thermal conductivity λ below 0.035 W / m.K and filling completely the space between the absorber and casing of solar collector have to be realized. Appropriate value for heat loss coefficient in the range from 1 to 3 W/m^2K is suitable [1], accordingly, value of heat loss for improved system is set to be 2 $W/m^2.K$. From Fig. 2, dependency of heat loss coefficient on thermal solar system performance is obvious. Higher heat loss coefficient of solar collector results in lower performance. The arrow indicates the value of the coefficient for the given system.
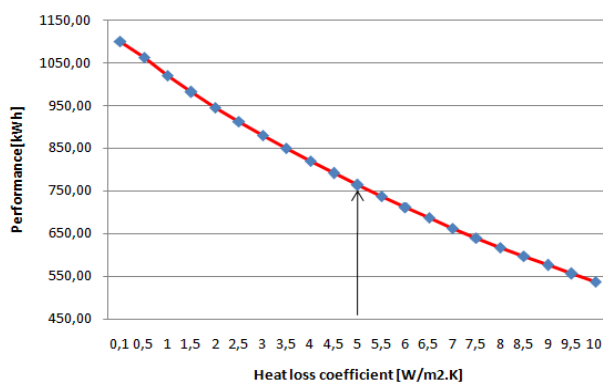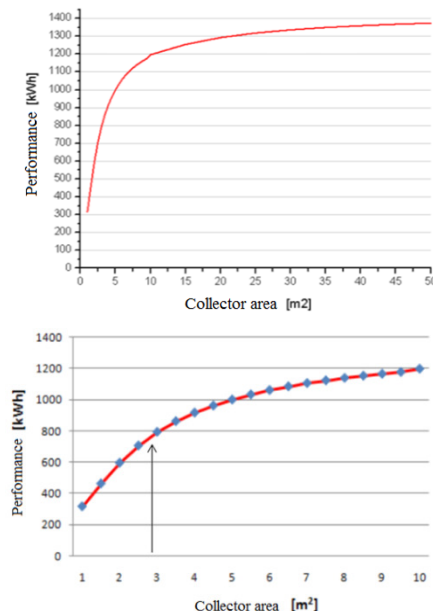

Thermal solar system performance according to heat loss coefficient [4]

Solar Collector Area

Aperture area of solar collector, which is actively working with solar radiation and gives the heat to heat transfer fluid, which should provide 85 to 100% of the DHW needs in the summer. For SDHW systems can be assumed that the aperture area is from 0.6 to 0.8 m^2 per person. For thermal solar system, which also supports space heating it is from 0.3 to 0.5 m^2 flat plate collector aperture area per m^2 floor area and 0.2 m^2 of vacuum tube solar collectors per m^2 floor area [2].

To compare the impact of collector area on thermal solar system performance calculations were carried out with different collector areas. With the exception of volume flow rate, all other variables in the system remain unchanged. From Fig. 3 it can be seen that after a certain collector area (in this case 10 m^2) is the transfer of heat from collectors non-efficient according to performance of thermal solar system. For a given system (arrow) is unreasonable to have more than 10 m^2 of collector area. Requirement for larger collector area will result in increasing of storage tank volume, dimension of pipes, pumps and other parameters, apart from often limited roof area and investment costs for larger solar collectors.

Thermal solar system performance according to collector area [4]
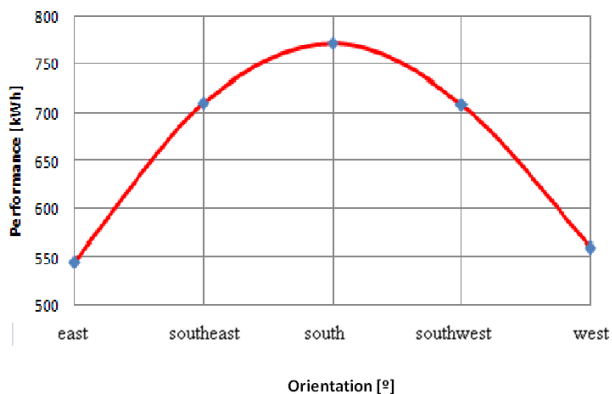
Solar Collector Tilt and Orientation

Correct choice of the solar collector tilt has a significant impact on the performance of thermal solar system, especially in systems designed to support space heating. Thermal solar system performance at various angles of inclination (tilts) of the collector area during the year is shown in Fig. 4a. In order to achieve highest performance during the year, tilt of solar collectors have to be from 45° to 50°, increasing or decreasing from this tilt of solar collector will result in performance degradation.
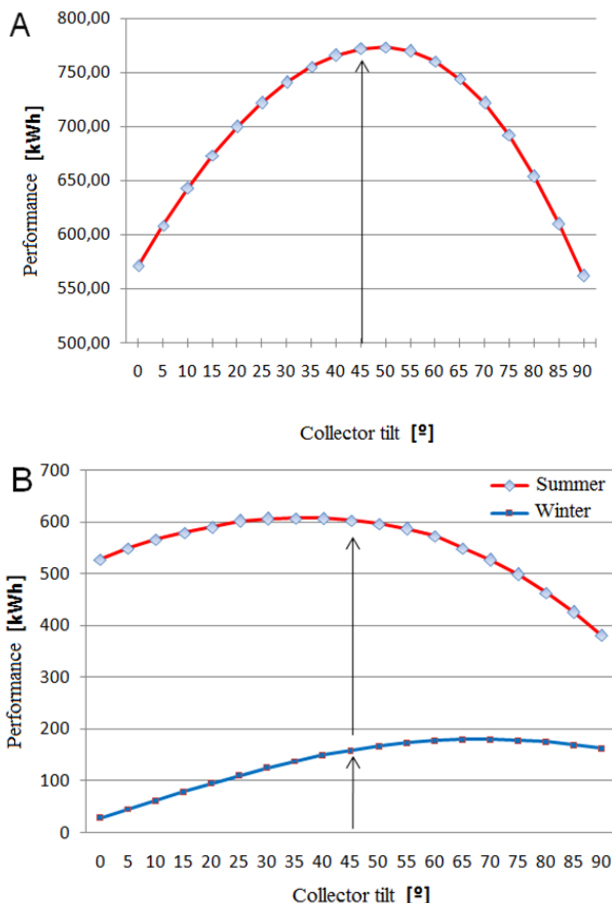
Influence of solar collector tilt on thermal solar system performance, a) Annualy, b) seasonal [4]

Thermal solar system performance at different tilts of the solar collector also varies during the season (summer period is from April to September and winter from October to March). In summer, when the intensity of solar radiation is higher, thermal solar system performance is about five times higher than in the winter period. Tilt of solar collector surface for the summer period should be from 35 to 40°, and during winter from 55° to 85° according to Fig. 4b.

Solar collectors should be located on the southern roof surface (azimuth 0°). Fluctuations of the position of the roof surface in the direction east / west results in a performance decreasing - max. 10%. In the Fig. 5 can be seen how thermal solar system performance is influenced by solar collector orientation.


Influence of solar collector orientation on thermal solar system performance [4]

Solar Storage Tank Volume

Other very important parameter of thermal solar system is to design suitable storage tank volume. Designing and installation of too large solar tanks have negative points, such as excessive investment costs or often limited space for placement of these storage tanks in residential buildings. Disadvantage is also heating of excessive amounts of DHW in larger tanks which is ultimately not consumed and after certain time will become colder, thereby reducing the overall performance of thermal solar system is achieved.
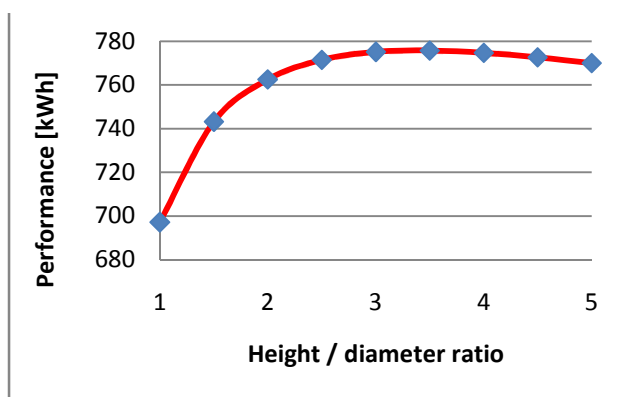
Thermal solar system performance by function of storage tank volume was calculated. The ratio of height and width (diameter) of tank remain unchanged. Fig. 5 show how the performance of thermal solar system is affected by storage tank volume. It is clear that the amount of about 150 litres best suits the thermal solar system in this case. Increasing or decreasing of the storage tank volume (150 l) will result in thermal solar system performance decreasing. With higher ratio comes higher performace. Initially, there is a strong relationship where total volume is between 105 and 160 liters. In this range the difference between system performances is about 6% (2% per 1 liter). This relationship subside between 160 and 240 liters (0.3% per 1 liter), and around 240-290 becomes an almost linear dependence (0.1% per 1 liter).
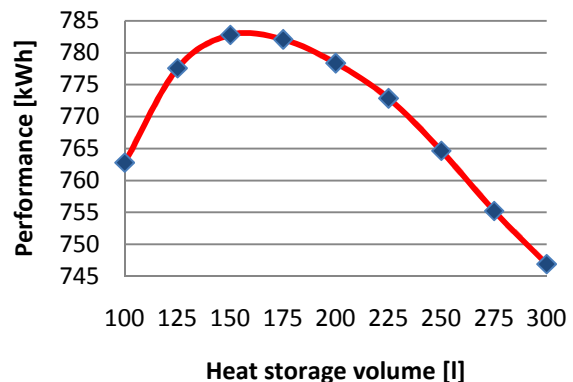
Thermal solar system performance influenced by heat storage volume [4]

Height / Diameter Ratio of the Storage Tank

When considering the spiral tank we have to pay special attention to select proper height/diameter ratio. It is very important, because using too large diameter in relation to the height of the tank will prevent efficient heating of domestic water by the spiral. Can be concluded that if the ratio is around 2 the better system performance, but we have to keep some reasonable limit to not design too slender tank resulting in increasing heat loss and relative small storage capacity to height of the tank. Also a good thermal stratification for spiral tank is obtained when the height/diameter ratio is 2 or higher. The height/diameter ratio is thus equal to or higher than the recommended ratio.

Thermal solar system performance influenced by height/diameter ratio [4]

As we can see in the Fig. 7, given thermal solar system is the most preferably when the SDHW tank height/diameter ratio is about 3.5. Increasing or decreasing tank H/D ratio from 3.5 will result in the thermal solar system performance decreasing.

This is caused by the fact that the thermal stratification is maintained better in the storage tank with a higher height/diameter ratio than in a tank with a low height/diameter ratio due to a lower downward thermal conductivity through the water and the tank walls. Therefore the auxiliary energy supply will be lower and the collector efficiency will be higher for systems with storage tanks with higher height/diameter ratios than for systems with tanks with low height/diameter ratio. However, for spiral storage tank with an auxiliary volume of 80 l, the height/diameter ratio of value 3 results in the highest thermal solar system performance. This is caused by the fact that the tank surface area and tank heat loss, is increasing for increasing height/diameter ratio, as long as the ratio is not too low. The increased thermal stratification achieved by an increased height/diameter ratio can from a certain value of height/diameter ratio no longer compensate increasing heat losses and result in lower thermal solar system performance, i. e. too high H/D ratio result in decreasing of thermal solar system performance. [3]

RESULTS

System performance can be improved of more than 31 % (Table 3) than in given system by changing four thermal solar system parameters such as heat loss coefficient and aperture area of used solar collector, storage tank volume and its height and diameter ratio (Table 2).

CHANGED PARAMETERS OF THERMAL SOLAR SYSTEM [4]

Thermal solar system	Heat loss coefficient (W/(m². K))	H/D ratio (-)	Tank volume (l)	Collector area (m²)
Given	5,13	2,56	228,7	2,78
Improved	2,00	3,5	175	3,00

RESULTS OF GIVEN AND IMPROVED THERMAL SOLAR SYSTEM CALCULATIONS BY SPIRALSOL [4]

	Net utilized solar energy (kWh)	System performance (kWh)	Solar fraction (%)	System solar fraction (%)
Given thermal s.s.	783,1	772	46,7	46
Improved thermal s.s.	1 027,9	1017	61,3	60,6
Improvement (%)	31	32	31	32

CONCLUSION

Thermal solar system was investigated and results show that the given system should have several improvements as well as different system parameters could impact system performance in general. For this reason it is very important to design thermal solar heating system carefully and advisedly to save both auxiliary energy and investments.

In literature can be found many ways how to improve a system or what to take into account during designing a whole system. Main factors, i.e. tank volume in correlation with collector area assuming that other parameters are properly selected such as thermal insulation of pipes and solar tank, auxiliary energy, back-up heater and pump in collector loop.

REFERENCES

[1] Furbo, S. Hot Water Tanks Storage for Solar Heating Systems. In Course 11117 Solar Heating Systems, Educational Notes 4, Lyngby: Technical University of Denmark, 2011

[2] Furbo, S. Low Flow Solar Heating Systems. In Course 11117 Solar Heating Systems, lecture 4, Lyngby: Technical University of Denmark, 2011

[3] Robert Hausner and Christian Fink, Stagnation Behaviour of Thermal Solar Systems. AEE INTEC

[4] Skalík, L., Lulkovičová, O. Solar Eergy System Components Optimalization. In: Nízkoteplotné vykurovanie 2012: Proceedings from 12th Conference. Dunajská Streda, Slovak Republic, 22.-23.5.2012. Bratislava: SSTP, 2012, p. 33-38. ISBN 978-80-89216-46-8

[5] Szente, I. Farkas, and P. Odry: The application of Thermopile Technology in high Energy Nuclear Power Plants, EXPRES 2014, pp.23-28, 2014, ISBN 978-86-85409-96-7

[6] Nyers J., Nyers A.: "Hydraulic Analysis of Heat Pump's Heating Circuit using Mathematical Model". 9rd IEEE ICCC International Conference" Proceedings-USB, pp 349-353, Tihany, Hungary. 04-08. 07. 2013. ISBN 978-1-4799-0061-9

District Heat Supply Based on Renewable Energy

Jenő Kontra
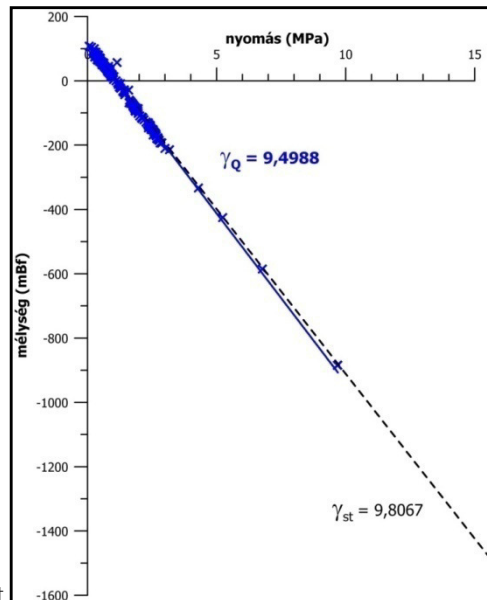
Budapest University of Technology and Economics
Department of Building Energetics and Services, Budapest, Hungary
kontra@egt.bme.hu; www.egt.bme.hu

Abstract— **Extension of district heat supply is a very important development task for a medium-size Hungarian town, Cegléd. District heat supply of two housing estates of this town is solved with gas heating at present. For establishing the heat source side of an additional district heat supply system for public buildings, the only solution is – considering favorable geothermal circumstances of the Hungarian Great Plain – renewable energy, namely thermal water based heating. This way, obsolete gas-burning boilers in public buildings of the town can be discarded and operational costs will reduce to about one quarter of the present gas heating. This planned geothermal heat supply operates with two new producing wells and one injection well in a closed pressurized system without degasification, consequently, there is no scale and carbon-dioxide generation in the system, and is faultless also in terms of environmental protection.**
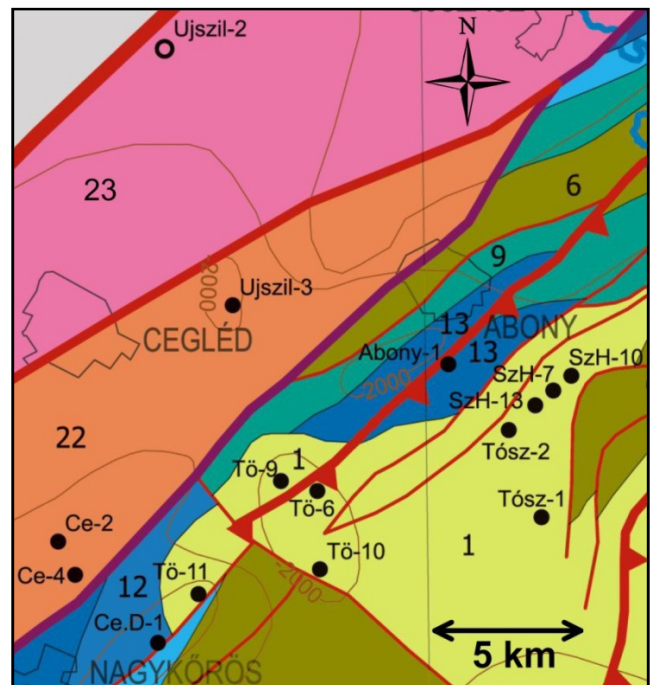
Fig. 1: Pre-cainozoic map of the wider environment of Cegléd (*HAAS et al. 2010*)

(*Red and lilac lines: tectonic elements; TISZA Main Unit; 6 – Lower Cretaceous basic volcanites and their redeposited marine sediments, 9 – Middle Jurassic–Lower Cretaceous pelagic limestone, flint limestone, 12 – Upper Triassic–Lower Jurassic siliciclastic set with fossil coal*)

content, 13 – Middle Triassic shallow-sea siliciclastic and carbonate set, 22 – Variscan granitoid rocks, 23 – Variscan metamorphit set)
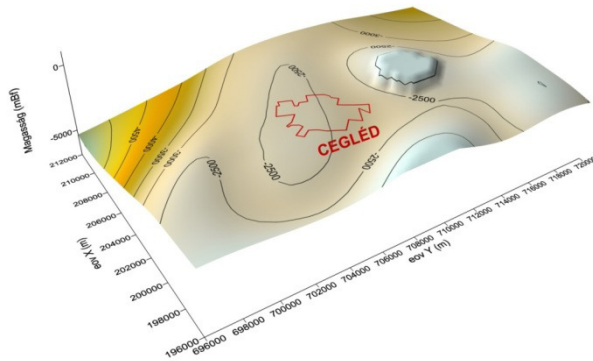
I.   CONDITION OF HEAT GENERATING SOURCES

Gas heating evaluation (boilers)
On the heat source side of the buildings heating operating currently, outdated gas boilers stand**.**
Heating appliances are out of date.

They are evaluated from the following main aspects:
  a.)   modernity status,
  b.)   wear and tear, physical aging,
  c.)   estimated useful life of appliances remained.

a.)   Modernity status
At present level of gas heating, only condensing heating technology can be regarded as modern where heating technological efficiency may reach 108-109%. Boilers with an efficiency lower than this are not suitable (FÉG-VESTALE, KOMFORT, ÉTI). Among the public buildings reviewed, only the headquarters of the municipality has a modern boiler. Consumption of all the others is disproportionately high; they do not correspond to the Hungarian energy-political targets as they operate with expensive imported gas, just for quoting a reason (see the images attached).

b.)   Wear and tear, physical aging
All but two of the boilers are in worn-out condition also physically. Some appliances have been operating for 25-35 years, they often need cost-intensive repairs, and their low efficiency goes with high consumption. Their estimated rest useful life is 0 to 1 year. All this justifies their disassembly.

As high-rank energy-political target, a renewable energy based reconstruction, namely geothermics shall be performed.

c.)   Estimated rest useful life of boilers is 0 to 3 years with considerable repair and spare parts costs.

Table 1

No.	Institution	Built in boiler's output [kW]	Energy carrier consumption (at present) GJ pro year			Heated volume [m³]	Calculated heating power [kW]
			2013	2014	till Oct. 2015		
1	Kossuth L. Secondary School	532	5,178	1,987	3,801	27,400	510
2	Gál József Sports Hall	1,025	1,673	1,322	1,636	20,603	750
3	Swimming Pool and Bath	510 + 320	4,147	3,810	3,918	-	470
4	Török János Agricultural and Medical Vocational Secondary School	735	2,487	2,790	2,346	22,854	635
5	Dózsa György Dormitory	702	2,185	2,147	2,274	8,650	620
6	Cegléd Vocational Secondary School of Economics and Information Technology	975	1,138	960	934	11,840	846
7	Várkonyi István Primary School*	460	1,266	1,183	1,250	4,102	418
8	Day Nursery in Deák Street	120	862	743	939	2,401	103
9	Nursery School in Deák Street	110	602	552	651	2,160	96

*including extension

II   DESIGN OF THE PROPOSED GEOTHERMAL HEAT SOURCE

As heat source of the new district heat system, two thermal water production wells, indicated by T_1 and T_2 on the city map, will serve. These wells will expectedly produce thermal water of 65°C, operate in controlled way with drowned pumps and with a maximum volume flow of 50m³/h each. Downed pumps are to be installed below the bubble point in the wells and

they will transfer thermal water within the pre-insulated grid on the track in the soil to be precisely defined during the detailed design.

In the thermal water center, a high-performance plate heat exchanger will be built in where thermal water exchanges heat to the district heat system with a nominal temperature drop of Δt= 30°C. In this closed system, soft water circulates between the thermal water center and the recipient heat centers of the individual buildings.

In the thermal water system in the recipient thermal water center, a subsurface reinforced concrete container of a volume of 200 m³ shall be constructed;

thermal water will be transferred from both production wells to this container from where the heat exchanger is supplied. It is a pressurized closed system. That is why neither CO_2 nor other gases escape from thermal water and no saline deposits occur (salts of Ca, Mg etc.) because hydro-carbonates remain in solution.

A proposed location of the thermal water center may be the territory of the operating heating plant of the present district heating. As an advantage, peak energy could be input here during the short winter periods when peak demand arises for some days. The present thermal well of the swimming pool and bath shall be excluded from thermal water supply as its consumption system is solved appropriately from the well of the bath.

We located the proposed new thermal water wells within the area defined in the thermal water geological expertise, at a distance of 1.3 km from each other, however, the exact places will be determined by various authorities, local governments and geologists during the working design.

The thermal water injection well (indicated by V) returning cooled down thermal water shall be situated in this territory. This well places the cooled down water of both production wells in the original producing depth. From the collection container of 50 m³ in the thermal water center for cooled down thermal water, automatically controlled recuperation with pumps will be realized after a 15μ filtering in full harmony with the production quantities.

The cooled down thermal water is transferred to the injection well in uninsulated HDPE pipes. We note here that post-utilization of this cooled down thermal water of nominal temperatures of 30 to 35°C can be performed by heat exchangers with very favorable COP – depending on future demands.

The thermal water based new district heat supply system is a double-pipe system filled with soft water, ending in the heat plant of each building directly. Pipes are laid down in soil on the indicated track to be finalized during design and they transfer heat to own recipient heat plant of each public building, calculated with a nominal temperature gradient of 80/60°C. The system has a radial design as shown in the enclosed graph.
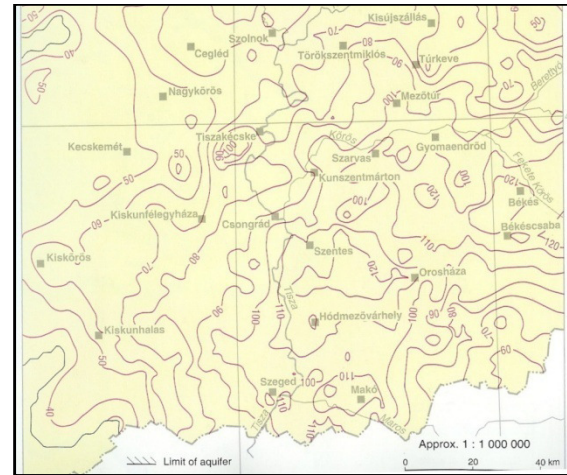

Fig. 4: Temperatures (°C) at the bottom of Upper Pannonian layers in the Southern Great Plain (Atlas of Geothermal Resources in Europe, 2002)
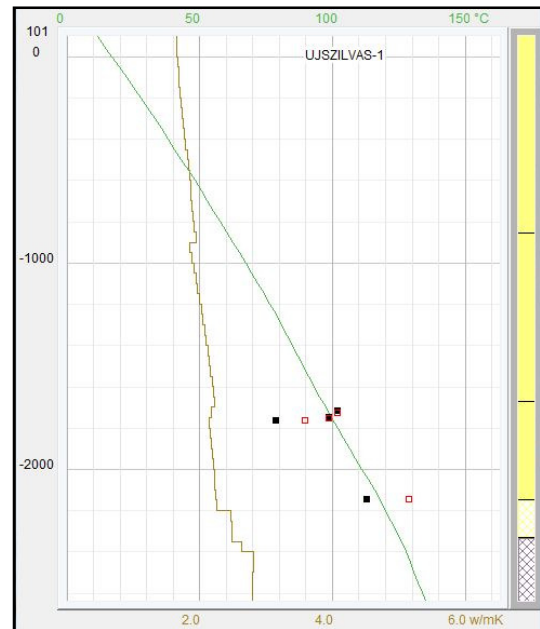

Fig. 5: Change of temperatures (°C) in function of depth (*square: measurement data, green line: approximating curve*) and change of heat-conveying capacity *(W/mK) (brown line) based on data of boring Újszilvás-1)*

From the heat source to the recipient heat plant, the system operates with a remote monitoring system where all operating properties are registered and collected.
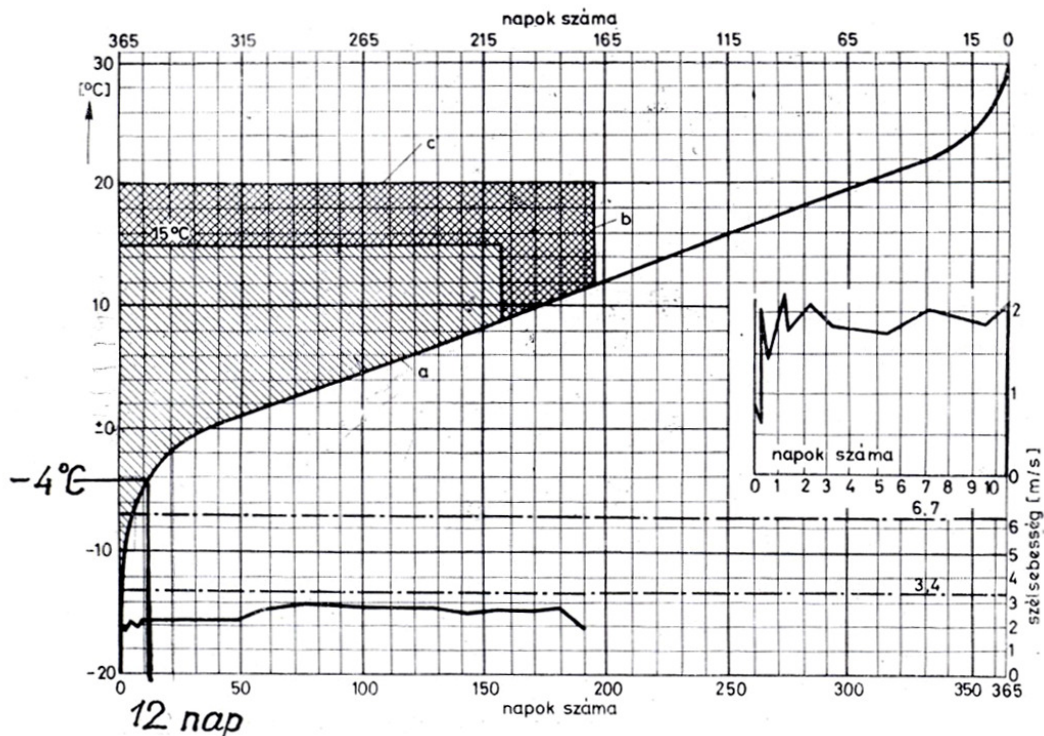
Fig. 6: Heat frequency curve

III IMPORTANCE OF THIS RESEARCH

By order of the town development company of Cegléd, geothermal circumstances of the town and its neighborhood have been examined. This study has confirmed that both temperature and quantity of expectable thermal water can be suitable heat source of the system, and places of new thermal wells have been determined.

The existing thermal wells can be used in district heat supply neither concerning water temperature nor heat load.

Thermal well II of the bath and swimming pool with an expected yield of 600l/sec planned at present will cover air engineering needs of the sports hall, can replace the gas supply of tent's heating in winter as well as can satisfy also the heat demand of the new thermal bathing-pool to be constructed.

In terms of building physics and heating technology, we have reviewed public buildings of the town specified for this study and have stated that building reconstruction is justified from point of view of heating technology and building physics.

Wear and tear as well as physical aging of heat generating equipment are considerable, most equipment and thermal centers shall be replaced. Reorganization of the heat generating side based on thermal water results in essential savings in energy costs and operating costs. According to our proposal, two production wells and one injection well are needed with some additional peak

energy (based on gas). We have defined the optimum track and dimensions of the grid.

Based on this and considering all elements of the system, we have elaborated the investment budget. Expectable savings in operating costs are significant, and this serves as justification for this investment. Establishment of a district heat supply system based on renewable energy is preferable also in terms of environmental protection due to lower carbon-dioxide emission and gas savings.

REFERENCES

[1] Garbai, L.-Kontra, J.: Zalaegerszeg város geotermális alapú távhőellátása (Geothermal sourced district heat supply of town Zalaegerszeg) (study), Budapest, 2015

[2] Kontra, J.-Varga, J.: Távhő Cselekvési Terv Geotermális energetikai fejezete (District Heat Action Plan, Section Geothermal Energetics) Budapest, 2013

[3] Kontra, J.: Lakitelek Népfőiskola geotermális energiahasznosítási és épületrekonstrukciós tervezés és tanulmány (Geothermal energy utilization and building reconstruction plan and study of Lakitelek College) Budapest, 2012

[4] J. Nyers, L. Garbai, A. Nyers: A modified mathematical model of heat pump's condenser for analytical optimization. International J. ENERGY. Vol. 80, pp. 706-714, 2015.

[5] Magyar Zoltán, Garbai László, Jasper Andor Risk-based determination of heat demand for central and district heating by a probability theory approach ENERGY AND BUILDINGS 110: pp. 387-395. (2016)

Blade Shape of Wind Turbine in the Study of Optimal Material Consumption

S. Mirjanic,* D. Jesić**, D. Golubović***, S. Kirin****

*University of Banja Luka, Faculty of Sciences, Banja Luka, sladjanamirjanic@yahoo.com
**International Technology and Menagement Academi, Novi Sad, Serbia, dusanjesic@hotmail.com
*** University of East Sarajevo, Faculty of Mechanical Engineering, Bosnia and Hercegovina,
Vuka Karadžića 30, 71123 East Sarajevo, e-mail: dusan.golubovic54@gmail.com
****Innovation centre of Faculty of Mechanical Engineering in Belgrade, 11000 Belgrade, Serbia,
snezanakirin@yahoo.com;

Abstract—**The paper analyze parameters that effect the propeller of wind turbine blade shape. The wind turbine blade has been designed by the use of data obtained by computer program. Comparison was made between three blades with different aerodynamic profile characteristic with same remaining input data and other two blades being designed with different wind velocities as design velocities. The results presented in the paper may be useful for optimization of the wind turbine blade shape of good characteristic, especially in the case where material consumption plays an important role.**

INTRODUCTION

The paper represent investigation and is based on relationships representing change of kinetic energy of wind in turning energy of blade of wind turbine [1, 2] and investigate some influenced parameters on optimal dimension of blade. Relative massive radial dimension of turbine for power on turbine shaft are obligated of analyses of turbine influenced on turbine round means blade. Reduction of longitudinal and transversal dimensions of the blade helps of the price reductions of turbine according mass unit, of installed power. The aim of the paper shows influence of the aerodynamic profiles of blade with different characteristic of wind speed on dimension of blade. It is also important influence of parameters of fast move on transversal dimension of turbine blade.

THE BASE RELATIONSHIPS FOR WIND TURBINE

In the papers [ ] is shown relationships that describe conection of influenced parameters (dinamic, geometric and aerodinamic) of working circle of turbine. From relationship (1) visible is direct influence of aerodinamic parameters of profile blade (C_L- parameter of buoyancy and C_D= K C_L- parameter of resin) on element of rotational power

dP_Q/dr which is posible get from diferential of the blade radius:

$$\frac{dP}{dr} = 0.5 C_L \rho l B \omega^2 V^2 r^2 (1 + a_2) \cdot [k_p^2 (1 + a_2)$$

$$^2 + (1 - a_1)^{~2}]^{~1/2} \frac{1}{k_p} \left(\frac{1 - a_1}{1 + a_2} - k k_p \right) \qquad (1)$$

A. INFLUENCE OF AERODINAMIC PROFILE OF THE BLADE SELECTION

With same input data in algoritm for PC are chozen distribution of cross section dimension of blade acording radius of blade l=f(r) of three diferent types of profilein NACA series, Fig 1. Higher diferences of transverzal dimensions of profile blade, with lengt l smaler are in profile beter caracteristic, C_L=f(a) is to expect result get here, what recommend on possible savings in material with good characteristic chosen. Blade of `Svedwinda` turbine bladeis on fig 1. This is of Svedish compani [] try chose profile of the blade for use out of commonly used from serial NACA from Danish and other producers of wind turbines. It is interesting to notice of curve difference character of curve l=f(r) in the area of small radius (r), according author of this paper is according Swedwind that for r=0 is ∞ value.

Don't knowing the algorithm of Swedish authors it is not possible to establish influence on that character theoretic distribution l=f(r) curve. According the paper [ ] it is possible to describe influence of factors a_1 and a_2 along the radius of blade.

B. INFLUENCE OF WIND SPEED ON DESIGNED TURBINE SPEED

According known basic equation of wind power which is possible take for wind ($v^{3/2}$). On the opposite side influence of rotational   mass inertia of turbine

127

aggregate conditioning of value of income wind speed (cut in) for working turbine start.

Need for turbine switch of during stormy (cut of) dictate reasons of authorised strenth of materijal, which is over come of when there is complicated dinamic load

If we talk about project of turbine for drive of asynchrony generator of current, regulation of turbine work in narrow interval of angular speed involved special access of projected turbine and regulation of inside turbine regulation system. Inside working interval of wind speed (cut of and cut out) logically is to choose project value of wind speed for entry value of optimal determination of blade contour. Which is wind speed in working interval is projected and how much is it conditioned of potential place where turbine will work. Answer of this question is not straightforward.

According one turbine is designed for given nominal power of electro generator which is equal or very near maximal speed of wind (for P_{max})according the others speed is nearer output energy what follows from simple analytic approach [3, 6]. By the first way round are smaller diameter than by the other way for same maximal power, what gives smaller price of 1 kW installed power. Both cases don't base on frequency of blowing defense v_{pr} gated from data's from future place what is for big systems very important. Designed blade for wind speed gives biggest energy during year (statistic of average investigation) on the place of use cud give maximal effect.

Because of missing of measured speed of wind on future place of turbine installation during longer time user of system producer gives aggregate of wonted installed power which gives energy on generator depends on potential of wind on the place of installation. Turbine blade is not designed on the base of wind speed which gives highest wind speed which gives highest energy of wind that gives highest energy of kW the installed power.
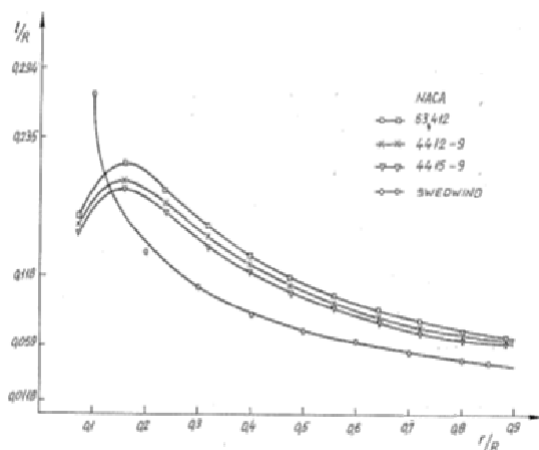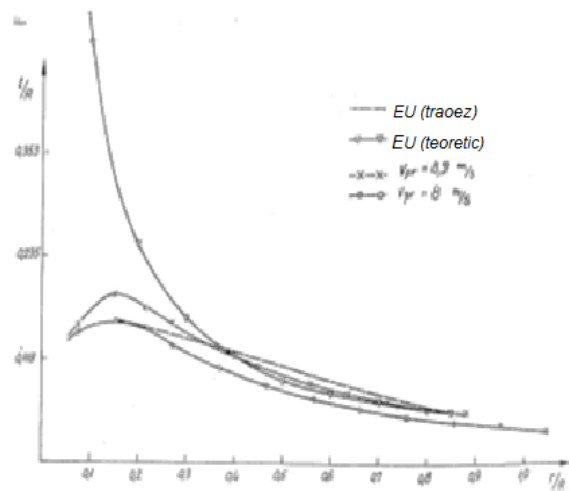

Figure 2 Distribution of blade chord (1) along the blade radius (r) for different velocities

TABLE I. Caparisons of two blade chords which have same entrance data but different v_{pr}

Same 0f the input data (power, no of revolutions, power factor, ρ density of material C_1, C_p profil character					
V_{pr}=8.0 m/s	10.66	2137	9742.9	56.115	0.525	8.017
V_{pr}=8.0 m/s	11.911	1843	9736.1	56.076	0.539	9.5
Results	Axial force kN	Tangential force kN	Torsional moment Nm	Turbine Power kW	C_p	Radius of circle m

Table 1 gives data for comparisons of programing two blades of same entry data but different v_{pr}. Blade with smaller value of v_{pr} is little longer but slim for same power of turbine than blade of higher v_{pr}. Higher parameter of power C_p of second blade can help higher sum of energy on same location of work.

Fig 2 shows influence of v_{pr} (value) on the transversal dimensions of blade. On the same Fig is shown theoretical blade chord European conventional turbine and trapeze shape of industrial blade.

When change l=f(r) as a function of speed k_p= R ω/r shows diagram on Figure 3 from which is visible that faster turbine have slim blade.

Figure 1 Distribution of blade chord (1) along the blade radius (r) for different aerodynamic characteristic
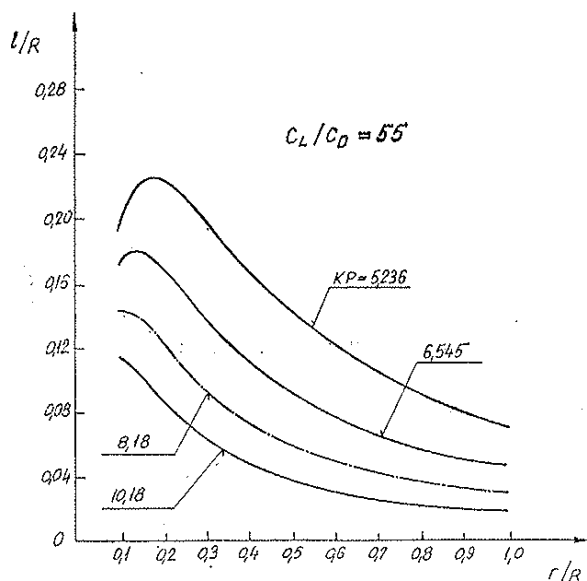
128

Figure 3 Distribution of blade chord (1) along the blade radius (r) for different tip-speed ratio

III CONCLUSION

In the age of growing investigation and use of wind turbine in the world with higher efficiency of transformation of wind energy, especially big units, presented influence could be useful for determination of price of 1 kW of the energy from wind

REFERENCES

[1] Labudovic B. at all, Obnovljivi izvori energije. Energetika Marketing, Zagreb, 2002

[2] Pavlovic, T., Milosavljevic, D., Mirjanic, D., Renewable sources of energy (in Serbian language), Akademija nauka i umjetnosti Republike Srpske, Banja Luka, 2013.

[3] Janicek F at all Obnovitelne zdroje energije 1, STU, Fakulta elektrotechniky a informatiki, Bratislava, 2007, pp162

[4] P Kovac, Z. Palkova Proizvodno masinstvo i Obnavljivi izvoei energije, FTH Izdavastvo, 2011, p 122

[5] Fragnel A.: Promotion of Renewable energy consumption in EU, 1st international Engineering,, Mostar, 2010 pp 57-62

[6] Gvozdenac D, Nakomcit-Smaragditis B., Gvozdenac-Urosevic B., Obnovljivi izvori energije, FTH, Izdavastvo, 2010, s208

[7] G Burcik at all: Potencijali solarne i vetro Energije u Srbiji (studija) Ministarstvo nauke I zastite zivotne sredine R Srbije, EE704-1052A, 2005

[8] Zlatanovic M et all: Energetski potencijal vetra Republike Srpske, Alternativni izvori energije I budicnost njihove primene, br 102 (OPN br 14), 2010, CANU, Podgorica , str,196-2015)

[9] J. Nyers, L. Garbai, A. Nyers: A modified mathematical model of heat pump's condenser for analytical optimization. International J. Energy. Vol. 80, pp. 706-714, 2015.

[10] http://www.energetskiportal.rs/obnovljivi-izvori-energije/energija-vetra/

EXPRES 2016

8th International Symposium on Exploitation of Renewable Energy Sources

---

In technical co-sponsors

- **Government** of Subotica

- **BME** University, Budapest

- **Óbuda** University, Budapest Hungary

- **Faculty of Economics**, Subotica

- **Tera Term** doo, Subotica,

In technical co-operation with

- **Annus Auto Saloon and Service,** Subotica
- **Đantar doo**, Bačka Topola
- **Mini Pani,** Subotica